

IDENTIFICATION AND MECHANISTIC INVESTIGATION OF
CLINICALLY IMPORTANT MYOPATHIC
DRUG-DRUG INTERACTIONS

Xu Han

Submitted to the faculty of the University Graduate School
in partial fulfillment of the requirements
for the degree of
Doctor of Philosophy
in the Department of Pharmacology and Toxicology,
Indiana University

March 2014

Accepted by the Graduate Faculty, Indiana University, in partial fulfillment of the requirements for the degree of Doctor of Philosophy.

David A. Flockhart, M.D., Ph.D., Chair

Robert R. Bies, Pharm.D., Ph.D.

Zeruesenay Desta, Ph.D.

Lang Li, Ph.D.

Sherry F. Queener, Ph.D.

Doctoral Committee

Sara K. Quinney, Pharm.D, Ph.D.

November 21, 2013

Jian-Ting Zhang, Ph.D.

Acknowledgements

First, I am truly grateful for having the opportunity to work with my research mentors, Dr. David Flockhart and Dr. Lang Li. This dissertation would not have been possible without their inspiration, guidance and support. I consider them as both mentors and close friends for their help for me to grow not only scientifically but also personally. They both have been incredibly supportive, have opened my eyes for me to find the future direction, have allowed me to receive additional scientific trainings that further expanded my knowledge and expertise, and have cultivated my critical thinking that would be vitally important for my future career. I also have learned from them the value of open-mindedness, hardworking, creativity, tolerance, patience and cooperative consciousness, from which I will surely benefit for the rest of my life.

I would also like to thank the members on my thesis committee, Dr. Sherry Queener, Dr. Sara Quinney, Dr. Zeruesenay Desta, Dr. Robert Bies and Dr. Jian-Ting Zhang. They have provided critical evaluation on my data and hypothesis that helped me to develop the dissertation. I want to especially thank Dr. Sara Quinney and Dr. Zeruesenay Desta for providing expert assistance and suggestions that are essential for me to complete the dissertation. I would also like to thank Dr. Sherry Queener for acting as my committee chair and for her understanding.

I must also thank the members, past and present, of the Division of Clinical Pharmacology and Dr. Lang Li's laboratory. It has been my pleasure to work in these friendly, diverse and supportive environments. I want to especially thank Dr. David Jones and Jessica Lu for their help on the development of the LC/MS/MS methods. I also want

to thank the members from Dr. Lang Li's laboratory, Zhiping Wang, Abhinita Subhadarshini and Shreyas D. Karnik, whose work on text mining laid the foundation for my dissertation, and ChienWei Chiang and Guanglong Jiang, who have been helpful in many ways. In addition, I must also thank Dr. Jefferey Elmendorf and Lixuan Xi for their enormous help on the work with myotubes.

Lastly, I sincerely thank my parents, especially my mother, for their love and support that made this journey possible. I also want to thank my friends who have helped and supported me through those frustrations and depressed times. I shall always remember, for the rest of my life, the encouraging words that they gave me and the joy that I have shared with them.

Xu Han

IDENTIFICATION AND MECHANISTIC INVESTIGATION OF CLINICALLY
IMPORTANT MYOPATHIC DRUG-DRUG INTERACTIONS

Drug-drug interactions (DDIs) refer to situations where one drug affects the pharmacokinetics or pharmacodynamics of another. DDIs represent a major cause of morbidity and mortality. A common adverse drug reaction (ADR) that can result from, or be exacerbated by DDIs is drug-induced myopathy. Identifying DDIs and understanding their underlying mechanisms is key to the prevention of undesirable effects of DDIs and to efforts to optimize therapeutic outcomes. This dissertation is dedicated to identification of clinically important myopathic DDIs and to elucidation of their underlying mechanisms. Using data mined from the published cytochrome P450 (CYP) drug interaction literature, 13,197 drug pairs were predicted to potentially interact by pairing a substrate and an inhibitor of a major CYP isoform in humans. Prescribing data for these drug pairs and their associations with myopathy were then examined in a large electronic medical record database. The analyses identified fifteen drug pairs as DDIs significantly associated with an increased risk of myopathy. These significant myopathic DDIs involved clinically important drugs including alprazolam, chloroquine, duloxetine, hydroxychloroquine, loratadine, omeprazole, promethazine, quetiapine, risperidone, ropinirole, trazodone and simvastatin. Data from *in vitro* experiments indicated that the interaction between quetiapine and chloroquine (risk ratio, RR, 2.17, p-value 5.29E-05) may result from the inhibitory effects of quetiapine on chloroquine metabolism by cytochrome P450s (CYPs). The *in vitro* data also suggested that the interaction between

simvastatin and loratadine (RR 1.6, p-value 4.75E-07) may result from synergistic toxicity of simvastatin and desloratadine, the major metabolite of loratadine, to muscle cells, and from the inhibitory effect of simvastatin acid, the active metabolite of simvastatin, on the hepatic uptake of desloratadine via OATP1B1/1B3. Our data not only identified unknown myopathic DDIs of clinical consequence, but also shed light on their underlying pharmacokinetic and pharmacodynamic mechanisms. More importantly, our approach exemplified a new strategy for identification and investigation of DDIs, one that combined literature mining using bioinformatic algorithms, ADR detection using a pharmacoepidemiologic design, and mechanistic studies employing in vitro experimental models.

David A. Flockhart, M.D., Ph.D., Chair

Table of Contents

List of Tables	xii
List of Figures	xiv
<i>Chapter 1. Introduction to clinical drug-drug interactions (DDIs)</i>	1
1. Prevalence and significance of drug–drug interactions (DDIs)	1
2. Mechanisms underlying drug interactions	3
3. Approaches to studying drug interactions.....	7
4. Rationale for a translational approach	9
5. Why is myopathy an appropriate outcome of interest?	12
6. Hypothesis and aims	14
<i>Chapter 2. Identification of DDIs associated with myopathy in a large scale</i>	17
1. Introduction.....	17
a. Data sources for large-scale DDI identification.....	17
b. Text mining using the published biomedical literature.....	21
c. Pharmacoepidemiology study designs for identification of DDIs	24
d. Hypothesis and aims	26
2. Methods.....	27
a. Text mining and prediction of potentially interacting drug pairs	27
b. Preparing data for pharmacoepidemiology analyses	28
c. Identification of DDIs associated with myopathy using case-control studies	30
3. Original results.....	32
a. Substrate and inhibitor drugs mined from the published literature.....	32

b.	Demographics and characteristics of the CDM dataset	33
c.	DDIs significantly associated with an increased risk of myopathy	34
4.	Discussion	35
	<i>Chapter 3. In vitro assessment of inhibition of Cytochrome P450s</i>	46
i.	Screening for inhibition of CYPs.....	46
1.	Introduction.....	46
a.	CYP450s are the major drug-metabolizing enzymes in humans	46
b.	Inhibition of CYPs is an important mechanism of DDIs	47
c.	<i>In vitro</i> systems for mechanistic studies of DDIs	49
d.	Approaches to evaluating enzyme kinetics.....	52
e.	Bioanalytical methods for studying DDIs.....	53
f.	Quantitative assessment of the risk of clinical drug interactions.....	54
g.	Hypothesis and aims	57
2.	Methods.....	57
a.	Materials	57
b.	Screening for inhibition of the major CYPs and determining IC ₅₀ s	58
c.	Determining dissociation constant (K _i) and mode of inhibition.....	59
d.	Assessing the risk of DDI using R values.....	60
3.	Original experimental results	62
a.	IC ₅₀ estimates	62
b.	Mode of inhibition and K _i estimates	63
c.	Predicted risk of clinical DDIs.....	64
4.	Discussion	66

ii. Investigating mechanism involved in the interaction between simvastatin and loratadine.....	95
1. Introduction.....	95
a. Why is the interaction between simvastatin and loratadine of particular interest?	95
b. Pharmacokinetics and biotransformation of simvastatin	96
c. Pharmacokinetics and biotransformation of loratadine	98
d. Mechanisms of DDIs with simvastatin or loratadine.....	99
e. Hypothesis and aims	100
2. Methods.....	101
a. Materials	101
b. Incubation with HLMs.....	101
c. Sample preparation	102
d. Analytical methods using LC/MS/MS.....	102
3. Original experimental results.....	104
a. Inhibition of simvastatin and simvastatin acid metabolism by loratadine and desloratadine	104
1) Inhibition profiles of loratadine and desloratadine for the major CYPs.....	105
2) IC ₅₀ s of loratadine and desloratadine for the depletion of simvastatin and simvastatin acid in HLMs	105
b. Inhibition of loratadine metabolism by simvastatin and simvastatin acid.....	106
1) Inhibition profiles of simvastatin and simvastatin acid for the major CYPs	107

2) IC ₅₀ s of simvastatin and simvastatin acid for desloratadine formation	
in HLM	107
3) Mode of inhibition and K _i estimates	108
4. Discussion	108
<i>Chapter 4. In vitro assessment of inhibition of OATPs</i>	123
1. Introduction	123
a. Role of transporters in drug disposition	123
b. OATPs: characteristics, role in drug disposition and clinical DDIs	125
c. Experimental systems for assessing uptake transporter activity	129
d. Prediction of transporter-mediated DDIs	133
e. Hypothesis and aims	135
2. Methods	136
a. Materials	136
b. Screening for inhibition of E ₂ 17βDG uptake	136
c. Estimating IC ₅₀ s	138
d. Prediction of OATP1B1/1B3-mediated DDIs	138
3. Original experiment results	139
a. Screening for inhibition of E ₂ 17βDG uptake	139
b. IC ₅₀ estimates	140
c. Predicted risk of OATP1B1/1B3-mediated DDIs	141
4. Discussion	141
<i>Chapter 5. In vitro assessment of direct myotoxicity</i>	156
1. Introduction	156

a. Pathogenic mechanisms underlying drug-induced myopathy	156
b. Rat L6 myotubes as a model system to assess myotoxicity.....	160
c. Methods to evaluate pharmacodynamic drug interactions.....	162
d. Hypothesis and aims	166
2. Methods.....	167
a. Materials	167
b. Cell culture and drug treatment.....	167
c. Gene expression of CKM and Myog	168
d. MTS/PMS assay.....	170
e. Screening for the inhibition of L6 myotube viability	171
f. Determining concentration-cell viability relationships.....	171
g. Determining the combined effect of simvastatin and desloratadine	172
3. Original experimental results	173
a. Gene expression of CKM and Myog	173
b. Screening for the inhibition of myotube viability.....	175
c. Concentration- cell viability relationships of tegaserod, desloratadine and simvastatin.....	175
d. The combined effect of simvastatin and desloratadine.....	176
4. Discussion.....	176
<i>Chapter 6. Summary</i>	189
Appendix: Permission to resue Table 4-1	192
References.....	199
Curriculum Vitae	

List of Tables

Table 1-1. The clinical spectrum of drug-induced myopathy.....	16
Table 2-1. The number of substrates and inhibitors of the major CYPs mined from the published literature.....	43
Table 2-2. Categories and frequencies of myopathy diagnoses.....	44
Table 2-3. Drug pairs significantly associated with an increased risk of myopathy	45
Table 3-1. Summary of incubation conditions of CYP fluorometric assays	81
Table 3-2. IC ₅₀ s (95% CI) (μM) for the inhibition of the major CYPs	82
Table 3-3. Mode of inhibition and K _i ± SD (μM).....	90
Table 3-4. Predicted f _{u,inc}	91
Table 3-5. Predicted R values	92
Table 3-6. Predicted AUCRs	94
Table 3-7. Kinetics of simvastatin and simvastatin acid metabolism in HLMs	111
Table 3-8. IC ₅₀ s of loratadine and desloratadine for the major CYPs	115
Table 3-9. IC ₅₀ s of simvastatin and simvastatin acid for the major CYPs	118
Table 3-10. Predicted R values	122
Table 4-1. Summary of characteristics of clinically important OATPs in humans	149
Table 4-2. Inhibition (%) of E ₂ 17βDG uptake at 100 μM.....	151
Table 4-3. IC ₅₀ s for the inhibition of E ₂ 17βDG uptake	153
Table 4-4. Predicted R values	155
Table 5-1. The experimental design to evaluate the combined effect of simvastatin and desloratadine	182

Table 5-2. Myotube death after 5 days of treatment.....185

List of Figures

Figure 3-1. Inhibition-concentration curves grouped by CYP.....	83
Figure 3-2. Examples of abnormal kinetics observed from fluorometric assays.....	86
Figure 3-3. Inhibition-concentration curves grouped by drug.....	87
Figure 3-4. Biotransformation of simvastatin in humans	112
Figure 3-5. Biotransformation of loratadine in humans.....	113
Figure 3-6. Chromatography of simvastatin, simvastatin acid and desloratadine	114
Figure 3-7. Depletion of simvastatin and simvastatin acid in relation to incubation time and HLM concentration	116
Figure 3-8. Inhibition of simvastatin and simvastatin acid metabolism in HLMs by loratadine, desloratadine and ketoconazole	117
Figure 3-9. Kinetics of loratadine metabolism in HLMs.....	119
Figure 3-10. IC ₅₀ curves of the inhibition of desloratadine formation by simvastatin and simvastatin acid in HLMs	120
Figure 3-11. K _i s for the inhibition of desloratadine formation by simvastatin and simvastatin acid in HLMs	121
Figure 4-1. The rate of E ₂ 17βDG uptake in cryopreserved rat hepatocytes	150
Figure 4-2. Inhibition of E ₂ 17βDG uptake in cryopreserved rat hepatocytes at 100 μM.....	152
Figure 4-3. IC ₅₀ curves for the inhibition of E ₂ 17βDG uptake.....	154
Figure 5-1. Gene expression of Myog and CKM	183
Figure 5-2. Cell viability (%) after 5 days of treatment as compared with DMSO	

controls.....	184
Figure 5-3. Concentration-cell viability relationships of tegaserod, desloratadine and simvastatin.....	186
Figure 5-4. Concentration-effect curves of simvastatin and desloratadine in combination.....	187
Figure 5-6. Combination index (CI) – fraction of inhibition (f_a) plot.....	188

Chapter 1. Introduction to clinical drug-drug interactions (DDIs)

1. Prevalence and significance of drug–drug interactions (DDIs)

The term “drug-drug interactions” (DDIs) refers to interactions between two coadministered drugs in which one drug affects the pharmacokinetics or pharmacodynamics of another. The coadministration of two drugs is usually safe with no detectable interaction. Some drugs are coadministered purposefully to improve therapeutic outcomes. Some coadministered drugs can cause significant pharmacokinetic interactions that are not clinically important under usual therapeutic circumstances. Clinically important DDIs are drug interactions that cause failure to achieve the therapeutic effects of either or both drugs, or that result in or exacerbate severe or life-threatening adverse drug reactions (ADRs). This thesis is focused on clinically important DDIs that are associated with ADRs.

ADRs are a leading cause of morbidity and mortality in health care. According to a report of the Institute of Medicine, an estimated 7,000 deaths occur annually due to ADRs [1]. In hospitalized patient populations. It is estimated that 6.7% hospitalized patients experience serious ADRs with a fatality rate of 0.32% each year [2]. This means that more than 2,216,000 serious ADR events occur, which cause 106,000 deaths annually. ADRs are also a huge financial burden on health care. Drug-related morbidity and mortality is estimated to cost \$30.1 to \$136.8 billion in the ambulatory setting in the US each year [3].

DDIs are a significant contributor to preventable ADRs. Leape *et al.* estimated that DDIs represent 3–5% of all in-hospital medication errors [4]. In an analysis with an

Italian spontaneous reporting database, it was estimated that 22% of patients exposed to potential DDIs experienced associated ADRs [5]. In addition, Becker *et al.* found that DDIs were responsible for approximately 0.054% of emergency department visits, 0.57% of hospital admissions and 0.12% of re-hospitalizations [6]. In 2010, there were 129.8 million emergency department visits, 100.7 million outpatient department visits and 35.1 million inpatient department discharges in the US [7], suggesting a substantial number of hospital visits due to DDIs. It is not surprising that DDIs also contribute to increased cost and duration of hospital stays [8].

The risk of DDIs increases linearly with age and the number of prescribed drugs [9]. In a database involving 471,732 individuals, one-third of the population were found to be exposed to polypharmacy, and 15% of the population exposed to polypharmacy were exposed to potential drug interactions.

As polypharmacy becomes more common, the prevalence of DDIs is expected to increase. The elderly are particularly susceptible to DDIs, due both to their advanced age and to polypharmacy. Gurwitz *et al.* estimated that more than 40% of the elderly population aged 65 or older use 5 or more medications, and 12% use 10 or more medications [11]. According to Bjerrum *et al.*, among the elderly with polypharmacy, 25% aged 60-79 years and 36% over 80 years were potentially exposed to DDIs [10]. DDIs were responsible for 4.8% of hospital admissions in the elderly population [7]. It is worth noting that, according to Björkman *et al.*, 10% of the potential DDIs could be avoided according to the Swedish interaction classification system [12].

DDIs are also one of the most common reasons for drug withdrawal. When alternative medications are available and warnings in drug labels fail to manage the risk

of DDIs, DDIs associated with severe or life-threatening ADRs may lead to withdrawal of drugs from the market or restriction in drug use [13]. The interaction between the nonsedating antihistamine terfenadine and ketoconazole is associated with a significantly increased risk of *torsade de pointes* and fatal arrhythmia [14]. Because fexofenadine and loratadine are able to meet the same medical needs with better safety profiles, terfenadine was ultimately withdrawn from the market when the warnings in its label failed to adequately reduce the incidence of the fatal interaction. The nonsedating antihistamine astemizole and gastroprokinetic cisapride were withdrawn for similar reasons [15, 16]. The calcium channel blocker mibefradil was withdrawn because its inhibitory effects on drug metabolism caused dangerous interactions with at least 25 other drugs, including common antibiotics, antihistamines, and cancer drugs [17].

2. *Mechanisms underlying drug interactions*

There are a number of mechanisms by which drugs interact. These mechanisms can be divided into three general categories: pharmaceutical, pharmacokinetic and pharmacodynamic. Pharmaceutical drug interactions are those that occur prior to systemic administration and are often due to drug incompatibility [18]. Pharmacokinetic drug interactions are those in which one drug affects the absorption, distribution, metabolism or excretion of another [13]. The drug that causes the interaction is often referred to as the precipitant drug, and the drug whose pharmacokinetics is affected is often referred to as the victim drug. Pharmacodynamic drug interactions are those in which two drugs with overtly similar pharmacological effects produce exaggerated or

diminished effects when used in combination without changes in pharmacokinetics [19, 20].

The mechanisms by which pharmacokinetic interactions occur are relatively well understood. One of the common mechanisms underlying pharmacokinetic DDIs is alteration in drug absorption. The absorption of a drug can be altered due to changes in gastric pH. For example, didanosine requires a neutral-to-basic pH to be absorbed and its formulations are buffered. Medications, such as ketoconazole and itraconazole, are known to require an acidic environment for dissolution. The absorption of these drugs can be significantly decreased when given concomitantly with didanosine [21, 22]. Chelation and adsorption of drugs can also cause changes in absorption. Quinolone antibiotics, when combined with magnesium- and aluminum-containing antacids, can form insoluble complexes that are unable to permeate the intestinal mucosa and be absorbed [23]. Concomitant administration of antibiotics, such as penicillin G and tetracycline, with adsorbents, such as cholestyramine, can result in decreased absorption of antibiotics [24]. Another mechanism involves changes in gastric emptying and intestinal motility. Gastroprokinetic drugs such as cisapride can reduce gastrointestinal transit time and decrease the extent of absorption of drugs which are poorly soluble or absorbed only in a limited area of the intestine [25]. It has been recognized that inhibition or induction of drug-metabolizing enzymes, such as the cytochromes P450s (CYPs) and uridine 5'-diphosphate (UDP)-glucuronosyltransferases (UGTs), expressed in enterocytes of the intestinal epithelia can affect bioavailability and potentially contribute to DDIs [26]. Of similar importance is uptake or efflux drug transporters located on the basolateral membrane of the enterocytes. Inhibition of uptake transporters, such as organic anion

transporting peptides (OATPs), can lead to decreased absorption. On the other hand, inhibition of efflux transporters, such as P-glycoprotein, can enhance bioavailability [27].

There has been a debate on whether alterations in plasma protein binding can cause DDIs by affecting drug distribution. Displacement of a victim drug from its plasma protein binding sites, such as albumin, can lead to an increase in the unbound plasma concentration. However, this increase is usually transient as redistribution and elimination occur immediately after displacement. Thus, DDIs involving plasma protein binding displacement may potentially be clinically significant if the victim drug is highly bound in plasma, has a narrow therapeutic index and a small volume distribution. A transient increase in drug concentrations may be clinically important with drugs such as warfarin and phenytoin; however, for majority of drugs, their mean steady-state unbound drug concentration will remain unchanged. Alteration in plasma protein binding is therefore usually not a significant mechanism of drug interactions [28, 29].

The most common and important mechanism of pharmacokinetic drug interactions is an alteration in drug metabolism. Inhibition of drug metabolism accounts for 76% of case reports involving pharmacokinetic DDIs identified in Vigibase™, an international database for drug safety maintained by the World Health Organization [30]. Most metabolism-based DDIs involve inhibition or induction of CYPs, a class of phase I enzyme that catalyze oxidation, reduction and hydrolysis reactions [31]. Drugs that are inhibitors or inducer of CYPs can significantly change the pharmacokinetics of other drugs, although these interactions may be attenuated by genetic polymorphisms of CYPs [32]. Inhibition of CYPs is the major mechanism that has led to regulatory withdrawal of drugs and label changes. A more detailed discussion on inhibition of CYPs as a

mechanism of DDIs is provided in Chapter 3. Less common is the occurrence of DDIs as a result of inhibition of phase II enzymes that are responsible for conjugation. A few studies have suggested that inhibition of UGTs can contribute to DDIs [33]. Recently, a number of clinically important DDIs have been attributed to inhibition of hepatic uptake transporters, OATPs in particular [34]. These transporters determine the availability of drugs for hepatic metabolism and can lead to significant changes in pharmacokinetics when inhibited. Further discussion on this mechanism of interaction can be found in Chapter 4.

Relatively few DDIs occur due to alterations in renal elimination. The most common renal drug interactions occur at the site of tubular secretion, involving competition for transporters [35]. A number of important drug transporters are expressed in renal proximal tubule cells, including organic cation transporters (OCTs), organic anion transporters (OATs), the multidrug resistance-associated proteins (MRPs), p-glycoprotein, and the multidrug and toxin extrusion proteins (MATEs) [36]. Inhibition of these transporters could cause DDIs by decreasing cellular drug uptake and impairing renal clearance. For example, MATE1 and OCT1 have been shown to be important for the tubular secretion of metformin [37, 38]. The inhibition of MATE1 and OCT1 by cimetidine [39] contributed to its interaction with metformin. Cimetidine was shown to decrease renal metformin clearance by 27% and to increase the AUC (0 to 24 h) and C_{\max} of metformin by 50% and 81%, respectively [40].

In contrast to pharmacokinetic drug interactions, pharmacodynamic interactions are less well studied and understood. Based on the outcome of combining two drugs, pharmacodynamic interactions can be either synergistic or antagonistic.

Pharmacodynamic DDIs can occur at the site of receptors or downstream signaling pathways [18]. The mechanisms underlying pharmacodynamic interactions are often difficult to study. This is in part because of the intrinsic complexity of biological systems that are usually involved in pharmacodynamic interactions. Also, some DDIs are dose-dependent and a DDI may not be recognizable unless an appropriately high dose of one or both drugs is given. In addition, variability in demographics, physiology, underlying disease state and genetic variations can mask the effects of potential DDIs [20]. Recent advances in system pharmacology hold promise for promoting discovery and understanding of pharmacodynamic DDIs.

3. *Approaches to studying drug interactions*

There are three general approaches to discovery and investigation of DDIs, *in vitro*, *in vivo* and *in populo* [41]. *In vitro* pharmacokinetic experiments use cells or cell-derived systems to characterize changes in drug metabolism and transport activity that may underlie DDIs [41]. Commonly used *in vitro* experimental systems include primary, cultured and cryopreserved hepatocytes, human liver microsomes and recombinant CYP and UGT enzymes [13]. *In vitro* methods are used routinely in drug development to evaluate the risk of DDIs for investigational drugs. They are particularly helpful means of uncovering underlying molecular mechanisms of DDIs observed clinically. The information obtained from *in vitro* experiments can be used to develop mathematical models to predict the changes in drug exposure due to DDIs *in vivo*. *In vitro* experiments thus allow investigation of DDIs without the expense and potential risks involved in

conducting human trials. However, data from *in vitro* experiments are often insufficient to assess the clinical significance of a DDI [41].

In vivo studies can involve clinical trials conducted in humans to evaluate the changes in pharmacokinetics, efficacy and the risk of ADRs that result from DDIs. Clinical studies investigating pharmacokinetic DDIs are in general small in size, involving 10 – 100 patients, and usually adopt a randomized or cross-over design [13]. Plasma concentrations are often closely monitored to estimate drug exposure and other important pharmacokinetic parameters. Efficacy and side effects may also be measured. Clinical studies, when appropriately designed and performed, can provide the most convincing evidence for conclusions as to whether one drug interacts with another [41]. Data from these studies serve as the basis for regulatory drug label changes. However, clinical studies are usually not able to provide mechanistic insight unless they use a probe substrate or an inhibitor that is specific to a target enzyme or a transporter. Also, clinical studies are often expensive and time-consuming to conduct. More importantly, it may not be ethically defensible to conduct a clinical trial and investigate the effect of a DDI on the risk of ADRs.

Finally, *in populo* studies are pharmacoepidemiology studies investigating the effects of DDIs on efficacy and ADRs in a large population [42]. It is rare to perform a large-scale prospective observational study to investigate a drug interaction. Most pharmacoepidemiology studies on DDIs are retrospective, taking advantage of existing data from past clinical trials and medical databases such as spontaneous reporting systems and electronic medical record (EMR) databases [43]. Pharmacoepidemiology studies are an important tool used to discover unknown DDIs, especially those leading to

significant clinical changes such as in therapeutic efficacy or in ADR risk. They are particularly useful in detecting and quantifying rare ADRs resulting from DDIs. Compared to prospective clinical trials, pharmacoepidemiology studies have the advantages of larger sample size, longer observation periods, a paucity of potential ethical issues, and are less expensive, less time consuming, and possess greater ability to provide more generalizable results [42]. However, pharmacoepidemiology studies are themselves often subject to the limitations inherent in the use of existing data. A biased result may be obtained when confounding factors such as demographics, comedications, comorbidities and disease states are not appropriately accounted for [42].

4. Rationale for a translational approach

The goal of research on DDIs is to identify them, understand them, treat them when possible and ultimately prevent them. Traditionally, research on DDIs adopts a bottom-up strategy that heavily relies on knowledge about individual drugs or proteins of relevance. Such knowledge may relate to how a drug is metabolized or transported, which drug-metabolizing enzymes or drug transporters can be inhibited or induced by a particular drug, or which common comedications are also substrates or inhibitors of the affected enzymes or transporters. This knowledge provides a scientific basis for predicting the changes in pharmacokinetics due to a potential DDI in humans. Clinical studies are then conducted to examine the clinical significance of DDIs that potentially occur. This strategy is well established and has been incorporated as a routine in drug development to evaluate the risk of DDIs of investigational drugs. The FDA requires *in vitro* characterization of drug metabolism and inhibition of the major CYPs and important

drug transporters for any investigational drug [13]. If a potential risk is predicted based on *in vitro* data, a clinical study is required to assess the potential of clinical DDIs with common comedications and probe substrates or inhibitors of the relevant proteins [13].

This knowledge-based bottom-up approach has well-defined targets. It is applied to a particular pair of drugs involving specific pathways, and looks for changes in particular effects. Although highly specific, this approach is inefficient for identification of unknown DDIs. Only a very small number of targets can be studied at a time [41]. As a result, many DDIs remain undetected for a fairly long time until they are suspected once we know enough about the metabolism or transport of the involved drugs. This approach is particularly inefficient for identification of DDIs that are clinically important as most DDIs predicted from *in vitro* data turn out to have no effect clinically.

As polypharmacy becomes more common and DDIs occur more frequently, research on DDIs must adapt to a high-throughput mode to discover and investigate unknown DDIs in a more efficient manner and with a stronger clinical orientation. This change can be achieved by taking advantage of the voluminous body of existing knowledge stored in the published literature and in large databases, identifying unknown DDIs that are actually of clinical consequence, and interpreting them mechanistically. We call this a ‘top-down’ approach.

Identification of unknown, yet clinically important DDIs involves testing the clinical significance of possibly interacting drug combinations. This is a challenging task when the number of potential DDIs to be studied is prohibitively large. There are 1492 small-molecule drugs approved by the FDA, and 1,112,286 two-drug combinations that could possibly interact. The clinical significance of any specific DDI can, in theory, be

tested with either clinical trials or pharmacoepidemiology studies; however, with such a large number of potential DDIs, clinical trials are obviously not a feasible option to identify clinically important DDIs. Pharmacoepidemiology studies provide a cost-effective and efficient alternative. Performing pharmacoepidemiology studies requires defining an outcome of interest at first. With the aim of identifying clinically important DDIs in mind, we need to begin with an outcome of interest that is clinically important. An outcome of interest also needs to be identifiable from a data source, phenotypically well-defined, and not extremely rare. Myopathy is an outcome that meets all these criteria and we have thus selected this phenotypic outcome as our outcome of interest. The selection of myopathy as the outcome of interest is discussed in detail later.

Even for pharmacoepidemiology studies with relatively frequent outcomes, evaluating such a huge number of potential DDIs is challenging, because the statistical power to detect DDIs decreases with the number of simultaneous tests, given a fixed sample size available from a database. It is therefore important to limit our ambition and reduce the search space to a subset of drug combinations instead of all of them. The question then becomes which subset of possible drug combinations to select for study. A reasonable choice is the subgroup of DDIs that we understand better and potentially have more confidence in providing mechanistic explanations. Inhibition of CYPs is the most important mechanism of pharmacokinetic DDIs [13]. It is also the DDI mechanism currently best understood. We have therefore limited our initial screening to DDIs that may result from inhibition of CYPs.

A small number of published studies have taken an approach similar to ours. Percha *et al.* used a network of interrelationships between drugs and enzymes mined from

the published literature to provide mechanistic explanations for known DDIs and to infer new DDIs [44]. Their work, however, did not distinguish data from *in vitro*, *in vivo* or *in populo* studies. Also, they did not examine whether the predicted DDIs were clinically relevant. The work by Tatonetti *et al.* represents a progress as they not only predicted DDIs but also examined the association of predicted DDIs with clinical phenotypes using data from an EMR database [45]. A limitation of their work is the lack of mechanistic investigation.

The simple presence of a pharmacoepidemiologic DDI does not allow one to infer its mechanism. Without knowing by what mechanisms an apparent DDI can occur, one cannot conclude with certainty that it is truly an interaction rather than a false positive due to methodological flaws. It is similarly difficult to provide a reasonable alternative with better therapeutic outcome and without drug interaction. As we predict DDIs from inhibition of CYPs, this is naturally the most likely mechanism of DDIs that are identified to be clinically important, but we also attempt to explore other possible mechanisms by which DDIs can occur as DDIs can be multifactorial.

5. *Why is myopathy an appropriate outcome of interest?*

There are a number of reasons for selecting myopathy as our outcome of interest. First, myopathy is a clinically important outcome. Drug-induced myopathy is among the most common causes of muscle disease [46]. The clinical presentation of drug-induced myopathy ranges from asymptomatic muscle enzyme elevation to chronic myopathy with severe weakness, and to massive rhabdomyolysis with acute renal failure. A summary of clinical presentations of drug-induced myopathy is displayed in Table 1-1 [47]. Muscular

weakness, myalgia and myositis are the most common clinical presentations of drug-induced myopathy [46]. In the SIDER 2 database [48], a database of drug side effects mined from the FDA's drug labels, there are 124 FDA-approved drugs associated with muscular weakness, 395 associated with myalgia and 51 associated with myositis. These muscle-related side effects can cause noncompliance or discontinuation of drug treatment and potentially compromise therapeutic outcome. The most severe form of myopathy, rhabdomyolysis, is a rare but life-threatening condition. There are over 150 drugs of various classes that have been associated with rhabdomyolysis, including statins, antimalarials, antihistamines, antidepressants and antipsychotics [49-51].

Second, myopathy can result from or be exacerbated by DDIs. One well recognized example is the interaction between cerivastatin and gemfibrozil. In a population-based cohort study, the risk of rhabdomyolysis associated with cerivastatin monotherapy was 10-fold higher than that with the use of other statins. The interaction of cerivastatin with gemfibrozil increased the risk of rhabdomyolysis 50-fold [52]. This interaction led to the withdrawal of cerivastatin from the market. Considering the number of drugs that can induce myopathy, it is reasonable to speculate that there potentially exists a large number of drug interactions associated with increased risk of myopathy.

Third, myopathy is an outcome that is relatively phenotypically well-defined and readily detectable in EMR databases. Although myopathy has a broad spectrum of clinical presentations as shown in Table 1-1, each condition is relatively well-defined. Patients with myopathy can be identified from EMR databases using diagnostic codes.

Lastly, myopathy is a relatively common ADR that enables detection of DDIs with sufficient statistical power. Given a fixed number of simultaneous tests, the

statistical power to detect DDIs increases with the sample size available from a database. If a rare outcome, such as rhabdomyolysis, were selected for pharmacoepidemiologic study, it is very likely that only a small number of patients with rhabdomyolysis would be identified from available databases. Analyses therefore would likely be under-powered to detect DDIs associated with this outcome.

6. Hypothesis and aims

The overall hypothesis of this thesis is that the combination of data mining and *in vitro* mechanistic studies can identify and shed mechanistic light on new DDIs that are associated with an increased risk of clinical myopathy. To test this hypothesis, DDIs associated with increased risk of myopathy will first be identified. The likelihood that such drug interactions are caused by changes in the activities of drug-metabolizing enzymes and/or drug transporters, or direct myotoxicity will then be assessed *in vitro*. Due to the limitations of current experimental techniques for studying drug transporters, only the drug transporters of most interest, namely, organic anion transporting polypeptide 1B1 and 1B3 (OATP1B1/1B3), will be studied. The mechanisms of drug interactions that are particularly important will be further investigated. To test this hypothesis, the following specific aims are pursued:

Aim 1: Predict and identify DDIs associated with increased risk of myopathy by mining the published literature and EMR databases.

Aim 2: Evaluate *in vitro* the likelihood that DDIs identified in Aim 1 are caused by inhibition of the major CYP isoforms.

Aim 3: Evaluate *in vitro* the likelihood that DDIs identified in Aim 1 are caused by inhibition of hepatic uptake transporters OATP1B1/1B3.

Aim 4: Evaluate *in vitro* the likelihood that DDIs identified in Aim 1 are caused by direct myotoxicity using rat L6 myotubes.

Table 1-1. The clinical spectrum of drug-induced myopathy [47]

Condition	Definition
Myopathy	General term to describe all skeletal muscle-related adverse effects
Asymptomatic CK elevation	CK elevation without muscle symptoms
Myalgia	Muscle pain or weakness without CK elevation
Myositis	Muscle symptoms with CK elevation typically < 10 x ULN
Rhabdomyolysis	Muscle symptoms with CK elevation typically > 10 x ULN, and with creatinine elevation (usually with brown urine and urinary myoglobin)

Note: CK, creatine kinase; ULN, upper limit of normal.

Chapter 2. Identification of DDIs associated with myopathy in a large scale

1. Introduction

a. Data sources for large-scale DDI identification

Historically, clinical DDIs were identified through review of case reports and case series in which severe adverse events occur during the coadministration of drugs. In recent decades, there has been a rapid growth in both volume and complexity of data that have developed into large databases. Traditional pharmacovigilance applies high-throughput signal detection algorithms to these databases in order to detect drug-event associations and more complex drug safety phenomena such as DDIs [53].

The primary data source for pharmacovigilance has been spontaneous reporting systems [53]. Spontaneous reporting systems are passive systems largely maintained by regulatory and health agencies collecting reports of suspected ADRs from health-care professionals, consumers, and pharmaceutical companies. The two most well-known of these are the FDA Adverse Event Reporting System (FAERS) [54] and the VigiBase™ system [55] maintained by the World Health Organization. Spontaneous reporting systems largely rely on voluntary reporting, except for pharmaceutical companies, which are required to report suspected ADRs [54]. The information provided by spontaneous reporting systems include the drug suspected to cause the ADE, concomitant drugs, indications, suspected events, and limited demographics [53]. Data within spontaneous reporting systems are often used for detecting drug-event signals for follow-up analysis via formal pharmacoepidemiologic studies and to discover complex relationships, such as DDIs, that are difficult to identify manually. Spontaneous reporting systems have

advantages of centralized data collection and processing, large sample size and public accessibility. The limitations of spontaneous reporting systems include 1) over-reporting of ADRs known to result from a drug and underreporting of those otherwise; 2) the fact that only patients who experience ADRs are reported; 3) the fact that they often lack enough detail to evaluate the causality between a drug or a drug combination and an ADR; 4) duplication of reporting; and 5) missing or incomplete data [56, 57].

Another data source that has been increasingly used for pharmacovigilance is electronic medical records (EMRs) [53]. EMRs contain a vast repository of disease and treatment data that could be mined for identification of DDIs. Compared to spontaneous reporting systems, the data within EMRs are chronological – they contain a more complete record of medical history, treatments, conditions and diagnoses of a patient. EMRs thus have more power to examine temporal relationships between drug administrations and ADRs [53]. EMRs also contain data from broader populations than spontaneous reporting systems can, as they are not restricted to patients who experience ADRs only [58]. However, EMRs are designed primarily for clinical care instead of research, so re-use of clinical EMR data for identification of DDIs can be challenging [53]. EMR data suffer from the common problems of observational data, including missing data and incorrect data [53]. ADRs may not be recorded as diagnostic or lab test codes, and may require further informatics processing before analysis [53]. Also, EMR data contain vast quantities of unstructured clinical narratives that are often the primary and richest source of patient information but are difficult to analyze using automated methods. In addition, EMR data are largely proprietary and involve legal and privacy issues concerning access to patient data [58-60].

In addition to spontaneous reporting systems and EMRs, a few other information sources have been used for detection and prediction of DDIs. These information sources are mined with methods integrating statistics, computer science, medicine, epidemiology, chemoinformatics and biology. It has been shown to be a powerful approach to uncover hidden relationships between coadministration of drugs and potential clinical consequences.

One such data source is the published literature on biomedical science. PubMed is the most widely used online literature search service. It contains over 20 million articles and continues to add 40,000 new abstracts each month [61]. The published literature contains not only DDIs observed clinically, but also the potential underlying mechanisms investigated in experiments. Extracting and summarizing data from the voluminous body of biomedical literature using automated algorithms has been shown to be a promising approach to identification and prediction of DDIs. One recent example is the work by Percha *et al.*, who text-mined the published literature for the interrelationship between drugs and proteins such as metabolic enzymes and drug transporters. The resulting network provided possible mechanistic explanations for drug pairs that interact, and enabled prediction of DDIs from known interacting drug pairs sharing similar mechanisms of interaction [44]. In addition, text mining of the biomedical literature has the potential to identify large numbers of DDIs in a cost-effective manner.

Data sources relating to drug information have been increasingly used to study and predict DDIs. DrugBank is a bioinformatics and cheminformatics database that contains not only detailed chemical, pharmacological and pharmaceutical data of drugs, but also information relating to sequence, structure and pathway of drug targets. The

drugs in DrugBank include not only FDA-approved small molecule and protein drugs, but also experimental ones [62]. The KEGG DRUG is a similar database for all the approved drugs in the US, Europe and Japan, and contains information on molecular structure, target, metabolizing enzymes, transporters, known DDIs, and other molecular interaction network information [63]. The World of Molecular Bioactivity (WOMBAT) is a database containing protein-ligand binding data mined from papers published in medicinal chemistry journals between 1975 and 2012 [64]. ChEMBL and BindingDB are similar databases that are publicly available. Assuming that ADRs are predictable from the interaction of drugs with molecular actors, these databases have been used to bridge the gap between molecular mechanism and clinically observed ADRs resulting from drugs or drug combinations. There are a number of examples using information in these databases and ADRs discovered in the post-market phase to develop better models predicting ADR profile of drugs [65-67]. The data from DrugBank and KEGG DRUG can potentially be used to construct gold-standard sets of known DDIs for development of new DDI detection methods. These databases may not only provide a basis for better understanding of mechanisms underlying DDIs, but also enable prediction of DDIs and the resulting clinical consequences.

Another useful source of data is drug labels which contain valuable information about ADRs and known drug interactions. The full text of drug labels for all the drugs, including both prescribed and over-the counter drugs, available in the US are provided on the National Library of Medicine DailyMed website (<http://dailymed.nlm.nih.gov/dailymed/about.cfm>). A similar resource for the drugs available in Japan can be obtained from the Japan Pharmaceutical Information Center

(JAPIC). The Side Effect Resource (SIDER) database contains drug-side effect relationships mined from the text of drug package inserts. In a study by Tatonetti *et al.*, data from the SIDER database were used to predict DDIs [45]. PharmGKB is a database that provides curated knowledge about the impact of genetic variations on drug response, which can be potentially useful to study DDIs with respect to pharmacogenetics. Also available from PharmGKB are OFFSIDES and TWOSIDES which are databases of drug effects derived from adverse event reports and of DDI side effects, respectively [45].

Last but not least, social networks and online forums can also contribute to the discovery of DDIs. Health-related social networks such as Ask a Patient (<http://www.askapatient.com/>), DailyStrength (<http://www.dailystrength.org/>) and Yahoo Health (<http://health.yahoo.net/>) provide patients a platform for discussing and sharing experience with medications. Mining those websites is a promising approach to obtaining information on DDIs experienced by patients. Although extracting useful information from posts on these websites can be very challenging, they have been shown to provide supplementary information on side effects and therapeutic effects of drugs [68]. By examining the posts related to the use of aromatase inhibitors (AI) on 12 message boards between 2002 and 2010, Mao *et al.* identified common side effects experienced by breast cancer patients taking AIs in relation to drug switching and discontinuation [69].

b. Text mining using the published biomedical literature

Text mining in the biomedical literature has been increasingly recognized as a powerful approach that can not only transform the archives of science into rapidly accessible searchable data, but also promote the discovery of new knowledge and

development of science [70, 71]. It has grown in the last few years to be one of the major bioinformatics tools [72]. In general, text mining refers to “the process of extracting interesting and nontrivial information and knowledge from unstructured text” [73]. It lies at the interface of several computer science disciplines including but not limited to artificial intelligence, pattern recognition, neural networks, natural language processing, information retrieval and machine learning [73].

There are three commonly used approaches to text mining in the biomedical literature [70]. One is co-occurrence-based methods that search for concepts occurring in the same sentence or abstract and posit a relationship between them [70]. This approach has been used to build many early biomedical text mining systems but is used less frequently today because it is error prone [70]. Two more commonly used and more sophisticated approaches are the rule- or knowledge- based approaches, and statistical- or machine-learning-based approaches [70]. A rule-based system uses certain rules as criteria for information extraction. The complexity of a rule-based text mining system depends on what rules are applied. Rules can be simply certain linguistic patterns that are used to find explicit statements of interest [74]. For example, the pattern “<gene> is <associated> with <disease>” can be used as the rule to find the statements about the association between a single gene and a disease. In more complicated cases, rules can be what relationships exist between sets of subjects, or what variant forms of a gene or a protein are mentioned [74]. Sophisticated linguistic and semantic analyses may be needed in such cases to recognize a variety of possible ways of making statements of interest [74]. In contrast, a statistical- or machine-learning-based approach uses a set of training data to build classifiers that serve as the basis for subsequent classification of full

sentences or documents to be analysed [74]. Rule-based text mining systems in general, although not always, are time-consuming to develop, whereas machine-learning-based systems may require a large amount of training data that is not always available [70]. As a result of their respective deficiencies, these two approaches are often used together to complement each other. Many text mining systems employ initial processing based on machine learning to classify whether or not a document is relevant, followed by rule-based post-processing to extract information from the documents [70].

Before performing text mining, a corpus needs to be constructed. A corpus is “a collection of text or speech material that has been brought together according to a set of predetermined criteria” as defined by Ali Farghaly [75]. An example of a pharmacokinetic corpus is the work by Wu *et al.* [76]. As summarized by Rzhetsk *et al.* [71], text mining pipelines in general contain the following major stages. (1) Information retrieval (IR). IR is the process that finds relevant information in an unstructured text source. It largely relies on PubMed that provides a searchable engine and automated methods for abstract download. 2) Named-entity recognition. Once the documents containing the information of interest are retrieved, an automated method is applied to scan each sentence and to identify the language entities of interest. The target entities are often predefined in a dictionary containing their synonyms and homonyms, so that an individual entity can be identified even though it may be referred to by several different names and acronyms. 3) Information extraction (IE). IE is a process that links the identified targeted entities using certain action words and assembles them into simple phrases that capture their relationship. For example, one may extract the sentences with the structure “gene is associated with disease”, where “gene” and “disease” are the target

entities and “associate” is the action word capturing their relationship. 4) Synthesis and use of the extracted information. There are a variety of ways to use the extract information depending on the goal of text mining [71]. Examples include answering a question about the relationship between two objects, collecting published experimental evidence supporting a set of conclusions, or examining the consistency of a statement in the literature. Extracted information can be used to construct a map or a network, a global description of the interrelationships between different categories of objects. One such example is the work by Coulet *et al.*, who mined 17 million MEDLINE abstracts and built a network of 40,000 relationships between genes, drugs and phenotypes [77]. Another example is the work by Wang *et al.*, who mined the published literature for numeric pharmacokinetic data of drugs [78].

c. Pharmacoepidemiology study designs for identification of DDIs

Cohort and case-control studies are the two major study designs used to examine the association between an ADR and a drug exposure in pharmacoepidemiologic research [42].

A cohort means “a group of people who share similar characteristics or experience within a defined period” [79]. A cohort study is a study that “identifies subsets of a defined population and follow them over time, looking for differences in their outcome”, as defined by Strom *et al.* [42]. Cohort studies can be either prospective or retrospective. The output measure of cohort studies is relative risk, which is the ratio of the incidence rate of an outcome in the exposed group to the incidence rate of the outcome in the unexposed group [42]. A relative risk of greater than, equal to and less

than 1 indicates the risk of the outcome in the exposed group is greater than, equal to and less than that of the unexposed group, respectively. An adjusted risk ratio can be calculated using regression to account for the effect of confounders [80]. Cohort studies are particularly useful when one is interested in studying multiple possible outcomes at a time from a single exposure, especially a relatively uncommon exposure [42]. One major advantage of cohort studies as compared to case-control studies is not having to select a control group [42]. However, retrospective cohort studies often suffer from problems associated with retrospectively collected data [42]. Prospective cohort studies can be time-consuming and expensive to perform as they require following a large cohort of subjects over time. For an event occurs at a low rate, the size of a cohort can be prohibitively large [42, 80].

In contrast, case-control studies are studies looking for differences in antecedent exposures between a group of cases with an event to a group of randomly selected control subjects without the event [42, 80]. The underlying assumption behind case-control studies is that cases and controls are selected from the same source population [80]. The exposure distribution in the source population is estimated from controls. For this reason, selection of controls is vitally important when performing a case-control study, as inappropriate controls can bring bias [42]. At the end of study, an odds ratio is calculated, which is a close estimate of relative risk when the disease under study is relatively rare [42]. Case-control studies are particularly useful when one is interested in multiple drug exposures as causes of an ADR [42]. They are also particularly useful when one is studying a relatively rare ADR, as the required sample size is markedly smaller than needed for a cohort study [42]. Because case-control studies are generally retrospective,

they are subject to limitations in the validity of retrospectively collected exposure information [42, 80].

A variation of the case-control study is the nested case-control study. In a nested case-control study, a group of individuals are followed over time, only a sample of controls are selected for each case matching on the risk factors [81]. The resulting odds ratio from a nested case-control study, when proper sampling is used, closely approximates the relative risk obtained from a classic cohort study [81]. One of the advantages of nested case-control studies is that they have better control on the confounding factors through matching than cohort and classical case-control studies, while avoiding complicated statistical analysis such as propensity score [81].

d. Hypothesis and aims

In this chapter, I hypothesize that data mining in the published literature and EMR databases can be used to predict and identify DDIs associated with increased risk of myopathy. To test this hypothesis, the following aims are pursued:

- 1) Use text mining to identify substrate and inhibitor drugs of the major CYP isoforms and to predict drug pairs that potentially interact via inhibition of CYPs;
- 2) Use an electronic medical record (EMR) database to identify predicted interacting drug pairs that are associated with increased risk of myopathy.

2. Methods

a. Text mining and prediction of potentially interacting drug pairs

Text mining was performed to identify the substrate and inhibitor drugs of the major drug-metabolizing CYP isoforms, including CYP1A2, CYP2A6, CYP2B6, CYP2C8, CYP2C9, CYP2C19, CYP2D6, CYP2E1 and CYP3A4/5. Using the data in DrugBank, our group constructed a list of non-redundant generic names of 1492 small molecule drugs approved by the FDA. A rule-based approach was used for information retrieval. A template comprising key terms was constructed to retrieve PubMed abstracts meeting the following criteria: 1) involving *in vitro* studies characterizing drug metabolism, inhibition or induction of the major CYPs, or mechanisms underlying a CYP-based DDI; 2) involving the typical *in vitro* experimental systems for such studies, including recombinant CYP enzymes, human liver microsomes (HLMs) and human hepatocytes; 3) involving any of the drugs on our drug list; and 4) involving any of the probe substrates and specific inhibitors of the major CYPs defined by the FDA [13].

A filter based on natural language processing was then applied to examine the linguistic expression pattern of each sentence in the retrieved abstracts and to identify the sentences with entities of interest. The identified sentences were those describing the relationship of a drug with a major CYP isoform or with another drug. Examples include ‘drug D is (not) metabolized/a substrate of CYP isoform E’, ‘drug D (not) inhibit CYP isoform E’, ‘drug D is (not) an inducer of CYP isoform E’, ‘there is (not) interaction between drug A and B’.

For information extraction, two students in our laboratory independently and manually curated all the extracted sentences in the context of the relevant abstracts to

make a call on the role of a drug to a CYP isoform, i.e. a substrate, an inhibitor or an inducer. There were a number of cases where the two curators could not agree. I then curated all the abstracts that were not agreed by them, and also a random subset (20%) of the abstracts for which they reached an agreement.

The information extracted was summarized as lists of substrates, inhibitors, and inducers of each of the major CYP isoforms. Assuming that a substrate and an inhibitor of a particular CYP isoform have a metabolic interaction, potentially interacting drug pairs were predicted by pairing a substrate and an inhibitor of a CYP isoform. Since the primary interest was in DDIs associated with increased risk of myopathy, which are more likely to result from increased systemic exposure, DDIs that potentially result from induction of CYP enzymes were not considered.

b. Preparing data for pharmacoepidemiology analyses

A subset of data from the Indiana Network for Patient Care (INPC) Common Data Model (CDM) was used for the subsequent analysis. The INPC is a health information exchange data repository containing electronic medical records on over 11 million patients throughout the state of Indiana. Derived from the INPC, the CDM contains coded prescribed medications, diagnosis, and observation data of 2.2 million patients between 2004 and 2009. The CDM also contains over 60 million drug dispensing events, 140 million patient diagnoses, and 360 million clinical observations such as laboratory values. A subset of the CDM data involving 817, 059 patients whose prescribed medication data were available were used for analysis. These data have been

anonymized and constructed specifically for research on adverse drug reactions through collaboration with the Observational Medical Outcomes Partnership project.

Before performing the analyses, the drugs on our list were first mapped to those in the dataset. In the CDM, a prescribed medication is coded as a “Concept” identified by its “Concept ID” and described in detail in its “Concept Name”. The concept name of a medication typically describes the generic name(s) of the drug ingredient(s), the dosage(s), the route of administration, the formulation, and the trade name. An example of the concept name of a combination medication is “Atropine 0.025 MG / difenoxin 1 MG Oral Tablet [Motofen]”. The data set has in total 54,490 unique medication concepts. The drugs on our list were mapped to the medication concepts in the CDM using lexical expression matching followed by manual review. Our group also examined in the data set which pairs of predicted interacting drugs were coadministered to patients. Coadministration was defined as the prescription windows of two drugs less than 30 days apart. This helped our group to filter out the predicted drug pairs that were not used together in clinical settings.

The diagnoses relevant to myopathy, our health outcome of interest, were then identified in the data set. A diagnosis is coded as a “Condition Concept” in the CDM, also identified by its “Concept ID” and described in detail in its “Concept Name”. Myopathy has a broad spectrum of clinical presentations (Table 1-1), ranging from asymptomatic creatine kinase (CK) elevation without any muscle symptoms to life-threatening rhabdomyolysis. Our group focused on the myopathy diagnoses with muscle symptoms including, but not limited to, myalgia, myositis, muscle weakness, polymyositis and rhabdomyolysis.

c. Identification of DDIs associated with myopathy using case-control studies

For each predicted potentially interacting drug pair, a retrospective case-control study was performed to examine the association between myopathy diagnosis and the concomitant use of the pair of drugs. Only myopathy diagnoses preceded by drug prescriptions were considered because the group attempted to infer the causal relationship between myopathy and drug exposures. In addition, only the association of drug prescriptions with the *first* diagnosis of myopathy in a sequence of myopathy diagnoses was considered, because drug prescribed following the first diagnosis may be used to treat myopathy and may be confounded. All the patients whose medication data were available were included in the study, except those who had their first diagnoses of myopathy within the first six months of the data set. This was because it was assumed that patients who did not have any subsequent diagnosis of myopathy within six months following the first diagnosis were cured, and that those who had the first diagnoses of myopathy within the first six months of the data set may have preexisting myopathy that was not captured in the data set.

The exposure window of a drug was defined as the prescription duration of the drug and 30 days after the prescription supply. It was assumed that the risk of myopathy due to a drug exposure was highest within this window. Cases were considered to include patients who had at least one myopathy diagnosis. For each case, an index time was defined as the time of the first myopathy diagnosis. If an index time was within the exposure window of a drug, then the case was considered to be exposed to the drug. For a given predicted interacting drug pair, the cases of the substrate-only (or the inhibitor-only) group were the cases who were exposed to the substrate only (or the inhibitor only), and

the cases of the combination group were the cases exposed to both the substrate and the inhibitor. Patients who had no myopathy diagnosis were considered to be in a control pool. To select controls for the substrate-only group, an index time was defined as the same as that of a randomly selected case who was exposed to the substrate. The controls for the substrate-only group were considered to include all the patients in the control pool who were exposed only to the substrate at the index time. The controls for the inhibitor-only group and the combination group were defined similarly.

The synergistic effect of the substrate and inhibitor drugs on myopathy was tested using logistic regression. For a given drug, the risk of myopathy was determined by the number of cases divided by the total number of cases and controls. The risk ratio (RR) was calculated as $\text{risk ratio} = \text{risk}_{12} / (\text{risk}_1 + \text{risk}_2)$, where risk_1 , risk_2 and risk_{12} were the risk of myopathy in the subjects of the substrate-only group, the inhibitor-only group and the combination group, respectively. A risk ratio of greater than, equal to and less than unity indicates synergism, additive effect or antagonism, respectively. Of our interest were drug pairs with RRs greater than unity, indicating increased risk of myopathy when combined. Because the risk of myopathy is known to be correlated with age and gender [82], these two factors were incorporated into the model as covariates. The type I error rate was corrected for multiple testing using the Bonferroni method. The p-value threshold was therefore 0.0000136 (0.05/3670). The analyses were performed using SAS (Cary, NC).

3. Original results

a. Substrate and inhibitor drugs mined from the published literature

The sentences of interest extracted from PubMed abstracts were manually reviewed to identify substrates, inhibitors and inducers of the major CYP isoforms, including CYP1A2, CYP2A6, CYP2B6, CYP2C8, CYP2C9, CYP2C19, CYP2D6, CYP2E1 and CYP3A4/5. The first two student curators reached agreement on 78% of the extracted sentences. I made the call for the remaining 22% of the abstracts where the disagreement existed, and verified the 20% of randomly selected subset for which the other two curators agreed upon. This manual curation performed in the information retrieval step ensured a high quality of the literature mining data.

Our data show that among the 1492 drugs approved by the FDA, 232 drugs were either substrates or inhibitors of at least one of the major CYP isoforms. The numbers of substrate inhibitor drugs for each of the major CYP isoforms are presented in Table 2-1. One hundred and forty nine drugs were identified as substrates of any major CYP isoforms, 102 (68%) of which were substrates of CYP3A4/5. This is consistent with the observation that CYP3A alone is responsible for the metabolism of over 50% of the prescription drugs metabolized by the liver [83]. 59 drugs were found to be substrates of multiple CYP isoforms. 123 drugs were identified as inhibitors of any major CYP isoforms, 50 of which were found to inhibit multiple isoforms. The number of inhibitors of CYP3A4/5, CYP2D6, CYP2C9, CYP1A2 and CYP2C19 were comparable.

b. Demographics and characteristics of the CDM dataset

Assuming that a substrate and an inhibitor of a particular CYP isoform had a metabolic interaction, 13,197 pairs of drugs in total were predicted to be potentially interacting via inhibition of the relevant CYP isoforms by pairing a substrate with an inhibitor of a CYP isoform. Because not all these theoretical drug combinations are coadministered clinically, the analyses were limited only to those that are clinically relevant. To identify the drug pairs coadministered clinically, the drugs approved by the FDA were first mapped to the medication concepts in the database. Of these, 1,293 out of 1492 drugs were mapped successfully, while 199 drugs could not be matched. The unmatched drugs were found to be banned drugs, illicit drugs, organic compounds, herbicide/insecticides, functional group derivatives, herbal extracts, DrugBank drugs absent from the CDM, and drug names that only exist in the published literature. By screening for drug pairs whose prescription windows were less than 30 days apart, 3670 out of 13,197 predicted DDIs were identified to be coadministered to the patients in the database.

59,572 out of 828,905 (7.2%) patients had at least one diagnosis of myopathy. The age and gender were missing for 11,846 (1.4%) patients in the population. For the 59,572 patients who were diagnosed with myopathy, the average age was 40.2 ± 23 years, and 489,669 (59.1%) were female. The average number of medications taken by this population was 3.8 ± 2.5 . Race is known to be a risk factor for myopathy, but data identifying patients' race were only available for 11.84% of the total population, and were not included in the subsequent analyses.

Twelve concept IDs relevant to myopathy were identified in our data set (Table 2-2). “Myalgia and myositis” was the most frequent diagnosis, accounting for 78% of the total myopathy diagnoses, followed by “Muscle weakness” (20%). There were in total 53 cases of rhabdomyolysis identified from the date set.

c. DDIs significantly associated with an increased risk of myopathy

Using a case-control study design, the effect of each individual predicted drug pair on myopathy was tested using a synergistic model. This model was used since it is relatively conservative and since it lends itself to providing useful mechanistic insights. The model tested whether the risk of coadministration of both drugs was significantly higher than the additive risk from taking either drug alone. The risk was adjusted for age and gender, two known risk factors for myopathy. Both factors were significantly predictive of the risk of myopathy. Females were found to have a higher risk of myopathy than males with an odds ratio of 1.64 ± 0.0039 . The risk of myopathy increased with age at a rate of $0.15\% \pm 0.0012\%$ per year.

There were 27 drug pairs significantly associated with the risk of myopathy. Many of these drug pairs involved narcotic analgesics such as fentanyl, hydrocodone, oxycodone, and a muscle relaxant tizanidine, which were likely administered to patients with myopathy to relieve muscle symptoms. The significant drug pairs involving these drugs were therefore not considered as myopathic. The remaining 15 pairs of drugs significantly associated with an increased risk of myopathy are shown in Table 2-3.

The identified significant DDIs involved clinically important drugs including alprazolam, chloroquine, duloxetine, hydroxychloroquine, loratadine, omeprazole,

promethazine, quetiapine, risperidone, ropinirole, trazodone and simvastatin. Apart from the interaction between promethazine and tegaserod, all the other interactions involved chloroquine, hydroxychloroquine, or loratadine. Eight significant DDIs involved chloroquine and hydroxychloroquine. They were found to interact with risperidone, quetiapine, loratadine, trazodone and duloxetine. The highest relative risks (RRs) were observed with the interactions of risperidone with chloroquine and hydroxychloroquine (RR = 3.36 and RR = 2.88, respectively). Six significant DDIs involved loratadine. In addition to the interactions with chloroquine and hydroxychloroquine, loratadine was found to also interact with ropinirole, simvastatin, duloxetine, alprazolam, and omeprazole.

4. Discussion

In this chapter, I have addressed the hypothesis that literature mining and large databases can be used to predict and identify DDIs associated with myopathy. Using automated algorithms and rigorous manual review, the published literature was text-mined. There were 232 drugs identified as either substrates or inhibitors of the major CYPs. 13,197 pairs of drugs were predicted to have metabolic interactions via inhibition of CYPs, 3670 of which were found to be coadministered to patients in an EMR database. Using a case-control study design and a synergistic model, fifteen drug pairs were further identified to be significantly associated with an increased risk of myopathy as compared to the additive risk from taking either of the drugs alone.

Only a small number of studies designed to identify and predict DDIs using knowledge mined from the published literature have been published. Percha *et al.* [44]

and Tari *et al.* [84] identified through text mining the interrelationships between drugs and metabolic enzymes from which DDIs were inferred. Our work shared a similar assumption that a DDI can arise when a substrate drug and an inhibitor drug of a CYP enzyme are coadministered. The goal of our text mining work was to predict CYP-based metabolic DDIs for which there is more supporting evidence in the published literature. Consequently, our approach had the following features that distinguished our work from those published previously. First, our approach was strongly mechanism-oriented. We aimed only to mine from the literature the drugs that are substrates or inhibitors of the major CYPs, from which we could predict CYP-based metabolic DDIs. A resulting limitation of our work was that we could not obtain an exhaustive list of potentially interacting drug pairs. Second, we defined substrate and inhibitor of the major CYPs using a set of strict criteria – the drugs that had been investigated in a typical *in vitro* experimental system using probe substrates or specific inhibitors defined by the FDA. We recognize that this likely led to exclusion of some true substrates and inhibitors and consequently a smaller number of predicted drug pairs. Of 1492 small molecule drugs approved by the FDA, only 149 (10%) and 123 (8.2%) drugs were identified as substrates and inhibitors of any major CYP isoform, respectively. However, these identified drugs met the “norm” definition of a substrate or an inhibition of a CYP isoform. Third, the information extraction process was performed manually by three curators, including me, reviewing the extracted relevant sentences. Although less efficient than automated methods, manual curation ensured a high accuracy in identifying substrate and inhibitors of the major CYPs. All these features add our confidence in predicting CYP-based metabolic DDIs. Similar to the work of Percha *et al.* [44] and Tari *et al.* [84], the text

mining performed by our group was limited to PubMed abstracts. As pointed out by Cohen *et al.* [70], extracting information from full text of the published literature remains a challenging task in the field of text mining.

When compared to work published previously, our approach also differs in that we took a step forward from predicting novel metabolic DDIs to identifying those of clinical consequence from predicted DDIs. By testing the association of the predicted DDIs with myopathy diagnoses in an EMR database, fifteen pairs of drugs were found to increase the risk of myopathy when coadministered. This is similar to the approach used by Tatonetti *et al.*, who identified DDIs shared by an entire drug class using a database of side effects and corroborated those DDIs in an EMR database [45].

None of the fifteen DDIs identified by us has been reported before. Eight of these DDIs involved chloroquine and hydroxychloroquine. Both chloroquine and hydroxychloroquine are antimalarial drugs indicated for the suppressive treatment and for acute attacks of malaria. In developed countries such as in the US, they are mainly used to treat rheumatoid arthritis and systemic lupus erythematosus. The labels of both drugs note skeletal muscle myopathy or neuromyopathy as one of the side effects. There are a number of case reports on chloroquine and hydroxychloroquine induced neuropathy, myopathy, and cardiomyopathy [85, 86]. In a prospective cohort study by Casado *et al.*, 119 Spanish rheumatic patients treated with chloroquine or hydroxychloroquine were followed over three years. Of those patients, 22 (18.5%) were found to have persistently elevated serum levels of muscle enzymes. The prevalence of antimalarial induced myopathy was estimated to be 9.2% with an annual incidence of 1.2% during follow-up. The prevalence of antimalarial induced muscle weakness was estimated to be 6.7%. The

authors also pointed out that in rheumatic patients, the initial mild symptoms of muscular injury are often masked by the underlying disease, which may explain why the diagnosis of antimalarial myopathy is usually difficult and often delayed [87]. Their data suggest that the prevalence of myopathy in patients taking antimalarial drugs are higher than that expected previously [86]. Our data show that chloroquine and hydroxychloroquine can interact with a variety of drugs to bring about an even higher risk of myopathy. However, to date, there is no published study investigating drug interactions with chloroquine and hydroxychloroquine with respect to the risk of myopathy. Our data thus call for scientific attention to drug interactions that may lead to exacerbated antimalarial induced myopathy.

Similarly, the risk of myopathy associated with the antihistamine loratadine has largely been unnoted. Loratadine was involved in six of 15 significant DDIs. Myalgia is one of the side effects of both loratadine and its major pharmacologically active metabolite, desloratadine [88, 89]. Desloratadine seems to be more myotoxic than loratadine. In randomized clinical trials, 2.1% of subjects treated with desloratadine experienced myalgia as compared to 1.8% treated with placebo, whereas less than 2% of subjects treated with loratadine experienced myalgia [88, 89]. Our data indicate that loratadine or desloratadine may be more myotoxic than they have been recognized, and they can pose even higher risk of myopathy when coadministered with other drugs.

A review of drug labels revealed that myopathy is also one of the side effects of several other drugs involved in the significant DDIs. Statin-induced myopathy is one of the well-known side effects of statins. The risk of rhabdomyolysis associated with high dose of simvastatin is so well recognized that the FDA issued a black box warning against daily use of the 80 mg dose of simvastatin. Alprazolam is an anxiolytic indicated

for the management of anxiety disorder and panic disorder. Its side effects include muscular cramps and muscle stiffness which can be associated with myopathy. The use of trazodone, an antidepressant, can cause musculoskeletal pains. Back pain, muscle weakness, myalgia, muscle cramps and leg pain have been reported with the use of omeprazole, a proton pump inhibitor. Some other drugs can cause back pain, which may also be associated with myopathy. Those include risperidone and quetiapine, two antipsychotic drugs indicated for the treatment of schizophrenia and bipolar disorder mania, ropinirole, a dopamine agonist used to treat Parkinson's disease and restless legs syndrome, and tegaserod, a serotonin agonist used to treat irritable bowel syndrome and constipation. There are also a number of case reports in which rhabdomyolysis occurred in patients treated with risperidone [90-93] or quetiapine [94-99]. The muscle-related side effects of these drugs indicate that it is possible that interaction with these drugs may cause increased risk of myopathy.

In addition to having a synergistically myopathic interaction, there are other possible explanations for the association of these drugs with increased risk of myopathy. One is that they may be used to treat diseases that co-occur with myopathy and related muscle symptoms. For example, risperidone [100], quetiapine [100, 101], alprazolam [102], tegaserod [103] and duloxetine [104] may be used to manage the symptoms of fibromyalgia. Notably, duloxetine is indicated for the management of chronic musculoskeletal pain, including fibromyalgia. In addition, these drugs can be associated because their common comedications are used to manage myopathy or other diseases co-occur with myopathy. Not being able to establish a causal relationship is one of the inherent limitations of any pharmacoepidemiologic study. This issue can potentially be

addressed by performing carefully designed pharmacoepidemiology study that account for confounding factors such as comedications and comorbidities. However, it can be challenging to perform such studies for a large number of potentially interacting drug pairs.

There are a number of known clinical drug interactions that are associated with an increased risk of myopathy, including the interactions between CYP3A4-metabolized statins (e.g. simvastatin, atorvastatin and lovastatin) and strong inhibitors of CYP3A4 such as ketoconazole, itraconazole, and erythromycin, and the interactions between OATP-transported statins (e.g. cerivastatin, pravastatin and rosuvastatin) and strong inhibitors of OATPs such as gemfibrozil and cyclosporine. However, none of these known myopathic drug interactions were identified in our analyses. One possible explanation is that physicians and pharmacists were aware of such interactions and advised the patients not to take the interacting drugs together.

There are a few limitations of our study due to the use of diagnostic codes to identify myopathy cases. Muscle weakness and muscle pain are relatively subjective feelings that rely on patients' self-report and are subject to psychological factors [105]. There is therefore a potential risk of misidentification of patients who actually experienced myopathy using diagnostic codes. This may be particularly problematic for identification of myopathy cases taking antipsychotic drugs such as risperidone and quetiapine. The plasma level of creatine kinase has been proposed to be used as a biomarker for myopathy [106]. However, according to our primary analysis, data on the plasma level of creatine kinase in the EMR database are not helpful in the identification of patients with myopathy for two reasons: 1) there are only a small number of patients

with such data, indicating that analysis to detect DDIs may be underpowered due to a small sample size; 2) the majority of data are indicative of myocardial infarction instead of myopathy. Another problem with identification of cases and controls is that we only identified patients with symptomatic myopathy and those with asymptomatic creatinine kinase elevation could not be identified. A potential improvement in identification of cases and controls may be achieved by reviewing clinical narratives, but this is technically challenging.

Our analyses using the data existing in an EMR database also suffer from the weaknesses shared by retrospective observational studies in general. First, the data in the CDM dataset are incomplete. Age and gender information was missing for 11,846 (1.4%) patients, and race data were only available for 11.84% of the population. Second, the validity of the data is difficult to verify. For example, coadministration of drugs was identified using prescription codes, which could be unreliable. Third, our analyses are subject to potential population biases introduced by the EMR database.

The synergistic model used to evaluate the combined effect of two drugs has a number of limitations as well. Suppose that there is a background prevalence, B , of myopathy that is independent of the effect of any drug. Then the true relative risk can be calculated as $RR' = (R_{12} - B) / [(R_1 - B) + (R_2 - B)]$, where $(R_{12} - B)$, $(R_1 - B)$ and $(R_2 - B)$ are the risk of myopathy in the combination, substrate and inhibitor group that are due *only* to the drugs. When R_{12} is greater than the sum of R_1 and R_2 as in the case of synergistic interaction, this RR' is greater than the RR we estimated as $RR = R_{12} / (R_1 + R_2)$. In other words, the methods underestimated the relative risk when two drugs under study interact synergistically. B was, however, not estimable in our case because any

patient with a myopathy diagnosis was classified into a treatment group. As a result of underestimated RRs, a number of drug pairs that in fact had small synergistic effects when used in combination were probably misidentified as not having interactions. A potential solution to this issue is to select a group of controls for each case, matching on demographics, comorbidity and comedication distribution and other confounding factors. In addition, for some drug pairs the number of cases in the combination group was small, and that may limit our power to detect significant DDIs.

Additional limitations of this specific pharmacoepidemiologic study include that dose and duration of exposure were not taken into consideration. The risk of myopathy is known to be both dose- and time- dependent for some drugs including statins. Unlike spontaneous reporting systems, data from EMR databases are longitudinal where time-to-event methods are applicable. However, we could not apply such methods to evaluate the effect of duration of exposure because the current methods cannot be directly applied to EMRs for detection of DDIs.

In spite of the limitations discussed above, we demonstrated that it is possible to identify new and clinically important DDIs using data mined from the published literature, followed by screening for DDIs associated with myopathy in an EMR database.

Table 2-1. The number of substrate and inhibitor drugs of the major CYPs mined from the published literature

CYP Pathway	The number of substrates	The number of inhibitors
CYP1A2	30	39
CYP2A6	1	9
CYP2B6	5	15
CYP2C19	5	31
CYP2C8	11	2
CYP2C9	30	39
CYP2D6	34	39
CYP2E1	8	6
CYP3A4/5	102	48
Total	149	123

Table 2-2. Categories and frequencies of myopathy diagnoses

Concept ID	Concept Name	Frequency
84675	Myalgia and myositis	48877
79908	Muscle weakness	12720
80800	Polymyositis	372
446370	Antilipemic and antiarteriosclerotic drugs causing adverse effects in therapeutic use	206
4217978	Myalgia and myositis, unspecified	185
73001	Myositis	53
439142	Myoglobinuria	52
4345578	Rhabdomyolysis	52
4218609	Muscle weakness (generalized)	22
4262118	Other myopathies	7
4147768	Myopathy, unspecified	1
4248141	Rhabdomyolysis	1

Table 2-3. Drug pairs significantly associated with an increased risk of myopathy

Drug 1	Drug 2	Risk Ratio	P-value	Risk₁	Risk₂	Risk₁₂	M₁	N₁	M₂	N₂	M₁₂	N₁₂
Chloroquine	Risperidone	3.36	4.47E-05	0.16	0.04	0.65	689	4417	373	10233	11	17
Hydroxychloroquine	Risperidone	2.88	1.37E-04	0.19	0.04	0.65	684	3634	373	10233	11	17
Loratadine	Chloroquine	2.21	1.27E-05	0.03	0.16	0.42	1528	45104	683	4405	35	84
Promethazine	Tegaserod	2.20	1.28E-05	0.03	0.07	0.21	2325	80012	259	3893	48	228
Chloroquine	Quetiapine	2.17	5.29E-05	0.15	0.08	0.50	676	4394	1055	13813	26	52
Loratadine	Ropinirole	2.05	3.47E-05	0.03	0.12	0.31	1527	45107	713	6121	42	136
Chloroquine	Trazodone	1.99	2.23E-05	0.15	0.09	0.49	674	4391	875	9635	35	72
Loratadine	Hydroxychloroquine	1.95	7.02E-05	0.03	0.19	0.43	1528	45105	678	3622	35	81
Hydroxychloroquine	Trazodone	1.76	2.02E-04	0.19	0.09	0.49	669	3608	875	9635	35	72
Chloroquine	Duloxetine	1.65	1.34E-10	0.14	0.15	0.48	614	4289	3688	25173	138	288
Loratadine	Simvastatin	1.60	4.75E-07	0.03	0.05	0.13	1447	44623	4256	88683	152	1184
Loratadine	Duloxetine	1.56	7.43E-09	0.03	0.15	0.28	1446	44914	3685	25117	181	647
Loratadine	Alprazolam	1.56	1.06E-09	0.03	0.07	0.16	1372	44426	3726	50734	236	1447
Hydroxychloroquine	Duloxetine	1.53	1.46E-08	0.17	0.15	0.49	609	3509	3688	25173	138	282
Loratadine	Omeprazole	1.33	4.45E-07	0.03	0.07	0.13	1322	44207	4617	70800	354	2796

Note: **Risk₁**, **Risk₂** and **Risk₁₂** designate the risk of myopathy in the subjects of the substrate drug group, the inhibitor drug group and the combination group, respectively; **M₁**, **M₂** and **M₁₂** are the number of cases of the substrate drug group, the inhibitor drug group and the combination group, respectively; **N₁**, **N₂** and **N₁₂** are the number of controls of the substrate drug group, the inhibitor drug group and the combination group, respectively.

Chapter 3. *In vitro* assessment of inhibition of Cytochrome P450s

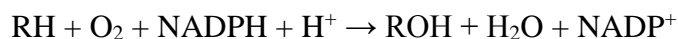
i. Screening for inhibition of CYPs

1. Introduction

a. *CYP450s are the major drug-metabolizing enzymes in humans*

The cytochrome P450 superfamily (CYPs) is a large and diverse group of heme-containing enzymes. The name P450 is derived from the maximum spectral absorbance peak at 450 nm when they are in the reduced and CO-bound form [31]. They catalyze the oxidation, peroxidation and reduction of endogenous metabolic intermediates such as steroids, prostaglandins and fatty acids, as well as xenobiotic substances such as drugs, toxins and environmental pollutants [31]. In humans, CYPs play a central role in phase I drug metabolism. They are responsible for metabolizing the vast majority of therapeutic drugs and thus have been the most studied xenobiotic metabolizing enzymes [83].

The activity of CYPs requires both a reducing agent (nicotinamide adenine dinucleotide phosphate [NADPH]) and molecular oxygen. A typical reaction catalyzed by CYPs is a monooxygenase reaction, in which one molecule of oxygen is reduced per substrate molecule (RH), with one oxygen atom appearing in the product and the other in the form of water [107, 108]:



In contrast to most enzymes in the body, CYPs are promiscuous [83]. A single CYP isoform can metabolize many structurally distinct chemicals, owing to their large and fluid binding pockets. A substrate drug can be metabolized by several CYPs at the same time, although this may occur at different rates. As a result, there is significant

overlapping substrate specificity amongst CYPs. This is one of the underlying reasons for drug interactions as one drug may compete for the binding pocket and reduce the metabolic rate of another drug [83].

There are 55 individual CYPs in 16 families have been identified in humans [108]. The isoforms that are most significant in drug metabolism are members of the CYP1, CYP2 and CYP3 families [109, 110]. Drug-metabolizing CYPs are most abundant in the liver [83]. They are also expressed throughout the gastrointestinal tract, and in lower amounts in lung, kidney, and even in the central nervous system [83]. Intracellularly, these enzymes are located in the lipophilic endoplasmic reticulum membranes [83]. In the liver, CYP1A2, CYP2B6, CYP2C8, CYP2C9, CYP2C19, CYP2D6 and CYP3A4 appear to be the most important forms [109]. Together, they are responsible for the metabolism of about 75% of all marketed drugs [111]. It is worth noting that CYP3A4 is the most abundant isoform in the liver, accounting for about 30% of the total liver CYP content [112]. CYP3A4 alone is responsible for the metabolism of nearly 50% of the prescription drugs metabolized by the liver [111]. CYP3A4 is also the most abundant isoform in the gastrointestinal tract and is subject to DDIs occurring during drug absorption [110].

b. Inhibition of CYPs is an important mechanism of DDIs

The central role of CYPs in drug metabolism render them a particularly important site of DDIs [111]. Clinically observed metabolic DDIs involving CYPs can be due to either induction or inhibition of enzyme activity. Compared to induction-mediated DDIs, inhibition-mediated DDIs are more common and more clinically significant. Amongst the

drugs that have been withdrawn from the market, a significant number have been due to inhibition-mediated interaction with a commonly co-administered drug [113].

Enzyme inhibition can occur via two main biochemical mechanisms, reversible or irreversible. Competitive inhibition and noncompetitive inhibition are the two most commonly observed mechanisms that result in reversible inhibition [107]. When a reversible inhibition occurs, a drug reversibly binds to the affected enzyme(s), either competing for the binding pocket, or allosterically reducing the metabolic capacity. As a result, there is a reduction in the metabolism and an increase in the systemic exposure of another drug, which may lead to an increased in the risk of adverse drug reactions [107]. An example is inhibition of terfenadine metabolism by ketoconazole. Terfenadine is an antihistamine primarily metabolized by CYP3A4. At clinical doses, terfenadine is almost undetectable in plasma due to high first pass metabolism and efficient systemic clearance. However, when co-administered with ketoconazole, an antifungal and a very potent inhibitor of CYP3A4, the plasma concentration of terfenadine dramatically increases to a level that prolongs the electrocardiographic QT interval. The severe inhibition of terfenadine metabolism by ketoconazole led to episodes of torsade de pointes and fatal arrhythmias in many patients [114]. The drug was ultimately withdrawn from clinical use.

Irreversible inhibition, or mechanism-based inhibition, can occur when a drug is metabolized by a CYP to a reactive intermediate which binds to the active site of the enzyme and inactivates it permanently. The body has to restore the pool through *de novo* synthesis of the enzyme which may take weeks. Irreversible inhibition thus has more profound effects on drug metabolism and accounts for some of the most potent clinically observed DDIs [13, 107]. One such example is mibefradil. Mibefradil is a calcium

channel antagonist and a potent metabolism-based inhibitor of CYP3A4/5 with a K_{inact} of 0.4 min^{-1} [115]. It was withdrawn from the market due to unacceptable risk of DDIs with many CYP3A4 substrate drugs, including midazolam and triazolam, whose AUC was increased by 8-fold and 9-fold, respectively, when coadministered with mibefradil [116, 117].

c. *In vitro* systems for mechanistic studies of DDIs

Understanding the underlying mechanism of a DDI enables physicians to prevent and treat them, and allows scientists to predict future DDIs sharing similar mechanisms. Thus elucidation of the mechanism of individual DDIs is key. *In vitro* experimental systems are one approach to characterizing metabolism-based DDIs. Commonly used *in vitro* experimental systems include recombinant CYP enzymes, human liver microsomes (HLMs), and human hepatocytes [118].

Recombinant CYP enzymes are human CYP enzymes heterologously expressed in baculovirus-cultured insect cells or an *E. coli*-based expression system [119]. Because these enzymes are easy and affordable to prepare and in general offer high reproducibility, they have become a routine and reliable resource for characterization of metabolism during drug development [13]. Since there is only a single CYP enzyme present in the system, these enzymes have the advantage of not requiring the use of a highly selective probe substrate [120]. They are particularly useful in studying metabolic routes that exist in low abundance *in vivo*, such as CYP2D6 and CYP2B6 [112]. On the other hand, the kinetics in the presence of a single CYP are less predictive of that *in vivo*, where multiple CYPs may compete and metabolism of a drug may be diverted to alternative routes when

the primary route is blocked [118]. Also, the levels of nonspecific binding, accessory proteins and/or protein-protein interactions are different from those of other systems, further widening the difference in *in vitro* kinetics between recombinant and native systems [118].

HLMs are vesicle-like artifacts that are prepared from human liver tissue. After homogenization and differential centrifugation, the endoplasmic reticulum membranes of hepatocytes reform into vesicles that are enriched with a panel of drug metabolizing enzymes including CYPs, flavinmonooxygenases, carboxylesterases, epoxide hydrolase and UGTs [121]. The level of cytochrome b5 and the relative abundance of proteins are more similar to what is observed *in vivo* as compared to recombinant enzymes [121]. HLMs thus represent a more physiologically relevant system in terms of enzyme composition. They have been routinely used to evaluate the metabolic stability and inhibition of CYPs and UGTs by drugs, and to identify which enzyme or enzymes are responsible for oxidizing or glucuronidating a drug [13, 118]. One of the disadvantages, though, is that they require the use of a highly selective probe substrate for studying a particular enzyme of interest, potentially complicating analytical procedures [118]. Also, certain CYP isoforms may be absent or in low abundance in the liver of a donor due to genetic variations, which can introduce variability in results obtained using HLMs prepared from such a donor [118]. The commonly used HLMs are therefore pooled from HLMs prepared using livers from many donors.

In recent years, human hepatocytes have been increasingly used to characterize drug metabolism and to evaluate DDIs. The most commonly used preparations include isolated primary hepatocytes and cryopreserved hepatocytes [122, 123]. These

preparations are particularly appealing as they are most representative of what occurs *in vivo* – they contain a full range of drug-metabolizing enzymes, including both phase I and phase II, and membrane drug transporters, as well as the intracellular apparatus for gene expression and protein modification [123]. This gives hepatocytes a unique advantage in studying (1) DDIs involving enzymes that are absent or present in low abundance in HLMs, (2) the interplay of drug transport and metabolism, and (3) enzyme induction and transporter regulation in response to drug treatment. However, the use of hepatocytes has been largely limited by availability [123]. In contrast to HLMs or recombinant CYPs, it is difficult to pool sufficiently large quantities of hepatocytes for detailed kinetic analysis [118]. Consequentially, CYP activity in hepatocytes is often measured under non-Michaelis-Menten conditions. In addition, metabolites produced from substrates may be conjugated, further complicating the analysis. Inter-individual variability and variation in preparation procedure also add difficulty to promoting their use [118]. Recent progress in culturing hepatic cell lines in 2D and 3D has shown a promise to overcome some of the limitations and may become a substitute of hepatocytes for *in vitro* studies in the future [124].

Due to the advantages and limitations of the systems discussed above, data generated using any individual system can only provide a piece of knowledge in the picture of drug metabolism. These systems therefore often need to be used together to obtain a more comprehensive understanding on the metabolism of a drug.

d. Approaches to evaluating enzyme kinetics

Biochemical reactions involving a single substrate are often assumed to follow Michaelis–Menten kinetics, as are most CYP-mediated drug metabolism reactions [125]. Determination of the kinetic parameters, K_m , V_{max} , and CL_{int} , for CYP catalyzed reactions is important to the characterization of drug metabolism. These parameters not only enable scientists to predict the clearance of a drug in humans, but also provide insights into non-linear pharmacokinetic behaviors and mechanisms of DDIs. There are two approaches to measuring Michaelis-Menten kinetics of a CYP reaction *in vitro*, namely, metabolite formation and substrate depletion.

Conventionally, evaluation of K_m and V_{max} involves the incubation of a substrate with a single recombinant CYP enzyme or HLM preparation. The rate of metabolites formation then is measured under the conditions where the initial reaction velocity is linear. In cases where a drug has multiple metabolites, this approach requires identification and analytical method development for quantifying each of the individual metabolites [118]. This approach thus may not be feasible in some cases.

Using the substrate depletion approach, incubations are conducted in the same way as using the conventional approach. Instead of following the rate of metabolite formation, the reaction velocity is measured by the rate of substrate disappearance from the incubation mixture. Consequently, K_m and V_{max} describe the overall metabolism of the substrate instead of formation of individual metabolites. When a predominant metabolite is formed, the kinetics estimates using the substrate depletion approach have been shown to be close to those obtained using the conventional approach [126]. The substrate depletion approach has several limitations as it requires consumption of a

substantial fraction of substrate to estimate the kinetics accurately. One is that it may violate the fundamental assumptions required for Michaelis-Menten kinetics. Also, it may not be applicable to drugs that have low intrinsic clearance. Furthermore, it may require a high enzyme concentration which could increase nonspecific binding and the experimental errors incurred in evaluation of kinetic parameters [126, 127].

e. Bioanalytical methods for studying DDIs

Advances in bioanalytical techniques used to study DDI have largely been made due to the need for screening of drug candidates with favorable metabolic and safety profiles in the early stages of drug development [128]. The traditional approach to *in vitro* DDI studies involves incubation of known probe substrates with CYP enzymes and measurement of change in the rate of metabolism in the presence of test compounds [13]. For example, inhibitors of CYP3A4 are usually identified by a decreased rate of the 1-hydroxylation of midazolam or the 6'-hydroxylation of testosterone in the presence of a test compound [129]. Such assays require time-consuming and labor-intensive analytical tools such as liquid chromatography (LC) coupled with UV detection or mass spectrometry (MS). The principle bottleneck in the application of LC/UV and LC/MS is the limited throughput, largely owing to the need for extracting analytes from an incubation mixture [128]. Although throughput has been significantly improved by newer techniques, it remains a challenge in the application of LC/UV or LC/MS in a drug development setting [118].

Absorbance- or fluorescence-based assays that do not require metabolite separation allow for simultaneous monitoring of a large number of reactions on plate

readers, thus enhancing sample throughput [130]. Examination of various O-alkyl derivatives of resorufin, fluorescein, 7-hydroxycoumarins, and 6-hydroxyquinolines as substrates of CYPs resulted in commercialization of some of these compounds for fluorometric assays testing inhibition of CYPs [131]. These assays in general involve non- or low- fluorescent substrates which produce high-fluorescent metabolites when incubated with CYPs. The rate of metabolism can be readily determined by monitoring the change in fluorescence which reflects the amount of fluorescent metabolites produced during a fixed period of time [130]. These assays can be easily adapted to a high-throughput setting where multiple compounds at various concentrations can be tested in one application. Compared with the traditional LC/MS, fluorometric assays are a highly efficient means for assessing DDIs. However, because these assays involve substrates which in general lack specificity for individual CYPs, their application has been largely limited to recombinant CYP enzymes where only a single enzyme is present [132]. Also, because of the complex kinetic patterns of CYPs, occasionally, IC_{50} s and K_i s resulted from fluorometric assays are poorly correlated with those obtained using conventional probe substrates [132].

f. Quantitative assessment of the risk of clinical drug interactions

Tremendous efforts have been made to develop an overarching prediction of the risk of DDIs *in vivo* using *in vitro* experiment data. A variety of mathematical models have been developed using data from experiments involving drug metabolism and inhibition of drug-metabolizing enzymes. These models fall into three categories with increasing level of complexity: basic models, mechanistic static models, and

comprehensive dynamic models that include physiological-based pharmacokinetic models (PBPK) [133].

The basic model is the one that has been most widely used largely due to its simplicity. It estimates the ratio (R value) of intrinsic clearance of a victim drug in the absence and presence of an inhibitor drug as $R = 1 + [I]/K_{i,u}$, where [I] is the maximal total (free and bound) systemic inhibitor concentration in plasma, and $K_{i,u}$ is the unbound reversible inhibition constant determined *in vitro* for the affected pathway [134]. This model assumes reversible CYP inhibition (competitive or non-competitive), that the victim drug is orally administered, cleared exclusively by a single metabolic pathway that is affected by the inhibitor, that the ‘well-stirred liver’ model for hepatic clearance applies, that negligible inhibition of first-pass metabolism in the gastrointestinal tract occurs, and constant inhibitor concentration [133]. To be conservative, [I] is estimated as the systemic total peak concentration, $C_{max, total}$ (bound and free), of an inhibitor drug at the highest proposed clinical dose. For CYP3A inhibitors that are dosed orally, [I] is estimated by $[I] = I_{gut} = \text{molar dose}/250 \text{ ml}$. For time-dependent inhibitors, the R value is estimated as $R = (K_{obs} + K_{deg})/K_{deg}$ and $K_{obs} = k_{inact}([I]/(K_I + [I]))$, where K_{deg} is the apparent first order degradation rate constant of the affected enzyme, k_{inact} and K_I are maximal inactivation rate constant and apparent inactivation constant, respectively, K_{obs} is the apparent inactivation rate constant and $K_{obs} = k_{inact} ([I]/(K_I + [I]))$ [13]. This approach in general over-predicts the risk of DDI, often due to the assumption of a single exclusive pathway [133].

In many cases, DDIs occur via simultaneous inhibition of multiple metabolic pathways. Mechanistic static models take into account all the interaction mechanisms by

incorporating the fraction of the affected drug metabolized by the inhibited enzyme ($f_{m,CYP}$), thus improving prediction accuracy [133]. These models also include parameters reflecting the change in bioavailability in the gut due to inhibition of enzymes in enterocytes and/or the change in first-pass metabolism. They share assumptions with those used in the basic model. A generalized form of this approach is as follows [135],

$$AUCR = \frac{AUC_{inhibited}}{AUC} = \frac{F_{inhibited}}{F} \frac{1}{\sum_i^n \frac{f_{m,CYP_i}}{1 + \sum_j^m \frac{[I]_j}{K_{i,j,unbound}}} + (1 - \sum_i^n f_{m,CYP_i})} \quad \text{Eq. 3-1}$$

where $F_{inhibited}$ and F are the bioavailability of a victim drug in the presence and absence of one or multiple inhibitor drugs, i and j denote multiple affected CYPs and inhibitors, respectively. These models have been shown to represent an improvement over the basic model and can provide more accurate predictions. One of the limitations of this model is that it “uses a single static estimate of *in vivo* concentration of an inhibitor drug to provide a point estimate of the average magnitude of change in the exposure to a victim drug” as made clear by Einolf *et al.* [133].

Mechanistic dynamic models take into account the dynamics of drug concentration after a dose. A typical example of such models is the Simcyp simulator. This software simulates the concentration-time profile of a target drug under a mechanistic framework with parameters describing the human body in demographic, anatomical, genetic and physiological aspects on a population level, the physicochemical characteristics of drugs, and clinical study design. Compared with the static models discussed above, it allows one to investigate the dynamics of a DDI and the effects of inhibitory metabolites, and to predict the variability in the magnitude of DDI in a representative population [112, 136].

Because the basic model provides a conservative prediction, the R value can serve as an initial estimate. Currently, the FDA recommends a stepwise model-based strategy for assessing the risk for a drug-drug interaction. For drugs with R values greater than 1.1 (or greater than 11 for CYP3A4 inhibitors), the use of a mechanistic model, either static or dynamic, is recommended for further evaluation. A predicted AUCR outside the window of 0.8-1.25 indicates a possible clinical DDI and conduct of a clinical study is required [13].

g. Hypothesis and aims

In this chapter, I hypothesize that alterations in CYP metabolic activity contribute to the significant myopathic DDIs identified previously. To test this hypothesis, the following aims are pursued:

- 1) Evaluate *in vitro* the drugs involved in the significant myopathic DDIs for their potential to inhibit the major drug-metabolizing CYPs;
- 2) Investigate in detail the mode of inhibition for significant inhibitors identified in Aim 1);
- 3) Quantitatively predict the risk of metabolism-based DDIs.

2. Methods

a. Materials

All drugs and metabolites were purchased from Toronto Research Chemicals Inc. (North York, ON, Canada). The fluorometric cytochrome P450 inhibition kits for CYP1A2, 2B6, 2C8, 2C9, 2C19, 2D6 and 3A4 were purchased from BD Biosciences

(San Jose, CA). Methanol and acetonitrile were purchased from Sigma-Aldrich (St. Louis, MO). Corning™ black 96-well polypropylene assay plates were purchased from Fisher Scientific (Pittsburgh, PA).

b. Screening for inhibition of the major CYPs and determining IC₅₀s

Cytochrome P450 inhibition kits were used to determine the IC₅₀s of the drugs for the major CYPs, including CYP1A2, CYP2B6, CYP2C8, CYP2C9, CYP2C19, CYP2D6 and CYP3A4. The assays were conducted following the manufacturer's manuals using the conditions that are summarized in Table 3-1 [130]. Briefly, the components were thawed and pre-warmed to 37 °C. The drugs were dissolved in methanol or acetonitrile. Organic solvents were kept below 2% for acetonitrile (1% for methanol and 0.2% for DMSO) of the final reaction volume since these solvents are known to inhibit CYP enzymes [137, 138]. In 96-well plates (maximum volume 300 µL), the drugs were diluted to a series of concentrations in a solution containing nicotinamide adenine dinucleotide phosphate (NADP⁺, final concentration 1.3 mM), MgCl₂ (final concentration 3.3 mM), glucose-6-phosphate (G6P, final concentration 3.3 mM) and glucose 6-phosphate dehydrogenase (final concentration 0.4 U/mL). The enzymes and substrates were diluted to desired concentrations in sodium phosphate reaction buffer (pH 7.4, final concentration 200 mM) and mixed. The mixture was pre-incubated at 37 °C for 10 min. Reactions were initiated with addition of the enzyme and substrate mixture to the cofactor and drug mixture. The final reaction volume of all assays was 200 µL. After incubating at 37 °C for a pre-specified period of time (15 to 45 min, see Table 3-1), the reactions were stopped by adding 75 µL of quenching solution (0.5M Tris base or 2N

NaOH, see Table 3-1). Fluorescence was determined using a BioTek Synergy 2 (Winooski, VT) fluorescence reader at excitation and emission wavelengths optimized to detect the metabolites. Each of the drugs was tested at eight concentrations in duplicate. The highest final concentration of the drugs ranged from 100 to 1000 μM depending on its solubility and the enzyme tolerance to organic solvents. The lowest final concentration ranged from 0.023 to 0.46 μM . Positive controls (see Table 3-1) were used to demonstrate the reproducibility of the assays. Fluorescence emission of the drugs alone at the relevant wavelengths was examined at the same concentrations as in assays. To estimate IC_{50} s, percent of inhibition was calculated using net fluorescence that was corrected for the background. The values of percent of inhibition were then fitted to a two- (Eq. 3-2) or four- (Eq. 3-3) parameter log-logistic model as follows,

$$\% \text{ Inhibition} = \frac{100}{1+10^{(\log \text{IC}_{50} - \log [I]) \times \text{Hill slope}}} \quad \text{Eq. 3-2}$$

$$\% \text{ Inhibition} = \text{Bottom} + \frac{\text{Top} - \text{Bottom}}{1+10^{(\log \text{IC}_{50} - \log [I]) \times \text{Hill slope}}} \quad \text{Eq. 3-3}$$

where top and bottom are the top and bottom asymptote of a sigmoidal inhibition curve, respectively. Data were analyzed using GraphPad Prism 5 software (La Jolla, CA).

c. Determining dissociation constant (K_i) and mode of inhibition

For the drug and pathway pairs which yielded IC_{50} values less than 20 μM , indicating a relatively potent inhibition, the mode of inhibition and K_i were determined. Fluorometric assays were adapted to test multiple substrate and inhibitor concentrations for a specific drug-enzyme pair in one setting. The reaction conditions and experimental procedures were the same as above except where indicated. More specifically, on a 96-well plate, the test drug was diluted to the desired concentrations in solutions containing

cofactors. A mixture of the enzyme and the substrate was created for each of the desired substrate concentrations before being added to the test drug. Since the substrate and inhibitor concentrations in such assays can affect the estimate of K_i , the selection of concentrations was guided by the IC_{50} estimates and the reported K_m s. In each experiment, the substrate was tested around 5x, 2x, 1x, 0.5x, and 0.2x K_m , and the inhibitor drug was tested around 5x, 2x, 1x, 0.5x, 0.2x, and 0x IC_{50} . Each combination of inhibitor drug and substrate concentration was tested in duplicate.

The net fluorescence signals were obtained by subtracting the background from the original readouts after correction for the fluorescence produced by the drugs alone, and were fitted to the model of competitive inhibition, non-competitive inhibition, uncompetitive inhibition or mixed inhibition using GraphPad Prism 5 software. The final model was identified using Dixon plots with the aid of the method described by Geng *et al.* [139]. Briefly, the apparent inhibition constants regardless of the inhibition mechanism ($K_{i,NR}$) were calculated using $K_{i,NR} = [I] * r / (1 - r)$, where $[I]$ is inhibitor concentration, and r is the ratio of the reaction velocity in the presence and absence of inhibitors. When the values of $K_{i,NR}$ were plotted against substrate concentrations, uncompetitive inhibitory reactions were identified with the characteristic decreasing trend, whereas data of competitive inhibition and noncompetitive inhibition formed a straight line with the slope being a positive number or zero, respectively.

d. Assessing the risk of DDI using R values

Following the recommendations from the FDA [13], for each inhibitor-pathway pair for which a K_i value was observed, I estimated the R values as $1 + [I]/K_{i,u}$, where $[I]$

is the peak total plasma inhibitor concentration, and (C_{max}) is the concentration at the highest proposed clinical dose obtained from the published literature (see Table 3-5). The highest C_{max} was used as a conservative prediction when multiple such C_{max} values had been reported. Because inhibition of CYP3A expressed in the gastrointestinal gut can cause changes in bioavailability and potentially lead to DDIs, the prediction involving inhibition of CYP3A uses an estimated concentration in the gut for inhibitors administered orally. Therefore, for drugs that inhibited CYP3A4 and are administered orally, [I] is estimated as $[I] = I_{gut} = \text{molar dose}/250 \text{ mL}$. $K_{i,u}$ is the unbound dissociation constant of an inhibitor drug, estimated by $K_{i,u} = f_{u,inc} * K_i$, where K_i is the dissociation constant of an inhibitor determined *in vitro*, $f_{u,inc}$ is the fraction of unbound inhibitor drug in *in vitro* incubation. The value of $f_{u,inc}$ was predicted using the Halifax-Houston model in the following equation (Eq. 3-4) [140],

$$f_{u,inc} = \frac{1}{1 + 10^{0.072(\log \frac{P}{D})^2 + 0.067 \log \frac{P}{D} - 1.126}} \quad \text{Eq. 3-4}$$

where $\log P$ and $\log D$ are the predicted partition coefficient and the distribution coefficient, respectively, obtained from DrugBank.

Consistent with the FDA guidelines for metabolism-based inhibitory DDIs [13], inhibitors of CYP3A4 with an R value of >11 , or inhibitor of other CYPs with an R value of >1.1 , were interpreted as possibly involving clinically meaningful DDIs. For inhibitor drugs with an R value greater than the cutoffs, AUCR was further predicted for the relevant myopathic drug pairs using the mechanistic static model in Eq. 3-1. To predict AUCR, the fraction of metabolism (f_m) of a victim drug via the affected pathway(s) was estimated by $f_{m,CYPi} = CL_{int,CYPi} / CL_{int, total}$, where $CL_{int,CYPi}$ is the intrinsic clearance via the affected pathway under consideration (CYP_i), and $CL_{int, total}$ is the total intrinsic

clearance. $CL_{int,CYPi}$ and $CL_{int,total}$ were obtained from the published literature. AUCRs between 1.25 and 2 were considered as clinically weak interactions; those between 2 and 5 as moderate inhibitory interactions; and those greater than 5 as clinically strong inhibitory interactions [13].

3. Original experimental results

To test the hypothesis that the DDIs identified previously are due, in part, to inhibition of important CYPs, I examined *in vitro* the potential of these drugs to inhibit the major CYPs using high-throughput fluorometric assays, and then predicted how likely inhibition of the CYPs contributes to the DDIs.

a. IC_{50} estimates

The thirteen drugs involved in the significant myopathic DDIs identified were screened for inhibition of the major CYP isoforms, including CYP1A2, CYP2B6, CYP2C8, CYP2C9, CYP2C19, CYP2D6 and CYP3A4. IC_{50} s are shown in Table 3-2, and the inhibition curves are displayed in Figure 3-1. At the highest concentration tested, some of the drugs did not show any inhibition, e.g. omeprazole for CYP2B6, or failed to produce 50% inhibition, e. g. chloroquine for CYP1A2 and CYP2B6. In either of these two situations, IC_{50} was designated as greater than the highest concentration tested. Some drugs exhibited abnormal kinetics in the assays for CYP2C8, CYP2C9 and CYP2C19. For example, omeprazole and trazodone showed activation rather than inhibition (Figure 3-2 A and B); loratadine and omeprazole seemed to inhibit CYP2C8 and CYP2C9, respectively, at lower concentrations but activate the enzymes at higher concentrations

(Figure 3-2 C and D); alprazolam and quetiapine exhibited inhibition at lower concentrations but activation at higher concentrations for CYP2C9, respectively (Figure 3-2 E and F). IC_{50} could not be determined for such cases and they are therefore labeled as ND in Table 3-2. The causes of such unusual kinetics are addressed in detail later.

IC_{50} s were evaluated for 60 drug-enzyme pairs. The inhibitory potential of individual drugs was highly variable across the CYPs, which was reflected in a wide range of IC_{50} values spanning from 0.34 μ M to 540 μ M. Using arbitrary cutoffs, the inhibitors were classified as relatively potent ($IC_{50} \leq 20 \mu$ M), relatively moderate (20μ M $\leq IC_{50} \leq 200 \mu$ M), or relatively weak ($IC_{50} \geq 200 \mu$ M). Twenty inhibitory reactions were identified as involving relatively potent inhibition, 28 as relatively moderate inhibition and 12 as relatively weak inhibition. It should be noted that a number of relatively potent inhibitors discovered here had not been reported before. For example, promethazine was identified as a relatively potent inhibitor of CYP1A2 ($IC_{50} = 1.0$ (0.8, 1.2)); ropinirole was a relatively potent and specific inhibitor of CYP2D6 ($IC_{50} = 0.85$ (0.79, 0.92)); tegaserod exhibited relatively potent inhibition for CYP2D6, 3A4 and 2C9 with an IC_{50} of 0.34, 5.6 and 7.9 μ M, respectively.

b. Mode of inhibition and K_i estimates

Since IC_{50} is substrate-dependent and therefore has limited ability to predict the risk of DDIs, the potency and mode of inhibition were further characterized. Considering that estimating dissociate constant (K_i) requires a large number of incubations, I focused on the drug-pathway pairs which were more likely to be involved in DDIs – those that exhibited a relatively potent inhibition with an IC_{50} less than 20 μ M. Drug-pathway pairs

involving omeprazole and CYP2C8 exhibited unusual kinetics, K_i and the mode of inhibition thus could not be determined. Inhibition was characterized in detail for eighteen drug – enzyme pairs (Table 3-3). The mode of inhibition was predominantly competitive, with K_i ranging from 0.25 μM to 20.1 μM . Noncompetitive inhibition was only observed for the inhibition of CYP2C19 by duloxetine.

c. Predicted risk of clinical DDIs

Following the FDA guidelines, I first estimated R values to obtain an initial assessment of the risk of clinical DDIs associated with the inhibitory reactions characterized above. To estimate R values, $f_{u,inc}$, the fraction of unbound drug in *in vitro* incubation, was predicted for each individual drug of interest and is shown in Table 3-4. The estimated $K_{i,us}$ and R values are shown in Table 3-5. With the R cutoff value of 11 for CYP3A4 inhibitor drugs and 1.1 for inhibitor drugs of other CYPs, six inhibitory reactions were considered as having potential to inhibit intrinsic clearance of other drugs via the affected pathway and cause clinical DDIs. With a predicted R value of 13, quetiapine was the only CYP3A4 inhibitor drug predicted to potentially be involved in clinical DDIs at its highest proposed clinical dose (800 mg). The other drugs that inhibited CYP3A4, including simvastatin, tegaserod and duloxetine, had R values that were much smaller than 11, suggesting a remote chance to interact with drugs mainly metabolized by CYP3A4. Duloxetine, promethazine, risperidone and ropinirole exhibited relatively potent inhibition for CYP2D6 and had estimated R values of 1.8, 1.3, 1.2 and 1.2, respectively. Because of the high peak plasma concentration, chloroquine also had an estimated R value across the borderline (R value =1.3), although its inhibition for

CYP2D6 was only relatively moderate ($K_{i,u} = 14.03 \mu\text{M}$). These drugs therefore had potential to interact with drugs that are exclusively metabolized by CYP2D6. The predicted risk of clinical DDIs for the other inhibitory reaction was considered to be negligible.

The six drugs with significant R values above the cut off limits were involved in eight significant myopathic DDIs identified previously. Since R values usually overestimate the risk of DDIs and are not specific for interacting drugs, the contribution of inhibition of CYPs to those significant DDIs was further evaluated using a mechanistic-static model. To account for the contribution of the affected pathway to the total metabolism of a victim drug, the fraction of metabolism (f_m) of the affected pathways, mostly CYP3A4 and CYP2D6, was estimated using data from the published literature. The AUCR was then predicted for scenarios where any of the six drugs was the perpetrator drug and the interacting drug was the victim drug. The estimated f_m and predicted R values are shown in Table 3-6.

The inhibition of CYP3A4 by quetiapine was predicted to result in a 1.25-fold increase in the AUC of chloroquine, although CYP3A4 only accounts for 25% of chloroquine metabolism [141]. Consistent with the definition by the FDA, this small predicted AUCRs indicates a weak clinical DDI between quetiapine and chloroquine. The predicted AUCRs suggested that the other drug pairs would not have significant interactions clinically.

4. Discussion

In the first part of this chapter, I have addressed the hypothesis that inhibition of the major CYPs contributes to the significant drug interactions previously identified. I first screened the thirteen drugs involved in those DDIs for inhibition of the major CYPs. Then I characterized the mode of inhibition and potency in detail for eighteen inhibitory reactions that yielded IC_{50} s less than 20 μ M. Next, I predicted the risk of metabolism-based DDI via inhibiting a single pathway for the reactions characterized in detail, and identified six drugs with significant potential to act as precipitant drugs and cause clinical DDIs. Lastly, for the myopathic DDIs involving any of these six drugs, I predicted the change in the AUC of the victim drugs in the presence of these drugs, and found that quetiapine and chloroquine may have a weak clinical drug interaction.

The examination of the potential to inhibit the CYPs provides a relatively comprehensive view on the drugs' inhibitory profile for the major drug-metabolizing enzymes. The inhibitory potential for CYP2B6 and CYP2C8 is particularly valuable since these two isoforms have been understudied. Such inhibitory profiles may not be available to the public, and are often lacking for drugs that were developed decades ago since the requirement by the FDA on evaluation of CYP inhibition by investigational drugs is only relatively recent. In general, the IC_{50} s presented in Table 3-2 and the K_i s presented in Table 3-3 are consistent with the inhibitory potential of these drugs published previously. My data represent not only a confirmation of some inhibitory profiles that have been published, but are also the first to provide such information on alprazolam, hydroxychloroquine, promethazine and quetiapine. Here, I discuss first the

consistency between my data and those that have been published. The clinical implication of these inhibitory profiles will be addressed later.

Alprazolam had a rather favorable inhibitory profile for the major CYPs by exhibiting only relatively weak inhibitory effects on CYP2B6, CYP2C8, CYP2C19 and CYP3A4. This may explain the lack of publications on its inhibitory potential for CYPs.

Chloroquine was identified as a relatively potent inhibitor of CYP2D6, a relatively moderate inhibitor of CYP2C8 and a relatively weak inhibitor of CYP3A4. It showed little inhibitory effect on the other isoforms. Further characterization of the inhibition of CYP2D6 revealed that chloroquine is a competitive inhibitor of this isoform with a K_i of 20.1 μM , that is consistent with the data of Biparo *et al.* and Masimirembwa *et al.* [142, 143], who reported that chloroquine was a competitive inhibitor of CYP2D6 with K_{is} of 12.4 μM and 15.3 μM , respectively. These data are consistent with the results of Projean *et al.*, who found that chloroquine was metabolized, in part, by CYP2D6 [141].

Duloxetine exhibited relatively potent inhibition of CYP1A2, CYP2C9, CYP2C19, CYP2D6 and CYP3A4, and relatively moderate inhibition of CYP2B6 and CYP2C8. The broad inhibitory effect of duloxetine across CYP isoforms suggests that duloxetine could be involved in drug interactions by simultaneously inhibiting multiple pathways. Paris *et al.* showed that duloxetine inhibited CYP isoforms 1A2, 2B6, 2C8, 2C9, 2C19, 2D6 and 3A4/5 with IC_{50} s of 50, 15, 60, >100, 27, 7 and 38 μM , respectively [144], which are comparable to our IC_{50} estimates of 9.6, 33.3, 35.9, 26.3, 12, 0.9 and 10.2 μM , respectively. It is worth noting that both sets of data identify CYP2D6 as the isoform most sensitive to duloxetine inhibition. Because duloxetine is a substrate of CYP2D6 [145], it was suspected that duloxetine is a mechanism-based inhibitor of

CYP2D6. However, the data of Chan *et al.* clearly showed that the inhibition of CYPs by duloxetine was not time-dependent [146]. I found that the inhibition of CYP1A2, CYP2D6 and CYP3A4 was competitive with K_i s of 4.7, 0.3 and 10.5 μM , respectively, and that of CYP2C19 was noncompetitive with a K_i of 2.9 μM . Knadler *et al.* reported that the K_i for the inhibition of CYP1A2, CYP2C19, CYP2D6 and CYP3A4 by duloxetine was 17.7, 7.1, 2.4 and 133 μM , respectively [147]. Compared with these K_i values determined using conventional CYP probe substrates, my K_i estimates are in a similar range for CYPs but are in general of smaller values.

The inhibitory profile of hydroxychloroquine resembles that of chloroquine in that it showed a relatively strong inhibition for CYP2D6, a relatively moderate inhibition for CYP2C8, a relatively weak inhibition for CYP3A4 and no inhibition for the other isoforms. The potential of hydroxychloroquine to inhibit CYPs *in vitro* has not been reported before, and my data are the first to provide such information.

Loratadine also exhibited a broad inhibitory effect on CYPs. It was a relatively potent inhibitor of CYP2D6, CYP2B6 and CYP2C9, a relatively moderate inhibitor of CYP2C19 and CYP3A4 and a relatively weak inhibitor of CYP1A2. My data showing the relatively potent inhibition of CYP2D6 and CYP2B6 by loratadine are consistent with the results of Nicolas *et al.* [148] and Walsky *et al.* [149], who reported that IC_{50} s of loratadine for CYP2D6 and CYP2B6 were 15 μM and 7.69 μM , respectively. I further found that the inhibitions of CYP2B6 and CYP2D6 by loratadine were both competitive with K_i s of 2.0 and 0.5 μM , respectively. The relatively moderate inhibition of CYP3A4 and weak inhibition of CYP1A2 are also consistent with the data presented by Nicolas *et al.* [148], who showed that IC_{50} s for these isoforms were 32 μM and >100 μM ,

respectively. Discrepancy exists in the inhibitory potencies for CYP2C9 and, more prominently, for CYP2C19. Lee *et al.* found that loratadine did not show significant inhibition for CYP2C9 and the IC_{50} was higher than 30 μM [150]; whereas my data indicate that loratadine was a relatively potent inhibitor of CYP2C9 with an IC_{50} of 12.35 μM and a K_i of 7.6 μM . A relatively potent inhibition of CYP2C19 by loratadine has been reported by many groups with IC_{50} ranging from 0.76 μM [151] to 2.80 μM [150], whereas my data show that this inhibition is only relatively moderate in potency with an IC_{50} of 21.3 μM . The inhibition of CYP2C19 by loratadine has been identified by other groups as competitive with a K_i ranging from 0.006 μM [152] to 0.61 μM [151]. The cause of these discrepancies may lie in the estimation of IC_{50} s. In the case of both CYP2C9 and CYP2C19, the observed inhibition-concentration curve of loratadine was in an incomplete sigmoidal shape and was rather flat across the concentrations (the light blue curves in Figure 3-1 CYP2C9A and CYP2C19.A), which would usually lead to inaccurate estimation of the model parameters. In addition, the IC_{50} of loratadine for CYP2C8 could not be evaluated due to unusual kinetics (Figure 3-2 C). A relatively potent inhibition of CYP2C8 by loratadine was reported by Walsky *et al.* with an IC_{50} of 3.36 μM [153].

Omeprazole was found to be a relatively potent inhibitor of CYP3A4, a relatively moderate inhibitor of CYP2C19, CYP1A2 and CYP2D6. The relatively moderate inhibition of CYP1A2 is consistent with the IC_{50} of 78 μM observed by Moody *et al.* [154]. The relatively weak the inhibition of CYP2D6 is consistent with the K_i values determined by others, ranging from 181.8 μM [155] to 302 μM [156]. Omeprazole has been identified as a mechanism-based inhibitor of CYP2C19 and CYP3A4 with K_{inact} S of

0.044 /min [157] and 0.099 /min [158], respectively. Since the inhibitory effect of a mechanism-based inhibitor is less apparent with shorter pre-incubation time as in the experiments, this may explain the discrepancy between my data and those showing omeprazole to be a relatively potent inhibitor of CYP2C19 [159, 160]. In addition, IC₅₀ of omeprazole for CYP2C9 could not be determined. Other groups have reported that omeprazole is a potent to moderate inhibitor of this isoform with a highly variable K_i ranging from 0.41 μM [161] [162] to 74.9 μM [163].

Promethazine was able to inhibit all the CYPs of interest. It was identified as a relatively inhibitor of CYP1A2 and CYP2D6, and a relatively moderate inhibitor of the other isoforms. I further found that promethazine was a competitive inhibitor of CYP2D6 with a K_i of 0.25 μM, which represents a more potent inhibition than those reported by Hamelin *et al.* [164] and He *et al.* [165] who reported a K_i of 1.9 μM and 9 μM, respectively, for this inhibitory reaction. He *et al.* also reported a relatively moderate inhibition of CYP2C9 by loratadine with an IC₅₀ of 88 μM [165], which is comparable to my IC₅₀ estimate (12.4 μM) in magnitude. The inhibitory effect of promethazine on the other CYP isoforms has never been reported.

Quetiapine exhibited a relatively potent inhibition for CYP3A4 and a relatively moderate inhibition for CYP2B6 and CYP2D6. Its potential to inhibit CYP2C8, CYP2C9 and CYP2C19 could not be evaluated. The inhibition of CYP3A4 was identified as competitive with a K_i of 0.75 μM. The inhibitory effects of quetiapine on CYPs have never been reported before.

Risperidone was found to be a relatively potent inhibitor of CYP2D6, a relatively moderate inhibitor of CYP2C9, CYP2C19 and CYP3A4, and a relatively weak inhibitor

of CYP2B6. The potent inhibition of CYP2D6 was identified as competitive with a K_i of 1.62 μM . Zimmerline *et al.* found that risperidone is a mechanism-based inhibitor of CYP2D6 with a K_{inact} of 0.005 /min [158]. The moderate inhibition of CYP3A4 was consistent with the K_i of 67 μM observed by Prakash *et al.*[166]. The same group also reported that the IC_{50} s of risperidone for CYP1A2, CYP2C9 and CYP2C19 were greater than 100 μM .

Ropinirole exhibited a relatively potent inhibition for CYP2D6 and weak or no inhibition for the other CYP isoforms. The potent inhibition of CYP2D6 was also observed by Wynalda *et al.* who reported an IC_{50} of 0.54 μM [167]. I further found that this inhibitory reaction was competitive with a K_i of 0.85 μM .

Tegaserod was a relatively potent inhibitor of CYP2D6, CYP2C9 and CYP3A4, a relatively moderate inhibitor of CYP2B6, and a relatively weak inhibitor of CYP1A2. The inhibition of CYP2D6, CYP2C9 and CYP3A4 was all found to be competitive with K_i s of 0.51 μM , 11.4 μM and 5 μM . A thorough investigation on the inhibitory effect of tegaserod on CYPs was conducted by Vickers *et al.* using conventional VYP probe substrates and HLMs [168]. They found that tegaserod was a relatively potent inhibitor of CYP1A2 and CYP2D6 with K_i s of 0.84 μM and 0.85 μM , respectively, and a relatively moderate inhibitor of CYP2C8, CYP2C9, CYP2C19 and CYP3A4 with IC_{50} s of ~130 μM , ~74 μM , ~153 μM , and ~107 μM , respectively. My data are consistent with those of Vickers *et al.* only with respect to the inhibition of CYP2D6.

Trazodone was found to be a moderate inhibitor of CYP2B6, CYP2D6 and CYP3A4. The inhibition of CYP3A4 is consistent with the IC_{50} of 22.7 μM reported by Kalgutkar *et al.* [169]. A stronger inhibitory effect on CYP2D6 was observed by Otton *et*

al., who showed that trazodone was a competitive inhibitor of this isoform with a K_i of 9 μM [170].

Simvastatin also exhibited inhibitory effect on many CYP isoforms. My data showed that simvastatin was a relatively potent inhibitor of CYP3A4, CYP2C9 and CYP2C8, and a relatively moderate inhibitor of CYP2C19, CYP2D6 and CYP2B6. The relatively moderate inhibition of CYP2C19 and the relatively potent inhibition of CYP2C8 and CYP2D4 are consistent with those observed elsewhere [129, 153, 171-173]. My estimate of K_i equal to 0.51 μM for inhibition of CYP3A4 is very close to that reported by Foti *et al.* (0.54 μM) [129]. Compared with my data, the inhibition of CYP2C9 was found to be much less potent with an IC_{50} ranging from 111.6 μM [174] to 287 μM [171]. Also, a slightly more potent inhibition of CYP2B6 was observed ($\text{IC}_{50} = 15.9 \mu\text{M}$) by Walsky *et al.* [149].

Evaluating the inhibitory effects of these drugs on the CYPs in a consistent system also allows comparing the inhibitory potential across the major CYPs. Figure 3-3 shows the inhibition-concentration curves grouped drug-wise. These drugs share a common trend of losing inhibitory selectivity at higher concentrations. Consistent with the values of IC_{50} s and K_i s, these plots suggest that some of the drugs can serve as selective inhibitors of specific CYP isoforms within certain concentration windows. For example, on the plot of chloroquine, the inhibition-concentration curve for CYP2D6 (hot pink) is clearly separated with those for the other isoforms on the right, indicating a more potent inhibition of CYP2D6. The blank space between the curve of CYP2D6 and those of the others corresponds to a window of concentration within which the inhibitory effect of chloroquine is relatively selective for CYP2D6. Apparently, chloroquine has a broad

“window of selectivity”. The range of concentration in which 70% inhibition of CYP2D6 was observed with no significant inhibitory effect on other isoforms was approximately from 20 μM to 100 μM . The same also applies to risperidone and ropinirole for inhibition of CYP2D6. The concentration window of ropinirole for selective inhibition of CYP2D6 is approximately 2 μM to 100 μM , and that of risperidone is approximately 3 μM to 20 μM . It should be noted that the inhibition-concentrations curves were obtained using recombinant CYP enzymes and fluorogenic probes. Further studies are warranted to examine the selectivity of inhibition using conventional CYP probes in HLMs where multiple isoforms are present.

The window of selective inhibition discussed above only applies to the CYP isoforms for which inhibitory potential could be evaluated, including those with $\text{IC}_{50\text{s}}$ designated as greater than the highest concentration tested. There are a number of cases where abnormal kinetics were observed and inhibitory potential could not be determined. The possibility remains that, in these cases, the test drug may be a potent inhibitor of the CYP isoform, and its window of selective inhibition taking account of all the major CYPs may consequently be different.

Among the abnormal kinetics observed, an apparent enzyme activation was observed with omeprazole in the assay of CYP2C8 and with trazodone in the assay of CYP2C19 (Figure 3-2 A and B). There are a few possible explanations for these apparent enzyme activations. One is that the test drug is also fluorescent at the wavelength that the metabolite of the fluorogenic probe is being detected. Amongst the drugs tested, only omeprazole, chloroquine and hydroxychloroquine exhibited fluorescence at the relevant wavelengths. However, enzyme activation observed with omeprazole remained even after

correction for the fluorescence of this drug. Another possibility is that the metabolites of the test drugs may be highly fluorescent at the relevant wavelengths, so the fluorescent signal may largely represent the amount of the metabolites of the test drug. It is also possible that the test drugs and/or its metabolites allosterically bind to the enzyme, rendering the enzyme more efficient in metabolizing the fluorogenic probes (positive cooperativity). These possible mechanisms, and their combination, may explain the monotonic increase in fluorescent signal with the test drug concentration. For the other abnormal kinetics showing activation at lower concentrations and inhibition at higher concentrations, or the opposite, the mechanism may be even more complex.

High-throughput fluorometric CYP inhibition assays enabled me to evaluate inhibitory potential of CYPs in a highly efficient way. However, this approach also represents one of the limitations of my study. While there is in general a good correlation between IC_{50} values determined using fluorogenic and conventional probes [132, 175], occasionally, IC_{50} values generated using fluorogenic probes can be very different from those using conventional probes [132, 175]. It is well recognized that IC_{50} values are dependent on probe substrate, which is particularly true for CYP3A4. CYP3A4 simultaneously binds and metabolizes multiple compounds in its active site. Therefore, cooperativity, activation, and complex inhibition kinetics are much more common with CYP3A4 than with enzymes of the CYP1 and CYP2 families [176, 177]. Also, the structural and physiochemical properties of fluorogenic probes are different from those of conventional probes [132]. These may explain the inconsistency between the IC_{50} values I observed and those from the published literature, all of which were determined with conventional probes. It follows that caution should be exercised when interpreting the

data from such fluorometric assays. In addition, I could not evaluate IC_{50} for some of the drugs in the assays involving CYP2C8, CYP2C9 and CYP2C19. It may be possible to evaluate the IC_{50} s in such cases using conventional probes.

In addition to the use of fluorescent probes, the use of recombinant CYP enzymes may also be problematic. The activities of purified recombinant CYP enzymes are known to be different in some respects from that observed in the liver or in HLMs [178]. This difference in enzymatic activity may cause inconsistency between IC_{50} s determined here and those that have been published. Future studies thus are warranted to validate the inhibitory potencies using HLMs or hepatocytes and conventional probes.

Another limitation of my *in vitro* study is that I did not examine the potential of these drugs as mechanism-based inhibitors of the CYPs. Some of these drugs are already known to be mechanism-based inhibitors, e.g. omeprazole for CYP2C19 and CYP3A4, and risperidone for CYP2D6. Since mechanism-based inhibition requires substrate activation, an inhibitory reaction involving a CYP isoform that also metabolizes its inhibitor drug can potentially be mechanism-based. For example, inhibition of CYP2D6 by chloroquine and promethazine might be mechanism-based because CYP2D6 is involved in the metabolism of these drugs. The predicted R values and AUCRs may consequently underestimate the risk of clinical DDIs for mechanism-based inhibitory reactions due to their more profound effects on enzyme activity than reversible inhibitions. This underestimation may result in a false conclusion that some DDIs identified previously are not caused by inhibition of CYPs.

The inhibitory potential obtained *in vitro* provided the basis for prediction of the risk of clinical DDIs *in vivo*. Applying the R value approach, I screened for inhibitory

reactions that potentially have clinical consequences. For the majority of the six drugs predicted with significant R values, there is little evidence for their potential to interact with other drugs clinically as precipitant drugs.

As a relatively potent inhibitor of CYP2D6, duloxetine had an R value of 1.78 and was predicted to interact with CYP2D6 substrate drugs. This is consistent with drug interactions that have been observed with duloxetine clinically. Skinner *et al.* showed that duloxetine increased the AUC of desipramine, an *in vivo* probe of CYP2D6, by 192% and 122% at a dose of 60 mg twice daily and 30 mg twice daily, respectively [145]. Coadministration of 40 mg of duloxetine twice daily with the CYP2D6 substrate tolterodine (2 mg twice daily) increased tolterodine steady state AUC and C_{max} by 71% and 64%, respectively, and prolonged the half-life of tolterodine by 14% [179]. Also, duloxetine increased the C_{max} and half-life of metoprolol, a CYP2D6 substrate, and decreased its clearance, leading to a 180% increase in the AUC [180]. However, duloxetine did not significantly change the pharmacokinetics of risperidone and aripiprazole [181], which are also CYP2D6 substrates. It therefore seems that the inhibitory effect of duloxetine on CYP2D6 is moderate from a clinical perspective.

Chloroquine was predicted to interact clinically with drugs that are exclusively metabolized by CYP2D6. The R value of 1.36 is due mostly to the high C_{max} (1547 ng/ml) that was reported for patients with malaria after receiving 1500 mg chloroquine for 3 days [182]. But even if predicted with a much lower C_{max} observed in healthy volunteers (838 ng/ml) [183], the resulting R value of 1.19 would still be significant. Since chloroquine has a long half-life of 146 to 333 hours [184], these C_{max} values are likely lower than that at steady state. More importantly, chloroquine is known to accumulate in

tissues including the liver and muscles [185]. The accumulation ratio of chloroquine was 795 ± 33 in viable isolated rat hepatocytes [186]. Therefore, the risk of chloroquine as a precipitant drug is likely substantially underestimated. Similar to the case of quetiapine, reports on pharmacokinetic drug interactions involving chloroquine as a precipitant drug are limited. Chloroquine increased the C_{\max} and AUC of paracetamol without affecting the elimination rate [187]. Chloroquine was also reported to reduce the bioavailability of ampicillin [188]. These studies, however, do not suggest a role of chloroquine in drug interactions by inhibiting CYP2D6. Future studies are needed to further evaluate the potential of chloroquine to act as a precipitant drug and its effect of the metabolism of other drugs by CYP2D6.

Promethazine was also predicted to interact with CYP2D6 substrate drugs with an R value of 1.31. There are very few studies suggesting the role of promethazine as a precipitant drug in DDIs by inhibiting CYP2D6. The steady state plasma concentration of haloperidol, a substrate of CYP2D6, during promethazine coadministration was significantly higher than those before the coadministration or 1 week after the discontinuation of promethazine [189]. Coadministration of promethazine was found to increase the plasma concentration and AUC of chloroquine, a substrate of CYP2D6, suggesting a possible mechanism of CYP26 inhibition [190].

Both ropinirole and risperidone were predicted with R values of 1.15, suggesting a small risk of interacting with CYP2D6 substrate drugs clinically. The R value of risperidone is likely to be an underestimate since the drug is known to be a mechanism-based inhibitor of CYP2D6. Both ropinirole and risperidone lack evidence of having clinical drug interactions as a precipitant drug. The only published study involving drug

interaction with ropinirole reported a small change in the C_{max} and AUC of digoxin with coadministration of ropinirole [191]. This weak interaction is unlikely due to inhibition of CYP2D6 by ropinirole. No published DDI study showing risperidone as a precipitant drug was found.

With a gut concentration estimated at the dose of 800 mg, quetiapine was predicted to cause DDIs with drugs that are exclusively metabolized by CYP3A4 (R value = 13). This seems at odds with the lack of publication on CYP3A4-based interactions with quetiapine given that CYP3A4 has such a broad substrate spectrum. The published DDIs studies involving quetiapine all observed it as a victim drug. Its pharmacokinetics were found to be affected by ketoconazole and carbamazepine, a CYP3A4 inhibitor and inducer, respectively [192], or by fluoxetine, a CYP2D6 inhibitor [193].

It is possible that the general lack of publications on clinical drug interactions with the drugs discussed here are because these drugs have rarely been evaluated clinically as precipitant drugs. Another possibility is that the clinical risk of drug interactions with these drugs were overpredicted using the R value approach. Future studies are warranted to investigate the potential of these drugs to act as inhibitors of CYPs *in vivo* and their clinical consequences.

Over-prediction of the risk of clinical DDIs using R values may be more prominent with the inhibitors of CYP3A4, for which a gut concentration that is normally much higher than the circulating concentration was assumed. However, in the case of quetiapine, the predicted risk using R value is supported by the predicted AUCR for the interaction of chloroquine with quetiapine. It should be noted that, even for chloroquine,

whose fraction of metabolism through CYP3A4 is only 0.25, quetiapine was predicted to result in 1.25-fold increase in the AUC when coadministered. The inhibitory effect of quetiapine on CYP3A4 would be more profound if a victim drug were metabolized by CYP3A4 to a larger extent. Considering that prediction of AUCR ignores the change in bioavailability due to inhibition of first-pass metabolism, this AUCR is likely an underestimate. On the other hand, the elimination of chloroquine is largely rate-limited by distribution rather than hepatic metabolism [184, 194]. The documented accumulation of chloroquine in the liver and muscles may further attenuate the overall effect of quetiapine on its pharmacokinetics.

The risk of clinical DDIs is likely under-predicted when chloroquine is the precipitant drug due to its hepatic accumulation. Since the C_{\max} of chloroquine used for predicting AUCRs is likely much lower than its hepatic concentration, the AUCRs of chloroquine vs. duloxetine and of chloroquine vs. risperidone likely under-predicted the effects of chloroquine on the pharmacokinetics of the victim drugs. PBPK models that incorporate the hepatic concentration of chloroquine and the victim drugs may provide better predictions. Clinical studies that evaluate chloroquine as a precipitant drug will be very helpful.

Aside from over-prediction in general and potential under-predictions in the case of chloroquine, the prediction of the risk of clinical DDIs has a major limitation that results from using the R value and AUCR approach. It is problematic to use a single static estimate of *in vivo* concentration of an inhibitor drug to provide a point estimate of the average magnitude of change in the exposure to a victim drug. The static nature of the two models may be particularly problematic for drugs that have relatively short half-lives

and whose circulating concentrations drop rapidly following a dose. One example is simvastatin, whose half-life can be as short as two hours [195]. The inhibitory effects of such drugs on the overall metabolism of a victim drug may be limited even when they are strong inhibitors of the relevant CYPs. In addition, the major CYPs, CYP2D6, CYP2C9 and CYP2C19 in particular, are known to be polymorphic. The risk of clinical DDIs with the drugs of interest may be overpredicted for some individual and under-predicted for others.

Table 3-1. Summary of incubation conditions of CYP fluorometric assays.

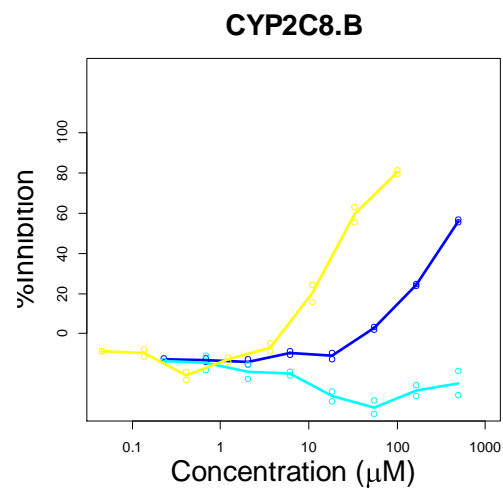
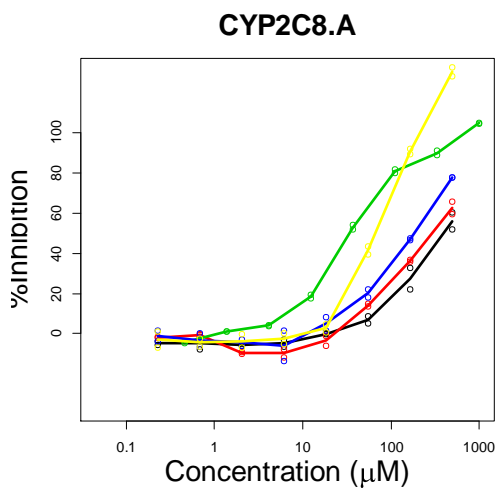
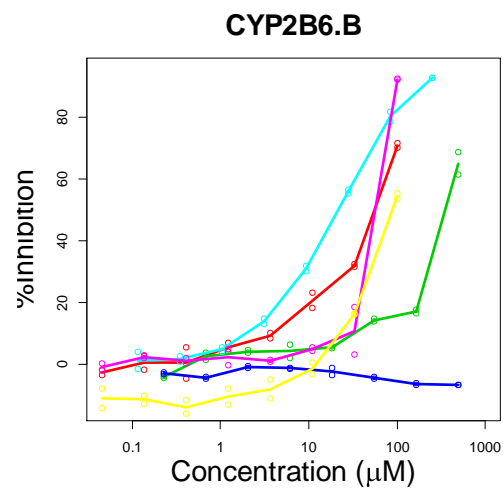
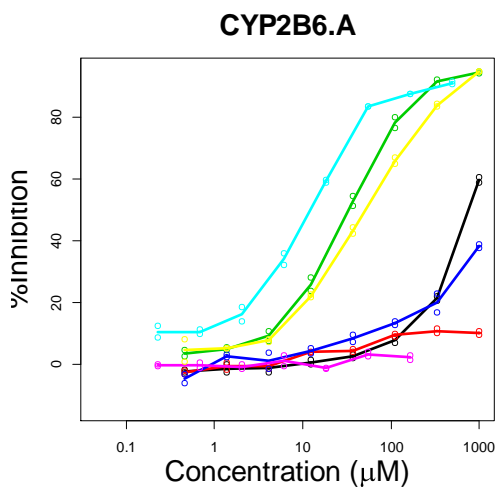
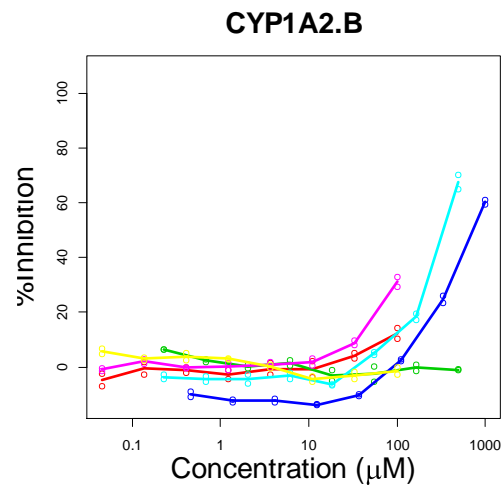
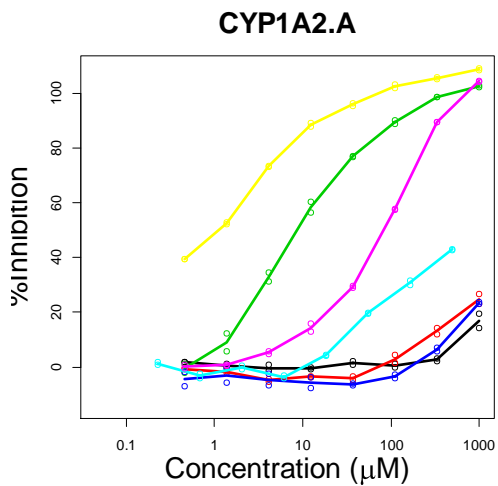
	CYP1A2	CYP2B6	CYP2C8	CYP2C9	CYP2C19	CYP2D6	CYP3A4
Substrate	CEC	EFC	DBF	MFC	CEC	AMMC	BFC
Substrate Concentration (μM)	5	2.5	1	75	25	1.5	50
Enzyme Concentration (nM)	2.5	5	9	5	2.5	7.5	5
$K_{m,app}$ (μM)	3.5		1	78	29	1	>200
$V_{max,app}$ (min^{-1})	3.4		0.4	2.1	0.016	1	1.5 @40uM
Buffer	50mM KPO_4	50mM KPO_4	50mM KPO_4	50mM KPO_4	50mM KPO_4	50mM KPO_4	200mM KPO_4
pH	7.4	7.4	7.4	7.4	7.4	7.4	7.4
Incubation Time (min)	15	30	40	45	30	30	30
Quenching Solution	0.5M Tris base	0.5M Tris base	2N NaOH	0.5M Tris base	0.5M Tris base	0.5M Tris base	0.5M Tris base
Metabolite	CHC	HFC	Fluorescein	HFC	CHC	AHMC	HFC
Ex/Em (nm)	410/460	410/530	485/538	410/530	410/460	390/460	410/530
Control inhibitor	Furaflyline	Tranlycypromine	Quercetin	Sulfaphenazole	Tranlycypromine	Quinidine	Ketoconazole

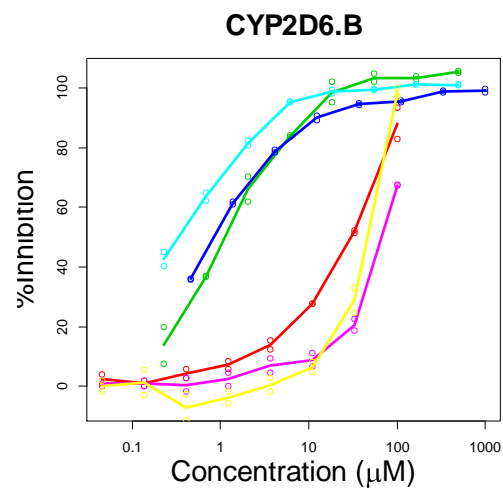
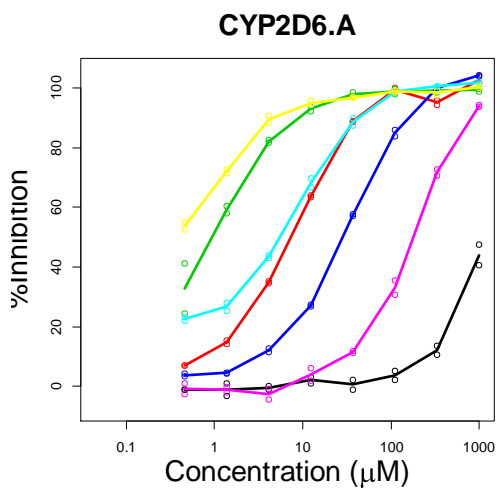
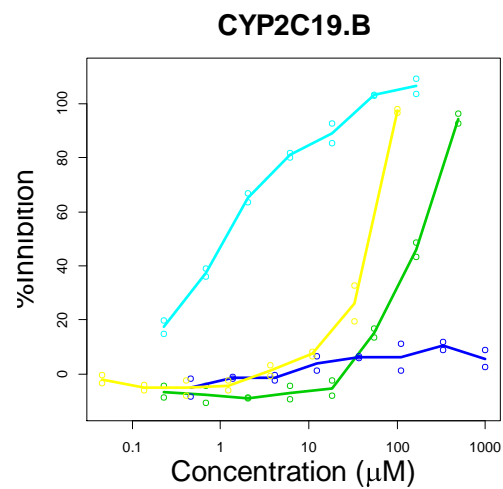
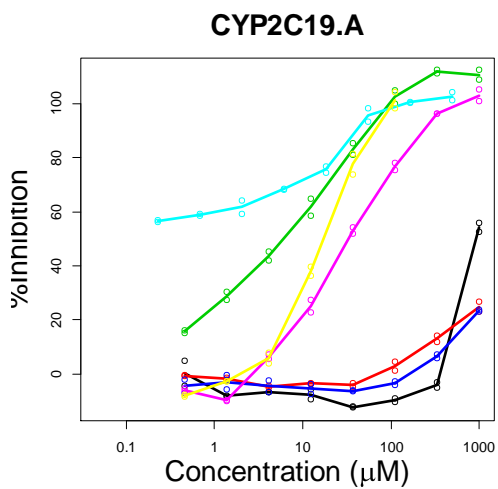
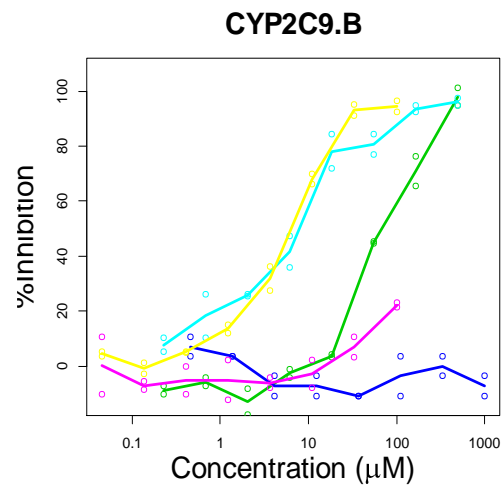
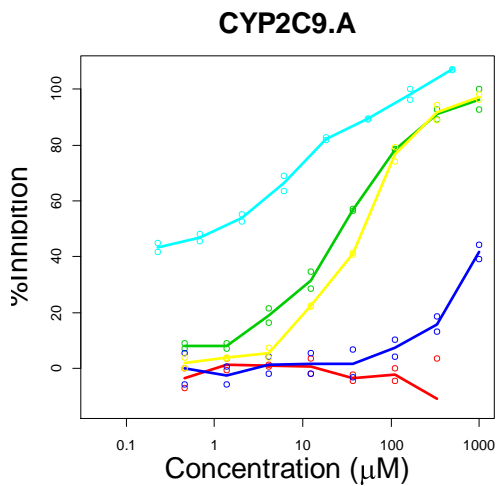
Note: CEC, 3-cyano-7-ethoxycoumarin; EFC, 7-Ethoxy-4-trifluoromethylcoumarin; DBF, Dibenzylfluorescein; MFC, 7-methoxy-4-trifluoromethylcoumarin; AMMC, 3-[2-(N,N-diethyl-N-methylammonium) ethyl]-7-methoxy-4-methylcoumarin; BFC, 7-benzyloxy-4-trifluoromethylcoumarin; CHC, 3-Cyano-7-hydroxycoumarin; 7-HC, 7-Hydroxycoumarin; HFC, 7-hydroxy-4-trifluoromethylcoumarin; AHMC, 3-[2-(N,N-diethylamino)ethyl]-7-hydroxy-4-methylcoumarin hydrochloride.

$K_{m,app}$, apparent Michealis Menton constant; $V_{max,app}$, apparent maximum reaction velocity; Ex, excitation wavelength; Em, emission wavelength.

Table 3-2. IC₅₀s (95% CI) (μM) for the inhibition of the major CYPs

	CYP1A2	CYP2B6	CYP2C8	CYP2C9	CYP2C19	CYP2D6	CYP3A4
Alprazolam	>100	773 (723.3, 826.1)	396.4 (321.3, 489.2)	ND	443.9 very wide	>1000	303.8 (261.7, 352.6)
Chloroquine	>1000	>1000	147.8 (80.2, 272.5)	>1000	>1000	8.0 (6.8, 9.4)	367.0 (326.5, 412.6)
Duloxetine	9.6 (8.3, 11.0)	33.3 (30.7, 36.1)	35.9 (31.7, 40.6)	26.3 (22.9, 30.2)	12.0 (8.6, 16.8)	0.9 (0.8, 1.1)	10.2 (9.7, 10.6)
Hydroxychloroquine	>1000	>1000	176.6 (75.43, 413.5)	>1000	>1000	27.1 (24.2, 30.5)	352.4 (323.9, 383.3)
Loratadine	630 (438, 906.3)	11.9 (9.9, 14.4)	ND	12.35 (7.8, 19.45)	21.3 (15.3, 29.7)	9.1 (8.3, 9.9)	33.2 (30.1, 36.6)
Omeprazole	112.1 (97.3, 129)	>1000	ND	ND	32.0 (25.9, 39.5)	190.7 (158.4, 229.5)	7.4 (7.0, 7.8)
Promethazine	1.0 (0.8, 1.2)	51.1 (46.7, 56)	106.9 (86.4, 131.9)	43.8 (39.3, 48.8)	40.8 (28.8, 57.8)	0.39 (0.35, 0.44)	48.5 (44.8, 52.6)
Quetiapine	>100	51.2 (42, 62.4)	ND	ND	ND	25.7 (21.7, 30.6)	4.5 (3.7, 5.5)
Risperidone	>500	358.9 (297.3, 433.3)	ND	75.0 (58.2, 99.3)	169.9 (140, 206.2)	1.0 (0.5, 2.0)	169.2 (143.7, 199.2)
Ropinirole	540.5 (319.9, 913.2)	>500	407.8 (279.2, 595.7)	>1000	>1000	0.85 (0.79, 0.92)	707.9 (648.2, 773.2)
Tegaserod	347.1 (307.4, 391.9)	20.8 (19.6, 22.1)	>500	7.9 (4.9, 12.9)	1.17 (0.95, 1.43)	0.34 (0.31, 0.38)	5.6 (4.8, 6.4)
Trazodone	>100	55.0 (48.8, 62.1)	ND	>100	ND	67.1 (59.6, 75.7)	67.7 (54.4, 84.4)
Simvastatin	>100	89.3 (65.8, 121.2)	17.2 (13.1, 22.7)	6.4 (5.3, 7.6)	43.4 (37.1, 50.7)	41.3 (35.1, 48.5)	4.3 (2.4, 7.8)





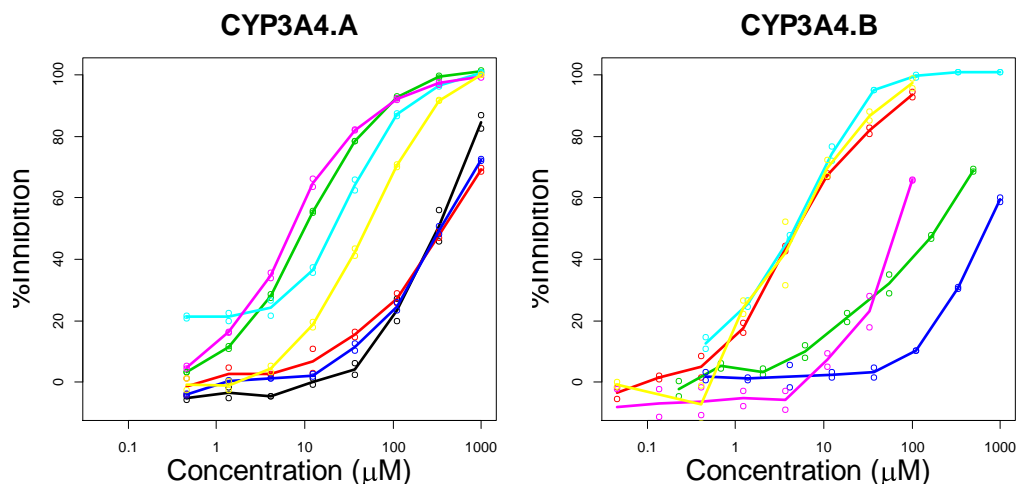


Figure 3-1. Inhibition-concentration curves grouped by CYP. The inhibitions by alprazolam (black), chloroquine (red), duloxetine (green), hydroxychloroquine (dark blue), loratadine (light blue), omeprazole (hot pink) and promethazine (yellow) are shown in panel A for the CYPs tested. The inhibitions by quetiapine (red), risperidone (green), ropinirole (dark blue), tegaserod (light blue), trazodone (hot pink) and simvastatin (yellow) are shown in panel B for the CYPs tested. Each drug was tested in duplicate shown in open circles. The lines connect the average % inhibition values of the two replicates at each concentration.

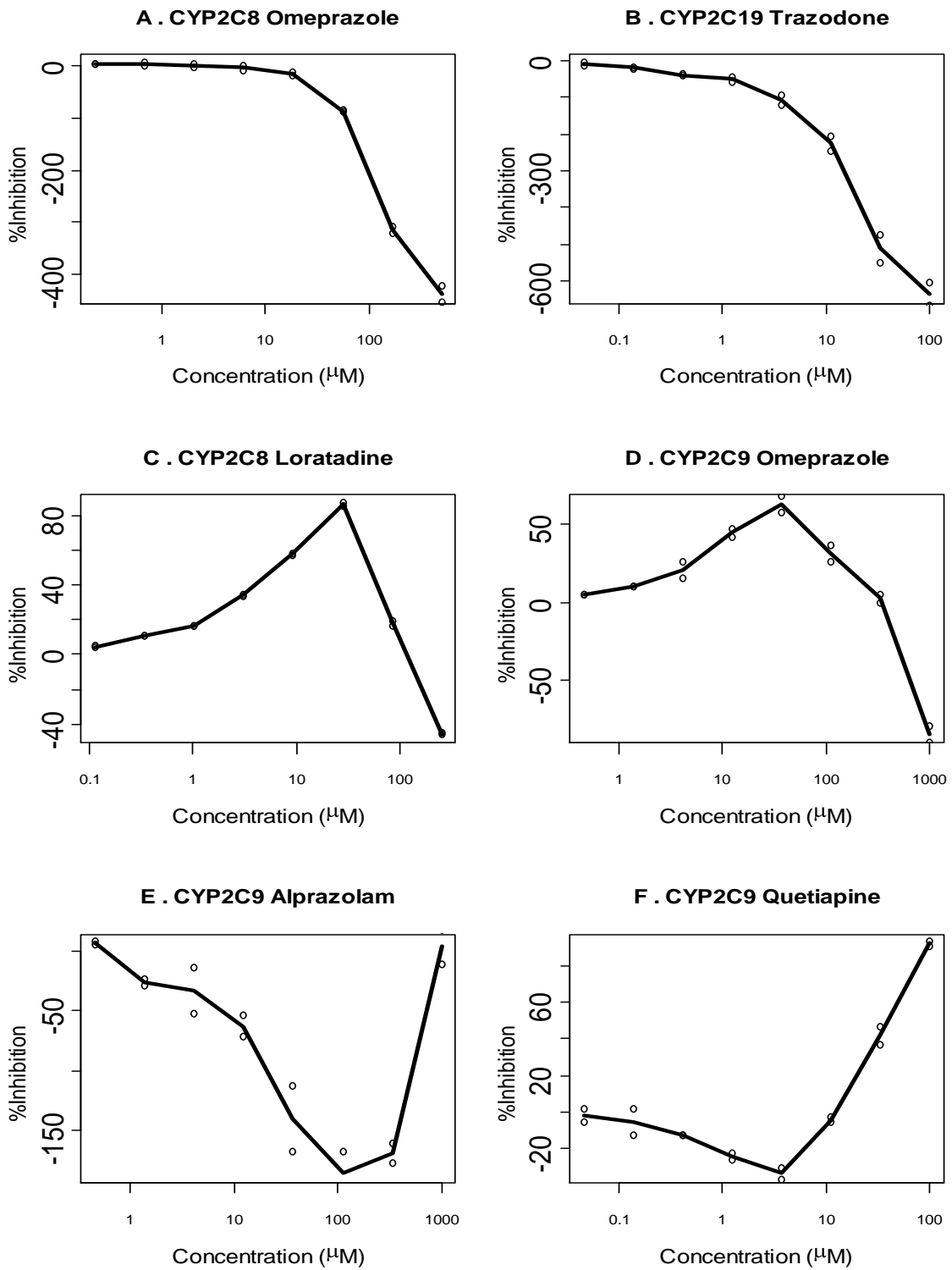
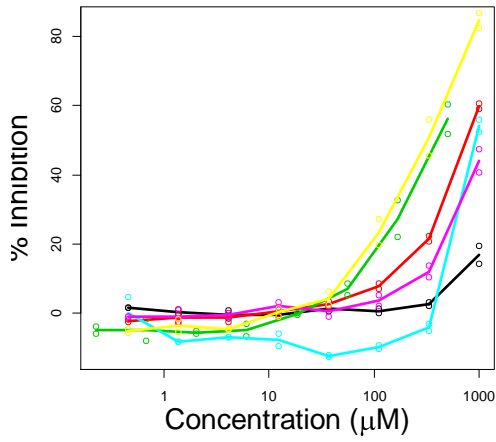
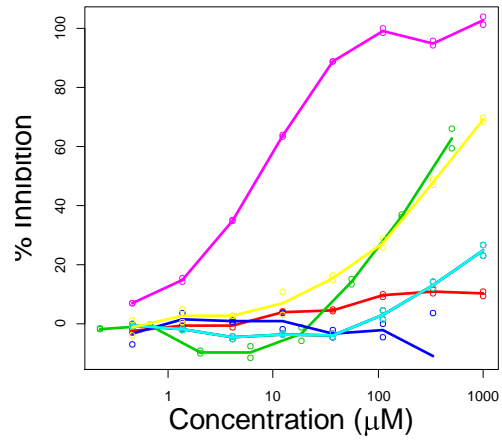


Figure 3-2. Examples of abnormal kinetics observed from fluorometric assays.

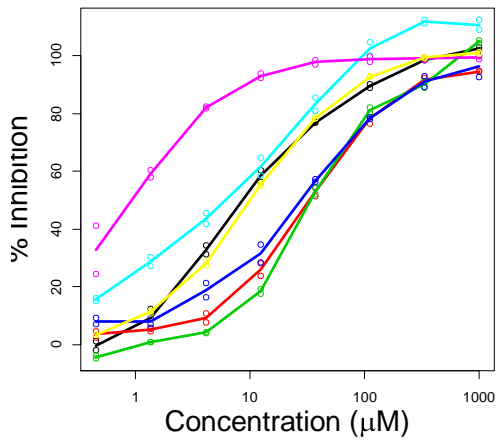
Alprazolam



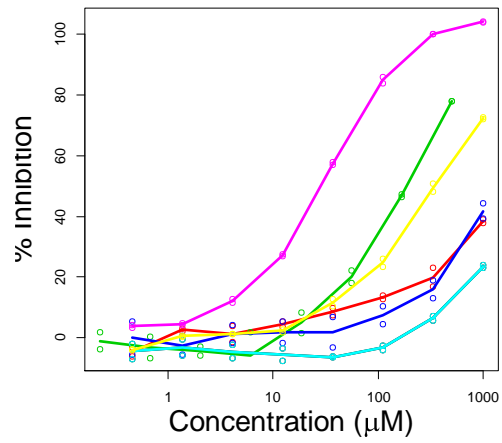
Chloroquine



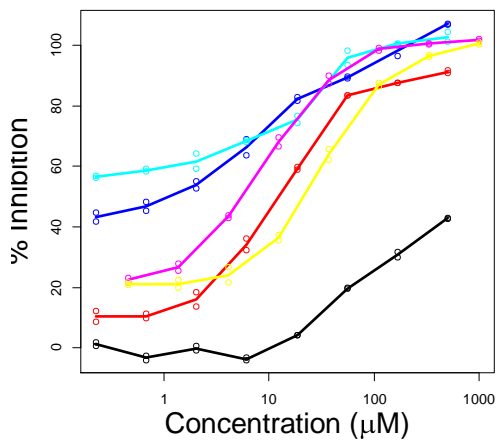
Duloxetine



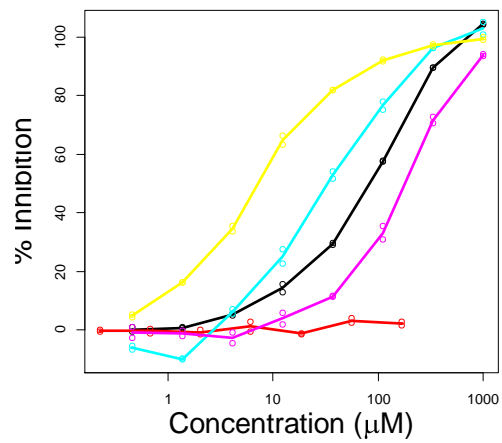
Hydroxychloroquine

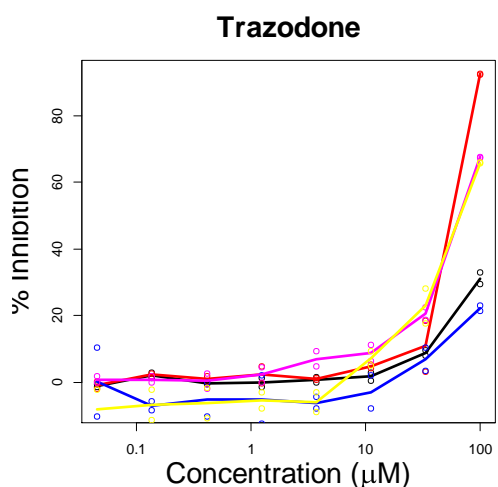
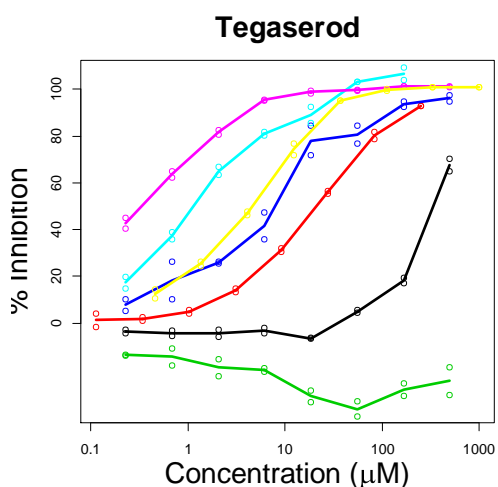
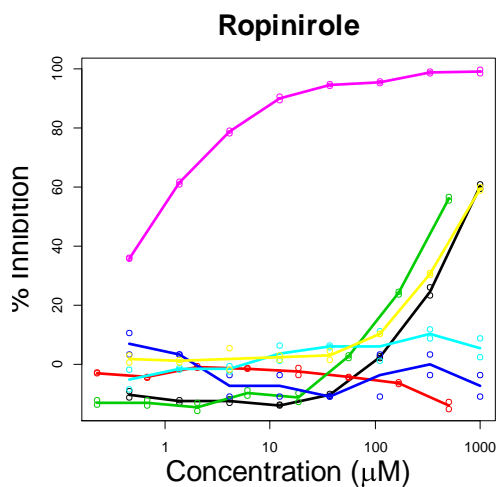
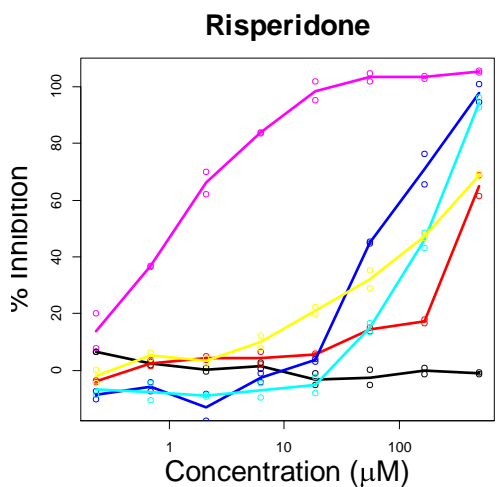
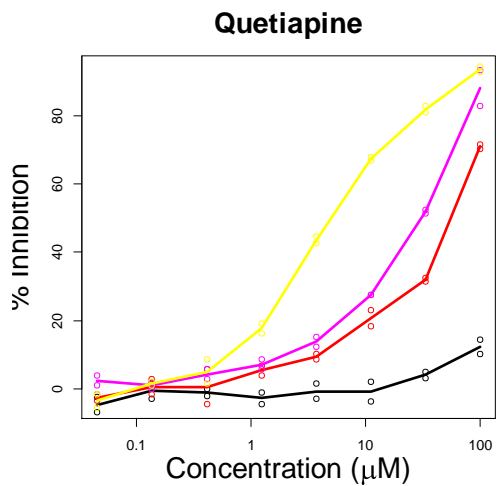
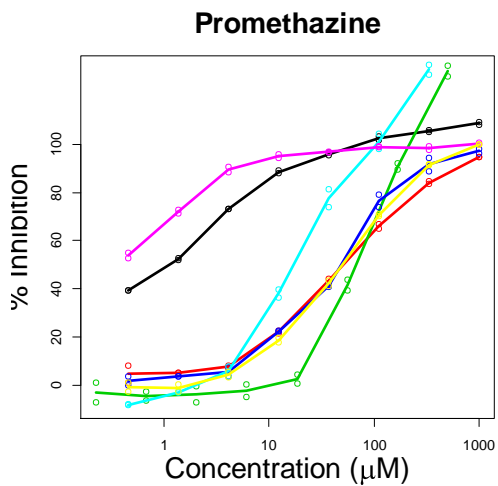


Loratadine



Omeprazole





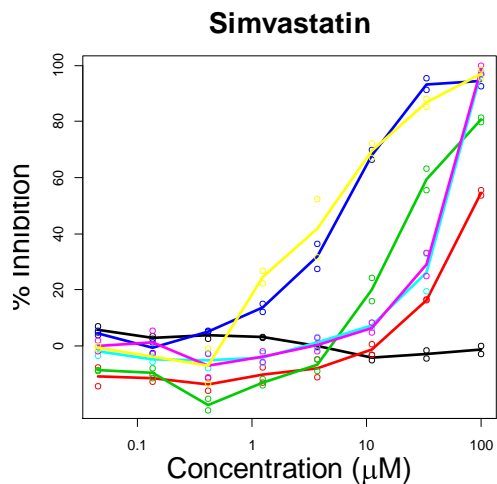


Figure 3-3. Inhibition-concentration curves grouped by drug. The fraction of inhibition is shown for CYP1A2 (black), CYP2B6 (red), CYP2C8 (green), CYP2C9 (dark blue), CYP2C19 (light blue), CYP2D6 (hot pink) and CYP3A4 (yellow) for each individual test drug. Each drug was tested in duplicate with individual values shown in open circles. The lines connect the average % inhibition values of the two replicates at each concentration.

Table 3-3. Mode of inhibition and $K_i \pm SD$ (μM)

	CYP1A2	CYP 2B6	CYP 2C9	CYP 2C19	CYP 2D6	CYP 3A4
Chloroquine					Competitive 20.1 \pm 2.9	
Duloxetine	Competitive 4.7 \pm 0.6			Noncompetitive 2.9 \pm 0.3	Competitive 0.3 \pm 0.03	Competitive 10.5 \pm 0.4
Loratadine		Competitive 2.0 \pm 0.3	Competitive 7.6 \pm 1.0		Competitive 0.5 \pm 0.08	
Promethazine					Competitive 0.25 \pm 0.03	
Quetiapine						Competitive 0.75 \pm 0.07
Risperidone					Competitive 1.62 \pm 0.19	
Ropinirole					Competitive 0.85 \pm 0.09	
Tegaserod			Competitive 11.4 \pm 2.8	Competitive 9.2 \pm 2.8	Competitive 0.51 \pm 0.06	Competitive 5.0 \pm 0.7
Simvastatin			Competitive 18.3 \pm 3.5			Competitive 0.51 \pm 0.1

Table 3-4 Predicted $f_{u,inc}$

Drug	Log D	Log P	Log k_a	$f_{u,inc}$
Chloroquine	1.59	4.412	-0.364	0.698
Duloxetine	2.31	4.809	-0.509	0.763
Loratadine	3.895	3.9	-1.126	0.930
Promethazine	3.4	4.887	-0.867	0.880
Quetiapine	2.51	2.6	-1.119	0.929
Risperidone	1.89	2.678	-1.028	0.914
Ropinirole	0.49	2.486	-0.705	0.835
Simvastatin	4.72	4.7	-1.127	0.931

Table 3-5 Predicted R values

Drug	Pathway	K_i (μM)	f_{u,inc}	K_{i,u} (μM)	C_{max} (ng/ml)	MW (g/mol)	[I] (μM)	R	R > 1.1 or > 11 for 3A4	C_{max} Reference
Quetiapine	3A4	0.75	0.93	0.70	-	383.5	8.344 ¹	12.97	+	-
Simvastatin	3A4	0.51	0.93	0.47	-	418.7	0.764 ²	2.61		-
Duloxetine	2D6	0.3	0.76	0.23	53.2	297.4	0.179	1.78	+	[196]
Chloroquine	2D6	20.1	0.70	14.03	1547	319.9	4.836	1.34	+	[183]
Promethazine	2D6	0.25	0.88	0.22	19.3	284.4	0.068	1.31	+	[197]
Tegaserod	3A4	5	0.92	4.61	-	301.39	0.796 ³	1.17		-
Risperidone	2D6	1.62	0.91	1.48	89.1	410.5	0.217	1.15		[198]
Ropinirole	2D6	0.85	0.84	0.71	26.9	260.4	0.103	1.15	+	[199]
Duloxetine	3A4	10.5	0.76	8.02	-	297.4	0.807 ⁴	1.10		-
Duloxetine	2C19	2.9	0.76	2.21	53.2	297.4	0.179	1.08		[196]
Duloxetine	1A2	4.7	0.76	3.59	53.2	297.4	0.179	1.05		[196]
Loratadine	2D6	0.5	0.93	0.47	4.12	382.9	0.011	1.02		[200]
Tegaserod	2D6	0.51	0.92	0.47	2.7	301.39	0.009	1.02		[201]
Loratadine	2B6	2	0.93	1.86	4.12	382.9	0.011	1.01		[200]
Simvastatin	2C9	18.3	0.93	17.03	25.4	418.7	0.061	1.00		[202]
Loratadine	2C9	7.6	0.93	7.07	4.12	382.9	0.011	1.00		[200]
Tegaserod	2C19	9.2	0.92	8.48	2.7	301.39	0.009	1.00		[201]
Tegaserod	2C9	11.4	0.92	10.51	2.7	301.39	0.009	1.00		[201]

Note:

1. [I] of quetiapine was estimated as the highest proposed clinical dose (800 mg /383.5 g/mol) divided by 250 mL.
2. [I] of simvastatin was estimated as the highest proposed clinical dose (80 mg/418.7 g/mol) divided by 250 mL.
3. [I] of tegaserod was estimated as the highest proposed clinical dose (6 mg/ 301.39 g/mol) divided by 250 mL.
4. [I] of duloxetine was estimated as the highest proposed clinical dose (60 mg/ 297.4 g/mol) divided by 250 mL.

Pathway designates the inhibited CYP isoform; **K_i** is the dissociation constant; **f_{u,inc}** is the fraction of unbound in incubation mixture; **C_{max} (ng/ml)** is the maximal plasma concentration of the inhibitor drug at the highest proposed clinical dose; **MW** is the molecular weight of the inhibitor drug; **[I]** is the inhibitor concentration used for R value prediction, and is equal to the highest proposed clinical dose divided by 250 ml for inhibitors of CYP3A4 or equal to C_{max} otherwise; **R** is the predicted R value.

Table 3-6. Predicted AUCRs

Precipitant Drug	Victim Drug	Pathway	f _m	K _{i,u} (μM)	[I] (μM)	AUCR	RR	P value	[I] Reference	f _m Reference
Quetiapine	Chloroquine	CYP3A4	0.25	0.70	2.82	1.25	2.17	5.29E-05	[203]	[141]
Chloroquine	Duloxetine	CYP2D6	0.65	14.03	4.84	1.20	1.65	1.34E-10	[183]	[204]
Chloroquine	Risperidone	CYP2D6	0.4	14.03	4.84	1.11	3.36	4.47E-05	[183]	[205]
Duloxetine	Chloroquine	CYP2D6	0.16	0.23	0.18	1.08	1.65	1.34E-10	[196]	[141]
		CYP3A4	0.25	8.02						
Duloxetine	Loratadine	CYP2C19	0.2	2.21	0.18	1.08	1.56	7.43E-09	[196]	[206]
		CYP2D6	0.1	0.23						
		CYP3A4	0.7	8.02						
Chloroquine	Quetiapine	CYP2D6	0.11	14.03	4.84	1.03	2.17	5.29E-05	[183]	[207]
Chloroquine	Loratadine	CYP2D6	0.1	14.03	4.84	1.03	2.21	1.27E-05	[183]	[206]
Ropinirole	Loratadine	CYP2D6	0.1	0.71	0.10	1.01	2.05	3.47E-05	[199]	[206]
Chloroquine	Trazodone	CYP2D6	0	14.03	4.84	1.00	1.99	2.23E-05	[183]	[208]
Promethazine	Tegaserod	CYP2D6	0	0.22	0.07	1.00	2.2	1.28E-05	[197]	[168]
Risperidone	Chloroquine	CYP2D6	0	1.48	0.22	1.00	3.36	4.47E-05	[198]	[141]

Note: **Pathway** designates the CYP isoforms that are inhibited by the precipitant drugs; **f_m**, fraction of metabolism carried out by the inhibited CYP pathway; **K_{i,u}**, unbound dissociation constant; **[I]**, the maximal plasma concentration of the precipitant drug at the highest proposed clinical dose; **AUCR**, the predicted ratio of area under plasma concentration-time curve of the victim drug in the presence vs. absence of the precipitant drug; **RR**, the relative risk of myopathy; **P value**, p value of RR.

ii. Investigating mechanisms involved in the interaction between simvastatin and loratadine

1. Introduction

Amongst the fifteen DDIs identified in Chapter 2, the interaction between simvastatin and loratadine was of particular interest. The second part of this chapter is dedicated to the mechanistic investigations on this specific interaction with regard to inhibition of CYP-mediated metabolism by the two drugs.

a. Why is the interaction between simvastatin and loratadine of particular interest?

First, the interaction involves drugs that are both widely prescribed to millions of patients. It may thus be relevant to a large patient population, and have a significant impact on public health. It follows that understanding the mechanism underlying the interaction could also benefit a large number of patients. Simvastatin (trade name Zocor™) is an antihypercholesterolemic agent in the “statin” class of HMG-CoA reductase inhibitors, and is indicated for hyperlipidemia and secondary prevention of coronary heart diseases and cardiovascular events. It has become standard practice to initiate statin therapy immediately after acute coronary syndromes, regardless of lipid levels. Simvastatin is the second-best selling statin of the seven statins currently on the market. Loratadine (trade name Claritin™, Alavert™) is a long-acting, non-sedating tricyclic antihistamine with selective peripheral histamine H₁ – receptor antagonistic activity. It is indicated for the relief of nasal and non-nasal symptoms of seasonal allergic

rhinitis and for the treatment of chronic idiopathic urticarial. Loratadine is one of most prescribed antihistamine [209].

Second, statin-induced myopathy represents a significant barrier to maximizing the benefits of statin therapy and can be exacerbated by DDIs. This compliance-limiting adverse drug reaction occurs in 5-20% of patients treated with statins [210]. Typical features of statin induced myopathy include fatigue, muscle pain, muscle weakness, muscle tenderness, cramping and tendon pain [211]. In 2012, the FDA issued a black box warning against the use of the 80 mg dose of simvastatin because of increased risk of myopathy and rhabdomyolysis with this dose [212]. Concomitant use of drugs that are known to increase the systemic exposure to simvastatin are contraindicated for increased risk of myopathy and rhabdomyolysis. A few examples of these drugs are gemfibrozil, ketoconazole, itroconazole, cyclosporine and danazol [213]. Investigations into the mechanism of the simvastatin-loratadine interaction may help us to identify other drugs interactions with simvastatin, or statins in general, that share similar mechanisms.

Third, myalgia is one of the common side effects of both loratadine and its major pharmacologically metabolite, desloratadine [88, 89]. Investigations on the interaction of simvastatin and loratadine may call public and scientific attention to loratadine-induced myopathy and DDIs that increase the risk for it, thereby potentially improving the outcomes of patients treated with loratadine.

b. Pharmacokinetics and biotransformation of simvastatin

Simvastatin is administered orally as an inactive lactone prodrug at doses of 10, 20 and 40 mg daily. The drug is well absorbed (60 – 85%) but its bioavailability is low

(5%) because of high hepatic extraction (>80%). Food has little effect on absorption or bioavailability of simvastatin. In plasma, 95-98% of the drug is protein-bound [214]. The plasma concentration of simvastatin was 25.4 ± 9.5 ng/mL (0.06 ± 0.02 μ M) following a 80-mg oral dose given once daily for 7 days to healthy adults [202].

Simvastatin lactone is hydrolyzed to the active β -hydroxyl form, simvastatin acid, both in the gastrointestinal tract and in the liver [215, 216]. The lactone and the acid exist in an equilibrium which is both pH- and temperature-dependent. The lactone is hydrolyzed to the acid both chemically and enzymatically by esterase and by paraoxonase, and the acid can be converted back to the lactone [216]. In the liver, both simvastatin and the acid are extensively metabolized. The major metabolites of simvastatin observed in human bile are 3'-hydroxy, 6' β -hydroxy and 6'-carboxy simvastatin [216]. Upon incubation of simvastatin with HLMs, 3'-hydroxy, 6'-exomethylene and 3', 5'-dihydrodiol simvastatin were the major metabolites identified in addition to the acid [217]. CYP3A4/5 were the major enzymes responsible for the metabolism of simvastatin in HLMs, with CYP3A4 exhibiting a 3-fold higher affinity than CYP3A5. TAO, a selective inhibitor of CYP3A4, inhibited the formation of 3'-hydroxy, 6'-exomethylene and 3', 5'-dihydrodiol simvastatin from simvastatin in HLMs by 25%, 75% and 40%, respectively. CYP2E1, and possibly CYP2B6, also contributed to simvastatin metabolism, but to a much less extent [26]. Simvastatin acid is also primarily metabolized by CYP3A (86%) with a minor contribution from CYP2C8 (14%) [218]. Upon incubation with HLMs, 3'-hydroxy, 6'-exomethylene and 3',5'-dihydrodiol simvastatin hydroxyl acid were the major metabolites formed from simvastatin acid [218]. Biotransformation of

simvastatin and the structures of its metabolites are illustrated in Figure 3-4. The kinetics of simvastatin metabolism in HLMs are described in Table 3-7.

Simvastatin is mainly eliminated through hepatic metabolism, with only 13% being renally excreted unchanged. The serum half-life of simvastatin is 2-5 hours, thus the optimal time of dosing is in the evening when hepatic cholesterol synthesis is most active [25-27].

c. Pharmacokinetics and biotransformation of loratadine

Loratadine is given orally at a recommended dose of 10 mg daily. It is rapidly absorbed following a single 10 mg dose. Maximal plasma concentrations are observed 1.3 hours and 2.4 hours after administration for loratadine and its major metabolite, desloratadine, respectively. The C_{max} s of loratadine and desloratadine were 4.1 ± 4.4 ng/mL (10.7 ± 11.4 nM) and 3.9 ± 2.4 ng/mL (12.5 ± 7.7 nM), respectively, following a 10 mg oral dose of loratadine [200]. Food and water intake can improve the bioavailability of loratadine [200]. In the plasma, 95-98% of loratadine is protein-bound.

In the liver, loratadine is extensively metabolized via descarboethoxylation to desloratadine, and by oxidation or glucuronidation. Desloratadine is a pharmacologically active metabolite. The major circulating metabolites of loratadine include 3-hydroxy-desloratadine glucuronide, dihydroxy-desloratadine-glucuronide, and several metabolites resulting from descarboethoxylation and oxidation. Upon incubation of loratadine with HLMs, the major metabolite formed is desloratadine. CYP3A4 is the predominant enzyme (70%) responsible for the conversion of loratadine to desloratadine, followed by CYP2C19 (20%) and CYP2D6 (10%) [206]. Desloratadine itself is eliminated by further

metabolism. Biotransformation of loratadine and the structures of its metabolites are illustrated in Figure 3-5.

Approximately 84% of a 10 mg dose of loratadine was excreted into urine (41%) and feces (43%) in the form of metabolites within 10 days after oral administration. The half-life of loratadine is 8 hours, while that of desloratadine is 28 hours [209].

d. Mechanisms of DDIs with simvastatin or loratadine

Almost all the clinically significant DDIs with simvastatin that have been documented are pharmacokinetic, with the one exception being ezetimibe. Ezetimibe enhances the cholesterol-lowering effect of simvastatin in humans by selectively inhibiting dietary cholesterol absorption in the gastrointestinal tract [219]. One of the major mechanisms underlying the pharmacokinetic DDIs with simvastatin is inhibition of simvastatin metabolism. Drugs that are strong inhibitors of CYP3A4, including certain antifungal medications (itraconazole, ketoconazole, posaconazole) and macrolide antibiotics (erythromycin, clarithromycin, telithromycin) as well as HIV protease inhibitors, have been found to significantly increase the systemic exposure to simvastatin and are contraindicated with any dose of the drug. For example, erythromycin increased the AUC of simvastatin and simvastatin acid by 6.2-fold and 3.9-fold, respectively [220]; the AUC of simvastatin was 3059% higher in the presence of ritonavir/saquinavir compared to that of simvastatin alone [221]; posaconazole increased the AUC of simvastatin by 5- to 11-fold and that of simvastatin acid by 5- to 8-fold during co-administration [222]. Some other drugs that inhibit CYP3A4 to a lesser extent are contraindicated with certain higher doses of simvastatin. These examples include

verapamil, diltiazem, amlodipine, ranolazine, amiodarone, dronedarone and ticagrelor. Since the incidence of statin-induced myopathy is dose-dependent, it is not surprising that the risk of myopathy in patients treated with simvastatin is higher during concomitant use of the above mentioned drugs. Patients receiving 20 to 80 mg of simvastatin daily were found to be 10-times more likely to experience myopathy with co-administration of verapamil than those without co-administration of verapamil [223].

As is the case for simvastatin, DDIs with loratadine are mostly due to inhibition of its metabolism. Loratadine has been found to interact with CYP3A4 inhibitors such as ketoconazole [224], clarithromycin [200], nefazodone [225] and cimetidine[224], which lead to a significantly increased systemic exposure to loratadine. The AUC of loratadine and desloratadine was increased by 76% and 49%, respectively, after coadministration with clarithromycin [200]. The plasma concentrations of loratadine and desloratadine were increased by 307% and 73%, respectively, after coadministration with ketoconazole [224]. Nefazodone increased the AUCs of loratadine and desloratadine by 39% and 12%, respectively. Moreover, the increased exposure to loratadine by nefazodone was associated with marked QTc prolongation that was correlated with loratadine plasma concentration [225]. These studies clearly demonstrate that CYP3A4 inhibitor drugs can significantly increase the systemic exposure to loratadine, thereby increasing the risk of adverse reactions to loratadine.

e. Hypothesis and aims

I wish to test the hypothesis that the interaction of simvastatin and loratadine is due, in part, to inhibition of metabolism, thereby leading to an increase in the systemic

exposure to either or both drugs and thus an increased risk of myopathy. To test this hypothesis, the following aims were pursued:

- 1) Assess *in vitro* to what extent loratadine and its active metabolite, desloratadine, inhibit the metabolism of simvastatin and its active form, simvastatin acid, through incubation with HLMs;
- 2) Assess *in vitro* to what extent simvastatin and simvastatin acid inhibit the metabolism of loratadine and desloratadine through incubation with HLMs.

2. Methods

a. Materials

All the drugs and the metabolites were purchased from Toronto Research Chemicals (North York, Ontario, Canada). Glucose-6-phosphate, NADP and glucose-6-phosphate dehydrogenase, acetonitrile (HPLC grade), methanol (HPLC grade), ammonium acetate and ammonium formate were purchased from Sigma-Aldrich (St. Louis, MO). Pooled human liver microsomes (HLMs) from 50 donors were purchased from BD Biosciences (Wobum, MA).

b. Incubation with HLMs

The drugs were dissolved and diluted in methanol to desired concentrations and were dried in a speed vacuum, followed by the addition of 200 mM potassium phosphate reaction buffer (pH 7.4) and HLMs. After pre-warming at 37 °C in a water bath for 5 min, reactions were initiated with the addition of a NADPH-regenerating system consisting of 1.3 mM NADP⁺, 3.3 mM glucose-6-phosphate, 3.3 mM MgCl₂, and 0.4 U/mL glucose-

6-phosphate dehydrogenase. In the negative control samples, the NADPH-regenerating system was replaced with the same volume of potassium phosphate reaction buffer. The final volume of the reaction mixture was 250 μL . The mixture was then incubated at 37 $^{\circ}\text{C}$ for an additional length of time that allows the reaction to be linear. The reaction was stopped with the addition of 500 μL ice-cold acetonitrile, followed by vigorous vortex-mixing.

c. Sample preparation

25 μL of internal standard (1 μM lovastatin for simvastatin and simvastatin acid, 1 μM fluoxetine for loratadine) were added to each sample. After brief centrifugation, the liquid phase was transferred to a disposable clean capped glass tube. Next, 500 μL of 100 mM ammonium acetate (pH 4.5) and 6 mL of hexane/ethyl acetate (50/50, v/v) were added to the samples of simvastatin and simvastatin acid; and 500 μL of glycine/NaOH and 6 mL of hexane/ethyl acetate (50/50, v/v) were added to the samples of loratadine. The samples were agitated for 15 min on a shaker, followed by centrifugation at 13,000 rpm and 4 $^{\circ}\text{C}$ for 10 min. The upper organic phase was transferred to a clean glass culture tube and was dried in a speed vacuum. The samples were reconstituted with 100 μL of mobile phase, and 80 μL were injected into the LC/MS/MS for analysis.

d. Analytical methods using LC/MS/MS

LC/MS/MS assays were developed for quantification of simvastatin, simvastatin acid and desloratadine. The MS/MS system was an API2000 MS/MS triple quadrupole system (Applied Biosystems, Foster City, CA) equipped with a turbo ion spray, coupled

with a Shimadzu (Columbia, MD) HPLC system consisting of an LC-20 AB pump and SIL-20A HT auto-sampler (Applied Biosystems/MDS Sciex, Foster City, CA), operating under Analyst 1.5.1 software. A flow rate of 0.3 mL/min was used for sample analysis on a Sonoma C₈ (West Berlin, NJ) analytical column (3 μ, 100 Å, 7.5 cm X 4.6 mm). The column was maintained at ambient temperature (~23 °C), while the auto-sampler temperature was set at 25 °C.

For quantification of simvastatin and simvastatin acid, an isocratic HPLC elution mobile phase was used, consisting of 85% acetonitrile and 15% ammonium acetate 5 mM (v/v). Lovastatin served as the internal standard. The turbo ionspray source temperature was optimized at 550 °C. The analytes were detected by monitoring the precursor→product ion transition using multiple reaction monitoring (MRM) scan mode. For simvastatin quantification, the MRM was performed at m/z 419.425→119.2 for simvastatin and 405.4→199.1 for lovastatin. Results were obtained using the following settings: curtain gas at 12, collision gas at 3, nebulizer gas (GS1) at 44, the turbo ionspray gas (GS2) at 35 and ionspray voltage at 5000. For simvastatin acid quantification, the MRM was performed at m/z 437.4→199.2 for simvastatin acid and 405.4→199.1 for lovastatin. Results were obtained using the following settings: curtain gas at 16, collision gas at 4, nebulizer gas (GS1) at 48, turbo ionspray gas (GS2) at 35 and ionspray voltage at 5500. The peak area was measured, and the peak area ratio of drug to internal standard and the concentration were calculated using Analyst 1.5.1 software. The limit of quantification was 50 nM for both simvastatin and simvastatin acid. The chromatography of simvastatin and simvastatin acid are presented in panel A and B of Figure 3-6.

For quantification of desloratadine, the mobile phase consisted of 85% methanol and 15% 25 mM ammonium formate. Fluoxetine served as the internal standard. The turbo ionspray source temperature was optimized at 500 °C. The MRM was performed at m/z 311.2→258.9 for desloratadine and 310.3→44.0 for fluoxetine. Results were obtained using the following settings: curtain gas at 14, collision gas at 6, nebulizer gas (GS1) at 40, turbo ionspray gas (GS2) at 30 and ionspray voltage at 5500. The peak area was measured, and the peak area ratio of drug to internal standard and the concentration were calculated using Analyst 1.5.1 software. The limit of quantification for desloratadine was 25 nM. The chromatography of desloratadine is presented in panel C of Figure 3-6.

3. Original experimental results

a. Inhibition of simvastatin and simvastatin acid metabolism by loratadine and desloratadine

I hypothesize that loratadine and/or desloratadine inhibit the hepatic metabolism of simvastatin and/or simvastatin acid, thereby increasing the systemic exposure to simvastatin and/or simvastatin acid. To test this hypothesis, I first examined *in vitro* the CYP inhibition profile of loratadine and desloratadine using fluorometric assays, in order to assess whether or not they have potential to inhibit the metabolism of simvastatin and simvastatin acid. Then I evaluated the impact of loratadine and desloratadine on the hepatic metabolism of simvastatin and simvastatin acid in a more physiologically relevant system, HLMS.

1) *Inhibition profiles of loratadine and desloratadine for the major CYPs*

Using fluorometric assays, the IC_{50} s of loratadine and desloratadine for the major CYPs were evaluated and are shown in Table 3-8. The IC_{50} of CYP2C8 could not be determined because of abnormal kinetics. Consistent with the previous definitions on inhibitory potency, the inhibitors with IC_{50} s less than 20 μ M were considered as relatively potent, those with IC_{50} s between 20 μ M and 200 μ M were considered as relatively moderate, and those with IC_{50} s greater than 200 μ M were considered as relatively weak. Loratadine was therefore a relatively potent inhibitor of CYP2D6, CYP2C9 and CYP2B6, a relatively moderate inhibitor of CYP2C19 and CYP3A4, and a relatively weak inhibitor of CYP1A2. Desloratadine exhibited relatively potent inhibition for CYP2D6 and CYP 3A4, relatively moderate inhibition for CYP2B6 and CYP 2C19, and relatively weak inhibition of CYP1A2 and CYP 2C9. The inhibitions, particularly those involving CYP3A4, indicated that both loratadine and desloratadine have the potential to inhibit the metabolism of simvastatin and simvastatin acid.

2) *IC_{50} s of loratadine and desloratadine for the depletion of simvastatin and simvastatin acid in HLMs*

Because both simvastatin and simvastatin acid are converted into multiple metabolites, measuring disappearance of substrate is preferred over monitoring metabolite formation as an approach to evaluating the rate of metabolism.

I first defined the experimental conditions under which the initial reaction velocity is linear. Upon incubation of 1 μ M simvastatin with 0.05 or 0.1 mg/ml HLMs for up to 30 min, simvastatin disappeared from the incubation mixture linearly for up to 10

min at both the HLM concentrations (Figure 3-7 A). Similarly, incubation of simvastatin acid with 0.2 or 0.4 mg/ml HLM showed that the metabolism was linear for up to 20 min (Figure 3-7 B). Since a sufficient amount of substrate needs to be depleted to detect an inhibition, in the subsequent incubations, simvastatin was incubated with 0.1 mg/ml HLMs for 10 min, and simvastatin acid was incubated with 0.4 mg/ml HLMs for 20 min.

To test whether loratadine and desloratadine inhibit the metabolism of simvastatin in HLMs, a single concentration of simvastatin was incubated with various concentrations of loratadine or desloratadine. Ketoconazole was used as a control inhibitor because it is well known to inhibit CYP3A4 and simvastatin metabolism. The IC_{50} s (95% CI) of loratadine, desloratadine and ketoconazole for simvastatin metabolism were 20.3 (11, 37.1) μ M, 12.3 (4.6, 33.2) μ M, and 1.7 (1.1, 2.8) μ M, respectively (Figure 3-8 A, C, E). Similarly, the effects of these drugs on the metabolism of simvastatin acid were evaluated. The IC_{50} s (95% CI) were 129.5 (75, 223.4) μ M, 86.0 (38.1, 194.3), and 0.48 (0.17, 1.38) μ M for loratadine, desloratadine and ketoconazole, respectively (Figure 3-8 B, D, F). The IC_{50} s suggested that loratadine and desloratadine had a greater impact on the hepatic metabolism of simvastatin than on that of simvastatin acid. In addition, desloratadine had more potential than loratadine to inhibit the metabolism of both simvastatin and simvastatin acid, consistent with its smaller IC_{50} for CYP3A4.

b. Inhibition of loratadine metabolism by simvastatin and simvastatin acid

I hypothesize that simvastatin and/or simvastatin acid inhibit the hepatic metabolism of loratadine, thereby increasing the systemic exposure to loratadine. Using the same approach, I tested this hypothesis first using CYP fluorometric assays to assess

whether or not simvastatin and simvastatin acid is able to inhibit loratadine metabolism. I then evaluated the impact of simvastatin and simvastatin acid on the hepatic metabolism of loratadine in HLMs.

1) Inhibition profiles of simvastatin and simvastatin acid for the major CYPs

Using fluorometric assays, the IC_{50} s of simvastatin and simvastatin acid that were estimated for the major CYPs are shown in Table 3-9. Simvastatin showed a relatively potent inhibition for CYP3A4, CYP2C9 and 2C8, relatively mild inhibition of CYP2D6, CYP2C19 and CYP2B6 and no inhibition of CYP1A2 at concentrations up to 100 μ M. Simvastatin acid showed a relatively potent inhibition of CYP3A4, a relatively mild inhibition for CYP2C8 and 2C9, and no effect on the other isoforms at concentrations up to 100 μ M.

2) IC_{50} s of simvastatin and simvastatin acid for desloratadine formation in HLMs

Because desloratadine is the major metabolite of loratadine, its formation rate was used to evaluate inhibition of loratadine metabolism. Since the K_m and V_{max} of loratadine metabolism had not been reported, I first investigated the kinetics of loratadine metabolism in HLMs in order to optimize experimental conditions for accurate estimation of inhibitory potency. Upon incubation of 50 μ M loratadine with 0.1 mg/ml HLMs for up to 60 min, the initial reaction velocity measured by the formation of desloratadine was found to be linear for up to 10 min (Figure 3-9 A). The metabolism of loratadine in HLMs exhibited typical Michaelis-Menten kinetics with a K_m of 0.90 ± 0.23 μ M and a V_{max} of 4.41 ± 0.25 nmol/min/mg HLMs (Figure 3-9 B).

To test whether simvastatin and simvastatin acid inhibit loratadine metabolism in HLMs, a single concentration of loratadine was incubated with various concentrations of simvastatin or simvastatin acid. The IC_{50} s (95%CI) of simvastatin and simvastatin acid for desloratadine formation was 8.2 (4.9, 13.8) μ M and 11.8 (6.8, 20.5) μ M, respectively (Figure 3-10).

3) *Mode of inhibition and K_i estimates*

Upon incubation of loratadine at various concentrations, both the inhibition by simvastatin and that by simvastatin acid were identified as noncompetitive with K_i s of 6.9 ± 0.8 μ M and 18.0 ± 3.6 μ M, respectively (Figure 3-11).

4. Discussion

During this work, I have addressed the hypothesis that the interaction of simvastatin and loratadine was due, in part, to the mutual inhibition of their metabolism. I found that both loratadine and desloratadine were able to inhibit the major CYP isoform involved in simvastatin metabolism - CYP3A4. They could also inhibit the metabolism of its active metabolite, simvastatin acid. To confirm these inhibitory effects, I further examined the metabolism of simvastatin and simvastatin acid in the presence of loratadine and desloratadine in pooled HLMs. I found that loratadine and desloratadine inhibited the depletion of simvastatin with IC_{50} s of 20.3 μ M and 12.3 μ M, respectively, and that of simvastatin acid with IC_{50} s of 129.5 μ M and 86.0 μ M, respectively. Assuming that these inhibitions are reversible, K_i s of these inhibitory reactions can be approximated using $IC_{50} / (1 + [S] / K_m)$. Given that these experiments were carried out at a substrate

concentration (1 μM) that was far below the K_m ($> 20.9 \mu\text{M}$ for simvastatin and $> 47 \mu\text{M}$ for simvastatin acid), the K_{iS} can be approximated by the IC_{50S} since $[S] / K_m$ approaches zero in these cases.

Because the IC_{50S} determined in HLMs represent the inhibitory potential for the total metabolism of the substrates, $R = 1 + [I]/K_{i,u}$ can be applied to estimate the ratio of total intrinsic clearance in the presence and absence of the inhibitor drugs. An R value in such cases can also be interpreted as a crude estimate of the change in the AUC of the substrate. With respect to the metabolism of simvastatin and simvastatin acid, the predicted R values of loratadine and desloratadine were close to unity due to the low circulating plasma concentrations (Table 3-10). These data imply that the inhibitory effects of loratadine and desloratadine on the metabolism of simvastatin and simvastatin acid observed *in vitro* are unlikely to produce any significant clinical consequences.

Using a similar approach, I also tested the effects of simvastatin and simvastatin acid on the metabolism of loratadine. Both simvastatin and simvastatin acid exhibited inhibition for the major CYPs, especially for CYP3A4, the isoform primarily responsible for loratadine metabolism, suggesting a possible inhibition of loratadine metabolism *in vivo*. The follow-up experiments using HLMs showed that simvastatin and simvastatin acid were able to inhibit the metabolism of loratadine to desloratadine with IC_{50S} of 8.2 μM and 11.8 μM , respectively. Both inhibitory reactions were further identified as noncompetitive with K_{iS} of 6.9 μM and 3.6 μM . The R values predicted for simvastatin and simvastatin acid, assuming the C_{max} of simvastatin acid equal to that of simvastatin (0.06 μM), were also close to unity (Table 3-10), indicating that the exposure to loratadine would not be significantly different with coadministration of simvastatin.

These data together suggest that inhibition of metabolism is unlikely to be an important mechanism underlying the interaction between simvastatin and loratadine observed in the population studies carried out as part of this work.

Table 3-7. Kinetics of simvastatin and simvastatin acid metabolism in HLMs [217, 218].

Metabolite	Simvastatin			Simvastatin Acid		
	3'-Hydroxy	6'-Exomethylene	3', 5'-Dihydrodiol	3'-Hydroxy	6'-Exomethylene	3', 5'-Dihydrodiol
K_m (μM)	20.9 ± 7.8	36.2 ± 15.5	35.0 ± 5.6	47 ± 12	47 ± 21	76 ± 35
V_{max} (pmol/min/mg)	2066.1 ± 799.5	1293.4 ± 447.1	2536.1 ± 1124.1	0.86 ± 0.26	0.59 ± 0.16	1.9 ± 1.8
CL_{int} (ml/min/mg)	0.098 ± 0.007	0.037 ± 0.011	0.072 ± 0.026	0.02 ± 0.01	0.015 ± 0.01	0.02 ± 0.01

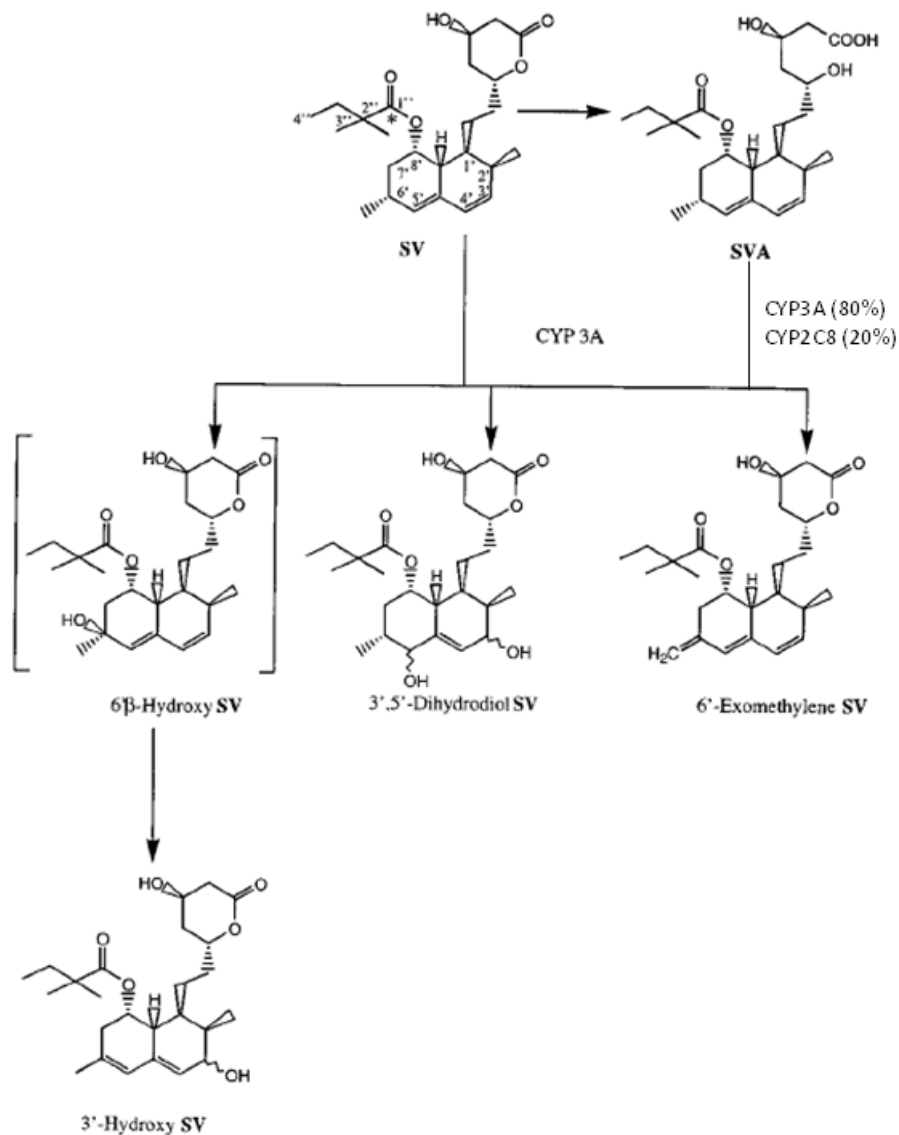


Figure 3-4. Biotransformation of simvastatin in humans [216, 218]. Note that the metabolism of simvastatin and simvastatin acid exists in parallel. The figure shows only the structures of simvastatin metabolites. Those of simvastatin acid metabolites are similar except that the lactone is replaced by an open acid.

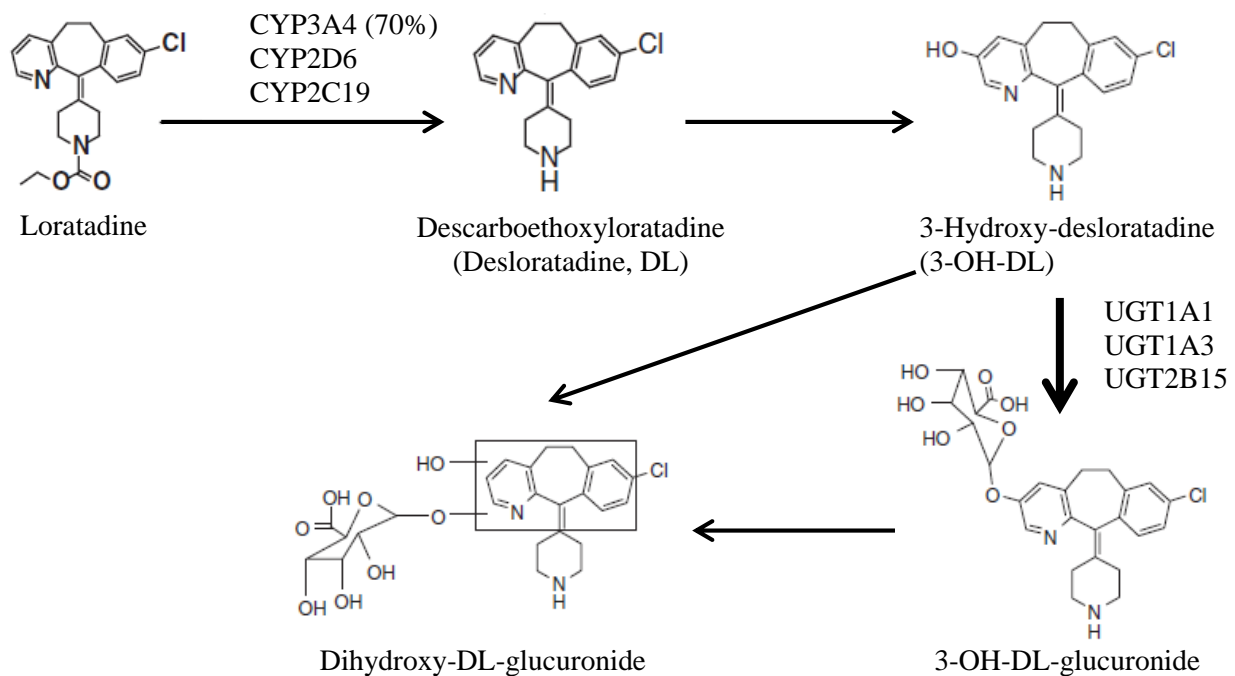


Figure 3-5. Biotransformation of loratadine in humans [209, 226].

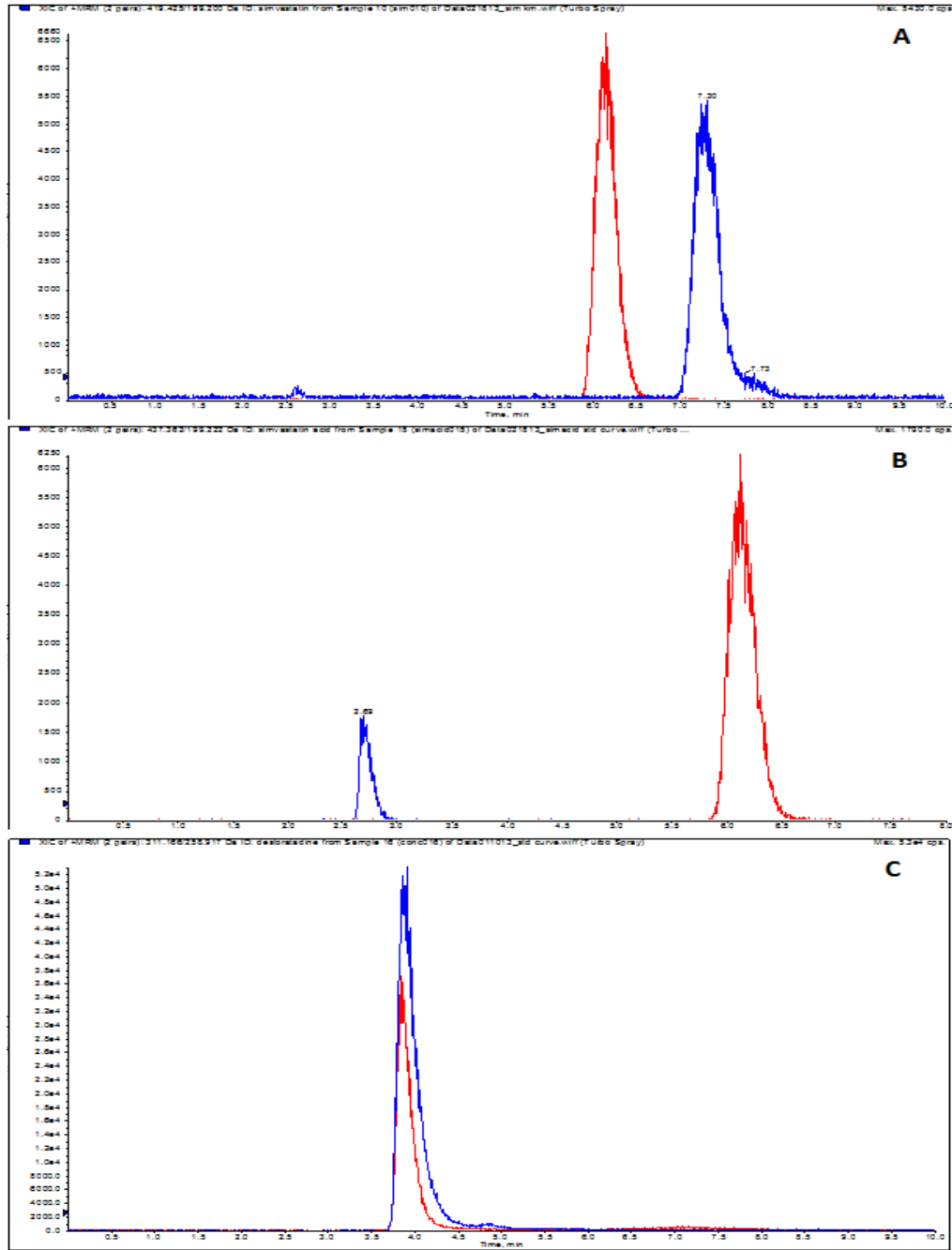


Figure 3-6. Chromatography of simvastatin (A), simvastatin acid (B) and desloratadine (C). Lovastatin served as the internal standard for simvastatin and simvastatin acid, and fluoxetine served as the internal standard for desloratadine. The analytes and the internal standards are shown in blue and red, respectively.

Table 3-8. IC₅₀s of loratadine and desloratadine for the major CYPs

	IC ₅₀ (95% CI, μM)						
	1A2	2B6	2C8	2C9	2C19	2D6	3A4
Loratadine	630 (438, 906.3)	11.9 (9.9, 14.4)	ND	12.35 (7.8, 19.45)	21.3 (15.3, 29.7)	9.1 (8.3, 9.9)	33.2 (30.1, 36.6)
Desloratadine	506.6 (397.2, 646.3)	29.3 (25.8, 33.4)	ND	158.9 (107.1, 235.7)	59.0 (43.2, 80.7)	14.0 (13.2, 14.9)	19.2 (17.6, 21.0)

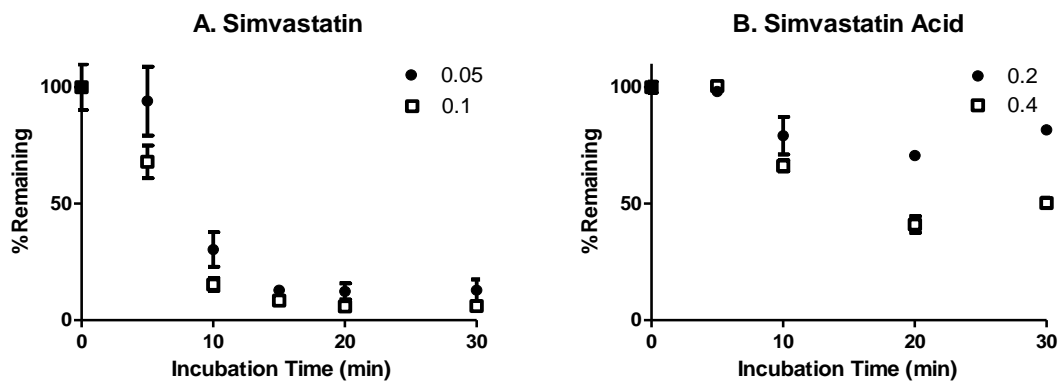


Figure 3-7. Depletion of simvastatin (A) and simvastatin acid (B) in relation to incubation time and HLM concentration. 1 μ M simvastatin was incubated with 0.05 (\bullet) and 0.1 (\square) mg/ml HLMs and disappeared linearly up to 10 min. 1 μ M simvastatin acid was incubated with 0.2 (\bullet) and 0.4 (\square) mg/ml HLMs and disappeared linearly also up to 10 min.

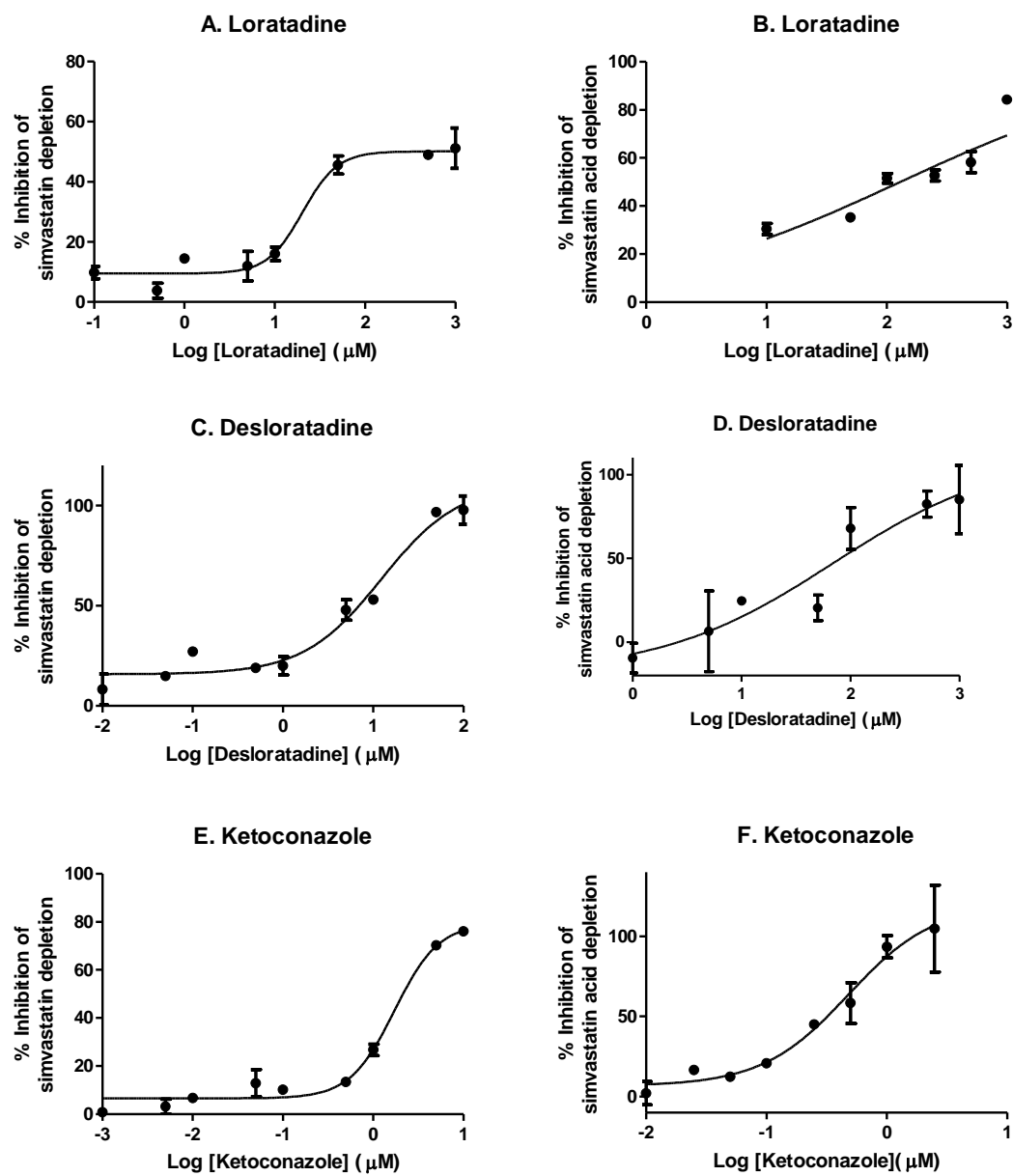


Figure 3-8. Inhibition of simvastatin (A, C, E) and simvastatin acid (B, D, F) metabolism in HLMs by loratadine (A and B), desloratadine (C and D), and ketoconazole (E and F).

Table 3-9. IC₅₀s of simvastatin and simvastatin acid for the major CYPs

	IC ₅₀ (95% CI, μM)						
	1A2	2B6	2C8	2C9	2C19	2D6	3A4
Simvastatin	>100	89.3 (65.8, 121.2)	17.2 (13.1, 22.7)	6.2 (5.4, 7.0)	43.4 (37.1, 50.7)	41.3 (35.1, 48.5)	3.1 (1.4, 7.2)
Simvastatin acid	>100	>100	50.7 (14.3, 179.7)	96.6 (53.5, 174.4)	>100	>100	10.7 (4.9, 23.3)

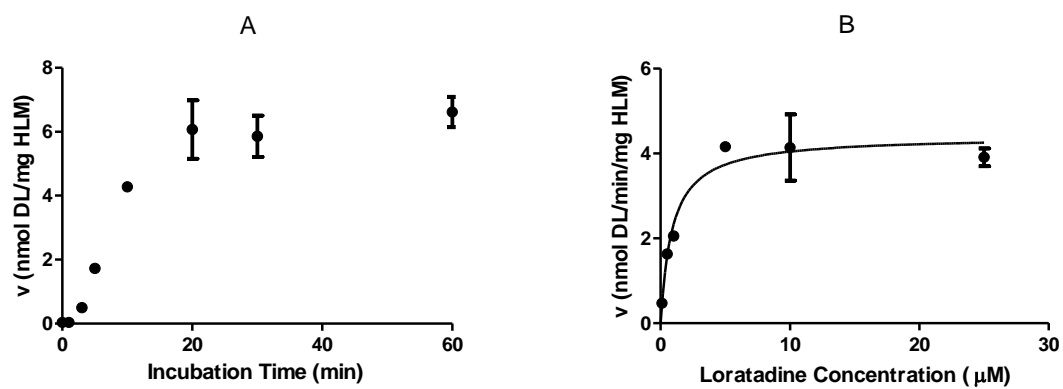


Figure 3-9. Kinetics of loratadine metabolism in HLMs. The metabolism of loratadine was linear for up to 10 min (A). The Michaelis-Menten kinetics of loratadine metabolism in HLMs is shown in (B). DL, desloratadine.

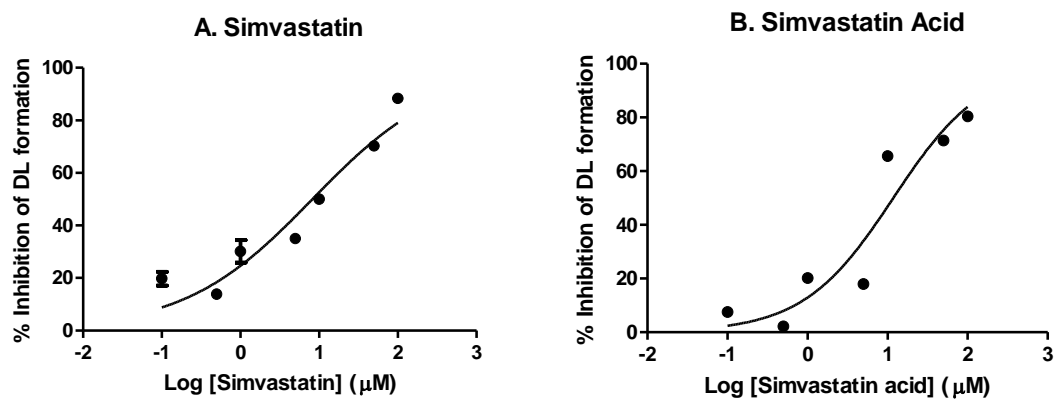


Figure 3-10. IC₅₀ curves of the inhibition of desloratadine (DL) formation by simvastatin (A) and simvastatin acid (B) in HLMs.

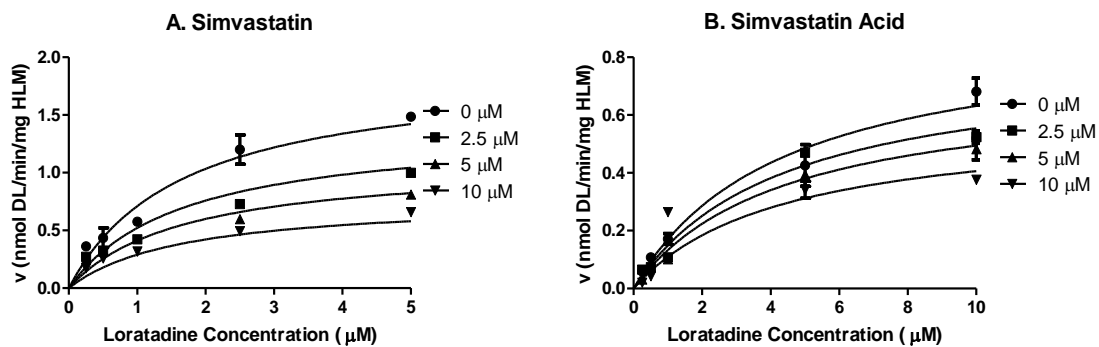


Figure 3-11. K_i s for the inhibition of desloratidine formation by simvastatin (A) and simvastatin acid (B) in HLMs.

Table 3-8 Predicted R values

Precipitant Drug	Victim Drug	K _i (μM)	f _{u,inc}	K _{i,u} (μM)	C _{max} (ng/ml)	MW (g/mol)	C _{max} (μM)	R value	C _{max} Reference
Loratadine	Simvastatin	20.3	0.93	18.89	4.12	382.9	0.01	1.00	[200]
Desloratadine	Simvastatin	12.3	0.73	9.02	3.89 ¹	310.8	0.01	1.00	[200]
Desloratadine	Simvastatin	12.3	0.73	9.02	4.69 ²	310.8	0.02	1.00	[227]
Loratadine	Simvastatin Acid	129.5	0.93	120.48	4.12	382.9	0.01	1.00	[200]
Desloratadine	Simvastatin Acid	86	0.73	63.08	3.89	310.8	0.01	1.00	[200]
Desloratadine	Simvastatin Acid	86	0.73	63.08	4.69	310.8	0.02	1.00	[227]
Simvastatin	Loratadine	6.9	0.93	6.42	25.4	418.7	0.06	1.01	[202]
Simvastatin Acid	Loratadine	3.6	0.93	3.35	25.4	436.6	0.06	1.02	[202]

Note:

1. Peak plasma concentration observed following a 10 mg oral dose of loratadine.
2. Peak plasma concentration observed following a 5 mg oral dose of desloratadine.

K_i designates the dissociation constant determined *in vitro*, and is approximated by the IC₅₀ for the inhibition of simvastatin and simvastatin acid; **f_{u,inc}**, the fraction of unbound in incubation mixtures; **K_{i,u}**, unbound dissociation constant estimated by $K_i * f_{u,inc}$; **C_{max}**, the maximal plasma concentration of the precipitant drug at the highest proposed clinical dose; **MW**, the molecular weight of the precipitant drug; **R value** is estimated as $R = 1 + [I]/K_{i,u}$.

Chapter 4. *In vitro* assessment of inhibition of OATPs

1. Introduction

a. Role of transporters in drug disposition

Approximately 900 transporter genes have been annotated in the human genome [228]. They encode for transporter proteins that are responsible for influx of essential nutrients and ions and the efflux of toxins, drugs and other xenobiotics. Transporter proteins thought to be involved in the pharmacokinetics and pharmacodynamics of drugs are from two superfamilies - the solute carrier (SLC) superfamily and the adenosine triphosphate (ATP) - binding cassette (ABC) superfamily [229]. Transporters important to pharmacokinetics generally are located in intestinal, renal and hepatic epithelia as well as in the endothelium of the blood-brain barrier, where they control the tissue distribution, selective absorption and elimination of drugs across cell membranes [83].

Transporters that belong to the ABC superfamily rely on ATP hydrolysis to actively pump their substrates across the cell membrane. There are 49 genes that have been identified encoding ABC proteins that can be grouped into seven families from ABCA to ABCG [230]. Many ABC transporters mediate the efflux of drugs and their metabolites from the intracellular space of the epithelial cells. They prevent xenobiotics from reaching vital organs such as the brain, the cerebrospinal fluid, the testis and the fetus. Active efflux via ABC transporters thus acts as a defense mechanism that the body uses to decrease exposure to potentially toxic xenobiotics. On the other hand, ABC transporter-mediated active efflux impairs the absorption and distribution of drugs to their target sites. P-glycoprotein (P-gp, ABCB1) and breast cancer resistance protein

(BCRP, ABCG2) expressed on the intestinal luminal membrane reduce drug absorption by pumping drug molecules that have entered enterocytes back into the gastrointestinal lumen. P-gp, BCRP and multidrug resistance proteins (MRPs) expressed in brain capillary endothelial cells prevent the drugs from passing the blood-brain barrier [36, 231]. Overexpressing efflux ABC transporters such as P-gp and BCRP is one of the mechanisms employed by cancer cells to develop resistance to chemotherapy. In addition, efflux via ABC transporters across the canalicular membrane of hepatocytes and the luminal membrane of kidney proximal tubule is an important mechanism for hepatobiliary and renal excretion of drugs and their metabolites [36, 83].

Transporters in the SLC superfamily mediate facilitated diffusion and active transporter of a variety of ions, endogenous compounds and xenobiotics. There are 315 genes annotated for SLC transporter proteins in the human genome, which are grouped into 48 families [231]. Many SLC transporters serve as drug targets, including serotonin (5-HT) transporter and dopamine transporters. Some other SLC transporters, such as ones from *SLCO*, *SLC15*, *SLC22* and *SLC47* families, have been shown to play a role in the absorption, distribution and excretion of drugs and clinical DDIs [36]. For example, organic anion transporting polypeptides (OATPs) and peptide transporter 1 (PEPT1) expressed in the intestinal apical membrane mediate the absorption of drugs. OATPs, organic anion transporters (OATs) and organic cation transporter (OCTs) expressed on the hepatic sinusoidal membrane and the basolateral membrane of kidney proximal tubules that mediate the hepatic and renal uptake of drugs from the blood.

There has been an increasing recognition in recent years that transporters from the ABC and SLC superfamilies play an important role in drug disposition and clinical DDIs.

In a white paper published by the International Transporter Consortium [36], seven transporters were identified as having compelling clinical evidence of involvement in pharmacokinetics and DDIs. These transporters included P-gp, BCRP, OATP1B1, OATP1B3, OCT2, OAT1 and OAT3 [36]. The white paper and the FDA guideline recommend characterizing *in vitro* the role of these transporters in the disposition of investigational drugs during drug development to assess their potential for clinical DDIs [13, 36].

b. OATPs: characteristics, role in drug disposition and clinical DDIs

Amongst the drugs transporters mentioned above, OATPs are of particular interest because they have been shown to be particularly important to pharmacokinetics and clinical DDIs. Also, OATPs have a broad substrate spectrum as discussed later. Since all the drugs involved in the significant DDIs identified previously are administered orally, it is possible that these drugs are substrates of OATPs and interact via inhibition of OATPs.

OATPs are a family of membrane transport proteins that mediate the sodium-independent transport of a diverse range of amphipathic organic anions, neutral compounds and even some cations. OATPs belong to the solute carrier (SLC) superfamily as members of the solute carrier organic anion transporter family (SLCO) [232]. In humans, eleven members have been identified and grouped into six subfamilies. The general predicted OATP structure consists of thirteen transmembrane domains [233]. The mechanism of transport is believed to involve anion exchange by coupling the cellular uptake of substrate with the efflux of neutralizing anions such as bicarbonate,

glutathione or glutathione-S-conjugates [232]. The endogenous substrates of OATPs include bile acids, steroid conjugates, thyroid hormones, prostaglandins and bilirubin glucuronide. OATPs are also responsible for the transport of a number of drugs and xenobiotic substances [234]. Table 4-1 provides a summary of characteristics of the OATPs in humans and examples of their substrates [235].

Particular attention has been paid to OATP1B1, 1B3 and 2A1 as they are the transporter proteins demonstrated to this point to be most engaged in drug disposition [232]. The mechanisms of hepatic uptake include passive diffusion along an electrochemical gradient, active transport for anionic compounds, and facilitative diffusion for cationic compounds [235]. Expressed on the sinusoidal membrane of hepatocytes, OATP1B1, 1B3 and 2A1 contribute to the active uptake of drugs from the portal venous blood into hepatocytes [236]. The substrates of OATP1B1, 1B3 and 2B1 are mainly anionic amphipathic compounds with relatively high molecular weights (>350) and low plasma-protein unbound fraction (<30%), such as bile salts (taurocholate), several conjugated metabolites of steroids including estradiol-17 β -D-glucuronide (E217 β DG), thyroid hormones (T3, T4), statins, angiotensin converting enzyme inhibitors, and angiotensin II receptor antagonists [237]. It is worth noting that there is a significant overlap in the substrate spectrum among these three OATPs.

Hepatic uptake is the prerequisite for the subsequent hepatic metabolism of drugs and the elimination of drugs themselves via the bile. Once a compound is in the intracellular space of a hepatocyte, it can be eliminated through any of the three routes: metabolism by hepatic enzymes, excretion into bile, or return to the sinusoids via sinusoidal efflux. At a given time, the intra-hepatocyte concentration of an OATP

substrate reflects the net balance between its hepatic uptake via OATPs and its hepatic clearance through metabolism, biliary excretion or sinusoidal efflux. OATPs thus are a determinant of the hepatic exposure for their substrates [235].

This explains the association of OATPs with pharmacokinetics, efficacy and toxicity of their substrate drugs. First, for a drug whose target site of action is in the liver, OATPs can affect its efficacy by determining its intracellular concentration in hepatocytes. One example is simvastatin which targets HMG-CoA reductase in hepatocytes. The active form of simvastatin, simvastatin acid, is a substrate of both OATP1B1 and 1B3 [238]. In individuals carrying the less functional variant allele at c.521T>C SNP of *SLCO1B1*, the gene that encodes for OATP1B1, the reduction in the LDL cholesterol following simvastatin therapy was 1.3% lower per variant allele [239]. Second, for a drug that is actively excreted into bile or rapidly metabolized in hepatocytes, its hepatic uptake is the rate-limiting step in its hepatic clearance. OATPs thus can play a major role in determining such a drug's hepatic elimination. This can be observed from the following equation,

$$CL_{int,all} = PS_{uptake} \times \frac{PS_{eff} + CL_{met}}{PS_{eff} + CL_{met} + PS_{back}} \quad \text{Eq. 4-1}$$

Where $CL_{int,all}$ is the overall hepatic clearance, PS_{uptake} is the rate of hepatic uptake, PS_{eff} is the rate of biliary excretion, CL_{met} is the clearance of hepatic metabolism, and PS_{back} is the efflux rate from hepatocytes to sinusoids. The overall hepatic clearance ($CL_{int,all}$) approaches the rate of hepatic uptake (PS_{uptake}) when the sinusoidal efflux (PS_{back}) is much smaller than the total clearance of hepatic metabolism and biliary excretion ($PS_{eff} + CL_{met}$) [240]. This is exemplified by atorvastatin, a substrate of OATP1B1 and 2B1 extensively metabolized by CYP3A4. In a study by Maeda *et al.*, following an oral

microdose (33 µg) of atorvastatin in healthy volunteers, the dose-normalized AUC was increased by 22-fold with coadministration of rifampin (a strong inhibitor of OATP1B1/1B3) but remained unchanged with intravenous coadministration of itraconazole (a strong inhibitor of CYP3A4) [241]. These data suggested that the hepatic clearance of atorvastatin was mainly determined by the rate of its hepatic uptake in humans. When the function of OATPs is impaired, due to either inhibition by drugs or genetic variation, OATP substrate drugs that are primarily eliminated through hepatic metabolism are expected to have reduced hepatic clearance and increased systemic exposure, potentially resulting in increased risk of toxicity at peripheral tissues. Taking simvastatin as an example again, in patients with the C allele at *SLCO1B1* rs4149056, the odds ratio for statin-induced myopathy was 4.5 per copy as compared with the wild type allele [239]. This observation is so clinically important that the Clinical Pharmacogenetics Implementation Consortium (CPIC) has published therapeutic guidelines for the use of simvastatin in the clinic based on the genotype of *SLCO1B1* [242].

It has been increasingly recognized that OATPs represents an important site of DDIs since mechanistic studies have revealed that the interaction between cerivastatin and cyclosporine was caused by inhibition of OATP1B1 [243, 244]. Potent inhibitors of OATPs, such as cyclosporine, rifampin, gemfibrozil and itraconazole, have been reported to cause significant clinical DDIs with the drugs that rely on OATPs for hepatic uptake. DDIs involving inhibition of hepatic uptake via OATPs often also involve inhibition of hepatic metabolism by CYPs, leading to a remarkable increase in the systemic exposure to the victim drugs and the risk of adverse events. A typical example is the interaction of

cerivastatin and gemfibrozil. The interaction is caused by both the inhibition of the hepatic uptake of cerivastatin via OATP1B1 by gemfibrozil, and the inhibition of cerivastatin metabolism through CYP2C8 by the glucuronide metabolite of gemfibrozil [245, 246]. Consequently, gemfibrozil increased the AUC of cerivastatin by 559% in a pharmacokinetic study [247]. It also increased the risk of rhabdomyolysis for cerivastatin by 5-fold in a population-based cohort study [52]. Another example is cyclosporine and atorvastatin. Cyclosporine not only inhibits the OATP1B1-dependent hepatic uptake of atorvastatin *in vitro* [248], but also inhibits atorvastatin metabolism by CYP3A4. Coadministration of cyclosporine was shown to increase the AUC of atorvastatin by 9- to -15- fold [235].

c. Experimental systems for assessing uptake transporter activity

Understanding and predicting the role of transporters in pharmacokinetics and DDIs require appropriate characterization of uptake and efflux kinetics *in vitro*. For uptake transporters, there are two general types of *in vitro* systems commonly used to study their kinetics, recombinant cell and whole-cell systems [249].

Recombinant cells, including *Xenopus laevis* oocytes or immortalized cell lines, overexpressing transporter proteins of interest are commonly used to estimate the kinetics and inhibition of uptake transporters [27]. Oocyte systems are established by injecting cDNA of the transporter to allow overexpression [236]. Because of the large volume of oocytes, the time course of the compound accumulation in oocytes can remain linear for a long period of time. Oocyte systems therefore have the advantage of providing high signal-to-noise ratios in assessing uptake of drugs [237]. However, due to cDNA

injection, oocyte systems are not appropriate for high-throughput screening and often show a large variability in the expression level of the transporter [237]. More importantly, some data suggest that transporter kinetic parameters determined using oocytes are not always comparable to those generated in mammalian cells [249].

Immortalized cell lines transfected with cDNAs and stably overexpressing single or multiple transporters are thus preferred over oocytes for studying uptake transporters [27]. They allow constitutive expression of the transporter proteins of interest under certain selection pressure. HEK293 and CHO cells are the two host mammalian cell lines most commonly used because they demonstrate low endogenous transporter activity and are easy to maintain [249]. Additional advantages of these cell lines include that they are cost-effective, easy to perform experiments, and applicable to high-throughput screening [249]. There are numerous examples demonstrating the value of these cell lines in studying DDIs involving hepatic uptake transporters. One such example is using HEK293 cells stably overexpressing OATP1B1 and OATP1B3 to examine the inhibition of OATP-mediated pravastatin uptake by several widely prescribed oral antidiabetic drugs [250]. As noted above, transporters often have overlapping substrate spectrums. Therefore, cell lines transfected with a single transporter often lack the endogenous uptake or efflux transporters to provide a complete transport mechanism for a drug. It may even be challenging to predict the true *in vivo* situation using cell lines transfected with multiple transporters [251]. In addition, a large variability has been observed with the data generated using these recombinant cell lines due to inconsistency in cell handling and experimental procedures [249].

Whole-cell systems refer to those derived cell lines such as Caco-2 and MDCK, and primary human or rodent hepatocytes. Caco-2 and MDCK cell lines are often used to study efflux transporters or the interplay between uptake and efflux transporters expressed in the intestine and in the kidneys, respectively [249]. These cell lines can also stably or transiently overexpress the transporters of interest when cDNA transfection methods are used. The cells are seeded on a permeable membrane support to form a tight polarized cell monolayer, with uptake transporters localized in the basolateral membrane and efflux transporters localized in the apical membrane. The transport of drugs is determined by measuring the flux through the cell monolayer from the basolateral compartment to the apical compartment [252, 253]. Because apparent uptake in these models is confounded by apical efflux, one of the limitations is possible misidentification of uptake transporter substrates for non-substrates due to saturation of efflux transporters [249].

Primary hepatocytes, either freshly isolated or cryopreserved, have been widely accepted as the gold-standard models for identification of substrates of hepatic uptake transporters and for prediction of hepatic clearance [249]. They can be optimized to estimate kinetic parameters specific to uptake, metabolism, or efflux, as well as the interplay of these processes [249]. Cryopreserved hepatocytes are more commonly used than freshly isolated hepatocytes because they are more available and the majority of hepatic drug transporters appear to be preserved [254]. For studying uptake transporters, primary hepatocytes are often used in suspension because transporter function decreases quickly when cells are plated [255]. However, technical difficulties may arise as the viability of suspended hepatocytes decreases more rapidly than that of plated hepatocytes

[256]. Primary hepatocytes have been shown to be valuable tools for mechanistic studies on DDIs. In a study by Noe *et al*, gemfibrozil inhibited the OATP1B1-, OATP2B1-, and OATP1B3-mediated fluvastatin transport in individually transfected cell lines by 97, 70, and 62%, respectively, whereas only 27% inhibition was observed for fluvastatin uptake into primary human hepatocytes [251]. This study highlighted the advantages of hepatocytes as compared with recombinant cell lines in investigating the role of uptake transporters in DDIs. The application of human primary hepatocytes to transporter studies has been greatly limited by hepatocyte availability. Rat hepatocytes are a useful substitute in some cases. There is no true homologue of human OATP1B1/1B3 in rodents, but rodent OATP1B2 has been found very similar in function and substrate specificity to those human isoforms [232, 257]. Another issue often encountered in transporter studies using hepatocytes is that, due to the lack of specific inhibitors and substrates, it is often challenging to determine which individual isoforms of specific uptake transporters are involved in uptake of compounds [249]. A common goal in this research is therefore to identify probe substrates and specific inhibitors for individual clinically important transporters and to set up standards for experimental procedures similar to those that are described previously for CYPs.

In addition to the *in vitro* systems discussed above, an *oatp1b2*^{-/-} knockout mouse model and humanized OATP1B1 and OATP1B3 transgenic mouse models have been developed. These mouse models have contributed to a better understanding of the role of hepatic uptake transporters for the disposition of drugs *in vivo* [257-260].

d. Prediction of transporter-mediated DDIs

Current methods for the prediction of DDIs due to inhibition of hepatic uptake focus on inhibition of OATPs. These methods are extensions of those derived for CYP-mediated DDIs and can be grouped into three classes, static models (R value), mechanistic static models and PBPK models [27].

The static model estimates an R value as $R = 1 + [I]_{\text{inlet,max}} / K_i$, where $[I]_{\text{inlet,max}}$ is the maximum inhibitor concentration at the inlet to the liver, and K_i is the dissociation constant determined for the affected uptake transporter *in vitro* [27]. $[I]_{\text{inlet,max}}$ is estimated as $[I]_{\text{inlet,max}} = C_{\text{max}} + (k_a \times \text{Dose} \times F_a F_g / Q_h)$, where C_{max} is the maximum systemic plasma concentration of the inhibitor drug, dose is the highest dose of the inhibitor in clinical use, $F_a F_g$ is the fraction of the inhibitor dose that reaches the liver, k_a is the absorption rate constant of the inhibitor, and Q_h is the estimated hepatic blood flow (1500 mL/min) [13]. When values of $F_a F_g$ and k_a are not available, the theoretical maximum of 1 and 0.1 min^{-1} are assumed, respectively, for a conservative prediction [13]. When IC_{50} is evaluated at a substrate concentration well below K_m for the uptake transporter, K_i can be approximated by IC_{50} based on $K_i = IC_{50} / (1 + [S]/K_m)$ [261]. In contrast to CYPs, well-defined probe substrates and specific inhibitor are not yet available for uptake transporters, and this issue contributes to the huge variability in the reported IC_{50} s for OATPs [27]. A universal cutoff for R value thus has not been identified [27]. The recommendation of the International Transporter Consortium is to determine IC_{50} with the relevant co-medication substrates and inhibitors [27]. The FDA sets an R cutoff of 1.25 for investigational drugs inhibiting OATP1B1 and OATP1B3, and requires a follow-up clinical study with rosuvastatin, pitavastatin or pravastatin as probe substrates

for a predicted R value ≥ 1.25 [13]. The R value approach assumes that the uptake of the victim drug is exclusively via the OATP under consideration, and that any other potential contributing factors are negligible. This assumption often leads to overestimation of the magnitude of DDI *in vivo* [27, 262].

It has been observed that the contribution of OATPs to total hepatic uptake is substrate-dependent [27]. In predicting the risk of DDIs involving OATP1B1, to account for the differential contribution of OATP1B1, a mechanistic model has been developed which incorporates the fraction of drug transported via OATP1B1 only (f_{OATP1B1}) and has the following form [27],

$$AUCR = \frac{AUC_i}{AUC} = \frac{CL_{act,uptake}}{CL_{act,uptake(i)}} = \frac{1}{\frac{f_{\text{OATP1B1}}}{1 + \frac{[I]_{inlet,max,unbound}}{K_i}} + (1 - f_{\text{OATP1B1}})} \quad Eq. 4 - 2$$

This model assumes that other potential contributing factors, such as other uptake transporters, efflux transporters and metabolism, are not affected by the inhibitor drug [27]. The successful application of this model is limited by (1) the general lack of f_{OATP1B1} estimates for OATP1B1 substrates, and (2) the sensitivity of the predicted AUCR to the input value of f_{OATP1B1} [27]. Furthermore, this model has the same caveat as its counterpart for CYP-based DDIs, that is, it uses “a static estimate of *in vivo* inhibitor concentration to provide a point estimate of the average magnitude of change in the exposure to any victim drug” as pointed out by Einolf *et al.* [133].

To address more complicated situations where DDIs involving multiple transporters and/or transporter-enzyme interplay, many scientists advocate the use of PBPK models [263]. There has been an increasing use of whole-body PBPK modeling to integrate estimates of active uptake, passive permeability, intracellular binding,

metabolism, and efflux measured *in vitro* to predict *in vivo* pharmacokinetics. Compared with static models, PBPK models have the advantage of being able to simulate the concentration–time course of the inhibitor drug at the actual site of interaction [136]. For example, PBPK models can simulate the intracellular concentration in enterocytes for predicting inhibition of efflux transporters and CYP3A4 expressed in the gut wall. It can also simulate hepatic inlet concentration for predicting inhibition of hepatic uptake, or intracellular concentration in hepatocytes for predicting inhibition of hepatic efflux transporters and metabolic enzymes. In addition, PBPK models can be extended to incorporate the effects of metabolites on relevant transporters or metabolic enzymes [136]. Examples of using PBPK models for prediction of transporter-mediated DDIs are limited. Nevertheless, the current mechanistic framework of PBPK models makes quantitative assessment of complex DDIs possible [27].

e. Hypothesis and aims

Since all the drugs involved in the significant DDIs identified previously are administered orally, it is possible that inhibition of hepatic uptake via OATP1B1/1B3 contributes to these interactions. In this chapter, I hypothesize that inhibition of OATP1B1/1B3 contributes to the significant myopathic DDIs identified previously by reducing hepatic uptake and thus the subsequent hepatic clearance of drugs, leading to increased systemic exposure and the risk of myopathy. To test this hypothesis, each drug involved in the significant DDIs identified previously needs to be evaluated as both a substrate and an inhibitor of OATP1B1/1B3. This approach is, however, unfeasible as current experimental techniques require radio-labeling each individual drug involved.

Since an inhibitor of a transporter is often also a substrate, I examined the ability of those drugs to inhibit OATP1B1/1B3 to probe their potential to be substrates of these transporters. The drugs were first screened for the inhibition of E₂17βDG uptake in cryopreserved rat hepatocytes. E₂17βDG is a substrate of rOATP1B2, a functional homologue of human OATP1B1/1B3 in rodents. The risk of OATP1B1/1B3-mediated DDIs in humans was then inferred from the inhibitory potencies determined.

2. Methods

a. Materials

All drugs and metabolites were purchased from Toronto Research Chemicals Inc. (North York, ON, Canada). Tritium-labeled estradiol-17 β-D-glucuronide ([³H] E₂17βDG) was purchased from Perkin Elmer (Waltham, MA). Cryopreserved rat hepatocytes were purchased from Life Technologies (Grand Island, NY). Acetonitrile, methanol and components of Krebs-Henseleit buffer (KHB) were purchased from Sigma-Aldrich (St. Louis, MO). Phosphate-buffered saline (PBS) and ScintiSafe™ Econo Cocktail (Scintanalyzed™) were purchased from Fisher Scientific (Pittsburgh, PA).

b. Screening for inhibition of E₂17βDG uptake

To examine the inhibitory potential of the drugs of interest for rOATP1B2, the uptake of E₂17βDG was determined in the presence of the drugs under study in suspended cryopreserved rat hepatocytes. [³H] E₂17βDG and the test drugs were dissolved in methanol and diluted to the desired concentrations in KHB buffer. Rat hepatocytes were thawed, washed and suspended in Krebs-Henseleit buffer containing 2

g/L glucose. Following counting of the number of viable cells using trypan blue, the hepatocyte suspension was adjusted to a density of 2×10^6 viable cells per ml and kept on ice until the start of uptake. Aliquotes (100 μ L) of cell suspension were then transferred to 2.5 mL tubes and were pre-warmed at 37 $^{\circ}$ C for 3 min in a shaker water bath, along with the solution containing radio-labeled E₂17 β DG and the test drugs. The uptake was initiated with the addition of equal volume (100 μ L) of the solution containing [³H] E₂17 β DG and the test drugs to the cells. The hepatocytes were further incubated with [³H] E₂17 β DG and the test drugs for a designated length of time at 37 $^{\circ}$ C. In parallel, the uptake studies were also performed on ice to estimate the rate of passive diffusion. The final concentration of [³H] E₂17 β DG was 1 μ M, 0.1 μ Ci. The final concentration of the test drugs were 100 μ M, and each drug was tested in triplicate. The final concentration of hepatocytes was 0.2×10^2 per reaction (or 1×10^6 cells / mL). To ensure the consistency of uptake assays, 10 μ M rifampin was used as a positive control in each experiment.

Uptake was stopped with the addition of 1 mL ice-cold PBS and immediate centrifugation at 4500 rpm for 1 min at 4 $^{\circ}$ C. To wash off the residual substrate and test drugs, the cells were re-suspended with 1 mL ice-cold PBS and centrifuged again. After removing supernatants, the cell pellets were lysed with 200 μ L of 50% acetonitrile in H₂O, followed by vigorous vortexing. The cell lysates were then transferred to scintillation counting vials, 3 mL scintillation fluid was added, and radioactivity was determined by liquid scintillation counting in a LS 6500 multipurpose scintillation counter (Beckman Coulter, Fullerton, CA).

For data analysis, the total radioactivity was taken to be the sum of the radioactivity found in the supernatant and that of the hepatocyte lysates. The fraction of

total uptake was the ratio of the radioactivity of hepatocyte lysate to the total radioactivity. The fraction of active uptake was the obtained by subtracting the uptake at 0 °C from the total uptake at 37 °C. The fraction of inhibition was determined by comparing the active uptake in the presence of test drugs with that in the absence of any test drugs.

c. Estimating IC₅₀s

IC₅₀ was determined for the drugs which yielded more than 50% inhibition of [³H] E₂17βDG uptake into hepatocytes at 100 μM in the screening. To determine IC₅₀s, uptake studies were performed as described previously, except that the inhibition of [³H] E₂17βDG uptake was evaluated at multiple inhibitor concentrations in triplicate. The selection of inhibitor concentrations was guided by the fraction of inhibition in the screening study. The fraction of inhibition was determined as described above. IC₅₀s were estimated by fitting the fraction of inhibition to a two- (Eq. 3-2) or four- (Eq. 3-3) parameter log-logistic model using GraphPad Prism 5 software.

d. Prediction of OATP1B1/1B3-mediated DDIs

Following the FDA guidelines, for each drug administered orally for which an IC₅₀ was observed, an R value was estimated as $R = 1 + [I]_{\text{inlet,max}} / K_i$. Because the concentration of E₂17βDG (1 μM) was well below its K_m [264, 265], the K_is were approximated by the IC₅₀s based on $K_i = IC_{50} / (1 + [S]/K_m)$ [261]. $[I]_{\text{inlet,max}}$ was estimated as $C_{\text{max}} + (k_a \times \text{Dose} \times F_a F_g / Q_h)$, where C_{max} was the maximum systemic plasma concentration of the inhibitor drug obtained from the published literature (see Table 4-4), dose was the highest proposed clinical dose of the inhibitor drug, F_aF_g was the fraction of

the inhibitor dose that reaches the liver, k_a was the absorption rate constant of the inhibitor obtained from the published literature, and Q_h was the estimated hepatic blood flow (1500 mL/min). For the drugs whose $F_a F_g$ and k_a were not available, these parameters were assumed to be 1 and 0.1 min^{-1} . For simvastatin acid, the C_{\max} and dose were assumed to be equal to those of simvastatin. Because rifampin is usually given as an intravenous injection, its R value was estimated as $R = 1 + [I]/K_i$, where $[I]$ is the C_{\max} following an injection at the highest proposed clinical dose (600 mg). K_i was similarly approximated by the IC_{50} .

3. Original experimental results

a. Screening for inhibition of $E_217\beta$ DG uptake

Cryopreserved rat hepatocytes were used to examine the potential of the drugs of interest to inhibit OATPs. The hepatic uptake of $E_217\beta$ DG is known to be mediated by OATP1B1 and 1B3 in humans, and by rOATP1B2 in rodents [264, 265]. $E_217\beta$ DG uptake has been widely used as a marker activity of those OATPs *in vitro*. To examine the potential of the thirteen drugs involved in the significant myopathic DDIs and their active metabolites (e.g. simvastatin acid and desloratadine) for inhibition of OATPs, these compounds were screened for inhibition of $E_217\beta$ DG uptake in cryopreserved rat hepatocytes.

Because $E_217\beta$ DG uptake via rOATP1B2 in rat hepatocytes follows Michaelis-Menten kinetics [264], uptake measured beyond the early linear phase can be confounded by efflux and metabolism [249]. Selection of appropriate time points in the initial linear phase is therefore critical for accurate determination of inhibitory potential. In

preliminary studies, I found that the velocity of E₂17βDG uptake into rat hepatocytes was linear for up to 1 min (Figure 4-1). All the subsequent uptake studies were thus performed within the 1 min linear phase.

The inhibition of 1 μM E₂17βDG uptake into rat hepatocytes by the compounds tested is summarized in Table 4-2. A bar plot showing the remaining uptake (%) as compared to the controls is displayed in Figure 4-2. Six drugs were found to inhibit more than 50% of E₂17βDG uptake at 100 μM, and they were simvastatin acid, quetiapine, risperidone, omeprazole, duloxetine and alprazolam. Noticeably, simvastatin acid inhibited E₂17βDG uptake completely (103.3 ± 0.5%) at 100 μM. Quetiapine also exhibited potent inhibition of E₂17βDG uptake (95.5 ± 0.4%) at 100 μM.

b. IC₅₀ estimates

For the six drugs that yielded more than 50% of inhibition of E₂17βDG uptake in the screening studies, IC₅₀s were further determined and are shown in Figure 4-3 and Table 4-3. Because the interaction of simvastatin and loratadine was of particular interest, the IC₅₀ of desloratadine was also determined although it only exhibited 45% of inhibition for E₂17βDG uptake in the screening studies. Rifampin, a known inhibitor of OATPs, served as a positive control inhibitor, and its IC₅₀ (95% CI) was 8.9 (6.6, 12) μM. Simvastatin acid and quetiapine exhibited potent inhibition for E₂17βDG uptake in the screening studies and their IC₅₀s were 4.3 (3.5, 5.3) and 16.9 (11.7, 24.4) μM, respectively. The IC₅₀s of duloxetine, omeprazole, alprazolam, desloratadine and risperidone were relatively large and suggested only weak inhibition of rOATP1B2 at clinically relevant concentrations.

c. Predicted risk of OATP1B1/1B3- mediated DDIs

Following the FDA guidelines, an R value was predicted for each drug for which an IC₅₀ was observed (Table 4-4). Assuming that the C_{max} and dose of simvastatin acid are equal to those of simvastatin, the R value for simvastatin acid was 3.85. The R values of quetiapine, omeprazole and duloxetine were 5.28, 1.2 and 1.2, respectively, also higher than the FDA recommended cutoff of 1.1 [13]. The R values of simvastatin acid and quetiapine were larger than that of rifampin (R value 3.4), a known inhibitor of OATP1B1/1B3 that can cause clinical DDIs by inhibiting OATP1B1/1B3. Since rOATP1B2 is a functional homologue of human OATP1B1/1B3, these data suggest that simvastatin acid, quetiapine, duloxetine and omeprazole may inhibit the transport activity of OATP1B1/1B3 in humans, and interact with drugs whose hepatic uptake is primarily mediated by OATP1B1/1B3. The predicted R values for the other drugs were close to unity, indicating a negligible risk of OATP1B1- and OATP1B3- mediated DDIs *in vivo*.

4. Discussion

In this chapter, I have addressed the hypothesis that the DDIs identified previously were caused, in part, by the inhibition of hepatic uptake via OATP1B1/1B3. The drugs and their relevant active metabolites were screened for inhibition of E₂17βDG uptake, a marker activity of rOATP1B2, in cryopreserved rat hepatocytes. Six drugs, namely, simvastatin acid, quetiapine, duloxetine, omeprazole, alprazolam and risperidone exhibited more than 50% of inhibition at 100 μM. IC₅₀s were further determined for these drugs and the risk of OATP-mediated DDIs was predicted. The IC₅₀ of desloratadine was determined too as its inhibition was close to 50% and the interaction between loratadine

and simvastatin was of particular interest. Simvastatin acid and quetiapine exhibited relatively potent inhibition of E₂17βDG uptake with IC₅₀s of 4.3, and 16.9 μM, respectively. Omeprazole and duloxetine exhibited moderate inhibition of E₂17βDG uptake with IC₅₀s of 84.3 μM and 56.8 μM, respectively. The predicted R values of simvastatin acid, quetiapine, omeprazole and duloxetine were 3.85, 5.28, 1.2 and 1.2, respectively, indicating that these drugs may interact with drugs that rely on OATP1B1/1B3 for hepatic uptake *in vivo*. It is worth noting that the predicted R values of simvastatin acid and quetiapine were larger than that of rifampin, indicating that these two drugs have more potential to cause clinical DDIs by inhibiting OATP1B1/1B3 than rifampin, a drug that is known to interact with OATP1B1/1B3 substrates.

The inhibitory potencies observed here are consistent with those published previously, demonstrating the validity of the experimental system. Rifampin, a known inhibitor of OATP1B1/1B3, inhibited E₂17βDG uptake with an IC₅₀ of 8.9 μM, which is consistent with the reported inhibitory activity of rifampin *in vivo* [266]. Simvastatin acid inhibited E₂17βDG uptake with an IC₅₀ of 4.3 μM. This is in line with the previous observation that simvastatin acid is a substrate of OATP1B1/1B3 in humans and inhibits the OATP1B1/1B3-dependent pravastatin uptake [7]. On the other hand, simvastatin lactone only reduced E₂17βDG uptake by 36.3%, consistent with the observation that simvastatin is not a substrate of OATP1B1/1B3 [267].

The other compounds tested here have never been reported to inhibit OATP1B1/1B3. Many of them, such as omeprazole and duloxetine, are clinically important drugs that are often involved in significant clinical DDIs. My data are the first to describe their potential to inhibit rOATP1B2 and shed light on their potential to be

involved in OATP-mediated DDIs in humans. Future studies are needed to confirm the inhibitory potentials observed for these drugs and to integrate these considerations into clinical thinking about drug interactions.

Quetiapine draws particular attention as it was identified as a relatively potent inhibitor of rOATP1B2, thus a potential inhibitor of human OATP1B1/1B3. The IC₅₀ of quetiapine (16.9 μM) was close to that of a known potent OATP1B1/1B3 inhibitor, rifampin. The high predicted R value of 5.28 underscored its potential to cause DDIs by inhibiting OATP1B1/1B3-mediated hepatic uptake. Future studies are required to characterize in detail the inhibition of human OATP1B1/1B3 by quetiapine and to investigate its potential to cause clinical DDIs.

Overall, the data indicate that the inhibition of hepatic uptake via OATP1B1/1B3 is not the major mechanism for the DDIs identified previously. Other than simvastatin acid and quetiapine, the drugs involved in those DDIs exhibited only relatively weak or moderate inhibition of OATP1B1/1B3. Since the drugs were screened for inhibition at 100 μM, a concentration that is much higher than the hepatic input concentration of any drug at clinical doses, a relatively weak or moderate inhibition indicates that the chance of inhibiting OATP1B1/1B3 *in vivo* is minimal. The majority of the DDIs identified previously therefore cannot be explained by inhibition of hepatic uptake via OATP1B1/1B3.

The predicted R value of simvastatin acid was 3.85, indicating a risk of OATP1B1/1B3-mediated DDI *in vivo*. For the interaction between simvastatin and loratadine, loratadine and its active metabolite, desloratadine, exhibited only relatively weak and moderate inhibition for E₂17βDG uptake, respectively. Since the predicted R

value of desloratadine was close to unity, both loratadine and desloratadine are unlikely to increase the risk of simvastatin-induced myopathy by inhibiting the hepatic uptake of simvastatin acid via OATP1B1/1B3. On the other hand, the inhibition of E₂17βDG uptake by desloratadine suggests that desloratadine might be a substrate of OATP1B1/1B3. With an R value of 3.85, simvastatin acid can potentially inhibit the uptake of desloratadine, thereby increasing the risk of loratadine-induced myalgia. However, as I assume that the C_{max} and dose of simvastatin acid is equal to those of simvastatin, the R value of simvastatin acid is likely an overestimate because a fraction of dose and C_{max} exists in the form of simvastatin which inhibited E₂17βDG uptake with much less potency. Future mechanistic studies are needed to examine whether desloratadine is a substrate of OATP1B1/1B3, and to explore the possibility that the inhibitory effects of simvastatin acid on the hepatic uptake of desloratadine contributes to the interaction of simvastatin with loratadine.

Both duloxetine and omeprazole were predicted to interact with OATP1B1/1B3 substrate drugs with a relatively small risk (R value 1.2). Their inhibitory effects on OATP1B1/1B3 might contribute to their interactions with loratadine as they may inhibit the hepatic uptake of desloratadine. However, since the predicted R values are small and likely over-estimated, these inhibitions may have only small effects on the pharmacokinetics of loratadine.

The predicted R value of quetiapine was 5.28, indicating a risk of OATP1B1/1B3-mediated DDI *in vivo*. However, chloroquine and its active metabolite, hydroxychloroquine, only caused 26.3% and 27.7% inhibition of E₂17βDG uptake, respectively, indicating that they are unlikely to be substrates of OATP1B1/1B3.

Therefore, the interaction between quetiapine and chloroquine is unlikely to be due to the inhibition of hepatic uptake of chloroquine or quetiapine via OATP1B1/1B3. For similar reasons, the interactions of duloxetine with chloroquine and hydroxychloroquine cannot be attributed to the inhibition of OATP1B1/1B3 by duloxetine, although duloxetine was predicted with a small risk of interacting with OATP1B1/1B3 substrate drugs (R value 1.2).

Using E₂17βDG uptake as a functional marker, I was able to provide mechanistic insights into the DDIs identified previously with respect to inhibition of hepatic uptake via OATP1B1/1B3. On the other hand, I was not able to evaluate the overall effect of a perpetrator drug on the hepatic uptake of a victim drug for those DDIs. Such information can only be obtained via examining the uptake of a victim drug into hepatocytes in the absence and presence of a perpetrator drug.

Since the R value approach assumes that other potential contributing factors, such as uptake via other transporters, metabolism and efflux, are negligible, and that the inhibitor drugs concentration is constantly as high as the maximal hepatic inlet concentration at the highest proposed clinical dose, the R values are likely be overestimates of risk [27]. This approach is thus only appropriate for providing an initial assessment and for ruling out drugs that are unlikely to be involved in DDIs. Since the fraction of uptake via OATP1B1/1B3 is unknown for the drugs of interest, the AUCR approach cannot be applied. To obtain more accurate estimates of the risk of OATP-mediated DDIs *in vivo* for simvastatin acid and quetiapine, more comprehensive models such as PBPK models may be required.

Although my data demonstrate E₂17βDG uptake in rat hepatocytes as a useful model for evaluating inhibition of OATP1B1/1B3, there are a few caveats inherent to this model which limit the interpretation of the results. First, there is a concern that the species difference between rat and human hepatocytes, more specifically, between rOATP1B2 and human OATP1B1/1B3, may limit the extrapolation of uptake data from rats to humans. Indeed, the uptake kinetics of E₂17βDG in cryopreserved rat hepatocytes were found to be different from those in cryopreserved human hepatocytes. While the K_m of E₂17βDG uptake in cryopreserved rat (12.9 μM) was very similar to that human hepatocytes (8.4 μM), the V_{max} in rat hepatocytes (1300 pmol/min/10⁶ cells) was 34-fold higher than that in human hepatocytes (33.1 pmol/min/10⁶ cells), and the CL_{uptake} in rat hepatocytes was 20-fold higher than that in human hepatocytes [32]. In fact, however, the inhibitory potential of rifampin for E₂17βDG uptake determined here in rat hepatocytes was consistent with that determined in cryopreserved human hepatocyte suspensions by De Bruyn *et al.*, who reported that rifampin inhibited 70% of E₂17βDG (1 μM) uptake at 25 μM [30]. Extrapolating from an IC₅₀ of 8.9 μM determined here in rat hepatocytes, rifampin would inhibit 73.7% of E₂17βDG uptake (1 μM) at 25 μM (based on inhibition (%) = 1 / (1 + IC₅₀ / [I]) [33]). These data indicate that IC₅₀s may be more dependent on the affinity than on the abundance of transporter proteins on the hepatocyte membrane. This observation may not be generalizable since the inhibition of E₂17βDG uptake by the other compounds of interest has never been similarly tested in human hepatocytes. A similar concern also arises from using cryopreserved hepatocytes instead of fresh isolated hepatocytes. It has been shown that the K_m of E₂17βDG uptake remained unchanged whereas the V_{max} and CL_{uptake} decreased on average by 47% after cryopreservation of

human hepatocytes [34]. It is possible that there is a discrepancy between IC_{50} s determined in cryopreserved rat hepatocytes and in fresh isolated human hepatocytes as a result of species difference and cryopreservation. Since IC_{50} s provide the basis for estimating R values, there is a possibility that this discrepancy translates into an underestimated or overestimated risk of OATP1B1/1B3-mediated DDIs. Future studies are thus warranted to confirm the inhibitory potencies of those drugs in fresh isolated human hepatocytes in order to predict the risk of OATP-mediated DDIs with more confidence.

In addition, the experimental procedure used here is different from the standard oil-filtration method with respect to stopping an uptake reaction. Using the oil-filtration method, uptake reactions are stopped by centrifuging samples that allow cells to pass through a thin layer of oil while leaving the aqueous incubation medium on the top of oil. A small number of cells may fail to pass through the oil layer, resulting in an underestimate of total uptake. Large variability has been observed using this method, partly due to the difficulties in sampling cells for radio-activity determination. Using my method, uptake reactions were stopped with the addition of ice-cold PBS followed by immediate centrifugation. Addition of ice-cold PBS, theoretically, would bring the temperature of incubation mixture down to close to 0 °C and would significantly reduce the rate of substrate concentration- and temperature-dependent active uptake. However, uptake may continue while the samples are kept on ice before centrifugation. Also, a small number of hepatocytes may be removed along with supernatant, potentially leading to an underestimate of total uptake. Further studies may be needed to compare the two methods. Nevertheless, using my methods, I was able to obtain data with consistency and

relatively small variability. The inhibitory potentials were consistent with those published previously, further providing the evidence for the validity of this method.

Lastly, there is debate as to the best approach to assessing the contribution of passive diffusion to overall uptake. The traditional approach, as used here, assumes that active uptake is negligible at 0 °C, and that passive diffusion can be approximated by total uptake at 0 °C. This approach is confounded by the fact that membrane fluidity and thus the rate of passive diffusion is temperature-dependent. Approximation of passive diffusion at 37 °C by total uptake at 0 °C may lead to underestimation of passive diffusion at 37 °C. Since active uptake is estimated by the difference between total uptake and passive diffusion, this approach likely leads to overestimation of active uptake at 37 °C. In my case, this may result in underestimated inhibitory potencies.

Table 4-1. Summary of characteristics of clinically important OATPs in humans [235].

Transporter	Gene symbol	Other name	Chromosome	Reference accession (mRNA)	Tissue distribution	Substrate drugs
OATP1A2	<i>SLCO1A2</i>	OATP-A OATP	12p12	NM_134431 NM_021094	brain, testis, prostate	fexofenadine, talinolol, pravastatin, pitavastatin, rosuvastatin, methotrexate, saquinavir, erythromycin, levofloxacin, gatifloxacin, ciprofloxacin, atrasentan, ouabain, imatinib, rocuronium
OATP1B1	<i>SLCO1B1</i>	OATP-C OATP2 LST-1	12p12	NM_006446	liver	benzylpenicillin, cefditoren, cefoperazone, cefoperazone, cefazolin, nafcillin, rifampicin, gimatecan, SN-38, pazopanib, atorvastatin, cerivastatin, fluvastatin, pitavastatin, pravastatin, rosuvastatin, ezetimibe glucuronide, bosentan, atrasentan, enalapril, olmesartan, valsartan, temocapril, torsemide, darunavir, lopinavir, saquinavir, caspofungin, fexofenadine, methotrexate, mycophenolic acid glucuronide, sirolimus, troglitazone sulfate
OATP1B3	<i>SLCO1B3</i>	OATP8 LST-2	12p12	NM_019844	liver	docetaxel, methotrexate, paclitaxel, SN-38, rifampicin, bosentan, atrasentan, olmesartan, telmisartan, valsartan, fexofenadine, digoxin, pitavastatin, rosuvastatin, fluvastatin, enalapril, erythromycin, imatinib, mycophenolic acid glucuronide, ouabain
OATP1C1	<i>SLCO1C1</i>	OATP-F	12p12.2	NM_017435	brain, testis	
OATP2A1	<i>SLCO2A1</i>	PGT	3q21	NM_005630	pancreas, lung, intestine, prostate	
OATP2B1	<i>SLCO2B1</i>	OATP-B	11q13	NM_007256 NM_001145212	intestine, liver, ovary, testis, spleen	fexofenadine, talinolol, celiprolol, atorvastatin, pravastatin, pitavastatin, rosuvastatin, benzylpenicillin, glibenclamide, montelukast
OATP3A1	<i>SLCO3A1</i>	OATP-D	15q26	NM_013272 NM_001145044	ubiquitous	benzylpenicillin
OATP4A1	<i>SLCO4A1</i>	OATP-E	20q13.33	NM_016354	ubiquitous	benzylpenicillin
OATP4C1	<i>SLCO4C1</i>	OATP-H	5q21.2	NM_180991	kidney	digoxin, ouabain, methotrexate
OATP5A1	<i>SLCO5A1</i>	OATP-J	8q13.3	NM_030958		
OATP6A1	<i>SLCO6A1</i>	GST OATP-I	5q21.1	NM_173488	testis	

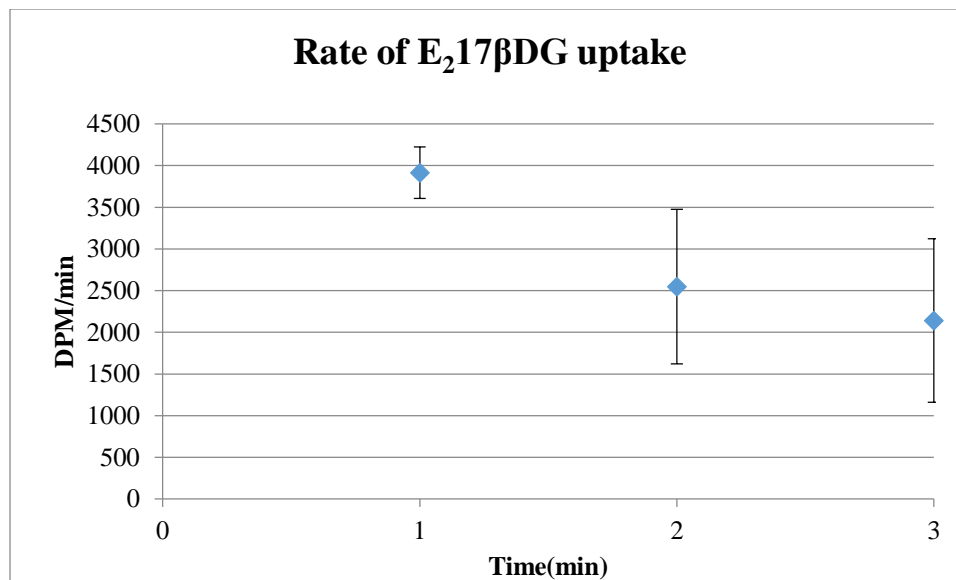


Figure 4-1. The rate of E₂17βDG uptake in cryopreserved rat hepatocytes. The uptake of E₂17βDG was linear up to 1 min.

Table 4-2. Inhibition (%) of E₂17βDG uptake at 100 μM

Drug	% Inhibition
Simvastatin Acid	103.3 ± 0.5
Quetiapine	95.5 ± 0.4
Risperidone	64.0 ± 5.9
Omeprazole	60.1 ± 4.8
Duloxetine	55.8 ± 0.9
Alprazolam	54.5 ± 0.3
Trazodone	48.4 ± 4.3
Desloratadine	44.9 ± 14.2
Simvastatin	36.3 ± 6.0
Hydroxychloroquine	27.7 ± 8.7
Chloroquine	26.3 ± 14.5
Tegaserod	24.6 ± 15.3
Ropinirole	23.7 ± 2.7
Loratadine	18.1 ± 10.9
Promethazine	17.7 ± 7.7

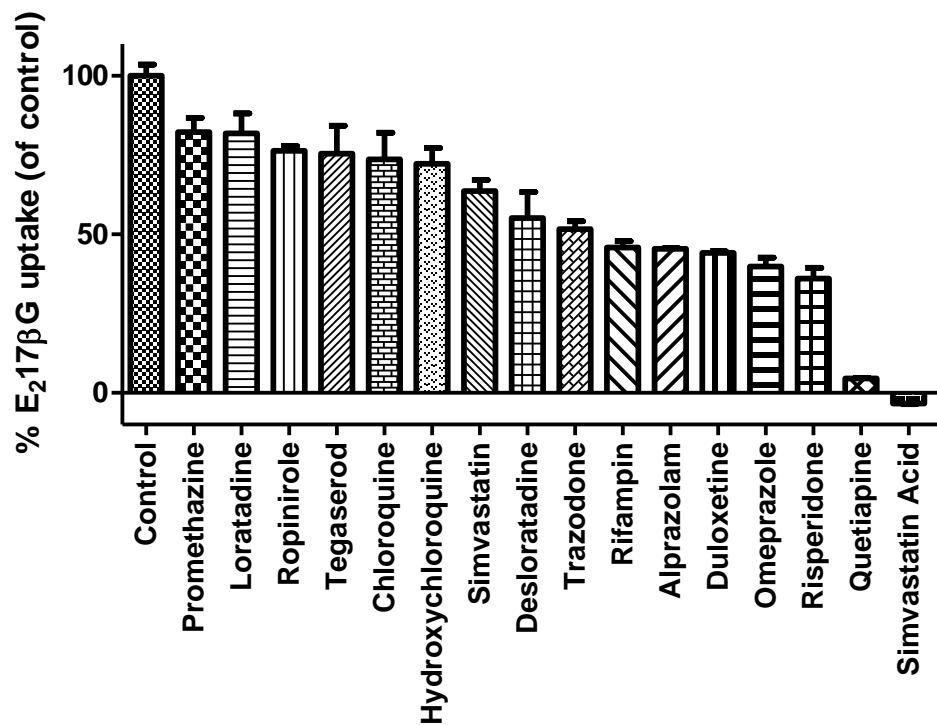


Figure 4-2. Inhibition of E₂17βDG uptake in cryopreserved rat hepatocytes at 100 μM.

Table 4-3. IC₅₀s for the inhibition of E₂17βDG uptake

Drug	IC₅₀ (μM)	95% CI
Simvastatin Acid	4.3	3.5, 5.3
Rifampin	8.9	6.6, 12
Quetiapine	16.9	11.7, 24.4
Duloxetine	56.8	45.1, 71.4
Omeprazole	84.3	49.8, 142.9
Alprazolam	99.5	79.5, 124.6
Desloratadine	140.5	111.4, 177.1
Risperidone	234.6	204, 269.8

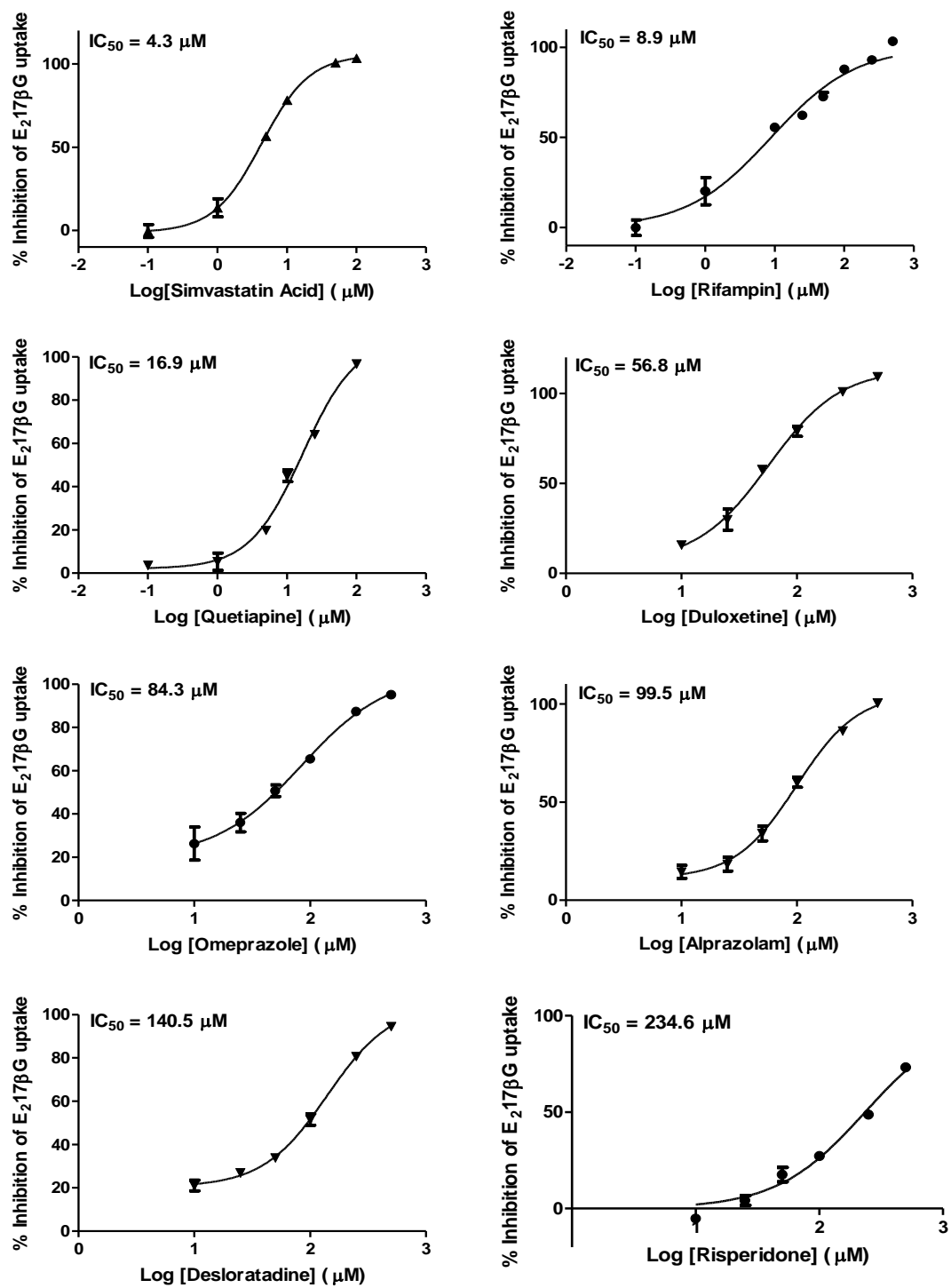


Figure 4-3. IC₅₀ curves for the inhibition of E₂17βDG uptake.

Table 4-4. Predicted R values

Drug	IC ₅₀ (μM)	Dose (mg)	MW (g/mol)	Dose (mmol)	C _{max} (ng/ml)	C _{max} (μM)	k _a (min ⁻¹)	F _a F _g	[I] _{inlet} (μM)	R	Reference
Quetiapine	16.9	400	383.5	1.043	1080	2.816	0.1	1	72.349	5.3	[203]
Simvastatin Acid	4.3	80	436.6	0.183	25.4	0.058	0.1	1	12.274	3.9	[202]
Rifampin	8.9		823		17400	21.143				3.4	[268]
Omeprazole	84.3	80	345.4	0.232	1432	4.146	0.1	1	19.586	1.2	[269]
Duloxetine	56.8	60	297.4	0.202	53.2	0.179	0.1	1	13.628	1.2	[270]
Alprazolam	99.5	3	308.8	0.010	102.9	0.333	0.1	1	0.981	1.0	[271]
Desloratadine	140.5	5	310.8	0.016	4.7	0.015	0.1	1	1.088	1.0	[272]
Risperidone	234.6	4	410.5	0.010	89.1	0.217	0.1	1	0.867	1.0	[198]

Note: **Dose** is the highest proposed clinical dose; **C_{max}** is the maximal plasma concentration at the highest proposed clinical dose; **k_a** is the absorption rate constant; **F_aF_g** is the fraction of the inhibitor dose that reaches the liver; **[I]_{inlet,max}** is the maximal inlet concentration of the inhibitor and was estimated as $C_{\text{max}} + (k_a \times \text{Dose} \times F_a F_g / Q_h)$, where Q_h is the hepatic blood flow (1500 mL/min). Because the values of k_a and $F_a F_g$ were not available conservative predictions, for conservative predictions, they were assumed to equal to the theoretical maxima of 0.1 min⁻¹ and 1, respectively.

Chapter 5. *In vitro* assessment of direct myotoxicity

1. Introduction

a. Pathogenic mechanisms underlying drug-induced myopathy

Drug-induced myopathy is among the most common causes of muscle disease. The clinical presentation of drug-induced myopathy ranges from asymptomatic muscle enzyme elevation to chronic myopathy with severe weakness and to massive rhabdomyolysis with acute renal failure. Over 150 drugs have been associated with rhabdomyolysis [49-51]. Mechanisms underlying drug-induced myopathy can be grossly classified as direct myotoxicity or immunologically induced inflammatory myopathy. Drugs that have been found to have direct myotoxicity include lipid-lowering drugs such as statins and fibrates, antimalarials such as chloroquine and hydroxychloroquine, glucocorticoids, cocaine, colchicine, antipsychotics such as phenothiazines, antiretrovirals such as zidovudine, and ipecac. Drugs that induce inflammatory myopathy through immunological system include statins, interferon alpha and penicillamine [273, 274]. Here, I limit the discussion to myopathies induced by statins and antimalarials only as they are the most relevant to the work described previously.

The mechanism underlying statin-induced myopathy has been extensively studied but remains unclear. The existing evidence suggests that it is likely to be multifactorial. Statins inhibit the conversion from HMG-CoA to mevalonate by HMG-CoA reductase (HMGCR), which is the rate-limiting step in cholesterol synthesis. By reducing mevalonate production, statins decrease endogenous cholesterol synthesis which contributes to their lipid-lowering effects. However, mevalonate is a precursor of

isoprenoids such as farnesyl pyrophosphate and geranylgeranyl pyrophosphate, both of which are required for modification of proteins by prenylation. Protein prenylation is important for producing many functional proteins such as small G proteins (e.g. Rho and Rab) that are essential for cell survival [275, 276]. The decreased protein prenylation by statins eventually causes increases in cytosolic calcium which lead to the activation of the proteolytic enzyme caspase-3 and to cell apoptosis. Importantly, the treatment with geranylgeranyl pyrophosphate blocked the toxic effects of the statins in vascular smooth muscle cells [277]. These data suggest that statin-induced myotoxicity may be mediated, at least in part, through apoptosis caused by depletion of isoprenoid intermediates and subsequent dysfunction of small G proteins.

Mevalonate also serves as a precursor for coenzyme Q10 (CoQ10, ubiquinone), an important component of the mitochondrial electron transport chain. This leads to the hypothesis that statin-induced CoQ10 deficiency is involved in the pathogenesis of statin myopathy. Indeed, circulating levels of CoQ10 has been found to be lower during statin treatment. However, the effect of statins on intramuscular levels of CoQ10 is controversial, and data on intramuscular CoQ10 levels in symptomatic patients with statin-induced myopathy are scarce. Although CoQ10 supplementation increases the circulating level of CoQ10, its effect on myopathic symptoms are contradictory. There is therefore insufficient evidence to conclude that there exists an etiologic role for CoQ10 deficiency in statin-induced myopathy [278-280].

Atrogen-1 can also be affected by statin-induced changes in lipid metabolism. Atrogen-1 is a muscle-specific ubiquitin protein ligase and a key player in skeletal muscle atrophy. The expression of atrogen-1 was found to be upregulated in muscle

biopsies from patients with statin induced-myopathy [281]. The knockdown of atrogen-1 in mice and in zebrafish abolished the myotoxicity of statins. Furthermore, statin-induced atrogen-1 expression and muscle damage in both of these systems were prevented by the treatment with geranylgeranol, a cell permeable precursor of geranylgeranyl pyrophosphate [282]. Thus, it has been speculated that statin myopathy may occur when an isoprenylation deficiency results in ineffective suppression of atrogen-1 [283].

Another suggested mechanism of statin-induced myopathy due to reduced lipid levels is destabilization of the sarcolemmal membrane in myocytes [284]. There is normally a dynamic equilibrium between plasma lipids and the myocyte membrane which can be disturbed by the depletion of plasma cholesterol due to statin treatment. However, this theory seems at odds with the observations that myotoxicity did not occur when cholesterol was lowered due to inhibition of squalene synthetase, an enzyme in the distal cholesterol synthesis pathway, in human skeletal myotubes [285]. In addition, patients with genetic variations resulting in cholesterol biosynthetic defects do not present with skeletal myopathy clinically [286]. These data suggest that statin-induced myopathy is more likely a consequence of isoprenoid depletion rather than reductions in membrane cholesterol content *per se*.

Mitochondrial dysfunction seems to be a phenotypic presentation that results from various molecular mechanisms in statin-induced myopathy. In addition to potentially impaired mitochondrial respiratory chain due to deficiency of CoQ10, the activities of citrate synthase and respiratory enzymes in mitochondria were reduced in patients taking statins [287]. Statins can trigger Ca²⁺-induced opening of the permeability transition pore and loss of mitochondrial membrane potential, followed by cytochrome c release

and cell apoptosis [288]. A recent study by Kwak *et al.* found that simvastatin induces myotube atrophy and cell loss associated with impaired ADP-stimulated maximal mitochondrial respiratory capacity, mitochondrial oxidative stress, and apoptosis in primary human skeletal myotubes, suggesting that mitochondrial dysfunction may underlie statin-induced myopathy [289].

In most cases, patients with statin-induced myopathy can completely recover within weeks or months after statins are discontinued. The observation that myopathy persists or progresses in some patients even after statin discontinuation suggests that inhibition of cholesterol synthesis is not the only mechanism underlying statin-induced myopathy. A subgroup of patients with persistent statin-induced myopathy was diagnosed with necrotizing autoimmune myopathy, a subtype of idiopathic inflammatory myopathy characterized by myocyte necrosis without significant inflammation. Statins were found to upregulate the expression of HMGCR, the major target of autoantibodies in patients with statin-induced necrotizing autoimmune myopathy. Regenerating muscle cells express high levels of HMGCR, which may sustain the immune response even after statins are discontinued [290]. This finding potentially provides a diagnostic test to help differentiate immune from non-immune statin myopathy.

Unlike statins, the antimalarial drugs chloroquine and hydroxychloroquine induce myopathy through their lysosomotropic effects [291]. Chloroquine and hydroxychloroquine have significant lysosomal affinity and can mediate autophagic protein degradation in lysosomes. Long term administration may result in the accumulation of these drugs which promotes accumulation of sequestered materials in

autophagic lysosomes [291]. This eventually leads to the development of the hallmark rimmed vacuoles in several tissues including muscles [292, 293].

b. Rat L6 myotubes as a model system to assess myotoxicity

Commonly used *in vitro* cell models of skeletal muscles include primary cell lines and immortalized cell lines such as rat L6 myotubes and mouse C2C12 myotubes [294]. Primary skeletal muscle cell lines developed from muscle biopsies can retain the metabolic characteristics of the donor tissue and are particularly useful for studying the effects of metabolic diseases on skeletal muscles [294]. Those developed from patients with myopathy can retain phenotypic traits of the donor related to myopathy pathogenesis [294]. Although primary skeletal muscle cell lines are a valuable *in vitro* model of skeletal muscles, their use has been limited by availability and their limited replicative potential in culture [295]. In contrast to primary cell lines, undifferentiated immortalized skeletal muscle cell lines can replicate indefinitely in culture. Cells can continue to undergo mitotic divisions and expand rapidly when maintained under appropriate culture conditions. In addition, immortalized skeletal muscle cell lines are able to retain many physiological functions similar to those of primary skeletal muscle cell lines. These cell lines therefore provide a readily available and replicable experimental model that is alternative to primary skeletal muscle cell lines [295].

The rat L6 cell line is the best *in vitro* cell model to study glucose uptake involving GLUT4 in muscle cells [296]. This is because rat L6 myotubes are most similar to human muscle cells in terms of translocation of GLUT4 upon insulin stimulation when compared to other cell models [296]. This cell line is also one of the most commonly

used *in vitro* cell models to investigate myogenesis as the underlying molecular mechanisms governing myogenesis are conserved from rats to humans [297]. The L6 cell line was established from embryonic or newborn rat thigh skeletal muscle cells and immortalized by treatment with a carcinogen, methyl cholanthrene [298]. The treatment with methyl cholanthrene enabled L6 myoblasts to last for months in a continuous state of replication without losing their potential to differentiate [298]. The undifferentiated myoblasts are mononucleated, spindle-shaped cells that can proliferate when cultured with a serum-rich medium. When they are confluent or are starved with less serum, they withdraw from the cell cycle, elongate, adhere and begin to differentiate [297]. Myocytes at this stage still have the ability to return to the cell cycle and proliferate. Those that commit to differentiation can elongate, migrate and fuse into postmitotic multinucleated myotubes that are terminally differentiated. Further differentiation of myotubes to form myofibers is associated with the appearance of cross-striation and contractility [295, 298].

Skeletal-muscle differentiation is a complex process coordinated by a number of factors. In addition to the extracellular matrix, which plays an important role in myocyte migration and fusion, many transcription factors that promote myogenesis have been discovered. Those include the members of the MyoD transcription factor family such as myogenin (Myog), Myf5 and Mef2. Under the regulation of P38/MAPK, Wnt and Sonic hedgehog, and the Notch/Delta pathway [297], the expression of myogenin increases during myoblast differentiation [299]. Also increasingly expressed are a number of muscle enzymes that closely associate with the metabolic capability of myofibers, including creatine kinase muscle type (CKM) [300, 301]. Creatine kinase is an enzyme

that catalyzes the conversion of creatine to create phosphocreatine and often used as a biomarker for differentiated myotubes [297].

The rat L6 cell line has been shown to be a useful model to evaluate myotoxicity of drugs. Itagaki *et al.* used L6 myotubes to investigate potential mechanisms underlying statin-induced myopathy, and found that hydrophobic simvastatin and fluvastatin decreased cell viability in a dose-dependent manner via apoptosis characterized by typical nuclear fragmentation and condensation as well as caspase-3 activation [277]. Sakamoto *et al.* identified Oatp1a4 and Oatp2b1 as the transporters mediating the uptake of pravastatin into L6 myotubes, suggesting a potential role of these transporters in statin-induced myopathy [302].

c. Methods to evaluate pharmacodynamic drug interactions

Two or more drugs that produce overtly similar effects can either produce exaggerated or diminished effects when used in combination [20]. When the combined effect is greater or less than that predicted by their individual effects, the combination is called synergism and antagonism, respectively [303]. Synergistic drug combinations are commonly used in the treatment of cancer, infectious diseases and pain so that desirable therapeutic effects can be achieved and adverse reactions can be avoided with lower doses [304]. When two drugs have synergistic toxicity, the adverse reactions could be exacerbated.

A number of methods have been developed to assess the nature and intensity of drug interactions. Greco *et al.* have summarized them as a strategy consisting of three steps [305]. The first step is to choose a good concentration-effect (dose-response)

structural model for each drug when applied individually [305]. A common choice is the Hill (or logistic) model (Eq. 5-1).

$$E = \frac{E_{max}(\frac{D}{D_m})^m}{1+(\frac{D}{D_m})^m} \quad \text{Eq. 5-1}$$

In Eq. 5-1, E is the measured effect (response), D is concentration of drug; E_{max} is the full range of response that can be affected by the drug; D_m is the median effect dose or concentration of drug (e.g. IC_{50} and ED_{50}), and m is a slope parameter [305]. Because data from real experiments rarely fit perfectly to an ideal curve, the second step is to choose an appropriate error model [305]. For example, a normal distribution is usually assumed for response measurements that are continuous; a binomial distribution can be assumed for proportions of failures or successes. A composite model then can be constructed from one structural model and one error model and used for fitting to experimental data. In the third step, one group of methods favored by mathematicians fits a combined action model to all of the data and estimates a parameter indicating the nature and intensity of an interaction. Another group of methods favored by pharmacologists is used more commonly. Such methods compare the observed combined effect with that predicted from a null reference model assuming no interaction [305]. Two commonly used null reference models are the Loewe additivity model and the Bliss independence model. The Loewe additivity model is in general considered a better reference model [305]. It is based on the idea that one drug cannot interact with itself. More specifically, in a sham experiment where a drug is combined with a diluted version of itself, the results would be additive [306]. A general mathematical description of Loewe additivity is shown in Eq. 5-2.

$$d. \quad 1 = \frac{D_1}{ID_{X,1}} + \frac{D_2}{ID_{X,2}} \quad \text{Eq. 5-2}$$

In Eq.5-2, $ID_{X,1}$, $ID_{X,2}$ are the concentrations of drugs to result in X% of effect for each respective drug alone, and D_1 , D_2 are concentrations of each drug in the mixture that yield X% inhibition.

Developed and introduced by Loewe *et al.* [306], the isobologram is the most famous and widely accepted method to assess the nature of two drug interactions. It applies the first two steps of the above strategy implicitly by estimating IC_{50} s using a Hill model and assuming normal distributions for continuous response data. In an isobologram, the diagonal NW-SE line connecting the IC_{50} s of two drugs when applied alone is the line of Loewe additivity. Points below the line indicate Loewe synergism and those above the line indicate Loewe antagonism. This approach has the advantages of being simple, flexible, intuitive and inexpensive. The disadvantages, though, include 1) it lacks objective statistical measures and intensity measures of an interaction; 2) scattered points around the additivity line may lead to false conclusions; 3) isobolograms often lead to waste of data since IC_{50} s cannot be estimated for dose-response curves with less than 50% effect, and consequently, it in general requires a large amount of data; and 4) many drug combinations have interactions that are not monotonically synergistic or antagonistic, and thus several isobols at particular effect levels (e.g. 10%, 25%, 50%, 75%, 90%) may not capture the nature of interaction entirely and may lead to false conclusion [305].

An algebraic analog of the isobologram is the method of Berenbaum *et al.* [307], in which an interaction index, I , is estimated using Eq. 5-3 to provide a quantitative measure of the intensity of an interaction.

$$I = \frac{D_1}{ID_{X,1}} + \frac{D_2}{ID_{X,2}} \quad \text{Eq. 5-3}$$

When $I > 1$, Loewe antagonism is claimed; when $I < 1$, Loewe synergism is claimed. This method shares similar strengths and limitations with the use of an isobologram [305].

In the spirit of Berenbaum *et al.*'s method, a widely used method developed by Chou *et al.* also provides a quantitative measure of the nature and intensity of an interaction [308]. The Chou's method involves estimating IC_{50} s and the slope parameter, m , for each drug when applied alone using the median effect equation (Eq. 5-4) [308] or its log-linearized form (Eq. 5-5) [308], where f_a is the fraction of effect affected by drug, f_u is the fraction remains unchanged and equal to $(1 - f_a)$.

$$\frac{f_a}{f_u} = \left(\frac{D}{D_m}\right)^m \quad \text{Eq. 5-4}$$

$$\log \frac{f_a}{f_u} = m \times \log(D) - m \times \log(D_m) \quad \text{Eq. 5-5}$$

The median effect equation (Eq. 5-4) is equivalent to the Hill model depicted in Eq. 5-1 but is derived from mass action enzyme kinetics. Assuming the two drugs are mutually exclusive, a combination index (CI) is then estimated using Eq. 5-6 [308]. A $CI > 1$ indicates antagonism; a $CI = 1$ indicates additivity; and a CI between 0 and 1 indicates synergism. A $CI - f_a$ plot is often produced by plotting CI values on y axis and f_a s on x axis.

$$CI = \frac{D_1/(D_1+D_2)}{D_{m1}(\frac{f_a}{f_u})^{1/m_1}} + \frac{D_2/(D_1+D_2)}{D_{m2}(\frac{f_a}{f_u})^{1/m_2}} \quad \text{Eq. 5-6}$$

The fundamental equation of this approach, the median effect equation (Eq. 5-4), is derived from basic mass action enzyme kinetics [308]. Thus, the estimable parameters have the potential to be biologically meaningful. This represents a major improvement since all the methods published previously have used empirical equations to describe

dose-response relationships. Also, the experimental design using this approach requires fewer data than other designs which are intended to be analyzed by isobolograms and other methods [308]. A $CI - f_a$ plot is able to provide a comprehensive view on the nature and intensity of interaction across the entire spectrum of effect [308]. However, this method also suffers from a number of limitations. The Eq. 5-6 is based on the assumption that the effects of two drugs are mutually exclusive [308]. This may not hold in cases involving complex biological systems [305]. As the method involved logarithmic transformation, the data points with more than 100% of effect produce a computational difficulty and have to be discarded. More importantly, large CI values often appear in the region near $f_a = 0$, indicating a strong antagonism, which has been proven an artifact when the interaction is truly synergistic [305].

d. Hypothesis and aims

I hypothesize that the significant myopathic DDIs identified previously are due, at least in part, to direct myotoxicity brought by individual drugs or their combinations. To test this hypothesis, the following aims are pursued:

- 1) Evaluate individual myotoxicity of the drugs involved in the significant DDIs, and their important metabolites, to differentiated rat L6 myotubes;
- 2) Examine the combined effects of drug pairs in which both drugs are significantly myotoxic.

2. Methods

a. Materials

Rat L6 myotubes were a generous gift from Dr. Jeffrey Elmendorf (Indiana University School of Medicine, Indianapolis, IN). All the drugs and the metabolites were purchased from Toronto Research Chemicals (Toronto, Canada). Fetal bovine serum (FBS) and Dulbecco's phosphate buffered saline (DPBS) were from Thermo Scientific™ HyClone™ (Waltham, MA). 24-well Falcon™ tissue culture plates were from Corning Life Sciences (Tewksbury MA). BioWhittake™ phosphate buffered saline (PBS) without calcium and magnesium were from Lonza (Walkersville, MD). CellTiter 96™ AQueous MTS reagent powder was from Promega™ (Madison, WI). Phenazine methosulfate (PMS), methanol and DMSO were from Sigma™ (St. Louis, MO). RNeasy mini kit and QuantiTect reverse transcription kit were from Qiagen Inc (Valencia, CA). α -Minimum essential medium (α -MEM), Gibco® antibiotic-antimycotic and 0.25% trypsin-EDTA (1X), TaqMan® gene expression master mix, Qubit RNA BR assay kit, MicroAmp fast optical 96-well reaction plate, MicroAmp optical adhesive film, TaqMan gene expression assay for CKM (assay ID Rn01644605_m1), myogenin (assay ID Rn01490689_g1), and GAPDH (assay ID Rn01775763_g1) were obtained from Life Technologies Corporation (Grand Island, NY).

b. Cell culture and drug treatment

Rat L6 muscle cells were cultured as previously detailed by Klip *et al.* [309] with slight modifications. Myoblast cells were maintained in continuous passages by trypsinization of subconfluent cultures using 0.25% trypsin. Cells were seeded at 7500

cells/well in 24-well plates, and were maintained in monolayer culture in α -MEM containing 10% FBS and 1% antibiotic-antimycotic solution (10,000 U/ml penicillin G, 10 mg/ml streptomycin and 25 mg/ml amphotericin B) in an atmosphere of 5% CO₂ at 37 °C. Five days after seeding, myoblasts were differentiated into multinucleated myotubes with 2% FBS. Cells were fed fresh medium every other day. All drug treatments were initiated when the majority of cells were differentiated myotubes (5 days after the initiation of differentiation and 10 days after seeding) and continued for 5 days. I chose this time window because it allows the longest possible time within the optimal drug treatment time window as determined by the expression profiles of CKM and Myog (see below).

c. Gene expression of CKM and Myog

The expression of creatine kinase muscle type (CKM) and myogenin (Myog) mRNA in rat L6 muscle cells on day 0 through day 13 after the initiation of differentiation was measured by real-time PCR. Cells were removed from culture on 24-well plates by trypsinization using 0.25% trypsin, and were stored immediately at -80 °C before extraction of total RNA. Total RNA of muscle cells was isolated using RNeasy mini kit in accordance with the manufacturer's instructions. The isolated RNA was quantified using the Qubit RNA BR assay kit and a Qubit® 2.0 fluorometer (Life Technologies Corporation, Grand Island, NY), immediately followed by reverse transcription. For each sample, cDNA was reverse-transcribed from 1 μ g of total RNA using QuantiTect reverse transcription kit following the manufacturer's instructions. The cDNAs were stored at -80 °C before use.

Real-time PCR was performed in triplicate for each sample. GAPDH served as an endogenous control to which the expression of CKM and Myog were normalized. Each reaction was carried out as a duplex reaction, employing a combination of a FAM-labeled CKM or Myog assay and a VIC dye-labeled GAPDH assay. All reactions were performed in MicroAmp fast optical 96-Well reaction plates covered by MicroAmp optical adhesive film. The final total volume was 20 μL per well, consisting of 1 μL of CKM or myog primer, 1 μL of GAPDH primer, 1 μL of cDNA, 10 μL of TaqMan master mix (2X) and 7 μL of nuclease-free water. Real-time PCR plates were run on a Bio-rad iCycler iQ PCR Thermal Cycler (Hercules, CA). Cycling conditions were 10 min / 95 $^{\circ}\text{C}$ initial denaturation / polymerase activation and 40 cycles each consisting of 15 s / 95 $^{\circ}\text{C}$ denaturation and 1min/60 $^{\circ}\text{C}$ annealing and elongation.

The gene expressions of CKM and Myog were quantified using the comparative C_T ($\Delta\Delta C_T$) method. Briefly, for each sample, the ΔC_T value was calculated as $\Delta C_T = C_{T \text{ target}} - C_{T \text{ reference}}$, where $C_{T \text{ target}}$ is the C_T value of CKM or Myog, and $C_{T \text{ reference}}$ is the C_T value of GAPDH. The $\Delta\Delta C_T$ value was calculated by $\Delta\Delta C_T = \Delta C_{T \text{ test sample}} - \Delta C_{T \text{ calibrator sample}}$. For Myog, the calibrator sample was the cells sampled on the day of differentiation (day 0). For CKM, because the gene expression was undetectable for the samples on day 0, 1 and 2, the cells sampled on day 3 since differentiation served as the calibrator sample. The standard error (SE) of $\Delta\Delta C_T$ was same as that of ΔC_T , and was calculated as $\text{SE}(\Delta C_T) = \text{SE}(\Delta\Delta C_T) = [\text{SE}(C_{T \text{ target}})^2 + \text{SE}(C_{T \text{ reference}})^2]^{1/2}$. The fold-change of gene expression relative to a calibrator sample was calculated as $2^{-\Delta\Delta C_T}$, with $2^{\Delta\Delta C_T + \text{SE}(\Delta\Delta C_T)}$ and $2^{\Delta\Delta C_T - \text{SE}(\Delta\Delta C_T)}$ as the upper and lower bound of standard error.

d. MTS/PMS assay

The CellTiter 96® aqueous non-radioactive cell proliferation (MTS/PMS) assay was used to measure cell viability after drug treatment. Similar to XTT and MTT assays, this assay involves bioreduction of a tetrazolium compound, MTS, by dehydrogenase enzymes in metabolically active cells in the presence of PMS. The resulting formazan product is soluble in cell culture medium and can be quantitated by the amount of light absorbance at 490 nm. The number of viable cells has a linear relationship with light absorbance at 490 nm [310].

A MTS solution (2 mg/mL) was prepared by dissolving MTS reagent powder in DPBS in a light-protected container. The solution was adjusted to pH 6 to 6.5 with 1N HCl, followed by filtration through a 0.2 µm filter into a sterile, light-protected container. Similarly, a PMS solution (0.92 mg/mL) was prepared by dissolving PMS in DPBS followed by filtration through a 0.2 µm filter into a sterile, light-protected container. Both MTS and PMS solutions were stored at -20 °C and protected from light before use.

For each 24-well plate to be assayed, 2 mL of MTS solution and 100 µL of PMS solution were added to 10 mL of α-MEM medium containing 2% FBS. 500 µL of this MTS/PMS-containing medium were added to each well. After incubating the plate for 3 hours in an atmosphere of 5% CO₂ at 37 °C, the light absorbance at 490 nm was recorded using Molecular Devices Spectramax M2e (Sunnyvale, CA). The assay was also carried out at the same time on an empty plate without any cells to estimate the background absorbance. For data analysis, the net absorbance was calculated as the difference between the absorbance of the samples and the background absorbance. Cell viability

was calculated as the net absorbance of treated cells divided by that of the DMSO treated control cells. The MTS/PMS assay is linear

e. Screening for the inhibition of L6 myotube viability

The compromise of L6 myotube viability was screened using the drugs involved in the significant myopathic DDIs identified previously, and using simvastatin acid, 3-hydroxy simvastatin (3OH simvastatin), desloratadine and 3-hydroxy desloratadine (3OH desloratadine), the important major metabolites of simvastatin and loratadine, respectively. The drugs and metabolites were dissolved in methanol and diluted in DMSO to desired concentrations before addition to α -MEM with 2% FBS. The final concentration was 10 μ M for all drugs, except for alprazolam and 3OH desloratadine which were tested at 5 μ M due to limited aqueous solubility. Each drug was tested in six replicate wells on the same plate. Cells treated with 0.1% DMSO on the same plate served as controls. The final concentration of DMSO was kept at 0.1% for all treatments. Cells were treated for 5 days from day 5 to day 10 after the initiation of differentiation. Experiments were repeated three times with different passages (passage #11 to #14) to ensure reproducibility of results.

f. Determining concentration – cell viability relationships

The viability of L6 myotubes at different concentrations was evaluated for drugs that yielded more than 50% inhibition in the screening study. These included tegaserod, desloratadine and simvastatin. For tegaserod, cells were treated at 0, 1, 2, 3, 4, 5, 6, 7, 8, 9 and 10 μ M. For desloratadine, cells were treated at 0, 1, 5, 7.5, 11, 17, 25 and 50 μ M.

For simvastatin, cells were treated at 0, 0.5, 1, 2, 5 and 10 μM . Each concentration was tested column-wise in four replicate wells on a 24-well plate. For tegaserod and desloratadine, concentrations were tested with two plates of cells from the same passage. Cells treated with 0.1% DMSO served as controls. All the treatments started on day 5 and ended on day 10 after the initiation of differentiation. The experiments were repeated multiple times with different passages (passage #11 to #14) of myotubes to ensure reproducibility of results. Cell viability was calculated as described above. IC_{50}s were estimated by fitting cell viability (%) and concentrations to a two- (Eq. 3-2) or four- (Eq. 3-3) parameter logistic model using GraphPad Prism V5.

g. Determining the combined effect of simvastatin and desloratadine

Fully differentiated myotubes were treated with simvastatin and desloratadine in combination on day 5 through day 10. The experimental design is displayed in Table 5-1. For 24-well plates 1 to 5, the dose response of simvastatin was tested column-wise at final concentrations of 0, 0.5, 1, 2, 4 and 8 μM , in the presence of desloratadine row-wise at final concentrations of 0, 5, 7.5, 10, 15 and 25 μM . Plates 6 to 10 were arranged similarly at the same concentration combinations except that the dose response of desloratadine was tested column-wise instead.

On plate 1 through 5, desloratadine at 0 μM was tested in row 1, 2, 3, 4 and 1 respectively. Simvastatin at 0 μM was tested similarly on plate 6 to 10. This design has several advantages. First, it is relatively balanced in that it provides eight replicates for each concentration combination involving 0 μM and six replicates for those otherwise. Second, it helps to control for potential batch effect among different plates by including

the combination (0 μ M, 0 μ M) on each plate which serves as the control for that plate. Third, the control combination (0 μ M, 0 μ M) appears in each row across plates, which helps to reduce confounding of an edge effect observed occasionally in the wells at corners. Lastly, the concentrations are evenly spaced on a logarithmic scale which helps with computation of interaction measures.

Combination index (CI) values were calculated as described by Chou *et al.* [308]. Cell viability, in this case was also the fraction unaffected (f_u), was first calculated as described above. Fractional inhibition (f_i) was calculated as $1 - f_a$. The slope factor m and IC_{50} of simvastatin and desloratadine were estimated by fitting the data of each drug when applied alone to Eq. 5-5. CI values were calculated using Eq. 5-6. A CI - f_a was constructed by plotting CI values and f_a on y and x axis, respectively.

3. Original experimental results

a. Gene expression of CKM and Myog

At any given time during myoblast differentiation, cells are a heterogeneous population consisting of proliferating myoblast, differentiating myocytes and terminally differentiated myotubes. I am most interested in the effects of drugs on differentiated myotubes as they are the victim of myotoxicity *in vivo*. Since the composition of a cell population may affect a drug's myotoxicity, I sought to select an optimal drug treatment window within which the majority of viable cells were healthy, fully differentiated myotubes that were not too senescent to confound the measurement of cell viability.

The expression of CKM and Myog are commonly used in skeletal muscle cell lines as biomarkers of myogenesis. For this reason, I examined the mRNA expression profile of

CKM and Myog in rat L6 muscle cells at various times after the initiation of differentiation. The results are presented in Figure 4-1. The expression of Myog (Figure 4-1, A) is expressed as fold-change relative to that on day 0 when differentiation was initiated. Because the mRNA expression was undetectable for CKM on day 0, 1 and 2, its mRNA levels are expressed as fold-change relative to that on day 3 after differentiation (Figure 4-1, B). The expression of Myog increased dramatically (645-fold) during the first three days of differentiation, then gradually decreased to 200-fold on the 10th day of differentiation, and remained relatively stable thereafter up to the 13th day. The change in the expression level of CKM was smaller than that of Myog. The expression of CKM increased beginning on the third day and spiked on the sixth day, followed by a gradual decrease thereafter.

These data are consistent with the results observed previously indicating that L6 myoblasts begin to express genes promoting differentiation upon the initiation of differentiation [297, 299, 300]. The gradual decrease in the expression of CKM and Myog may be due to an aging cell population. These expression profiles suggest that myotubes can be treated as early as day 5 and up to day 10 after the initiation of differentiation. Because I sought to test the worst-case scenario of drug myotoxicity, and because many of the drugs of interest are long-term treatments, I selected the longest possible time window, from day 5 to day 10 after the initiation of differentiation, as the treatment window for the subsequent experiments.

b. Screening for the inhibition of myotube viability

Cell viability was evaluated after 5 days of treatment with the drugs and metabolites of interest. Apart from alprazolam and 3OH desloratadine, which had limited aqueous solubility and were tested at 5 μM , all the other drugs were tested at a final concentration of 10 μM . Myotubes treated with tegaserod, simvastatin, desloratadine and simvastatin acid exhibited significantly decreased viability as compared to those treated with DMSO (Figure 5-2). Tegaserod was the most potent myotoxin (97.98% cell death), followed by desloratadine (73.66%), simvastatin (73.28%) and simvastatin acid (32.95%) at 10 μM (Table 5-1). It is worth noting that several drugs seemed to improve cell viability significantly after 5 days of treatment. Cells treated with chloroquine, hydroxychloroquine and promethazine were 46.8%, 43.4% and 42.1% more viable than those treated with DMSO as measured using the MTS/PMS assay. The data from three repeated experiments with myotubes of different passages were consistent.

c. Concentration-cell viability relationships of tegaserod, desloratadine and simvastatin

Because treatment with tegaserod, simvastatin and desloratadine resulted in more than 50% myotube death, their concentration-effect curves were characterized with myotubes treated at various concentrations. Tegaserod inhibited myotube viability with an IC_{50} (95% CI) of 4.32 μM (4.15, 4.49) (Figure 5-3 A). Its concentration-effect curve was characterized by a steep drop between 3 μM to 6 μM . The IC_{50} s (95% CI) of desloratadine and simvastatin were 10.94 μM (9.24, 12.96), and 1.64 μM (1.05, 2.56), respectively (Figure 5-3 B and C).

d. The combined effect of simvastatin and desloratadine

To test whether there is a myotoxic interaction between simvastatin and desloratadine, their combined effect on myotube viability was examined by treating myotubes with a range of concentrations of both drugs. In general, the concentration-effect curves of simvastatin shifted leftward with increasing concentration of desloratadine (Figure 5-4, A). The same trend was observed with the concentration curves of desloratadine in the presence of simvastatin (Figure 5-4, B). Using the method of Chou *et al.* [308], combination index (CI) values indicating the intensity of interaction were calculated and plotted against fractional inhibitory effect on myotube viability (f_a). The CI – f_a plot is shown in Figure 5-5, in which the points above the horizontal line at CI = 1 indicate antagonism, and those below the line indicate synergism. Most CI values were greater than zero and less than unity, indicating that the interaction between simvastatin and desloratadine was synergistic, such that the drugs notably increased each other's myotoxic effect. It follows that examination of each individual drug's effect would have underestimated the toxicity of the combination.

4. Discussion

In this chapter, I have addressed the hypothesis that direct myotoxicity of the individual drugs or their combinations contributes to the significant DDIs identified previously. An optimal drug treatment window between day 5 and day 10 after the initiation of differentiation was selected for rat L6 myotubes, based on the gene expression profiles of CKM and Myog, two marker genes of myogenesis. After 5 days of treatment, tegaserod, desloratadine and simvastatin caused significant decreases in the

viability of fully differentiated myotubes at 10 μM . Their $\text{IC}_{50\text{s}}$ for inhibition of viability were 4.32 μM , 10.94 μM and 1.64 μM , respectively. Simvastatin and desloratadine were further found to have a synergistic myotoxic interaction when applied in combination.

Both simvastatin and simvastatin acid induced cell death after 5 days of treatment, whereas 3-hydroxy simvastatin, one of the major circulating metabolites, was well tolerated by myotubes under these conditions. Simvastatin-induced myotoxicity observed here was consistent with the data of Kawk *et al.*, who found that simvastatin induced 60% - 80% cell death at 10 μM in primary skeletal muscle cells after 2 days of treatment using the MTS/PMS assay [289]. At 10 μM , simvastatin was about 2-fold more myotoxic than simvastatin acid. This is consistent with the observation of Skottheim *et al.*, who found that simvastatin lactone was 37-fold more potent in inducing of myotoxicity than its acid form in human primary skeletal myotubes [311]. These data suggest that simvastatin-induced myopathy is due mainly to simvastatin lactone, rather than its downstream metabolites.

Unlike simvastatin, loratadine-induced myopathy seems largely due to its active metabolite desloratadine. Both loratadine and 3-hydroxy desloratadine were well tolerated by myotubes at concentrations up to 10 μM . Its major metabolite desloratadine caused 73.66% of cell death at 10 μM after 5 days of treatment. Neither loratadine nor desloratadine has been reported before to be toxic to muscle cells of any type. My data are the first suggesting that desloratadine myotoxicity may be responsible for myopathy associated with loratadine and desloratadine. The data showing that desloratadine is more myotoxic than loratadine in L6 myotubes seems consistent with the higher occurrence of myalgia in patients treated with desloratadine than in those treated with loratadine. In

randomized clinical trials, 2.1% of subjects treated with desloratadine experienced myalgia, whereas less than 2% of subjects treated with loratadine experienced the same side effect [88, 89]. The myotoxicity of desloratadine and its association with myalgia in humans need to be further evaluated both in human muscle cells and *in vivo*.

This thesis also provides the first description of the myotoxicity of tegaserod. Tegaserod induced myotube death with an IC_{50} of 4.36 μ M. Its concentration – cell viability curve was characterized by a steep decrease between 3 and 6 μ M, indicating that tegaserod may induce cell death through a mechanism that requires tegaserod concentration to cross a certain threshold. Tegaserod is a partial 5-hydroxytryptamine receptor 4 (5-HT₄) agonist and a potent (5-HT_{2B}) antagonist. There are a number of published studies investigating its inotropic effect on cardiomyocytes [312] and smooth muscle cells [313], which may be related to its toxicity to L6 myotubes. Future studies are needed to investigate whether tegaserod has similar effects on human muscle cells.

The drugs were screened for myotoxicity at 10 μ M, a concentration that is much higher than the circulating concentration of any of these drugs. This concentration is also likely higher than the intramuscular concentrations of these drugs except for those of chloroquine and hydroxychloroquine, which are known to accumulate in tissues including muscle [185]. This high screening concentration allowed me to rule out the possibility of myotoxicity *in vivo* for the drugs that did not cause significant myotube death *in vitro*. Therefore, for those non-myotoxic drugs, direct myotoxicity is unlikely the mechanism for the relevant DDIs. On the other hand, this high concentration limits the interpretation of the myotoxicity of simvastatin, desloratadine and tegaserod in a clinical setting. It is possible that at clinical doses, the intramuscular concentrations of these three

drugs are never as high as those used in my experiments, and their toxicity to human muscle cells *in vivo* are minimal. It is, however, also possible that at clinical doses, these drug are toxic enough to induce certain molecular changes that contribute to clinical myopathy in humans, but not as toxic as to induce apoptosis of muscle cells as determined here. Future studies should evaluate the actual myotoxicity of these drugs in humans at clinical doses.

Chloroquine and hydroxychloroquine are known to be toxic to muscle cells. However, my data show that, instead of being myotoxic, they were able to improve the viability of myotubes after 5 days of treatment. The MTS/PMS assay used to evaluate cell viability depends on dehydrogenase enzymes in metabolically active cells. As dehydrogenase enzymes are mostly located in mitochondria, this assay largely measures the collective metabolic activity of mitochondria in the cell population being assayed. Since the myotoxicity of chloroquine and hydroxychloroquine are caused by their lysosomotropic effects, the MTS/PMS assay may not be able to detect myotoxicity of such drugs. This implies that the MTS/PMS assay is only appropriate for evaluating myotoxicity induced by changes in mitochondrial activity. Future studies are warranted to assess the possibility that these drugs induce myotoxicity through other mechanisms.

As was the case for chloroquine and hydroxychloroquine, ropinirole, trazodone, quetiapine and promethazine also seemed to improve cell viability. Considering the high screening concentration that should, in theory, be toxic to cells, the data on these drugs might be an artifact of the MTS/PMS assay. The increased signal at the end of treatment might be cause by dehydrogenase activation of these drugs. They might be able to improve the overall metabolic activity of mitochondria, or to change the

microenvironment in mitochondria, so that dehydrogenase is more efficient in converting MTS to the light-absorbing product.

There are a number of limitations inherent to the use of rat L6 myotubes as the model system. Although rat L6 myotubes are a good model for investigating muscular glucose uptake [296] and myogenesis [297], they may not be the most appropriate model for evaluating drug-induced myopathy. In addition, although these cells have been used by other groups for *in vitro* evaluation of myotoxicity of statins [277, 302] and fibrates [314], they have never been used to examine myotoxicity of other drug or any drug combinations. The validity of this cell model may need to be further assessed, especially for evaluation of myotoxicity resulting from drug combinations. The species difference between rat and human would limit the interpretation of the data in a clinical setting. Future studies using primary human muscle cells may be helpful to further evaluate the myotoxicity of the drugs of interest.

Using Chou *et al.*'s CI method, I identified a synergistic interaction between simvastatin and desloratadine in inducing myotube death. Most CI values are between zero and unity, and tend to decrease with increasing inhibition of cell viability. This suggests that at higher concentrations of simvastatin and desloratadine, where their combined toxic effect on myotubes are larger, the synergism between them is also stronger. There are a few large CI values indicating a strong antagonism in the region near $f_a=0$. As pointed out by Greco *et al.*, these may be an artifact resulting from methodological flaw. I could not obtain an isobologram for this drug combination because most of the concentration-effect curves could not provide reliable estimates of IC_{50} s. Further analysis of the response surface may provide a more comprehensive view

of the nature and intensity of this interaction. Nonetheless, my data suggest that the synergistic myotoxicity of simvastatin and desloratadine may contribute to the interaction between simvastatin and loratadine. Because the data were obtained using concentrations likely much higher than the intramuscular concentrations at the clinical doses, future studies are needed to validate my results *in vivo* and in humans. As discussed in chapter 3, both simvastatin and loratadine are clinically important drugs that are used by a huge number of patients. If this synergistic toxicity is confirmed to be clinically relevant, simvastatin and loratadine should probably not be used together as they commonly are. Patients may need to switch to other statins or other antihistamines to avoid the harm of this synergistic interaction while achieving favorable therapeutic effects.

Table 5-1. The experimental design to evaluate the combined effect of simvastatin and desloratadineNote: The concentration combination in each well is shown as simvastatin concentration μM * desloratadine concentration μM .

Dose-response of simvastatin in the presence of desloratadine							Dose-response of desloratadine in the presence of simvastatin						
	A	B	C	D	E	F		A	B	C	D	E	F
Plate 1							Plate 6						
1	0 * 0	0.5 * 0	1 * 0	2 * 0	4 * 0	8 * 0	1	0 * 0	0 * 5	0 * 7.5	0 * 10	0 * 15	0 * 25
2	0 * 5	0.5 * 5	1 * 5	2 * 5	4 * 5	8 * 5	2	0.5 * 0	0.5 * 5	0.5 * 7.5	0.5 * 10	0.5 * 15	0.5 * 25
3	0 * 7.5	0.5 * 7.5	1 * 7.5	2 * 7.5	4 * 7.5	8 * 7.5	3	1 * 0	1 * 5	1 * 7.5	1 * 10	1 * 15	1 * 25
4	0 * 10	0.5 * 10	1 * 10	2 * 10	4 * 10	8 * 10	4	2 * 0	2 * 5	2 * 7.5	2 * 10	2 * 15	2 * 25
Plate 2							Plate 7						
1	0 * 5	0.5 * 5	1 * 5	2 * 5	4 * 5	8 * 5	1	0.5 * 0	0.5 * 5	0.5 * 7.5	0.5 * 10	0.5 * 15	0.5 * 25
2	0 * 0	0.5 * 0	1 * 0	2 * 0	4 * 0	8 * 0	2	0 * 0	0 * 5	0 * 7.5	0 * 10	0 * 15	0 * 25
3	0 * 7.5	0.5 * 7.5	1 * 7.5	2 * 7.5	4 * 7.5	8 * 7.5	3	1 * 0	1 * 5	1 * 7.5	1 * 10	1 * 15	1 * 25
4	0 * 15	0.5 * 15	1 * 15	2 * 15	4 * 15	8 * 15	4	4 * 0	4 * 5	4 * 7.5	4 * 10	4 * 15	4 * 25
Plate 3							Plate 8						
1	0 * 7.5	0.5 * 7.5	1 * 7.5	2 * 7.5	4 * 7.5	8 * 7.5	1	1 * 0	1 * 5	1 * 7.5	1 * 10	1 * 15	1 * 25
2	0 * 10	0.5 * 10	1 * 10	2 * 10	4 * 10	8 * 10	2	2 * 0	2 * 5	2 * 7.5	2 * 10	2 * 15	2 * 25
3	0 * 0	0.5 * 0	1 * 0	2 * 0	4 * 0	8 * 0	3	0 * 0	0 * 5	0 * 7.5	0 * 10	0 * 15	0 * 25
4	0 * 25	0.5 * 25	1 * 25	2 * 25	4 * 25	8 * 25	4	8 * 0	8 * 5	8 * 7.5	8 * 10	8 * 15	8 * 25
Plate 4							Plate 9						
1	0 * 10	0.5 * 10	1 * 10	2 * 10	4 * 10	8 * 10	1	2 * 0	2 * 5	2 * 7.5	2 * 10	2 * 15	2 * 25
2	0 * 15	0.5 * 15	1 * 15	2 * 15	4 * 15	8 * 15	2	4 * 0	4 * 5	4 * 7.5	4 * 10	4 * 15	4 * 25
3	0 * 25	0.5 * 25	1 * 25	2 * 25	4 * 25	8 * 25	3	8 * 0	8 * 5	8 * 7.5	8 * 10	8 * 15	8 * 25
4	0 * 0	0.5 * 0	1 * 0	2 * 0	4 * 0	8 * 0	4	0 * 0	0 * 5	0 * 7.5	0 * 10	0 * 15	0 * 25
Plate 5							Plate 10						
1	0 * 0	0.5 * 0	1 * 0	2 * 0	4 * 0	8 * 0	1	0 * 0	0 * 5	0 * 7.5	0 * 10	0 * 15	0 * 25
2	0 * 5	0.5 * 5	1 * 5	2 * 5	4 * 5	8 * 5	2	0.5 * 0	0.5 * 5	0.5 * 7.5	0.5 * 10	0.5 * 15	0.5 * 25
3	0 * 15	0.5 * 15	1 * 15	2 * 15	4 * 15	8 * 15	3	4 * 0	4 * 5	4 * 7.5	4 * 10	4 * 15	4 * 25
4	0 * 25	0.5 * 25	1 * 25	2 * 25	4 * 25	8 * 25	4	8 * 0	8 * 5	8 * 7.5	8 * 10	8 * 15	8 * 25

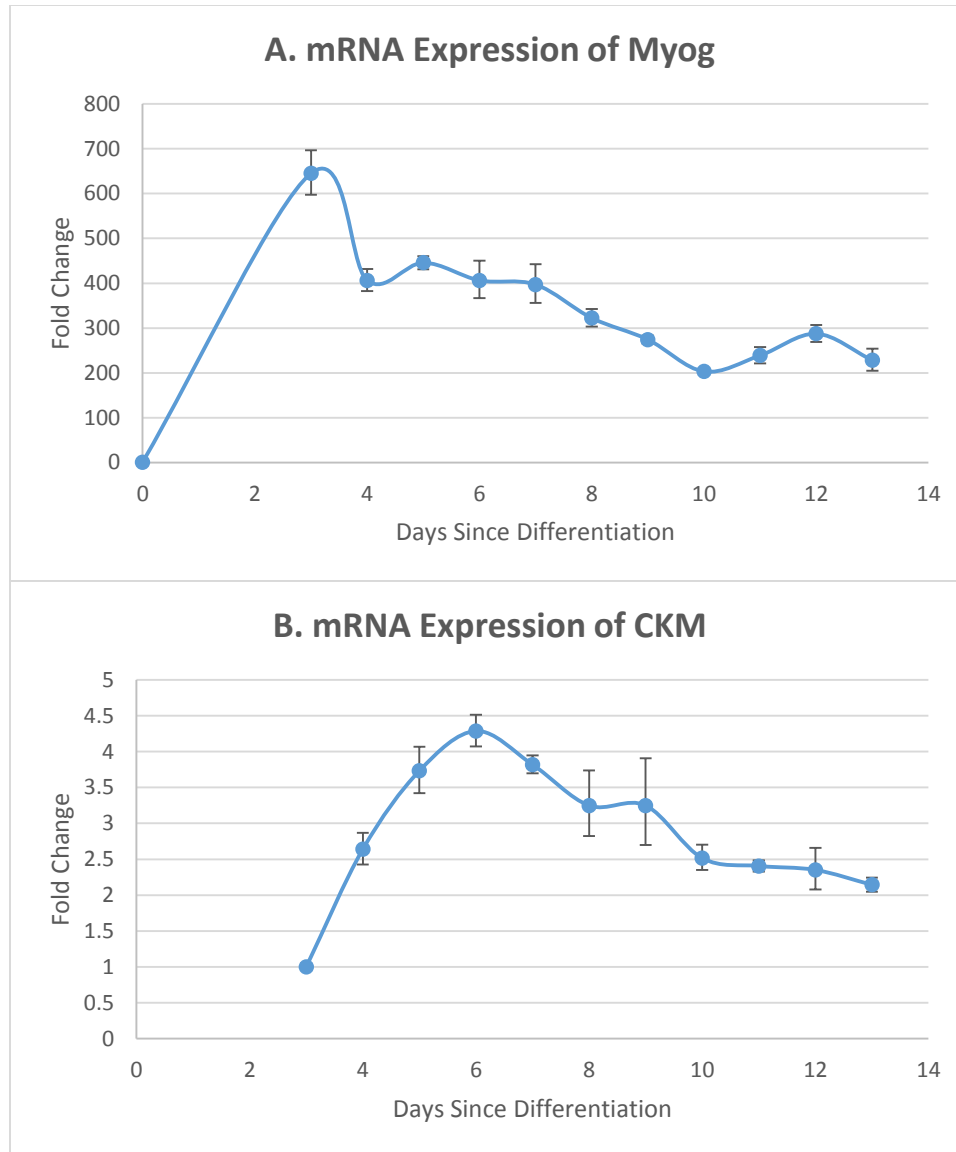


Figure 5-1. Gene expression of Myog (A) and CKM (B). The mRNA expression of Myog and CKM is expressed as fold-change relative to that on day 0 when differentiation was initiated.

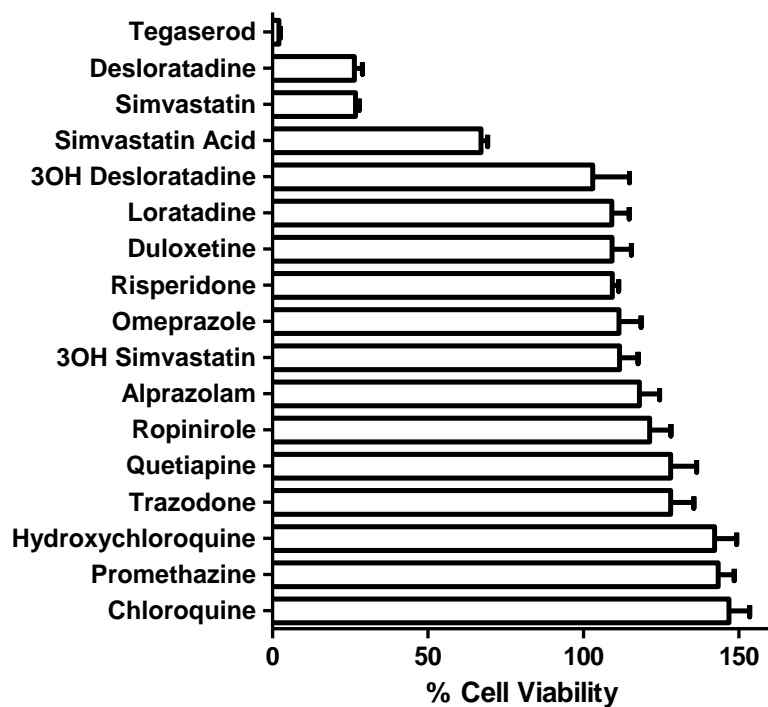


Figure 5-2. Cell viability (%) after 5 days of treatment as compared with DMSO controls. The drugs were tested with six replicates at 10 μ M except for alprazolam and 3OH desloratadine which were tested at 5 μ M.

Table 5-2. Myotube death after 5 days of treatment.

Drug	% Cell death (\pmSEM)
Tegaserod	97.9 \pm 0.4
Desloratadine	73.7 \pm 2.6
Simvastatin	73.3 \pm 1.1
Simvastatin Acid	33 \pm 2.1
3OH Desloratadine	-3 \pm 11.8
Loratadine	-9.1 \pm 5.6
Duloxetine	-9.2 \pm 6.2
Risperidone	-9.3 \pm 2
Omeprazole	-11.4 \pm 7.1
3OH Simvastatin	-11.6 \pm 6
Alprazolam	-18 \pm 6.5
Ropinirole	-21.3 \pm 6.9
Trazodone	-28 \pm 7.5
Quetiapine	-28 \pm 8.4
Hydroxychloroquine	-42.1 \pm 7.2
Promethazine	-43.4 \pm 5.1
Chloroquine	-46.8 \pm 6.649

Note: All the drugs were tested at 10 μ M except for alprazolam and 3OH desloratadine which were tested at 5 μ M.

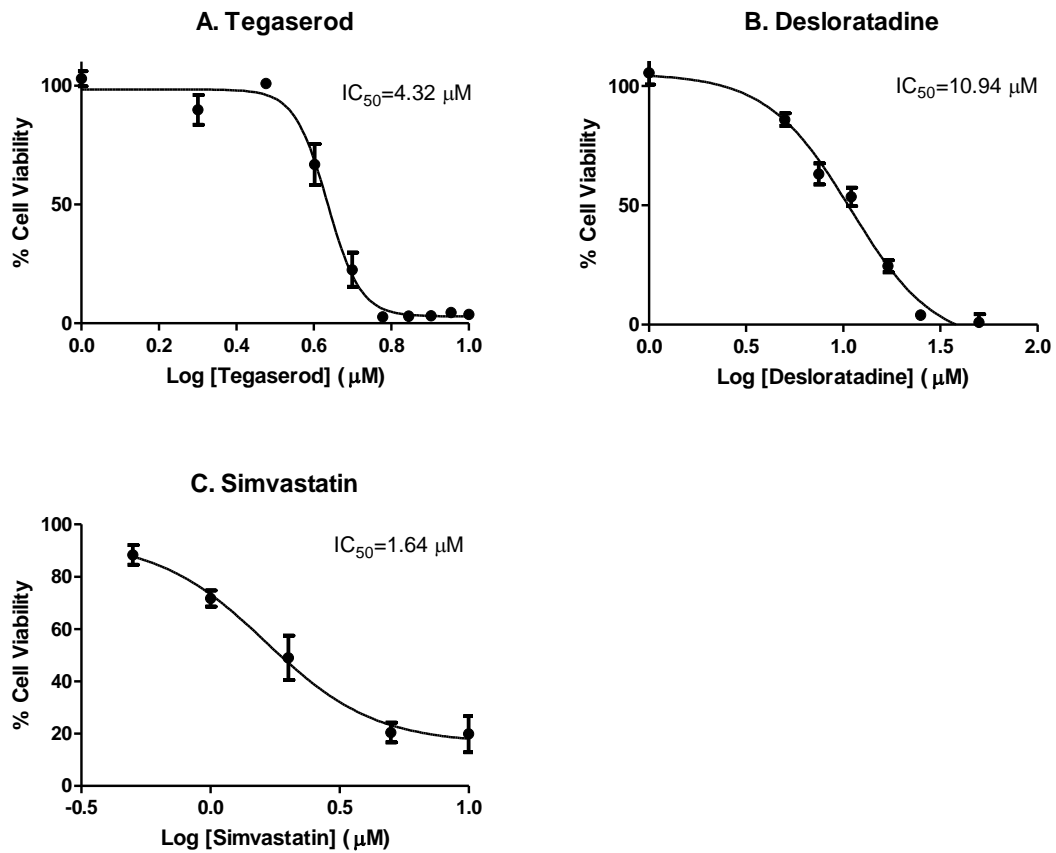


Figure 5-3. Concentration-cell viability relationship of tegaserod (A), desloratadine (B), and simvastatin (C). Fully differentiated myotubes were treated at 1, 2, 3, 4, 5, 6, 7, 8, 9 and 10 μM of tegaserod, 1, 5, 7.5, 11, 17, 25 and 50 μM of desloratadine, and 0.5, 1, 2, 5 and 10 μM of simvastatin for 5 days with at least four replicates.

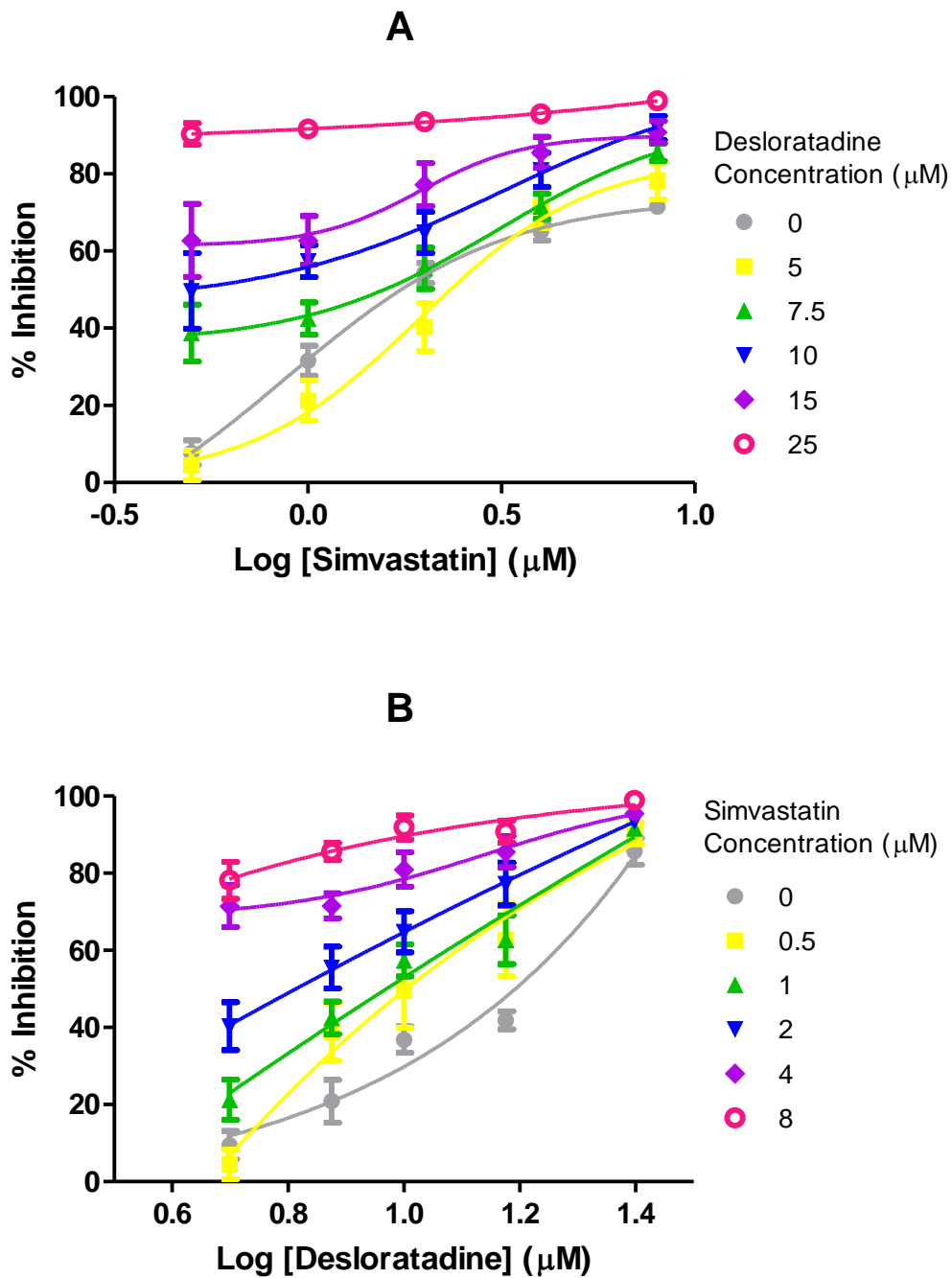


Figure 5-4. Concentration-effect curves of simvastatin and desloratadine in combination. The concentration-inhibition (%) curves of simvastatin in the presence of desloratadine are shown in panel A and those of desloratadine in the presence of simvastatin are shown in panel B.

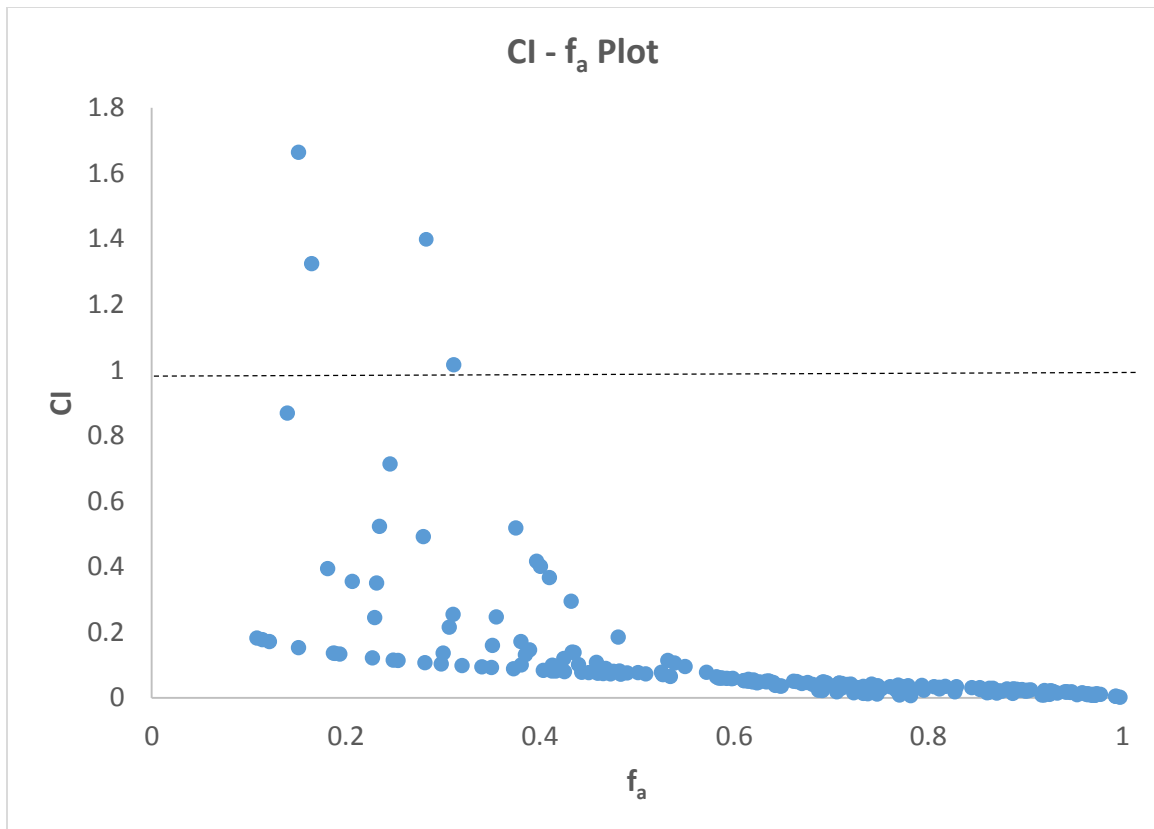


Figure 5-6. Combination index (CI) – fraction of inhibition (f_a) plot. The points above the horizontal dash line at $CI = 1$ indicate antagonism, and those below the line indicate synergism.

Chapter 6. Summary

In this thesis, I have tested the hypothesis that the combination of data mining and *in vitro* mechanistic studies can identify and shed mechanistic light on new DDIs that are associated with an increased risk of clinical myopathy.

Text mining of the published literature identified 232 drugs as either substrates or inhibitors of the major CYPs. 13,197 pairs of drugs were predicted to have metabolic interactions via inhibition of CYPs, 3670 of which were subjected to a pharmacoepidemiology study using a synergistic model and the data from an EMR database. Fifteen drug pairs were identified to be significantly associated with an increased risk of myopathy as compared to the additive risk from taking either of the drugs alone. These significant myopathic DDIs involved thirteen clinically important drugs including alprazolam, chloroquine, duloxetine, hydroxychloroquine, loratadine, omeprazole, promethazine, quetiapine, risperidone, ropinirole, trazodone and simvastatin. Many of these thirteen drugs were identified as inhibitors of the major CYPs *in vitro*. Their mechanisms and potencies were further characterized across eighteen inhibitory reactions that yielded IC_{50} s less than 20 μ M. Duloxetine, promethazine, risperidone, ropinirole, quetiapine and chloroquine were predicted to potentially act as precipitant drugs and cause clinical DDIs. When these interactions were carefully examined using the AUCR approach, the AUCR for the interaction between quetiapine and chloroquine was 1.25, indicating a weak clinical drug interaction. The risk of clinical DDIs for the other inhibitory reactions was predicted to be negligible.

Detailed studies on the interaction between loratadine and simvastatin revealed that loratadine and desloratadine were able to inhibit the metabolism of simvastatin and simvastatin acid, and that simvastatin and simvastatin acid were able to inhibit the metabolism of loratadine. However, these inhibitory reactions were relatively weak or moderate, and were unlikely to result in any clinically meaningful effect.

Simvastatin acid and quetiapine were identified as relatively potent inhibitors of E₂17βDG uptake via OATP1B1/1B3. Their predicted R values were 3.85 and 5.28, respectively, larger than that of rifampin (R value 3.4), a drug that is known to cause clinical DDIs by inhibiting OATP1B1/1B3. These data suggest that simvastatin acid and quetiapine may interact with drugs that rely on OATP1B1/1B3 for hepatic uptake *in vivo*. The inhibitory effect of simvastatin acid may contribute to the interaction between simvastatin and loratadine by inhibiting the hepatic uptake of desloratadine via OATP1B1/1B3.

Tegaserod, desloratadine and simvastatin were able to induce significant apoptosis in fully differentiated myotubes. Their IC₅₀s for inhibition of viability were 4.32 μM, 10.94 μM and 1.64 μM, respectively. Simvastatin and desloratadine were further found to have a synergistic myotoxic interaction when applied in combination, which may contribute to the interaction between simvastatin and loratadine.

These data suggest that the interaction between quetiapine and chloroquine may be due to the inhibition of the metabolism of chloroquine by quetiapine. The data also suggest that the interaction between simvastatin and loratadine may result from the inhibition of OATP1B1/1B3 by simvastatin acid and from synergistic myotoxicity of simvastatin and desloratadine.

Finally, with these data, I have demonstrated that our approach, that combines literature mining using bioinformatics algorithms, ADR detection using a pharmacoepidemiology design, and mechanistic studies employing *in vitro* experimental models, can identify and shed mechanistic light on new DDIs that are associated with an increased risk of clinical myopathy.

Appendix: Permission to Reuse Table 4-1

Rightslink Printable License

<https://s100.copyright.com/App/PrintableLicenseFrame.jsp?publis...>

JOHN WILEY AND SONS LICENSE TERMS AND CONDITIONS

Feb 01, 2014

This is a License Agreement between Xu Han ("You") and John Wiley and Sons ("John Wiley and Sons") provided by Copyright Clearance Center ("CCC"). The license consists of your order details, the terms and conditions provided by John Wiley and Sons, and the payment terms and conditions.

All payments must be made in full to CCC. For payment instructions, please see information listed at the bottom of this form.

License Number	3320280239055
License date	Feb 01, 2014
Licensed content publisher	John Wiley and Sons
Licensed content publication	Biopharmaceutics and Drug Disposition
Licensed content title	Clinical significance of organic anion transporting polypeptides (OATPs) in drug disposition: their roles in hepatic clearance and intestinal absorption
Licensed copyright line	Copyright © 2012 John Wiley & Sons, Ltd.
Licensed content author	Yoshihisa Shitara, Kazuya Maeda, Kazuaki Ikejiri, Kenta Yoshida, Toshiharu Horie, Yuichi Sugiyama
Licensed content date	Jan 20, 2013
Start page	45
End page	78
Type of use	Dissertation/Thesis
Requestor type	University/Academic
Format	Print and electronic
Portion	Figure/table
Number of figures/tables	1
Original Wiley figure/table number(s)	Table 1
Will you be translating?	No
Title of your thesis / dissertation	IDENTIFICATION AND MECHANISTIC INVESTIGATION OF CLINICALLY IMPORTANT MYOPATHIC DRUG-DRUG INTERACTIONS
Expected completion date	Mar 2014
Expected size (number of pages)	226
Total	0.00 USD
Terms and Conditions	

TERMS AND CONDITIONS

This copyrighted material is owned by or exclusively licensed to John Wiley & Sons, Inc. or one of its group companies (each a "Wiley Company") or a society for whom a Wiley

Company has exclusive publishing rights in relation to a particular journal (collectively "WILEY"). By clicking "accept" in connection with completing this licensing transaction, you agree that the following terms and conditions apply to this transaction (along with the billing and payment terms and conditions established by the Copyright Clearance Center Inc., ("CCC's Billing and Payment terms and conditions"), at the time that you opened your RightsLink account (these are available at any time at <http://myaccount.copyright.com>).

Terms and Conditions

1. The materials you have requested permission to reproduce (the "Materials") are protected by copyright.
2. You are hereby granted a personal, non-exclusive, non-sublicensable, non-transferable, worldwide, limited license to reproduce the Materials for the purpose specified in the licensing process. This license is for a one-time use only with a maximum distribution equal to the number that you identified in the licensing process. Any form of republication granted by this license must be completed within two years of the date of the grant of this license (although copies prepared before may be distributed thereafter). The Materials shall not be used in any other manner or for any other purpose. Permission is granted subject to an appropriate acknowledgement given to the author, title of the material/book/journal and the publisher. You shall also duplicate the copyright notice that appears in the Wiley publication in your use of the Material. Permission is also granted on the understanding that nowhere in the text is a previously published source acknowledged for all or part of this Material. Any third party material is expressly excluded from this permission.
3. With respect to the Materials, all rights are reserved. Except as expressly granted by the terms of the license, no part of the Materials may be copied, modified, adapted (except for minor reformatting required by the new Publication), translated, reproduced, transferred or distributed, in any form or by any means, and no derivative works may be made based on the Materials without the prior permission of the respective copyright owner. You may not alter, remove or suppress in any manner any copyright, trademark or other notices displayed by the Materials. You may not license, rent, sell, loan, lease, pledge, offer as security, transfer or assign the Materials, or any of the rights granted to you hereunder to any other person.
4. The Materials and all of the intellectual property rights therein shall at all times remain the exclusive property of John Wiley & Sons Inc or one of its related companies (WILEY) or their respective licensors, and your interest therein is only that of having possession of and the right to reproduce the Materials pursuant to Section 2 herein during the continuance of this Agreement. You agree that you own no right, title or interest in or to the Materials or any of the intellectual property rights therein. You shall have no rights hereunder other than the license as provided for above in Section 2. No right, license or interest to any trademark, trade name, service mark or other branding ("Marks") of WILEY or its licensors is granted hereunder, and you agree that you shall not assert any such right, license or interest with respect thereto.
5. NEITHER WILEY NOR ITS LICENSORS MAKES ANY WARRANTY OR REPRESENTATION OF ANY KIND TO YOU OR ANY THIRD PARTY, EXPRESS, IMPLIED OR STATUTORY, WITH RESPECT TO THE MATERIALS OR THE

ACCURACY OF ANY INFORMATION CONTAINED IN THE MATERIALS, INCLUDING, WITHOUT LIMITATION, ANY IMPLIED WARRANTY OF MERCHANTABILITY, ACCURACY, SATISFACTORY QUALITY, FITNESS FOR A PARTICULAR PURPOSE, USABILITY, INTEGRATION OR NON-INFRINGEMENT AND ALL SUCH WARRANTIES ARE HEREBY EXCLUDED BY WILEY AND ITS LICENSORS AND WAIVED BY YOU.

6. WILEY shall have the right to terminate this Agreement immediately upon breach of this Agreement by you.

7. You shall indemnify, defend and hold harmless WILEY, its Licensors and their respective directors, officers, agents and employees, from and against any actual or threatened claims, demands, causes of action or proceedings arising from any breach of this Agreement by you.

8. IN NO EVENT SHALL WILEY OR ITS LICENSORS BE LIABLE TO YOU OR ANY OTHER PARTY OR ANY OTHER PERSON OR ENTITY FOR ANY SPECIAL, CONSEQUENTIAL, INCIDENTAL, INDIRECT, EXEMPLARY OR PUNITIVE DAMAGES, HOWEVER CAUSED, ARISING OUT OF OR IN CONNECTION WITH THE DOWNLOADING, PROVISIONING, VIEWING OR USE OF THE MATERIALS REGARDLESS OF THE FORM OF ACTION, WHETHER FOR BREACH OF CONTRACT, BREACH OF WARRANTY, TORT, NEGLIGENCE, INFRINGEMENT OR OTHERWISE (INCLUDING, WITHOUT LIMITATION, DAMAGES BASED ON LOSS OF PROFITS, DATA, FILES, USE, BUSINESS OPPORTUNITY OR CLAIMS OF THIRD PARTIES), AND WHETHER OR NOT THE PARTY HAS BEEN ADVISED OF THE POSSIBILITY OF SUCH DAMAGES. THIS LIMITATION SHALL APPLY NOTWITHSTANDING ANY FAILURE OF ESSENTIAL PURPOSE OF ANY LIMITED REMEDY PROVIDED HEREIN.

9. Should any provision of this Agreement be held by a court of competent jurisdiction to be illegal, invalid, or unenforceable, that provision shall be deemed amended to achieve as nearly as possible the same economic effect as the original provision, and the legality, validity and enforceability of the remaining provisions of this Agreement shall not be affected or impaired thereby.

10. The failure of either party to enforce any term or condition of this Agreement shall not constitute a waiver of either party's right to enforce each and every term and condition of this Agreement. No breach under this agreement shall be deemed waived or excused by either party unless such waiver or consent is in writing signed by the party granting such waiver or consent. The waiver by or consent of a party to a breach of any provision of this Agreement shall not operate or be construed as a waiver of or consent to any other or subsequent breach by such other party.

11. This Agreement may not be assigned (including by operation of law or otherwise) by you without WILEY's prior written consent.

12. Any fee required for this permission shall be non-refundable after thirty (30) days from receipt

13. These terms and conditions together with CCC's Billing and Payment terms and conditions (which are incorporated herein) form the entire agreement between you and

WILEY concerning this licensing transaction and (in the absence of fraud) supersedes all prior agreements and representations of the parties, oral or written. This Agreement may not be amended except in writing signed by both parties. This Agreement shall be binding upon and inure to the benefit of the parties' successors, legal representatives, and authorized assigns.

14. In the event of any conflict between your obligations established by these terms and conditions and those established by CCC's Billing and Payment terms and conditions, these terms and conditions shall prevail.

15. WILEY expressly reserves all rights not specifically granted in the combination of (i) the license details provided by you and accepted in the course of this licensing transaction, (ii) these terms and conditions and (iii) CCC's Billing and Payment terms and conditions.

16. This Agreement will be void if the Type of Use, Format, Circulation, or Requestor Type was misrepresented during the licensing process.

17. This Agreement shall be governed by and construed in accordance with the laws of the State of New York, USA, without regards to such state's conflict of law rules. Any legal action, suit or proceeding arising out of or relating to these Terms and Conditions or the breach thereof shall be instituted in a court of competent jurisdiction in New York County in the State of New York in the United States of America and each party hereby consents and submits to the personal jurisdiction of such court, waives any objection to venue in such court and consents to service of process by registered or certified mail, return receipt requested, at the last known address of such party.

Wiley Open Access Terms and Conditions

Wiley publishes Open Access articles in both its Wiley Open Access Journals program [<http://www.wileyopenaccess.com/view/index.html>] and as Online Open articles in its subscription journals. The majority of Wiley Open Access Journals have adopted the [Creative Commons Attribution License](#) (CC BY) which permits the unrestricted use, distribution, reproduction, adaptation and commercial exploitation of the article in any medium. No permission is required to use the article in this way provided that the article is properly cited and other license terms are observed. A small number of Wiley Open Access journals have retained the [Creative Commons Attribution Non Commercial License](#) (CC BY-NC), which permits use, distribution and reproduction in any medium, provided the original work is properly cited and is not used for commercial purposes.

Online Open articles - Authors selecting Online Open are, unless particular exceptions apply, offered a choice of Creative Commons licenses. They may therefore select from the CC BY, the CC BY-NC and the [Attribution-NoDerivatives](#) (CC BY-NC-ND). The CC BY-NC-ND is more restrictive than the CC BY-NC as it does not permit adaptations or modifications without rights holder consent.

Wiley Open Access articles are protected by copyright and are posted to repositories and websites in accordance with the terms of the applicable Creative Commons license referenced on the article. At the time of deposit, Wiley Open Access articles include all changes made during peer review, copyediting, and publishing. Repositories and websites that host the article are responsible for incorporating any publisher-supplied amendments or

retractions issued subsequently.

Wiley Open Access articles are also available without charge on Wiley's publishing platform, **Wiley Online Library** or any successor sites.

Conditions applicable to all Wiley Open Access articles:

- The authors' moral rights must not be compromised. These rights include the right of "paternity" (also known as "attribution" - the right for the author to be identified as such) and "integrity" (the right for the author not to have the work altered in such a way that the author's reputation or integrity may be damaged).
- Where content in the article is identified as belonging to a third party, it is the obligation of the user to ensure that any reuse complies with the copyright policies of the owner of that content.
- If article content is copied, downloaded or otherwise reused for research and other purposes as permitted, a link to the appropriate bibliographic citation (authors, journal, article title, volume, issue, page numbers, DOI and the link to the definitive published version on Wiley Online Library) should be maintained. Copyright notices and disclaimers must not be deleted.
 - Creative Commons licenses are copyright licenses and do not confer any other rights, including but not limited to trademark or patent rights.
- Any translations, for which a prior translation agreement with Wiley has not been agreed, must prominently display the statement: "This is an unofficial translation of an article that appeared in a Wiley publication. The publisher has not endorsed this translation."

Conditions applicable to non-commercial licenses (CC BY-NC and CC BY-NC-ND)

For non-commercial and non-promotional purposes individual non-commercial users may access, download, copy, display and redistribute to colleagues Wiley Open Access articles. In addition, articles adopting the CC BY-NC may be adapted, translated, and text- and data-mined subject to the conditions above.

Use by commercial "for-profit" organizations

Use of non-commercial Wiley Open Access articles for commercial, promotional, or marketing purposes requires further explicit permission from Wiley and will be subject to a fee. Commercial purposes include:

- Copying or downloading of articles, or linking to such articles for further redistribution, sale or licensing;
- Copying, downloading or posting by a site or service that incorporates advertising with such content;

- The inclusion or incorporation of article content in other works or services (other than normal quotations with an appropriate citation) that is then available for sale or licensing, for a fee (for example, a compilation produced for marketing purposes, inclusion in a sales pack)
- Use of article content (other than normal quotations with appropriate citation) by for-profit organizations for promotional purposes
- Linking to article content in e-mails redistributed for promotional, marketing or educational purposes;
- Use for the purposes of monetary reward by means of sale, resale, license, loan, transfer or other form of commercial exploitation such as marketing products
- Print reprints of Wiley Open Access articles can be purchased from: corporatesales@wiley.com

The modification or adaptation for any purpose of an article referencing the CC BY-NC-ND License requires consent which can be requested from RightsLink@wiley.com.

Other Terms and Conditions:

BY CLICKING ON THE "I AGREE..." BOX, YOU ACKNOWLEDGE THAT YOU HAVE READ AND FULLY UNDERSTAND EACH OF THE SECTIONS OF AND PROVISIONS SET FORTH IN THIS AGREEMENT AND THAT YOU ARE IN AGREEMENT WITH AND ARE WILLING TO ACCEPT ALL OF YOUR OBLIGATIONS AS SET FORTH IN THIS AGREEMENT.

v1.8

If you would like to pay for this license now, please remit this license along with your payment made payable to "COPYRIGHT CLEARANCE CENTER" otherwise you will be invoiced within 48 hours of the license date. Payment should be in the form of a check or money order referencing your account number and this invoice number RLNK501216348.

Once you receive your invoice for this order, you may pay your invoice by credit card. Please follow instructions provided at that time.

**Make Payment To:
Copyright Clearance Center
Dept 001
P.O. Box 843006
Boston, MA 02284-3006**

For suggestions or comments regarding this order, contact RightsLink Customer Support: customer@copyright.com or +1-877-622-5543 (toll free in the US) or

+1-978-646-2777.

Gratis licenses (referencing \$0 in the Total field) are free. Please retain this printable license for your reference. No payment is required.

References

1. Medicine., C.o.Q.o.H.C.i.A.I.o., *To Err Is Human: Building a Safer Health System*. 2000, Washington, D.C.: National Academy Press.
2. Lazarou, J., B.H. Pomeranz, and P.N. Corey, *Incidence of adverse drug reactions in hospitalized patients: a meta-analysis of prospective studies*. JAMA, 1998. **279**(15): p. 1200-5.
3. Johnson, J.A. and J.L. Bootman, *Drug-related morbidity and mortality. A cost-of-illness model*. Arch Intern Med, 1995. **155**(18): p. 1949-56.
4. Leape, L.L., et al., *Systems analysis of adverse drug events. ADE Prevention Study Group*. JAMA, 1995. **274**(1): p. 35-43.
5. Leone, R., et al., *Identifying adverse drug reactions associated with drug-drug interactions: data mining of a spontaneous reporting database in Italy*. Drug Saf, 2010. **33**(8): p. 667-75.
6. Becker, M.L., et al., *Hospitalisations and emergency department visits due to drug-drug interactions: a literature review*. Pharmacoepidemiol Drug Saf, 2007. **16**(6): p. 641-51.
7. Prevention, C.f.D.C.a. *Hospital Utilization*. 2010; Available from: <http://www.cdc.gov/nchs/fastats/hospital.htm>.
8. Terleira, A., et al., *Effect of drug-test interactions on length of hospital stay*. Pharmacoepidemiol Drug Saf, 2007. **16**(1): p. 39-45.
9. Lin, C.F., C.Y. Wang, and C.H. Bai, *Polypharmacy, aging and potential drug-drug interactions in outpatients in Taiwan: a retrospective computerized screening study*. Drugs Aging, 2011. **28**(3): p. 219-25.
10. Bjerrum, L., et al., *Exposure to potential drug interactions in primary health care*. Scand J Prim Health Care, 2003. **21**(3): p. 153-8.
11. Gurwitz, J.H., et al., *Incidence and preventability of adverse drug events among older persons in the ambulatory setting*. JAMA, 2003. **289**(9): p. 1107-16.
12. Bjorkman, I.K., et al., *Drug-drug interactions in the elderly*. Ann Pharmacother, 2002. **36**(11): p. 1675-81.
13. FDA, *Guidance for Industry: Drug Interaction Studies —Study Design, Data Analysis, Implications for Dosing, and Labeling Recommendations*. 2012.
14. Monahan, B.P., et al., *Torsades de pointes occurring in association with terfenadine use*. JAMA, 1990. **264**(21): p. 2788-90.
15. Gottlieb, S., *Antihistamine drug withdrawn by manufacturer*. BMJ, 1999. **319**(7201): p. 7.
16. Griffin, J.P., *Prepulsid withdrawn from UK & US markets*. Adverse Drug React Toxicol Rev, 2000. **19**(3): p. 177.
17. Billups, S.J. and B.L. Carter, *Mibefradil withdrawn from the market*. Ann Pharmacother, 1998. **32**(7-8): p. 841.
18. Becker, D.E., *Adverse drug interactions*. Anesth Prog, 2011. **58**(1): p. 31-41.
19. Hinder, M., *Pharmacodynamic Drug–Drug Interactions*, in *Drug Discovery and Evaluation: Methods in Clinical Pharmacology*, H. Vogel, J. Maas, and A. Gebauer, Editors. 2011, Springer Berlin Heidelberg. p. 367-376.

20. Tallarida, R.J., *Drug synergism: its detection and applications*. J Pharmacol Exp Ther, 2001. **298**(3): p. 865-72.
21. Horowitz, H.W., U.P. Jorde, and G.P. Wormser, *Drug interactions in use of dapsone for Pneumocystis carinii prophylaxis*. Lancet, 1992. **339**(8795): p. 747.
22. Moreno, F., et al., *Itraconazole-didanosine excipient interaction*. JAMA, 1993. **269**(12): p. 1508.
23. Lomaestro, B.M. and G.R. Bailie, *Quinolone-cation interactions: a review*. DICP, 1991. **25**(11): p. 1249-58.
24. Campbell, N.R. and B.B. Hasinoff, *Iron supplements: a common cause of drug interactions*. Br J Clin Pharmacol, 1991. **31**(3): p. 251-5.
25. Piscitelli, S.C. and K. Rodvold, *Drug interactions in infectious diseases*. 2nd ed. Infectious disease. 2005, Totowa, N.J.: Humana Press. x, 534 p.
26. Najar, I.A., et al., *Involvement of P-glycoprotein and CYP 3A4 in the enhancement of etoposide bioavailability by a piperine analogue*. Chem Biol Interact, 2011. **190**(2-3): p. 84-90.
27. Zamek-Gliszczynski, M.J., et al., *ITC recommendations for transporter kinetic parameter estimation and translational modeling of transport-mediated PK and DDIs in humans*. Clin Pharmacol Ther, 2013. **94**(1): p. 64-79.
28. Rolan, P.E., *Plasma protein binding displacement interactions--why are they still regarded as clinically important?* Br J Clin Pharmacol, 1994. **37**(2): p. 125-8.
29. Sansom, L.N. and A.M. Evans, *What is the true clinical significance of plasma protein binding displacement interactions?* Drug Saf, 1995. **12**(4): p. 227-33.
30. Strandell, J. and S. Wahlin, *Pharmacodynamic and pharmacokinetic drug interactions reported to VigiBase, the WHO global individual case safety report database*. Eur J Clin Pharmacol, 2011. **67**(6): p. 633-41.
31. Danielson, P.B., *The cytochrome P450 superfamily: biochemistry, evolution and drug metabolism in humans*. Curr Drug Metab, 2002. **3**(6): p. 561-97.
32. Belpaire, F.M. and M.G. Bogaert, *Cytochrome P450: genetic polymorphism and drug interactions*. Acta Clin Belg, 1996. **51**(4): p. 254-60.
33. Kiang, T.K., M.H. Ensom, and T.K. Chang, *UDP-glucuronosyltransferases and clinical drug-drug interactions*. Pharmacol Ther, 2005. **106**(1): p. 97-132.
34. Koenen, A., et al., *Current understanding of hepatic and intestinal OATP-mediated drug-drug interactions*. Expert Rev Clin Pharmacol, 2011. **4**(6): p. 729-42.
35. Lepist, E.I. and A.S. Ray, *Renal drug-drug interactions: what we have learned and where we are going*. Expert Opin Drug Metab Toxicol, 2012. **8**(4): p. 433-48.
36. Giacomini, K.M., et al., *Membrane transporters in drug development*. Nature reviews. Drug discovery, 2010. **9**(3): p. 215-36.
37. Tsuda, M., et al., *Involvement of human multidrug and toxin extrusion 1 in the drug interaction between cimetidine and metformin in renal epithelial cells*. J Pharmacol Exp Ther, 2009. **329**(1): p. 185-91.
38. Wang, D.S., et al., *Involvement of organic cation transporter 1 in hepatic and intestinal distribution of metformin*. J Pharmacol Exp Ther, 2002. **302**(2): p. 510-5.
39. Ito, S., et al., *Competitive inhibition of the luminal efflux by multidrug and toxin extrusions, but not basolateral uptake by organic cation transporter 2, is the*

- likely mechanism underlying the pharmacokinetic drug-drug interactions caused by cimetidine in the kidney. *J Pharmacol Exp Ther*, 2012. **340**(2): p. 393-403.
40. Somogyi, A., et al., *Reduction of metformin renal tubular secretion by cimetidine in man*. *Br J Clin Pharmacol*, 1987. **23**(5): p. 545-51.
 41. Duke, J.D., et al., *Literature based drug interaction prediction with clinical assessment using electronic medical records: novel myopathy associated drug interactions*. *PLoS Comput Biol*, 2012. **8**(8): p. e1002614.
 42. Strom, B.L., S.E. Kimmel, and S. Hennessy, *Pharmacoepidemiology*. 5th ed. 2012, Chichester, West Sussex, UK: Wiley-Blackwell. p.
 43. Szarfman, A., J.M. Topping, and P.M. Doraiswamy, *Pharmacovigilance in the 21st century: new systematic tools for an old problem*. *Pharmacotherapy*, 2004. **24**(9): p. 1099-104.
 44. Percha, B., Y. Garten, and R.B. Altman, *Discovery and explanation of drug-drug interactions via text mining*. *Pac Symp Biocomput*, 2012: p. 410-21.
 45. Tatonetti, N.P., et al., *Data-driven prediction of drug effects and interactions*. *Sci Transl Med*, 2012. **4**(125): p. 125ra31.
 46. Miller, M.L. *Drug-induced myopathies*. 2013; Available from: <http://www.uptodate.com/contents/drug-induced-myopathies>.
 47. Bellosta, S. and A. Corsini, *Statin drug interactions and related adverse reactions*. *Expert Opin Drug Saf*, 2012. **11**(6): p. 933-46.
 48. *SIDER 2: Side Effect Resouce*. Available from: <http://sideeffects.embl.de/>.
 49. Zuckner, J., *Drug-related myopathies*. *Rheum Dis Clin North Am*, 1994. **20**(4): p. 1017-32.
 50. Prendergast, B.D. and C.F. George, *Drug-induced rhabdomyolysis--mechanisms and management*. *Postgrad Med J*, 1993. **69**(811): p. 333-6.
 51. Curry, S.C., D. Chang, and D. Connor, *Drug- and toxin-induced rhabdomyolysis*. *Ann Emerg Med*, 1989. **18**(10): p. 1068-84.
 52. Graham, D.J., et al., *Incidence of hospitalized rhabdomyolysis in patients treated with lipid-lowering drugs*. *JAMA*, 2004. **292**(21): p. 2585-90.
 53. Harpaz, R., et al., *Novel data-mining methodologies for adverse drug event discovery and analysis*. *Clinical pharmacology and therapeutics*, 2012. **91**(6): p. 1010-21.
 54. Administration, U.F.a.D. *FDA Adverse Event Reporting System (FAERS) (formerly AERS)*. Available from: <http://www.fda.gov/Drugs/GuidanceComplianceRegulatoryInformation/Surveillance/AdverseDrugEffects/>.
 55. Centre, T.U.M. *VigiBase™*. Available from: <http://www.umc-products.com/DynPage.aspx?id=73590&mn1=1107&mn2=1132>.
 56. Bate, A. and S.J. Evans, *Quantitative signal detection using spontaneous ADR reporting*. *Pharmacoepidemiol Drug Saf*, 2009. **18**(6): p. 427-36.
 57. Stephenson, W.P. and M. Hauben, *Data mining for signals in spontaneous reporting databases: proceed with caution*. *Pharmacoepidemiol Drug Saf*, 2007. **16**(4): p. 359-65.
 58. Schneeweiss, S. and J. Avorn, *A review of uses of health care utilization databases for epidemiologic research on therapeutics*. *J Clin Epidemiol*, 2005. **58**(4): p. 323-37.

59. Schneeweiss, S., *A basic study design for expedited safety signal evaluation based on electronic healthcare data*. *Pharmacoepidemiol Drug Saf*, 2010. **19**(8): p. 858-68.
60. Denny, J.C., *Chapter 13: Mining electronic health records in the genomics era*. *PLoS Comput Biol*, 2012. **8**(12): p. e1002823.
61. Pustejovsky, J., et al., *Robust relational parsing over biomedical literature: extracting inhibit relations*. *Pac Symp Biocomput*, 2002: p. 362-73.
62. Knox, C., et al., *DrugBank 3.0: a comprehensive resource for 'omics' research on drugs*. *Nucleic Acids Res*, 2011. **39**(Database issue): p. D1035-41.
63. Backman, J.T., et al., *Plasma concentrations of active simvastatin acid are increased by gemfibrozil*. *Clin Pharmacol Ther*, 2000. **68**(2): p. 122-9.
64. *WOMBAT (World of Molecular BioActivity)*. Available from: World of Molecular Bioactivity
65. Pouliot, Y., A.P. Chiang, and A.J. Butte, *Predicting adverse drug reactions using publicly available PubChem BioAssay data*. *Clin Pharmacol Ther*, 2011. **90**(1): p. 90-9.
66. Matthews, E.J., et al., *Identification of structure-activity relationships for adverse effects of pharmaceuticals in humans: Part C: use of QSAR and an expert system for the estimation of the mechanism of action of drug-induced hepatobiliary and urinary tract toxicities*. *Regul Toxicol Pharmacol*, 2009. **54**(1): p. 43-65.
67. Matthews, E.J. and A.A. Frid, *Prediction of drug-related cardiac adverse effects in humans--A: creation of a database of effects and identification of factors affecting their occurrence*. *Regul Toxicol Pharmacol*, 2010. **56**(3): p. 247-75.
68. Robert Leaman, L.W., Ryan Sullivan, Annie Skariah, Jian Yang, Graciela Gonzalez, *Towards Internet-Age Pharmacovigilance: Extracting Adverse Drug Reactions from User Posts to Health-Related Social Networks*. *Proceedings of the 2010 Workshop on Biomedical Natural Language Processing, ACL 2010*, 2010: p. 117-125.
69. Mao, J.J., et al., *Online discussion of drug side effects and discontinuation among breast cancer survivors*. *Pharmacoepidemiol Drug Saf*, 2013. **22**(3): p. 256-62.
70. Cohen, K.B. and L. Hunter, *Getting started in text mining*. *PLoS Comput Biol*, 2008. **4**(1): p. e20.
71. Rzhetsky, A., M. Seringhaus, and M.B. Gerstein, *Getting started in text mining: part two*. *PLoS Comput Biol*, 2009. **5**(7): p. e1000411.
72. Altman, R.B., *Introduction to translational bioinformatics collection*. *PLoS Comput Biol*, 2012. **8**(12): p. e1002796.
73. Vishwadeepak Singh Baghela 1, D.S.P.T., *Text mining approaches to extract interesting association rules from text documents*. *IJCSI International Journal of Computer Science Issues*, 2012. **9**(3): p. 545-552.
74. Hunter, K.B.C.a.L., *Natural Language Processing and Systems Biology*, in *Artificial intelligence and systems biology*, P.F. Dubitzky W, Editor., Springer Verlag: Berlin.
75. Farghaly, A., *Handbook for Language Engineers*. 2003.
76. Wu, H.Y., et al., *An integrated pharmacokinetics ontology and corpus for text mining*. *BMC Bioinformatics*, 2013. **14**: p. 35.

77. Coulet, A., et al., *Using text to build semantic networks for pharmacogenomics*. J Biomed Inform, 2010. **43**(6): p. 1009-19.
78. Wang, Z., et al., *Literature mining on pharmacokinetics numerical data: a feasibility study*. J Biomed Inform, 2009. **42**(4): p. 726-35.
79. *Cohort study*. Available from: http://en.wikipedia.org/wiki/Cohort_study.
80. Etminan, M. and A. Samii, *Pharmacoepidemiology I: a review of pharmacoepidemiologic study designs*. Pharmacotherapy, 2004. **24**(8): p. 964-9.
81. Etminan, M., *Pharmacoepidemiology II: the nested case-control study--a novel approach in pharmacoepidemiologic research*. Pharmacotherapy, 2004. **24**(9): p. 1105-9.
82. Chatzizisis, Y.S., et al., *Risk factors and drug interactions predisposing to statin-induced myopathy: implications for risk assessment, prevention and treatment*. Drug safety : an international journal of medical toxicology and drug experience, 2010. **33**(3): p. 171-87.
83. Goodman, L.S., et al., *Goodman & Gilman's pharmacological basis of therapeutics*. 12th ed. 2011, New York: McGraw-Hill. 2084 p.
84. Tari, L., et al., *Discovering drug-drug interactions: a text-mining and reasoning approach based on properties of drug metabolism*. Bioinformatics, 2010. **26**(18): p. i547-53.
85. Stein, M., M.J. Bell, and L.C. Ang, *Hydroxychloroquine neuromyotoxicity*. J Rheumatol, 2000. **27**(12): p. 2927-31.
86. Avina-Zubieta, J.A., et al., *Incidence of myopathy in patients treated with antimalarials. A report of three cases and a review of the literature*. Br J Rheumatol, 1995. **34**(2): p. 166-70.
87. Casado, E., et al., *Antimalarial myopathy: an underdiagnosed complication? Prospective longitudinal study of 119 patients*. Ann Rheum Dis, 2006. **65**(3): p. 385-90.
88. Merck, *CLARITIN® Product Information*.
89. Merck, *CLARINEX® Product Information*.
90. Vives, S., et al., *[Rhabdomyolysis and renal failure secondary to interaction between simvastatin, ciclosporin A and risperidone in an allogeneic stem cell transplantation patient]*. Med Clin (Barc), 2008. **131**(17): p. 676.
91. Patier, J.L., et al., *[Rhabdomyolysis caused by the association of simvastatin and risperidone]*. Med Clin (Barc), 2007. **129**(11): p. 439.
92. Zink, M., et al., *A case of pulmonary thromboembolism and rhabdomyolysis during therapy with mirtazapine and risperidone*. J Clin Psychiatry, 2006. **67**(5): p. 835.
93. Webber, M.A., et al., *Rhabdomyolysis and compartment syndrome with coadministration of risperidone and simvastatin*. J Psychopharmacol, 2004. **18**(3): p. 432-4.
94. Velasco-Montes, J., I. Orinuela-Gonzalez, and A.Z. Sanjuan-Lopez, *Rhabdomyolysis secondary to quetiapine*. Actas Esp Psiquiatr, 2012. **40**(2): p. 97-9.
95. Ceri, M., et al., *Comment on: low-dose quetiapine-induced severe rhabdomyolysis*. Ren Fail, 2011. **33**(4): p. 463-4.

96. Dickmann, J.R. and L.M. Dickmann, *An uncommonly recognized cause of rhabdomyolysis after quetiapine intoxication*. Am J Emerg Med, 2010. **28**(9): p. 1060 e1-2.
97. Stephani, C. and C. Trenkwalder, *Rhabdomyolysis after low-dose quetiapine in a patient with Parkinson's disease with drug-induced psychosis: a case report*. Mov Disord, 2010. **25**(6): p. 790-1.
98. Himmerich, H., et al., *Possible case of quetiapine-induced rhabdomyolysis in a patient with depression treated with fluoxetine*. J Clin Psychopharmacol, 2006. **26**(6): p. 676-7.
99. Smith, R.P., et al., *Quetiapine overdose and severe rhabdomyolysis*. J Clin Psychopharmacol, 2004. **24**(3): p. 343.
100. Calandre, E.P. and F. Rico-Villademoros, *The role of antipsychotics in the management of fibromyalgia*. CNS Drugs, 2012. **26**(2): p. 135-53.
101. Potvin, S., et al., *Add-on treatment of quetiapine for fibromyalgia: a pilot, randomized, double-blind, placebo-controlled 12-week trial*. J Clin Psychopharmacol, 2012. **32**(5): p. 684-7.
102. Russell, I.J., et al., *Treatment of primary fibrositis/fibromyalgia syndrome with ibuprofen and alprazolam. A double-blind, placebo-controlled study*. Arthritis Rheum, 1991. **34**(5): p. 552-60.
103. Reitblat, T., et al., *Patients treated by tegaserod for irritable bowel syndrome with constipation showed significant improvement in fibromyalgia symptoms. A pilot study*. Clin Rheumatol, 2009. **28**(9): p. 1079-82.
104. Angeletti, C., et al., *Duloxetine and Pregabalin for Pain Management in Multiple Rheumatic Diseases Associated with Fibromyalgia*. Pain Pract, 2012.
105. Ursin, H., I.M. Endresen, and G. Ursin, *Psychological factors and self-reports of muscle pain*. Eur J Appl Physiol Occup Physiol, 1988. **57**(3): p. 282-90.
106. Thompson, P.D., P. Clarkson, and R.H. Karas, *Statin-associated myopathy*. JAMA : the journal of the American Medical Association, 2003. **289**(13): p. 1681-90.
107. Guengerich, F.P., *Cytochrome p450 and chemical toxicology*. Chem Res Toxicol, 2008. **21**(1): p. 70-83.
108. Laine, R., *Metabolic stability: main enzymes involved and best tools to assess it*. Current drug metabolism, 2008. **9**(9): p. 921-7.
109. Shimada, T., et al., *Interindividual variations in human liver cytochrome P-450 enzymes involved in the oxidation of drugs, carcinogens and toxic chemicals: studies with liver microsomes of 30 Japanese and 30 Caucasians*. J Pharmacol Exp Ther, 1994. **270**(1): p. 414-23.
110. Paine, M.F., et al., *The human intestinal cytochrome P450 "pie"*. Drug Metab Dispos, 2006. **34**(5): p. 880-6.
111. Wienkers, L.C. and T.G. Heath, *Predicting in vivo drug interactions from in vitro drug discovery data*. Nat Rev Drug Discov, 2005. **4**(10): p. 825-33.
112. Rostami-Hodjegan, A. and G.T. Tucker, *Simulation and prediction of in vivo drug metabolism in human populations from in vitro data*. Nat Rev Drug Discov, 2007. **6**(2): p. 140-148.

113. Huang, S.M., et al., *Drug interaction studies: study design, data analysis, and implications for dosing and labeling*. Clinical pharmacology and therapeutics, 2007. **81**(2): p. 298-304.
114. Honig, P.K., et al., *Terfenadine-ketoconazole interaction. Pharmacokinetic and electrocardiographic consequences*. JAMA, 1993. **269**(12): p. 1513-8.
115. Prueksaritanont, T., et al., *Metabolic interactions between mibefradil and HMG-CoA reductase inhibitors: an in vitro investigation with human liver preparations*. Br J Clin Pharmacol, 1999. **47**(3): p. 291-8.
116. Backman, J.T., et al., *Mibefradil but not isradipine substantially elevates the plasma concentrations of the CYP3A4 substrate triazolam*. Clin Pharmacol Ther, 1999. **66**(4): p. 401-7.
117. Veronese, M.L., et al., *Effect of mibefradil on CYP3A4 in vivo*. J Clin Pharmacol, 2003. **43**(10): p. 1091-100.
118. Walsky, R.L. and S.E. Boldt, *In vitro cytochrome P450 inhibition and induction*. Current drug metabolism, 2008. **9**(9): p. 928-39.
119. Masimirembwa, C.M., et al., *Heterologous expression and kinetic characterization of human cytochromes P-450: validation of a pharmaceutical tool for drug metabolism research*. Drug Metab Dispos, 1999. **27**(10): p. 1117-22.
120. Bjornsson, T.D., et al., *The conduct of in vitro and in vivo drug-drug interaction studies: a Pharmaceutical Research and Manufacturers of America (PhRMA) perspective*. Drug metabolism and disposition: the biological fate of chemicals, 2003. **31**(7): p. 815-32.
121. Asha, S. and M. Vidyavathi, *Role of human liver microsomes in in vitro metabolism of drugs-a review*. Appl Biochem Biotechnol, 2010. **160**(6): p. 1699-722.
122. Gomez-Lechon, M.J., J.V. Castell, and M.T. Donato, *An update on metabolism studies using human hepatocytes in primary culture*. Expert Opin Drug Metab Toxicol, 2008. **4**(7): p. 837-54.
123. Gomez-Lechon, M.J., et al., *Human hepatocytes as a tool for studying toxicity and drug metabolism*. Curr Drug Metab, 2003. **4**(4): p. 292-312.
124. Godoy, P., et al., *Recent advances in 2D and 3D in vitro systems using primary hepatocytes, alternative hepatocyte sources and non-parenchymal liver cells and their use in investigating mechanisms of hepatotoxicity, cell signaling and ADME*. Arch Toxicol, 2013. **87**(8): p. 1315-530.
125. Houston, J.B. and K.E. Kenworthy, *In Vitro-In Vivo Scaling of CYP Kinetic Data Not Consistent with the Classical Michaelis-Menten Model*. Drug Metabolism and Disposition, 2000. **28**(3): p. 246-254.
126. Obach, R.S. and A.E. Reed-Hagen, *Measurement of Michaelis constants for cytochrome P450-mediated biotransformation reactions using a substrate depletion approach*. Drug metabolism and disposition: the biological fate of chemicals, 2002. **30**(7): p. 831-7.
127. Emoto, C., et al., *Methodologies for investigating drug metabolism at the early drug discovery stage: prediction of hepatic drug clearance and P450 contribution*. Curr Drug Metab, 2010. **11**(8): p. 678-85.

128. Hop, C.E., et al., *High throughput ADME screening: practical considerations, impact on the portfolio and enabler of in silico ADME models*. *Current drug metabolism*, 2008. **9**(9): p. 847-53.
129. Foti, R.S., et al., *Selection of alternative CYP3A4 probe substrates for clinical drug interaction studies using in vitro data and in vivo simulation*. *Drug Metab Dispos*, 2010. **38**(6): p. 981-7.
130. Miller, V.P., et al., *Fluorometric high-throughput screening for inhibitors of cytochrome P450*. *Annals of the New York Academy of Sciences*, 2000. **919**: p. 26-32.
131. Donato, M.T., et al., *FLUORESCENCE-BASED ASSAYS FOR SCREENING NINE CYTOCHROME P450 (P450) ACTIVITIES IN INTACT CELLS EXPRESSING INDIVIDUAL HUMAN P450 ENZYMES*. *Drug Metabolism and Disposition*, 2004. **32**(7): p. 699-706.
132. Cohen, L.H., et al., *In vitro drug interactions of cytochrome p450: an evaluation of fluorogenic to conventional substrates*. *Drug metabolism and disposition: the biological fate of chemicals*, 2003. **31**(8): p. 1005-15.
133. Einolf, H.J., *Comparison of different approaches to predict metabolic drug-drug interactions*. *Xenobiotica*, 2007. **37**(10-11): p. 1257-94.
134. Blanchard, N., et al., *Qualitative and quantitative assessment of drug-drug interaction potential in man, based on Ki, IC50 and inhibitor concentration*. *Curr Drug Metab*, 2004. **5**(2): p. 147-56.
135. Rostami-Hodjegan, A. and G. Tucker, *'In silico' simulations to assess the 'in vivo' consequences of 'in vitro' metabolic drug-drug interactions*. *Drug Discovery Today: Technologies*, 2004. **1**(4): p. 441-448.
136. Yeo, K.R., M. Jamei, and A. Rostami-Hodjegan, *Predicting drug-drug interactions: application of physiologically based pharmacokinetic models under a systems biology approach*. *Expert Rev Clin Pharmacol*, 2013. **6**(2): p. 143-57.
137. Li, D., et al., *Effect of regular organic solvents on cytochrome P450-mediated metabolic activities in rat liver microsomes*. *Drug Metab Dispos*, 2010. **38**(11): p. 1922-5.
138. Easterbrook, J., et al., *Effects of organic solvents on the activities of cytochrome P450 isoforms, UDP-dependent glucuronyl transferase, and phenol sulfotransferase in human hepatocytes*. *Drug Metab Dispos*, 2001. **29**(2): p. 141-4.
139. Geng, W., *A method for identification of inhibition mechanism and estimation of Ki in in vitro enzyme inhibition study*. *Drug metabolism and disposition: the biological fate of chemicals*, 2003. **31**(11): p. 1456-7.
140. Hallifax, D. and J.B. Houston, *Binding of drugs to hepatic microsomes: comment and assessment of current prediction methodology with recommendation for improvement*. *Drug metabolism and disposition: the biological fate of chemicals*, 2006. **34**(4): p. 724-6; author reply 727.
141. Projean, D., et al., *In vitro metabolism of chloroquine: identification of CYP2C8, CYP3A4, and CYP2D6 as the main isoforms catalyzing N-desethylchloroquine formation*. *Drug metabolism and disposition: the biological fate of chemicals*, 2003. **31**(6): p. 748-54.

142. Masimirembwa, C.M., J.A. Hasler, and I. Johansson, *Inhibitory effects of antiparasitic drugs on cytochrome P450 2D6*. European journal of clinical pharmacology, 1995. **48**(1): p. 35-8.
143. Bapiro, T.E., et al., *Application of higher throughput screening (HTS) inhibition assays to evaluate the interaction of antiparasitic drugs with cytochrome P450s*. Drug Metab Dispos, 2001. **29**(1): p. 30-5.
144. Paris, B.L., et al., *In vitro inhibition and induction of human liver cytochrome p450 enzymes by milnacipran*. Drug metabolism and disposition: the biological fate of chemicals, 2009. **37**(10): p. 2045-54.
145. Skinner, M.H., et al., *Duloxetine is both an inhibitor and a substrate of cytochrome P4502D6 in healthy volunteers*. Clinical pharmacology and therapeutics, 2003. **73**(3): p. 170-7.
146. Chan, C.Y., et al., *Reversible time-dependent inhibition of cytochrome P450 enzymes by duloxetine and inertness of its thiophene ring towards bioactivation*. Toxicol Lett, 2011. **206**(3): p. 314-24.
147. Knadler, M.P., et al., *Duloxetine: clinical pharmacokinetics and drug interactions*. Clinical pharmacokinetics, 2011. **50**(5): p. 281-94.
148. Nicolas, J.M., et al., *In vitro inhibition of human liver drug metabolizing enzymes by second generation antihistamines*. Chemico-biological interactions, 1999. **123**(1): p. 63-79.
149. Walsky, R.L., A.V. Astuccio, and R.S. Obach, *Evaluation of 227 drugs for in vitro inhibition of cytochrome P450 2B6*. J Clin Pharmacol, 2006. **46**(12): p. 1426-38.
150. Lee, C.A., et al., *Identifying a selective substrate and inhibitor pair for the evaluation of CYP2J2 activity*. Drug Metab Dispos, 2012. **40**(5): p. 943-51.
151. Barecki, M.E., et al., *In vitro characterization of the inhibition profile of loratadine, desloratadine, and 3-OH-desloratadine for five human cytochrome P-450 enzymes*. Drug metabolism and disposition: the biological fate of chemicals, 2001. **29**(9): p. 1173-5.
152. Foti, R.S. and J.L. Wahlstrom, *CYP2C19 inhibition: the impact of substrate probe selection on in vitro inhibition profiles*. Drug Metab Dispos, 2008. **36**(3): p. 523-8.
153. Walsky, R.L., E.A. Gaman, and R.S. Obach, *Examination of 209 drugs for inhibition of cytochrome P450 2C8*. J Clin Pharmacol, 2005. **45**(1): p. 68-78.
154. Moody, G.C., et al., *Fully automated analysis of activities catalysed by the major human liver cytochrome P450 (CYP) enzymes: assessment of human CYP inhibition potential*. Xenobiotica, 1999. **29**(1): p. 53-75.
155. Kosugi, Y., et al., *Evaluation of cytochrome P450-mediated drug-drug interactions based on the strategies recommended by regulatory authorities*. Xenobiotica, 2012. **42**(2): p. 127-38.
156. VandenBranden, M., et al., *Interaction of human liver cytochromes P450 in vitro with LY307640, a gastric proton pump inhibitor*. Pharmacogenetics, 1996. **6**(1): p. 81-91.
157. Ogilvie, B.W., et al., *The proton pump inhibitor, omeprazole, but not lansoprazole or pantoprazole, is a metabolism-dependent inhibitor of CYP2C19: implications for coadministration with clopidogrel*. Drug Metab Dispos, 2011. **39**(11): p. 2020-33.

158. Zimmerlin, A., M. Trunzer, and B. Faller, *CYP3A time-dependent inhibition risk assessment validated with 400 reference drugs*. Drug Metab Dispos, 2011. **39**(6): p. 1039-46.
159. Ring, B.J., et al., *In vitro interaction of the antipsychotic agent olanzapine with human cytochromes P450 CYP2C9, CYP2C19, CYP2D6 and CYP3A*. Br J Clin Pharmacol, 1996. **41**(3): p. 181-6.
160. Li, X.Q., et al., *Comparison of inhibitory effects of the proton pump-inhibiting drugs omeprazole, esomeprazole, lansoprazole, pantoprazole, and rabeprazole on human cytochrome P450 activities*. Drug metabolism and disposition: the biological fate of chemicals, 2004. **32**(8): p. 821-7.
161. Zhao, X.J. and T. Ishizaki, *A further interaction study of quinine with clinically important drugs by human liver microsomes: determinations of inhibition constant (K_i) and type of inhibition*. Eur J Drug Metab Pharmacokinet, 1999. **24**(3): p. 272-8.
162. Kumar, V., et al., *CYP2C9 inhibition: impact of probe selection and pharmacogenetics on in vitro inhibition profiles*. Drug Metab Dispos, 2006. **34**(12): p. 1966-75.
163. Furuta, S., et al., *Inhibition of drug metabolism in human liver microsomes by nizatidine, cimetidine and omeprazole*. Xenobiotica, 2001. **31**(1): p. 1-10.
164. Hamelin, B.A., et al., *In vitro characterization of cytochrome P450 2D6 inhibition by classic histamine H1 receptor antagonists*. Drug metabolism and disposition: the biological fate of chemicals, 1998. **26**(6): p. 536-9.
165. He, N., et al., *Inhibitory effects of H1-antihistamines on CYP2D6- and CYP2C9-mediated drug metabolic reactions in human liver microsomes*. European journal of clinical pharmacology, 2002. **57**(12): p. 847-51.
166. Prakash, C., et al., *Identification of the major human liver cytochrome P450 isoform(s) responsible for the formation of the primary metabolites of ziprasidone and prediction of possible drug interactions*. Br J Clin Pharmacol, 2000. **49 Suppl 1**: p. 35S-42S.
167. Wynalda, M.A. and L.C. Wienkers, *Assessment of potential interactions between dopamine receptor agonists and various human cytochrome P450 enzymes using a simple in vitro inhibition screen*. Drug metabolism and disposition: the biological fate of chemicals, 1997. **25**(10): p. 1211-4.
168. Vickers, A.E., et al., *In vitro metabolism of tegaserod in human liver and intestine: assessment of drug interactions*. Drug metabolism and disposition: the biological fate of chemicals, 2001. **29**(10): p. 1269-76.
169. Kalgutkar, A.S., et al., *Assessment of the contributions of CYP3A4 and CYP3A5 in the metabolism of the antipsychotic agent haloperidol to its potentially neurotoxic pyridinium metabolite and effect of antidepressants on the bioactivation pathway*. Drug Metab Dispos, 2003. **31**(3): p. 243-9.
170. Otton, S.V., et al., *Inhibition by fluoxetine of cytochrome P450 2D6 activity*. Clin Pharmacol Ther, 1993. **53**(4): p. 401-9.
171. Cohen, L.H., et al., *Equally potent inhibitors of cholesterol synthesis in human hepatocytes have distinguishable effects on different cytochrome P450 enzymes*. Biopharm Drug Dispos, 2000. **21**(9): p. 353-64.

172. Jenkins, S.M., et al., *Studies to further investigate the inhibition of human liver microsomal CYP2C8 by the acyl-beta-glucuronide of gemfibrozil*. Drug Metab Dispos, 2011. **39**(12): p. 2421-30.
173. Zahno, A., et al., *Effects of drug interactions on biotransformation and antiplatelet effect of clopidogrel in vitro*. Br J Pharmacol, 2010. **161**(2): p. 393-404.
174. Takanohashi, T., et al., *Prediction of the metabolic interaction of nateglinide with other drugs based on in vitro studies*. Drug Metab Pharmacokinet, 2007. **22**(6): p. 409-18.
175. Stresser, D.M., et al., *Substrate-dependent modulation of CYP3A4 catalytic activity: analysis of 27 test compounds with four fluorometric substrates*. Drug metabolism and disposition: the biological fate of chemicals, 2000. **28**(12): p. 1440-8.
176. Atkins, W.M., *Implications of the allosteric kinetics of cytochrome P450s*. Drug discovery today, 2004. **9**(11): p. 478-84.
177. Kenworthy, K.E., et al., *Multisite kinetic models for CYP3A4: simultaneous activation and inhibition of diazepam and testosterone metabolism*. Drug metabolism and disposition: the biological fate of chemicals, 2001. **29**(12): p. 1644-51.
178. Proctor, N.J., G.T. Tucker, and A. Rostami-Hodjegan, *Predicting drug clearance from recombinantly expressed CYPs: intersystem extrapolation factors*. Xenobiotica, 2004. **34**(2): p. 151-78.
179. Hua, T.C., et al., *Effect of duloxetine on tolterodine pharmacokinetics in healthy volunteers*. British journal of clinical pharmacology, 2004. **57**(5): p. 652-6.
180. Preskorn, S.H., et al., *Comparison of duloxetine, escitalopram, and sertraline effects on cytochrome P450 2D6 function in healthy volunteers*. Journal of clinical psychopharmacology, 2007. **27**(1): p. 28-34.
181. Hendset, M., et al., *The effect of coadministration of duloxetine on steady-state serum concentration of risperidone and aripiprazole: a study based on therapeutic drug monitoring data*. Therapeutic drug monitoring, 2010. **32**(6): p. 787-90.
182. McChesney, E.W., et al., *Studies of the metabolism of some compounds of the 4-amino-7-chloroquinoline series*. The Journal of pharmacology and experimental therapeutics, 1966. **151**(3): p. 482-93.
183. Na-Bangchang, K., et al., *The pharmacokinetics of chloroquine in healthy Thai subjects and patients with Plasmodium vivax malaria*. Br J Clin Pharmacol, 1994. **38**(3): p. 278-81.
184. Gustafsson, L.L., et al., *Disposition of chloroquine in man after single intravenous and oral doses*. Br J Clin Pharmacol, 1983. **15**(4): p. 471-9.
185. Adelusi, S.A. and L.A. Salako, *Tissue and blood concentrations of chloroquine following chronic administration in the rat*. J Pharm Pharmacol, 1982. **34**(11): p. 733-5.
186. MacIntyre, A.C. and D.J. Cutler, *Role of lysosomes in hepatic accumulation of chloroquine*. J Pharm Sci, 1988. **77**(3): p. 196-9.

187. Adjepon-Yamoah, K.K., N.M. Woolhouse, and L.F. Prescott, *The effect of chloroquine on paracetamol disposition and kinetics*. Br J Clin Pharmacol, 1986. **21**(3): p. 322-4.
188. Ali, H.M., *Reduced ampicillin bioavailability following oral coadministration with chloroquine*. J Antimicrob Chemother, 1985. **15**(6): p. 781-4.
189. Suzuki, A., et al., *Histamine H1-receptor antagonists, promethazine and homochlorcyclizine, increase the steady-state plasma concentrations of haloperidol and reduced haloperidol*. Therapeutic drug monitoring, 2003. **25**(2): p. 192-6.
190. Graham, D.J., et al., *Incidence of hospitalized rhabdomyolysis in patients treated with lipid-lowering drugs*. JAMA : the journal of the American Medical Association, 2004. **292**(21): p. 2585-90.
191. Taylor, A., et al., *The effect of steady-state ropinirole on plasma concentrations of digoxin in patients with Parkinson's disease*. British journal of clinical pharmacology, 1999. **47**(2): p. 219-22.
192. Grimm, S.W., et al., *Effects of cytochrome P450 3A modulators ketoconazole and carbamazepine on quetiapine pharmacokinetics*. Br J Clin Pharmacol, 2006. **61**(1): p. 58-69.
193. Potkin, S.G., et al., *Effect of fluoxetine and imipramine on the pharmacokinetics and tolerability of the antipsychotic quetiapine*. J Clin Psychopharmacol, 2002. **22**(2): p. 174-82.
194. Ducharme, J. and R. Farinotti, *Clinical pharmacokinetics and metabolism of chloroquine. Focus on recent advancements*. Clin Pharmacokinet, 1996. **31**(4): p. 257-74.
195. Mauro, V.F., *Clinical pharmacokinetics and practical applications of simvastatin*. Clinical pharmacokinetics, 1993. **24**(3): p. 195-202.
196. Ehiemua, A.O., et al., *Effect of promethazine on the metabolism of chloroquine*. European journal of drug metabolism and pharmacokinetics, 1988. **13**(1): p. 15-7.
197. Strenkoski-Nix, L.C., et al., *Pharmacokinetics of promethazine hydrochloride after administration of rectal suppositories and oral syrup to healthy subjects*. Am J Health Syst Pharm, 2000. **57**(16): p. 1499-505.
198. Zhou, Z.L., et al., *Multiple dose pharmacokinetics of risperidone and 9-hydroxyrisperidone in Chinese female patients with schizophrenia*. Acta Pharmacol Sin, 2006. **27**(3): p. 381-6.
199. Hubble, J., et al., *Linear pharmacokinetic behavior of ropinirole during multiple dosing in patients with Parkinson's disease*. J Clin Pharmacol, 2000. **40**(6): p. 641-6.
200. Carr, R.A., et al., *Steady-state pharmacokinetics and electrocardiographic pharmacodynamics of clarithromycin and loratadine after individual or concomitant administration*. Antimicrobial agents and chemotherapy, 1998. **42**(5): p. 1176-80.
201. Appel-Dingemanse, S., et al., *Multiple-dose pharmacokinetics confirm no accumulation and dose proportionality of the novel promotile drug tegaserod (HTF 919)*. Eur J Clin Pharmacol, 2001. **56**(12): p. 889-91.

202. Bergman, A.J., et al., *Simvastatin does not have a clinically significant pharmacokinetic interaction with fenofibrate in humans*. J Clin Pharmacol, 2004. **44**(9): p. 1054-62.
203. DeVane, C.L. and C.B. Nemeroff, *Clinical pharmacokinetics of quetiapine: an atypical antipsychotic*. Clin Pharmacokinet, 2001. **40**(7): p. 509-22.
204. Lobo, E.D., et al., *In vitro and in vivo evaluations of cytochrome P450 1A2 interactions with duloxetine*. Clinical pharmacokinetics, 2008. **47**(3): p. 191-202.
205. Fang, J., M. Bourin, and G.B. Baker, *Metabolism of risperidone to 9-hydroxyrisperidone by human cytochromes P450 2D6 and 3A4*. Naunyn Schmiedebergs Arch Pharmacol, 1999. **359**(2): p. 147-51.
206. Ghosal, A., et al., *Metabolism of loratadine and further characterization of its in vitro metabolites*. Drug metabolism letters, 2009. **3**(3): p. 162-70.
207. Hasselstrom, J. and K. Linnet, *In vitro studies on quetiapine metabolism using the substrate depletion approach with focus on drug-drug interactions*. Drug metabolism and drug interactions, 2006. **21**(3-4): p. 187-211.
208. Rotzinger, S., J. Fang, and G.B. Baker, *Trazodone is metabolized to m-chlorophenylpiperazine by CYP3A4 from human sources*. Drug metabolism and disposition: the biological fate of chemicals, 1998. **26**(6): p. 572-5.
209. Ramanathan, R., et al., *Disposition of loratadine in healthy volunteers*. Xenobiotica; the fate of foreign compounds in biological systems, 2007. **37**(7): p. 753-69.
210. Sathasivam, S., *Statin induced myotoxicity*. Eur J Intern Med, 2012. **23**(4): p. 317-24.
211. Bruckert, E., et al., *Mild to moderate muscular symptoms with high-dosage statin therapy in hyperlipidemic patients--the PRIMO study*. Cardiovasc Drugs Ther, 2005. **19**(6): p. 403-14.
212. Administration, U.S.F.a.D. *Zocor (simvastatin): Label Change - New Restrictions, Contraindications, and Dose Limitations*. 2011; Available from: <http://www.fda.gov/safety/medwatch/safetyinformation/safetyalertsforhumanmedicinalproducts/ucm258384.htm>.
213. Merck & Co., I., *ZOCOR (simvastatin) Tablets*, T.F.a.D. Administration, Editor.
214. Desager, J.P. and Y. Horsmans, *Clinical pharmacokinetics of 3-hydroxy-3-methylglutaryl-coenzyme A reductase inhibitors*. Clin Pharmacokinet, 1996. **31**(5): p. 348-71.
215. Prueksaritanont, T., et al., *Interconversion pharmacokinetics of simvastatin and its hydroxy acid in dogs: effects of gemfibrozil*. Pharm Res, 2005. **22**(7): p. 1101-9.
216. Vickers, S., et al., *In vitro and in vivo biotransformation of simvastatin, an inhibitor of HMG CoA reductase*. Drug Metab Dispos, 1990. **18**(4): p. 476-83.
217. Prueksaritanont, T., et al., *In vitro metabolism of simvastatin in humans [SBT]identification of metabolizing enzymes and effect of the drug on hepatic P450s*. Drug metabolism and disposition: the biological fate of chemicals, 1997. **25**(10): p. 1191-9.
218. Prueksaritanont, T., B. Ma, and N. Yu, *The human hepatic metabolism of simvastatin hydroxy acid is mediated primarily by CYP3A, and not CYP2D6*. British journal of clinical pharmacology, 2003. **56**(1): p. 120-4.

219. Kosoglou, T., et al., *Pharmacodynamic interaction between the new selective cholesterol absorption inhibitor ezetimibe and simvastatin*. Br J Clin Pharmacol, 2002. **54**(3): p. 309-19.
220. Kantola, T., K.T. Kivisto, and P.J. Neuvonen, *Erythromycin and verapamil considerably increase serum simvastatin and simvastatin acid concentrations*. Clinical pharmacology and therapeutics, 1998. **64**(2): p. 177-82.
221. Fichtenbaum, C.J., et al., *Pharmacokinetic interactions between protease inhibitors and statins in HIV seronegative volunteers: ACTG Study A5047*. AIDS, 2002. **16**(4): p. 569-77.
222. Krishna, G., et al., *Effect of posaconazole on the pharmacokinetics of simvastatin and midazolam in healthy volunteers*. Expert Opin Drug Metab Toxicol, 2012. **8**(1): p. 1-10.
223. Neuvonen, P.J., M. Niemi, and J.T. Backman, *Drug interactions with lipid-lowering drugs: mechanisms and clinical relevance*. Clinical pharmacology and therapeutics, 2006. **80**(6): p. 565-81.
224. Kosoglou, T., et al., *Evaluation of the pharmacokinetics and electrocardiographic pharmacodynamics of loratadine with concomitant administration of ketoconazole or cimetidine*. British journal of clinical pharmacology, 2000. **50**(6): p. 581-9.
225. Abernethy, D.R., et al., *Loratadine and terfenadine interaction with nefazodone: Both antihistamines are associated with QTc prolongation*. Clinical pharmacology and therapeutics, 2001. **69**(3): p. 96-103.
226. Ramanathan, R., et al., *Disposition of desloratadine in healthy volunteers*. Xenobiotica; the fate of foreign compounds in biological systems, 2007. **37**(7): p. 770-87.
227. Affrime, M., et al., *A pharmacokinetic profile of desloratadine in healthy adults, including elderly*. Clinical pharmacokinetics, 2002. **41 Suppl 1**: p. 13-9.
228. Anderle, P., Y. Huang, and W. Sadee, *Intestinal membrane transport of drugs and nutrients: genomics of membrane transporters using expression microarrays*. Eur J Pharm Sci, 2004. **21**(1): p. 17-24.
229. Ekins, S., et al., *Future directions for drug transporter modelling*. Xenobiotica, 2007. **37**(10-11): p. 1152-70.
230. Borst, P. and R.O. Elferink, *Mammalian ABC transporters in health and disease*. Annu Rev Biochem, 2002. **71**: p. 537-92.
231. Hediger, M.A., et al., *The ABCs of solute carriers: physiological, pathological and therapeutic implications of human membrane transport proteins* Introduction. Pflugers Arch, 2004. **447**(5): p. 465-8.
232. Niemi, M., *Role of OATP transporters in the disposition of drugs*. Pharmacogenomics, 2007. **8**(7): p. 787-802.
233. Konig, J., et al., *Pharmacogenomics of human OATP transporters*. Naunyn Schmiedebergs Arch Pharmacol, 2006. **372**(6): p. 432-43.
234. Hagenbuch, B. and C. Gui, *Xenobiotic transporters of the human organic anion transporting polypeptides (OATP) family*. Xenobiotica, 2008. **38**(7-8): p. 778-801.
235. Shitara, Y., et al., *Clinical significance of organic anion transporting polypeptides (OATPs) in drug disposition: their roles in hepatic clearance and intestinal absorption*. Biopharm Drug Dispos, 2013. **34**(1): p. 45-78.

236. Srimaroeng, C., J.L. Perry, and J.B. Pritchard, *Physiology, structure, and regulation of the cloned organic anion transporters*. *Xenobiotica*, 2008. **38**(7-8): p. 889-935.
237. Yoshida, K., K. Maeda, and Y. Sugiyama, *Hepatic and Intestinal Drug Transporters: Prediction of Pharmacokinetic Effects Caused by Drug-Drug Interactions and Genetic Polymorphisms*. *Annu Rev Pharmacol Toxicol*, 2012.
238. Hsiang, B., et al., *A novel human hepatic organic anion transporting polypeptide (OATP2). Identification of a liver-specific human organic anion transporting polypeptide and identification of rat and human hydroxymethylglutaryl-CoA reductase inhibitor transporters*. *J Biol Chem*, 1999. **274**(52): p. 37161-8.
239. Link, E., et al., *SLCO1B1 variants and statin-induced myopathy--a genomewide study*. *N Engl J Med*, 2008. **359**(8): p. 789-99.
240. Maeda, K. and Y. Sugiyama, *The use of hepatocytes to investigate drug uptake transporters*. *Methods Mol Biol*, 2010. **640**: p. 327-53.
241. Maeda, K., et al., *Identification of the rate-determining process in the hepatic clearance of atorvastatin in a clinical cassette microdosing study*. *Clinical pharmacology and therapeutics*, 2011. **90**(4): p. 575-81.
242. Wilke, R.A., et al., *The clinical pharmacogenomics implementation consortium: CPIC guideline for SLCO1B1 and simvastatin-induced myopathy*. *Clin Pharmacol Ther*, 2012. **92**(1): p. 112-7.
243. Shitara, Y., et al., *Inhibition of transporter-mediated hepatic uptake as a mechanism for drug-drug interaction between cerivastatin and cyclosporin A*. *J Pharmacol Exp Ther*, 2003. **304**(2): p. 610-6.
244. Shitara, Y., et al., *In vitro and in vivo correlation of the inhibitory effect of cyclosporin A on the transporter-mediated hepatic uptake of cerivastatin in rats*. *Drug Metab Dispos*, 2004. **32**(12): p. 1468-75.
245. Ogilvie, B.W., et al., *Glucuronidation converts gemfibrozil to a potent, metabolism-dependent inhibitor of CYP2C8: implications for drug-drug interactions*. *Drug Metab Dispos*, 2006. **34**(1): p. 191-7.
246. Shitara, Y., et al., *Gemfibrozil and its glucuronide inhibit the organic anion transporting polypeptide 2 (OATP2/OATP1B1:SLC21A6)-mediated hepatic uptake and CYP2C8-mediated metabolism of cerivastatin: analysis of the mechanism of the clinically relevant drug-drug interaction between cerivastatin and gemfibrozil*. *J Pharmacol Exp Ther*, 2004. **311**(1): p. 228-36.
247. Backman, J.T., et al., *Gemfibrozil greatly increases plasma concentrations of cerivastatin*. *Clin Pharmacol Ther*, 2002. **72**(6): p. 685-91.
248. Amundsen, R., et al., *Cyclosporine A, but not tacrolimus, shows relevant inhibition of organic anion-transporting protein 1B1-mediated transport of atorvastatin*. *Drug Metab Dispos*, 2010. **38**(9): p. 1499-504.
249. Brouwer, K.L., et al., *In vitro methods to support transporter evaluation in drug discovery and development*. *Clin Pharmacol Ther*, 2013. **94**(1): p. 95-112.
250. Bachmakov, I., et al., *Interaction of oral antidiabetic drugs with hepatic uptake transporters: focus on organic anion transporting polypeptides and organic cation transporter 1*. *Diabetes*, 2008. **57**(6): p. 1463-9.
251. Noe, J., et al., *Substrate-dependent drug-drug interactions between gemfibrozil, fluvastatin and other organic anion-transporting peptide (OATP) substrates on*

- OATP1B1, OATP2B1, and OATP1B3*. Drug Metab Dispos, 2007. **35**(8): p. 1308-14.
252. Press, B. and D. Di Grandi, *Permeability for intestinal absorption: Caco-2 assay and related issues*. Current drug metabolism, 2008. **9**(9): p. 893-900.
 253. Jin, H. and L. Di, *Permeability--in vitro assays for assessing drug transporter activity*. Current drug metabolism, 2008. **9**(9): p. 911-20.
 254. Li, M., et al., *Identification of interspecies difference in efflux transporters of hepatocytes from dog, rat, monkey and human*. Eur J Pharm Sci, 2008. **35**(1-2): p. 114-26.
 255. Ishigami, M., et al., *Evaluation of the uptake of pravastatin by perfused rat liver and primary cultured rat hepatocytes*. Pharm Res, 1995. **12**(11): p. 1741-5.
 256. Kimoto, E., et al., *Characterization of Organic Anion Transporting Polypeptide (OATP) Expression and Its Functional Contribution to the Uptake of Substrates in Human Hepatocytes*. Mol Pharm, 2012.
 257. Zaher, H., et al., *Targeted disruption of murine organic anion-transporting polypeptide 1b2 (Oatp1b2/Slco1b2) significantly alters disposition of prototypical drug substrates pravastatin and rifampin*. Mol Pharmacol, 2008. **74**(2): p. 320-9.
 258. van de Steeg, E., et al., *Complete OATP1B1 and OATP1B3 deficiency causes human Rotor syndrome by interrupting conjugated bilirubin reuptake into the liver*. J Clin Invest, 2012. **122**(2): p. 519-28.
 259. van de Steeg, E., et al., *Influence of human OATP1B1, OATP1B3, and OATP1A2 on the pharmacokinetics of methotrexate and paclitaxel in humanized transgenic mice*. Clin Cancer Res, 2013. **19**(4): p. 821-32.
 260. Zimmerman, E.I., et al., *Contribution of OATP1B1 and OATP1B3 to the disposition of sorafenib and sorafenib-glucuronide*. Clin Cancer Res, 2013. **19**(6): p. 1458-66.
 261. Cheng, Y. and W.H. Prusoff, *Relationship between the inhibition constant (K_I) and the concentration of inhibitor which causes 50 per cent inhibition (I₅₀) of an enzymatic reaction*. Biochemical pharmacology, 1973. **22**(23): p. 3099-108.
 262. Xu, Y., et al., *Computational models for predicting interactions with membrane transporters*. Curr Med Chem, 2013. **20**(16): p. 2118-36.
 263. Abbott, N.J., D.E. Dolman, and A.K. Patabendige, *Assays to predict drug permeation across the blood-brain barrier, and distribution to brain*. Current drug metabolism, 2008. **9**(9): p. 901-10.
 264. Kouzuki, H., et al., *Contribution of sodium taurocholate co-transporting polypeptide to the uptake of its possible substrates into rat hepatocytes*. J Pharmacol Exp Ther, 1998. **286**(2): p. 1043-50.
 265. Shitara, Y., et al., *Function of uptake transporters for taurocholate and estradiol 17beta-D-glucuronide in cryopreserved human hepatocytes*. Drug metabolism and pharmacokinetics, 2003. **18**(1): p. 33-41.
 266. De Bruyn, T., et al., *Determination of OATP-, NTCP- and OCT-mediated substrate uptake activities in individual and pooled batches of cryopreserved human hepatocytes*. Eur J Pharm Sci, 2011. **43**(4): p. 297-307.
 267. Kameyama, Y., et al., *Functional characterization of SLCO1B1 (OATP-C) variants, SLCO1B1*5, SLCO1B1*15 and SLCO1B1*15+C1007G, by using*

- transient expression systems of HeLa and HEK293 cells.* Pharmacogenet Genomics, 2005. **15**(7): p. 513-22.
268. Administration, F.a.D., *RIFADIN®(rifampin capsules USP) and RIFADIN® IV (rifampin for injection USP).*
269. Kovacs, P., et al., *High-dose omeprazole: use of a multiple-dose study design to assess bioequivalence and accuracy of CYP2C19 phenotyping.* Ther Drug Monit, 1999. **21**(5): p. 526-31.
270. Tianmei, S., et al., *Pharmacokinetics and tolerability of duloxetine following oral administration to healthy Chinese subjects.* Clin Pharmacokinet, 2007. **46**(9): p. 767-75.
271. Greenblatt, D.J., et al., *Alprazolam pharmacokinetics, metabolism, and plasma levels: clinical implications.* The Journal of clinical psychiatry, 1993. **54 Suppl**: p. 4-11; discussion 12-4.
272. Affrime, M., et al., *A pharmacokinetic profile of desloratadine in healthy adults, including elderly.* Clin Pharmacokinet, 2002. **41 Suppl 1**: p. 13-9.
273. Sieb, J.P. and T. Gillessen, *Iatrogenic and toxic myopathies.* Muscle Nerve, 2003. **27**(2): p. 142-56.
274. Lane, R.J. and F.L. Mastaglia, *Drug-induced myopathies in man.* Lancet, 1978. **2**(8089): p. 562-6.
275. Matzno, S., et al., *Statin-induced apoptosis linked with membrane farnesylated Ras small G protein depletion, rather than geranylated Rho protein.* J Pharm Pharmacol, 2005. **57**(11): p. 1475-84.
276. Sakamoto, K., et al., *Rab-small GTPases are involved in fluvastatin and pravastatin-induced vacuolation in rat skeletal myofibers.* FASEB J, 2007. **21**(14): p. 4087-94.
277. Itagaki, M., et al., *Possible mechanisms underlying statin-induced skeletal muscle toxicity in L6 fibroblasts and in rats.* J Pharmacol Sci, 2009. **109**(1): p. 94-101.
278. Marcoff, L. and P.D. Thompson, *The role of coenzyme Q10 in statin-associated myopathy: a systematic review.* J Am Coll Cardiol, 2007. **49**(23): p. 2231-7.
279. Chatzizisis, Y.S., C. Vaklavas, and G.D. Giannoglou, *Coenzyme Q10 depletion: etiopathogenic or predisposing factor in statin associated myopathy? Am J Cardiol, 2008. 101(7): p. 1071.*
280. Schaars, C.F. and A.F. Stalenhoef, *Effects of ubiquinone (coenzyme Q10) on myopathy in statin users.* Curr Opin Lipidol, 2008. **19**(6): p. 553-7.
281. Hanai, J., et al., *The muscle-specific ubiquitin ligase atrogin-1/MAFbx mediates statin-induced muscle toxicity.* J Clin Invest, 2007. **117**(12): p. 3940-51.
282. Cao, P., et al., *Statin-induced muscle damage and atrogin-1 induction is the result of a geranylgeranylation defect.* FASEB J, 2009. **23**(9): p. 2844-54.
283. Mammen, A.L. and A.A. Amato, *Statin myopathy: a review of recent progress.* Curr Opin Rheumatol, 2010. **22**(6): p. 644-50.
284. Morita, I., et al., *Enhancement of membrane fluidity in cholesterol-poor endothelial cells pre-treated with simvastatin.* Endothelium, 1997. **5**(2): p. 107-13.
285. Flint, O.P., et al., *Inhibition of cholesterol synthesis by squalene synthase inhibitors does not induce myotoxicity in vitro.* Toxicol Appl Pharmacol, 1997. **145**(1): p. 91-8.

286. Baker, S.K., *Molecular clues into the pathogenesis of statin-mediated muscle toxicity*. Muscle Nerve, 2005. **31**(5): p. 572-80.
287. Paiva, H., et al., *High-dose statins and skeletal muscle metabolism in humans: a randomized, controlled trial*. Clin Pharmacol Ther, 2005. **78**(1): p. 60-8.
288. Sirvent, P., et al., *Simvastatin triggers mitochondria-induced Ca²⁺ signaling alteration in skeletal muscle*. Biochem Biophys Res Commun, 2005. **329**(3): p. 1067-75.
289. Kwak, H.B., et al., *Simvastatin impairs ADP-stimulated respiration and increases mitochondrial oxidative stress in primary human skeletal myotubes*. Free Radic Biol Med, 2012. **52**(1): p. 198-207.
290. Mammen, A.L., et al., *Autoantibodies against 3-hydroxy-3-methylglutaryl-coenzyme A reductase in patients with statin-associated autoimmune myopathy*. Arthritis Rheum, 2011. **63**(3): p. 713-21.
291. Estes, M.L., et al., *Chloroquine neuromyotoxicity. Clinical and pathologic perspective*. Am J Med, 1987. **82**(3): p. 447-55.
292. Kumamoto, T., et al., *Experimental chloroquine myopathy: morphological and biochemical studies*. Eur Neurol, 1989. **29**(4): p. 202-7.
293. Kimura, N., et al., *Role of ubiquitin-proteasome proteolysis in muscle fiber destruction in experimental chloroquine-induced myopathy*. Muscle Nerve, 2009. **39**(4): p. 521-8.
294. Sundaram, C., *Muscle Biopsy*. 2012, InTech.
295. Sun, L., et al., *Glucocorticoids differentially regulate degradation of MyoD and Id1 by N-terminal ubiquitination to promote muscle protein catabolism*. Proc Natl Acad Sci U S A, 2008. **105**(9): p. 3339-44.
296. Yap, A., et al., *Rat L6 myotubes as an in vitro model system to study GLUT4-dependent glucose uptake stimulated by inositol derivatives*. Cytotechnology, 2007. **55**(2-3): p. 103-8.
297. Cui, Z., et al., *Preliminary quantitative profile of differential protein expression between rat L6 myoblasts and myotubes by stable isotope labeling with amino acids in cell culture*. Proteomics, 2009. **9**(5): p. 1274-92.
298. Yaffe, D., *Retention of differentiation potentialities during prolonged cultivation of myogenic cells*. Proc Natl Acad Sci U S A, 1968. **61**(2): p. 477-83.
299. Larson, D.E., et al., *Coordinated decreases in rRNA gene transcription factors and rRNA synthesis during muscle cell differentiation*. Proc Natl Acad Sci U S A, 1993. **90**(17): p. 7933-6.
300. Pontecorvi, A., et al., *Selective degradation of mRNA: the role of short-lived proteins in differential destabilization of insulin-induced creatine phosphokinase and myosin heavy chain mRNAs during rat skeletal muscle L6 cell differentiation*. EMBO J, 1988. **7**(5): p. 1489-95.
301. Nadal-Ginard, B., *Commitment, fusion and biochemical differentiation of a myogenic cell line in the absence of DNA synthesis*. Cell, 1978. **15**(3): p. 855-64.
302. Sakamoto, K., H. Mikami, and J. Kimura, *Involvement of organic anion transporting polypeptides in the toxicity of hydrophilic pravastatin and lipophilic fluvastatin in rat skeletal myofibres*. Br J Pharmacol, 2008. **154**(7): p. 1482-90.
303. Tallarida, R.J., *Quantitative methods for assessing drug synergism*. Genes Cancer, 2011. **2**(11): p. 1003-8.

304. Tallarida, R.J., *Combination analysis*. Adv Exp Med Biol, 2010. **678**: p. 133-7.
305. Greco, W.R., G. Bravo, and J.C. Parsons, *The search for synergy: a critical review from a response surface perspective*. Pharmacol Rev, 1995. **47**(2): p. 331-85.
306. Loewe, S.M., H., *Effect of combinations: mathematical basis of problem*. Arch. Exp. Pathol. Pharmacol., 1926. **114**: p. 313-326.
307. Berenbaum, M.C., *A method for testing for synergy with any number of agents*. J Infect Dis, 1978. **137**(2): p. 122-30.
308. Chou, T.C., *Theoretical basis, experimental design, and computerized simulation of synergism and antagonism in drug combination studies*. Pharmacological reviews, 2006. **58**(3): p. 621-81.
309. Khayat, Z.A., et al., *Rapid stimulation of glucose transport by mitochondrial uncoupling depends in part on cytosolic Ca²⁺ and cPKC*. Am J Physiol, 1998. **275**(6 Pt 1): p. C1487-97.
310. Promega, *CellTiter 96® Aqueous Non-Radioactive Cell Proliferation Assay Protocol*.
311. Skotheim, I.B., et al., *Statin induced myotoxicity: the lactone forms are more potent than the acid forms in human skeletal muscle cells in vitro*. European journal of pharmaceutical sciences : official journal of the European Federation for Pharmaceutical Sciences, 2008. **33**(4-5): p. 317-25.
312. Chai, W., et al., *Inotropic effects of prokinetic agents with 5-HT₄ receptor agonist actions on human isolated myocardial trabeculae*. Life Sci, 2012. **90**(13-14): p. 538-44.
313. Celtek, S., et al., *5-HT₄ receptor agonists enhance both cholinergic and nitrergic activities in human isolated colon circular muscle*. Neurogastroenterol Motil, 2006. **18**(9): p. 853-61.
314. Liu, A., et al., *Biphasic regulation of intracellular calcium by gemfibrozil contributes to inhibiting L6 myoblast differentiation: implications for clinical myotoxicity*. Chem Res Toxicol, 2011. **24**(2): p. 229-37.

Curriculum Vitae

Xu Han

EDUCATION

Indiana University

Indianapolis, IN

Ph.D. in Pharmacology, 2014

Advisors: Lang Li PhD and David A. Flockhart MD, PhD

Purdue University

Indianapolis, IN

M.S. in Applied Statistics, 2013

Peking University

Beijing, China

B.S. in Biotechnology, 2008

Outstanding Academic Progress Award, 2007

RESEARCH EXPERIENCE

Indiana University; with Lang Li PhD and David A. Flockhart MD, PhD

Doctoral thesis: Identification and mechanisms of clinically important drug-drug interactions in drug-induced myopathy

- Curated substrate and inhibitor drugs of the major human cytochrome P450s (CYPs) identified using bioinformatic tools
- Identified novel clinically important drug-drug interactions associated with increased risk of myopathy in an electronic medical record database using pharmacoepidemiologic methods
- Investigated mechanisms of the identified drug-drug interactions in *in vitro* systems, including human liver microsomes for assessing inhibitory potency for CYPs, rat hepatocytes for assessing inhibition of transporters, and rat myocytes for assessing direct myotoxicity

Pharmacokinetic Modeling of Paroxetine in the Context of CYP2D6 Pharmacogenetics

- Developed a physiology-based pharmacokinetic (PBPK) model for paroxetine to describe and predict its disposition with regard to CYP2D6 phenotype
- Determined CYP2D6 genotype for 200+ clinical samples

Peking University; with Shuo Lin PhD and Bo Li PhD

Function of z13 and z13h in the development of pancreas in zebrafish

- Investigated the spacial and temporal gene expression of *z13* and *z13h* in zebrafish embryos using *in situ* hybridization

AWARDS & HONORS

2012 Presidential Trainee Award, ASCPT

2012 David Goldstein Trainee Award, ASCPT

2007 Outstanding Academic Progress Award, Peking University, Beijing, China

SOFTWARE SKILL

Proficient in R and SAS. Experienced with SIMCYP Simulator and NONMEM.

PUBLICATIONS

Peer-reviewed Articles

1. **Han X**, Duke JD, Wang Z, Subhadarshini A, Karnik SD, Li X, Hall SD, Jin Y, Callaghan JT, Overhage MJ, Flockhart DA, Strother RM, Quinney SK, Li L. Literature based drug interaction prediction with clinical assessment using electronic medical records: novel myopathy associated drug interactions. *PLoS Comput Biol*. 2012 Aug;8(8):e1002614.
2. Wu HY, Karnik S, Subhadarshini A, Wang Z, Philips S, **Han X**, Chiang C, Liu L, Boustani M, Rocha LM, Quinney SK, Flockhart D, Li L. An integrated pharmacokinetics ontology and corpus for text mining. *BMC Bioinformatics*. 2013 Feb 1;14:35. doi: 10.1186/1471-2105-14-35.
3. Liu J, Flockhart PJ, Lu D, Lv W, Lu WJ, **Han X**, Cushman M, Flockhart DA. Inhibition of cytochrome p450 enzymes by the e- and z-isomers of norendoxifen. *Drug Metab Dispos*, 2013. 41(9): p. 1715-20.
4. **Han X**, H. Schelleman, C.M. Brensinger, S.K. Quinney, W.B. Bilker, D.A. Flockhart, L. Li, S. Hennessy. Pharmacoeconomic and *in Vitro* Evaluation of Potential Drug-Drug Interactions of Sulfonylureas with Fibrates and Statins. *British Journal of Clinical Pharmacology*. (Under preparation)

Published Abstracts

1. **X. Han**, S. K. Quinney, D. A. Flockhart, L. Li. An auto-inhibition pharmacokinetics model for paroxetine. *Clinical pharmacology and therapeutics*, 2010. 87(Supplement 1s): S53.
2. **X. Han**, Z. Wang, A. Subhadarshini, S. Karnik, R. M. Strother, S. D. Hall, Y. Jin, D.A. Flockhart, S. K. Quinney, J. D. Duke, L. Li. Novel Translational Paradigm for Drug-drug Interaction Research: A Combination of Literature-Based Discovery, Electronic Medical Records and *In Vitro* DDI Screening Assays. *Clinical pharmacology and therapeutics*, 2012. 91(Supplement 1s): S2.
3. **X. Han**, S. Quinney, T. Skaar, J. Elmendorf, D. Flockhart, L. Li. New myotoxic drug interactions between statins and rifampicin. *Clinical pharmacology and therapeutics*, 2013. 93(Supplement 1s): S44.

Podium Presentations

1. **X. Han**, Z. Wang, A. Subhadarshini, S. Karnik, R. Strother, D. Flockhart, S. Quinney, J. Duke, L. Li. Novel Translational Paradigm for Drug-drug Interaction Research: A Combination of Literature-Based Discovery, Electronic Medical Records and *In Vitro* DDI Screening Assays. ASCPT Annual Meeting; Washington DC, March, 2012.

Poster Presentations

1. **X. Han**, S. K. Quinney, D. A. Flockhart, L. Li. An Auto-inhibition Pharmacokinetic Model for Paroxetine. ASCPT Annual Meeting; Atlanta, Georgia, March, 2010.
2. **X. Han**, Sara Quinney, David Flockhart, Lang Li. Paroxetine Auto-inhibition Pharmacokinetic Modeling. ACOP Annual Meeting; San Diego, California, April, 2011.

3. **X. Han**, Z. Wang, A. Subhadarshini, S. Karnik, R. Strother, D. Flockhart, S. Quinney, J. Duke, L. Li. Novel Translational Paradigm for Drug-drug Interaction Research: A Combination of Literature-Based Discovery, Electronic Medical Records and *In Vitro* DDI Screening Assays. ASCPT Annual Meeting; Washington DC, March, 2012.
4. **X. Han**, Z. Wang, A. Subhadarshini, S. Karnik, R. Strother, D. Flockhart, J. Overhage, S. Quinney, J. Duke, L. Li. A Translational Bioinformatics Approach to Drug Interaction Identification and Validation. AMIA Annual Symposium, San Francisco, California, March, 2012.
5. **X. Han**, Z. Wang, A. Subhadarshini, S. Karnik, R. M. Strother, S. Hall, D. Flockhart, S. K. Quinney, J. D. Duke, L. Li. Clinical Myopathy as a Starting Point for Identification of New Myopathic Drug Interactions. AAPS Annual Meeting and Exhibition; Chicago, Illinois, October, 2012.
6. **X. Han**, J. Elmendorf, S. Quinney, T. Skaar, D. Flockhart, L. Li. New myotoxic drug interactions between statins and rifampin. ASCPT Annual Meeting; Indianapolis, Indiana, March, 2013.

MAJOR COURSES

Pharmacology: Clinical Pharmacokinetics, Principles of Pharmacology, Clinical Trials, Pharmacoepidemiology, Bioinformatics and System Biology

Statistics: Applied Regression Analysis, Experimental Design, Multivariate Analysis, Survival Analysis, Longitudinal Data Analysis, Generalized Linear Model, Nonlinear Mixed Effect Models

PROFESSIONAL AFFILIATIONS

- | | |
|-----------------|---|
| 2010 to present | American Society for Clinical Pharmacology and Therapeutics (ASCPT) |
| 2010 to 2011 | American Society of Pharmacometrics (ASOP) |
| 2012 to present | American Association of Pharmaceutical Scientists (AAPS) |
| 2012 to present | British Pharmacological Society (BPS) |

CERTIFICATES & WORKSHOPS

- | | |
|------|---|
| 2010 | SIMCYP Simulator Certificate Training Program, Indianapolis, IN |
| 2010 | Pharmacometrics Modeling with R Workshop, ACOP, San Diego, CA |
| 2012 | International Transporter Consortium Workshop Two (ITCW2), ASCPT |
| 2013 | Quantitative Systems Pharmacology Pre-conference, ASCPT |
| 2013 | Adaptive Clinical Trials in Drug Development Pre-conference, ASCPT |
| 2013 | Clinical Pharmacology Curriculum Review Course Post-conference, ASCPT |
| 2013 | AAPS Workshop on Drug Transporters in ADME, Bethesda, MD |

CONFERENCES

- | | |
|------------|-------------------------------------|
| 2010 March | ASCPT Annual Meeting; Atlanta, GA |
| 2011 April | ASOP Annual Meeting; San Diego, CA |
| 2012 March | ASCPT Annual Meeting; Washington DC |

2012 October	AAPS Annual Meeting and Exhibition; Chicago, IL
2012 November	BPS Annual Meeting; London UK
2012 December	IQPC 3 rd Annual Clinically Relevant Drug Transporters; London, UK
2013 March	ASCPT Annual Meeting; Indianapolis, IN